Mapping the next forest generation – the potential of national forest inventory data for identifying regeneration gaps

Leonie C. Gass[1], ORCID: 0009-0002-6339-1363, leonie.gass@uni-bayreuth.de, +49-921 / 55 5653

Lisa Hülsmann[1,2], ORCID: 0000-0003-4252-2715, lisa.huelsmann@uni-bayreuth.de

[1]Ecosystem Analysis and Simulation (EASI) Lab, University of Bayreuth, Bayreuth, Germany

[2]Bayreuth Center of Ecology and Environmental Research (BayCEER), University of Bayreuth, Bayreuth, Germany

Abstract

In light of global change and forest disturbances, there is an increasing recognition of the importance of forest regeneration to ensure future generations of trees. However, despite the importance of forest regeneration, there is a lack in spatial information on the current availability of trees in the seedling and sapling stage. In this study, we aimed to evaluate the potential to predict species-specific forest regeneration densities using regeneration data typically recorded within National Forest Inventories (NFIs). We then calculated three indicators for regeneration quantity and quality to locate potential gaps of regeneration under a changing climate. We successfully calibrated regeneration density models for 22 tree species using generalised additive models (GAMs) using regeneration density data from the 2012 German NFI and 44 environmental predictors. Subsequently, the models were used to create regeneration density maps for the German forest area at high spatial resolution (1 ha). Regeneration gaps were evaluated in terms of low total density (<1,000 ha^{-1}), low species richness (≤2 species) and a high proportion (≥75%) of regeneration at high future cultivation risk. Our results indicate gaps in terms of total regeneration density and species richness for 13.4% and 47.1% of the forest area of Germany, respectively. A lack of climate-adapted species was found for 25.2%, exemplarily assessed for the Bavarian forest area. Along this example, we show how such results can be used to identify areas that require additional silvicultural

intervention in order to increase the resilience of future forests. Our study highlights the potential of NFI data, particularly that on forest regeneration, and demonstrates the applicability of regeneration indicator maps for forest management and policymakers in times of change.

Keywords

Forest regeneration, species distribution models SDMs, generalized additive models GAMs, sapling density, species richness, climate-adapted species, cultivation risk

Introduction

Forests are ecosystems of global importance including their value for human well-being. However, forest ecosystems are increasingly affected by ongoing climate change. In Europe, repeated droughts have caused increased spread of pests and diseases, defoliation of trees (Potočić et al., 2021), reduced tree growth (Martinez del Castillo et al., 2022) and higher tree mortality (George et al., 2022; Senf et al., 2020). The consequences are more open canopies and more and larger disturbances (Senf & Seidl, 2021). This dynamic constitutes a partial loss of a forest generation, which makes it necessary to consider the subsequent generation, the regenerating trees that are in the seedling and sapling stage.

Forest regeneration determines present and future forest resilience under increasing disturbances and higher canopy mortality. A high density of seedlings and saplings can accelerate the regrowth of a closed canopy, avoid arrested succession (Royo & Carson, 2006) and serve as an advanced start of post-disturbance forest reorganization (Seidl et al., 2024; Seidl & Turner, 2022). Furthermore, regeneration is key for the species composition and stand structure of future mature stands, and thus is targeted by management to adapt forests to climate change (Fischer et al., 2016; Löf et al., 2018). While natural regeneration is the dominant regeneration type in many European forest systems, seeding, planting and cutting treatments are selectively applied to ensure forest regeneration, increase the proportion of climate-adapted tree species and create more mixed forest

stands (Erdozain et al., 2024; Löf et al., 2019). To assess how well forest regeneration is adapted to future climate developments and where targeted forestry measures would be necessary, regional quantification of regeneration is needed. Hence, it is essential to monitor small tree stages at large scales and at high spatial resolution.

One of the most important data sources on forests at large spatial scales are national forest inventories (NFIs). Besides statistically representative information on mature trees at regular time intervals, most European NFIs also include assessments of regeneration, i.e. trees below the threshold of diameter at breast height (dbh; Gschwantner et al., 2022; McRoberts et al., 2011). Forest regeneration is often measured as local regeneration densities by counting individuals per tree species and size class within small sampling areas, e.g. from 12 m^2 to 79 m^2 (Gschwantner et al., 2024; McRoberts et al., 2011). The potential of such NFI regeneration data is largely untapped and underestimated. First, despite the intense collection of forest regeneration information, the level of detail in the NFI reports is low. The reports either provide no information on forest regeneration (Lackner et al., 2023) or only the dominant type of regeneration, such as natural regeneration or planting, aggregated at the national level (e.g. Bundesministerium für Ernährung und Landwirtschaft, 2024; Rigling & Schaffer, 2015). NFI reports thus lack information on the quantity and quality of forest regeneration, such as total seedling and sapling density, tree species richness or species composition. Second, it is a widespread perception that inference on forest regeneration and its patterns along large environmental gradients using NFI data is challenging or impossible due to high spatial heterogeneity, many interacting stochastic processes (Price et al., 2001; Shoemaker et al., 2020) and the relatively small plot size for regeneration assessments. Nevertheless, NFI and regional inventory data on forest regeneration have been used to identify important drivers of regeneration (e.g. Axer et al., 2021; Martini et al., 2024; Vayreda et al., 2013) and to calibrate empirical models of regeneration distributions (Hasenauer et al., 2000; Kolo et al., 2017). This suggests that NFI regeneration data may have the potential to map the next generation of forests at large spatial scales.

A common approach to creating continuous maps from NFI sample plot data is to use species distribution models (SDMs; Hernández et al., 2014; Xu et al., 2025), which make use of a species' ecological niche. SMDs are fitted for tree species at national and continental scale to create detailed maps of current tree species distributions (Blickensdörfer et al., 2024; Bonannella et al., 2022) and gain insights into potential tree species distributions under climate change (e.g. Dyderski et al., 2018; Lima et al., 2024). However, these attempts focus on large trees above the dbh threshold. Although the drivers of regeneration are becoming better understood (e.g. Axer et al., 2021; Martini et al., 2024; Vayreda et al., 2013), empirical models have not been applied to predict regeneration in space. The advantages of such regeneration maps would be their ability to provide information at unobserved locations, allowing for regional assessment of the current status and potential gaps of regeneration quantity and quality at high spatial resolutions and at large spatial scales. Such species-specific regeneration maps could be used for early detection of post-disturbance reorganisation (Seidl et al., 2024), initialisation of dynamic forest simulation models (Díaz-Yáñez et al., 2024) and deriving regeneration indicators to inform forest management (Fischer et al., 2016).

Important indicators for the ability of forest regeneration to contribute to a more resilient next forest generation are its total density, species richness and proportion of climate-adapted species (Cerioni et al., 2024; König et al., 2022). High total regeneration density maintains the ability to establish the next forest generation (Hanbury-Brown et al., 2022). High species richness can reduce losses of productivity and biomass under more extreme climatic conditions and increased of disturbances (Mori et al., 2021; Sebald et al., 2021). For example, it can provide insurance, trait complementarity and facilitation (Jactel et al., 2017). A high proportion of climate-adapted species can indicate better resilience of the future mature forest stand and high economic value under climate change (Erdozain et al., 2024; Hanewinkel et al., 2013). Evaluation of these indicators at high spatial resolution is essential to assess regeneration as a potential for future forests.

Here, we assess the potential of regeneration density models calibrated with NFI data to infer and evaluate the current quantity and quality of forest regeneration at high spatial resolution. We built flexible species-specific regeneration models using the untapped regeneration density data of the German NFI in combination with 44 environmental variables, describing the environmental preferences of the tree species in early life stages. Subsequently, we used the regeneration models to predict the regeneration density per tree species for the German forest area at a resolution of 1 ha (100 x 100 m). We then assessed indicators of potential regeneration gaps by quantifying the currently available total regeneration density. Additionally, we evaluated regeneration quality, which is defined as species richness and the proportion of climate-adapted tree species in early life stages, the latter indicated as a low proportion of regeneration at high cultivation risk. We show that NFI regeneration data and derived products have high potential to inform solutions to current challenges of forest management and global change at regional, national, and continental scales.

Materials and Methods

We combined regeneration density observations from the German NFI to map the forest regeneration across Germany and evaluate potential regeneration gaps using a three-step approach. First, we combined the NFI regeneration data with environmental data to construct species-specific regeneration models (Figure 1). Second, we evaluated the predictive performance of the regeneration models using 10-fold spatially blocked cross-validation and used the validated models to predict regeneration densities for the forest area of Germany. Third, we mapped indicators of regeneration quantity and quality, demonstrating their potential application for Bavaria. The full workflow of modelling and data analysis can be found at https://github.com/LeonieCG/GermanRegenerationMaps2012 and https://doi.org/10.5281/zenodo.15552196.

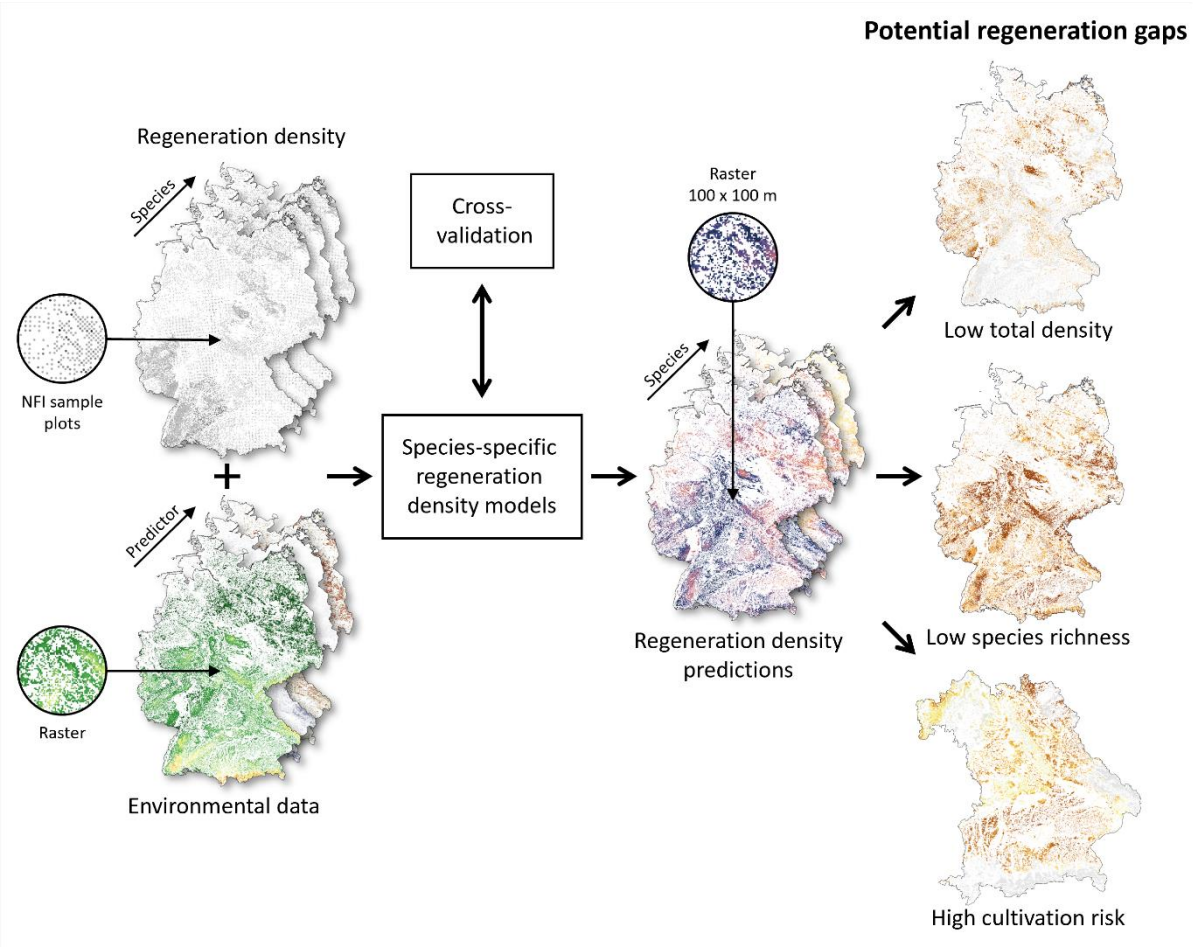

Figure 1: Workflow and criteria for the identification of potential regeneration gaps across German forests. To generate species-specific maps of current forest regeneration, we calibrated species-specific regeneration density models using data from the German National Forest Inventory (NFI). These maps allowed us to identify regions where forest regeneration has too low total density, low species richness, or high future cultivation risk. Map lines delineate study areas and do not necessarily depict accepted national boundaries.

Regeneration data

We used forest regeneration data from the most recent published German NFI (Bundeswaldinventur), conducted in 2011 and 2012 (Thünen-Institut, 2015). The German NFI is conducted every ten years to assess tree and stand characteristics that are representative of the German forests. The sampling design is based on a regular grid with each cluster point consisting of four sample plots (survey design detailed in Riedel et al., 2017). We used regeneration counts assessed at each sample plot, with individuals counted per species and size category within subplots

of 2 m radius (12.57 m^2). The size categories for regeneration were defined as: Category 1: >50-130 cm in height, Category 2: >130 cm in height - 4.9 cm dbh, Category 5: 5.0-5.9 cm dbh, Category 6: 6.0-6.9 cm dbh. Individuals were counted regardless of regeneration type, i.e. no distinction was made between natural, sown or planted regeneration. For our analyses, we summed up the counted individuals per species across all categories and evaluated data availability and average abundance for each tree species. Within the German NFI, the most common tree species in the regeneration were *Fagus sylvatica* L. (29.9% of the total regeneration), *Picea abies* (L.) H.Karst. (16.9%) and *Acer pseudoplatanus* L. (8.7%; Table S2). The tree species *Sorbus domestica* L. had no records, although it would be part of the German NFI regeneration protocol and was therefore excluded from further analysis. In total, our regeneration dataset covered information of 43 tree species at 59,848 NFI plot locations.

Predictors of regeneration patterns

To calibrate the predictive species distribution models, we used 44 environmental predictors related to topography, soil, macroclimate, microclimate, stand structure, space and time (Table 1). The environmental predictor values were preferably obtained from the NFI (meta) data and, if not available, from a corresponding raster layer at each NFI plot location (Table 1). Predictor information at each plot location was retrieved by the Thünen-Institute, as the true plot locations are not published. The regeneration density and environmental datasets were then combined, and observations with missing predictor values were removed. The resulting dataset consisted of 52,305 NFI plot observations used for model calibration (full dataset is available at https://doi.org/10.5281/zenodo.15550864).

For the prediction of forest regeneration, we prepared information on the environmental variables for the entire forest area of Germany. The base raster layer of the forest area was created by recalculating the forest area map by Langer et al. (2022) to a 1 ha resolution and to the coordinate system of the cultivation risk maps (see below). Then, each predictor raster dataset was transformed

using the base raster layer, and all datasets were set to the same coordinate system, extent and resolution. The predictors *coordinate* and *conspecific basal area*, were only available at NFI plot location and not as raster layers. Raster layers for *x* and *y coordinates* were created using the cell centroid coordinates of the base layer. Whereas the raster layers for *conspecific basal area* were derived using the NFI basal area data and the same modelling and prediction approach used for regeneration (see below).

Table 1: Predictor variables used for the calibration of the species-specific regeneration density models.

Category	Variable	Unit	Spatial extent	Spatial resolution	Measurement time	Reference
Topography	Eastness exposition	-	Europe	25 x 25 m	2011	Derived from Thünen-Institut (2015) or from European Environment Agency (2016)
	Northness exposition	-				
	Elevation above sea level	meters	Europe	25 x 25 m	2011	Thünen-Institut (2015) or European Environment Agency (2016)
Soil	Available water capacity	%	Europe	500 x 500 m	2009	Ballabio et al. (2016)
	Bulk density	t m³				
	Clay	%				
	Coarse fragments	%				
	Sand	%				
	Silt	%				
	$CaCO_3$	g kg^{-1}	Europe	500 x 500 m	2009-2012	Ballabio et al. (2019)
	Cation exchange capacity	cmol kg^{-1}				
	C-N-ratio	-				
	K	mg kg^{-1}				
	N	g kg^{-1}				
	P	mg kg^{-1}				
	pH in CaCl	-				
	Available water capacity in effective rooting depth	mm	Germany	250 x 250 m	NA	Duijnisveld (2015)
	Water and wetness probability index	%	Europe	20 x 20 m	2015	European Environment Agency (2018b)
	organic carbon	%	Europe	1000 x 1000 m	1800-2000	Jones et al. (2005)
	Total NH_4 immission	eq ha^{-1} a^{-1}	Germany	1000 x 1000 m	2013-2015	Schaap et al. (2018)
	Total NO_3 immission	eq ha^{-1} a^{-1}				
	Total N immission	eq ha^{-1} a^{-1}				
Macroclimate	Climatic water balance over the GDD period	mm	Europe	30 x 30 arcsec	1979–2013	Heiland et al. (2022)
	Climatic water balance	mm				
	Growing degree days	°C d				
	Mean annual precipitation	mm	Global	30 x 30 arcsec	1981-2010	Karger et al. (2017, 2018)
	Precipitation seasonality	%				
	Mean daily minimum air temperature of the coldest month	°C				

	Mean annual air temperature	°C				
	Annual range of air temperature	°C				
	Mean diurnal air temperature range	°C				
	Temperature seasonality	0.01 °C				
	Aridity index	-	Global	30 x 30 arcsec	1970-2000	Trabucco and Zomer (2019)
	Potential evapotranspiration	0.0001 mm				
Microclimate	Minimum temperature of the coldest month	°C	Europe	25 x 25 m	2000-2020	Haesen et al. (2023)
	Mean annual temperature	°C				
	Annual temperature range	°C				
	Mean diurnal temperature range	°C				
	Temperature seasonality	0.01 °C				
Stand structure	Tree cover density	%	Europe	20 x 20 m	2011-2013	European Environment Agency (2018a)
	Conspecific basal area (from angle count unit 1 and 2)	m^2 ha^{-1}	Germany	100 x 100 m	2011-2012	Thünen-Institut (2015) and this study
Space	Federal state of Germany	-	Germany	none and 100 x 100 m	2013 and 2022	Thünen-Institut (2015) and derived from Bundesamt für Kartographie und Geodäsie (2022)
	NFI plot coordinate x and y value (anonymized)	-	Germany	1000 x 1000 m	2016	Thünen-Institut (2015) and this study
Time	Month and year of NFI measurement	-	Germany	none	2011-2012	Thünen-Institut (2015)

Regeneration models

As predictive species-specific models of forest regeneration density, we calibrated generalized additive models (GAMs; Wood, 2017) with a negative binomial distribution and a log link function. We used GAMs with cubic regression splines (Wood et al., 2016) to allow for a broad spectrum of non-linear relationships between regeneration densities and our chosen environmental predictors. In addition, we included variables of space and time in our models. The time variable is used to account for seasonal differences in growing conditions and detection probability during the sampling period and consists of *month and year of NFI measurement*. We used the anonymized *plot coordinates* provided by the NFI to account for unobserved spatial predictors. These anonymized plot coordinates are the actual plot coordinates that have been transferred to a 1 x 1 km grid and then returned as grid cell coordinates (Hennig, 2022). We also included *federal state* as a predictor to account for potential differences in incentives of regeneration establishment and management of regeneration between states. Environmental predictors were included as fixed effects, whereas *month and year of*

NFI measurement and *federal state* were included as random effects in our models. *Plot coordinates* were included using a tensor product smooth to account for unexplained spatial variability in the regeneration densities. GAM smoothness selection and estimation of the negative binomial functions theta value was performed using fast restricted maximum likelihood estimation. Basis dimensions of smoothing splines were kept at moderate complexities for environmental fixed effects (k = 10) and were set to 25 in x and 50 in y direction for spatial effects. We allowed fixed effects to be shrunk to zero, serving as a variable selection technique (Wood, 2017), and used a ridge penalty for random effects.

To interpolate conspecific basal area for the German forest area to predict regeneration, the same model structure with basal area as the response, a Tweedie distribution and a log link function was used. We calibrated basal area models for each regeneration tree species which remained after model evaluation (see below) and used the same prediction approach as described for regeneration density, without cross-validation. The plausibility of the species-specific basal area distributions was assessed by visual comparison with distribution maps of the European atlas of forest tree species (Caudullo et al., 2016).

Models were fitted with the function bam() suited for large data sets (Wood et al., 2015) from the R package mgcv (v.1.9.1, Wood, 2023).

Model evaluation

Statistical assumptions of the regeneration models were assessed based on simulated residuals generated with the package DHARMa (v.0.4.6, Hartig, 2022). We visually evaluated distributional and residual assumptions as well as zero-inflation resulting in no critical violations (plots of simulated residuals can be found in Supplementary Material 1). To ensure that the observations are spatially independent, even though we are having a clustered sampling design for the NFI, we tested for spatial autocorrelation within scaled simulated residuals per cluster. We found a tendency for spatial autocorrelation for the regeneration models of *Betula pendula* Roth*, Betula pubescens* Ehrh., *Quercus*

petraea (Matt.) Liebl. and *Tilia* spp. (*T. platyphyllos* Scop. and *T. cordata* Mill.; see Table S1). However, given the models' satisfactory performance in cross-validation (see the subsequent paragraph), we assume that they generalize across space and likely capture meaningful spatial patterns.

In a next step, predictive model performance was assessed using a 10-fold spatially blocked cross-validation with the package blockCV (v.3.1.4; Valavi et al., 2019, 2024). Blocks were set up with hexagonal block shapes and block sizes corresponding to the spatial autocorrelation range of the response variables. Block sizes were found to be too large for some species, resulting in less than 10 blocks. In these cases, we set the range to 300 km resulting in 11 blocks for Germany (Table S1). For each fold, the mean absolute error (MAE) as an indicator for model performance (Chai & Draxler, 2014) and pseudo-R^2 (Cameron & Windmeijer, 1997) as an indicator of explanatory power were computed for the test and training data. For MAE, we calculated the relative MAE from the test and training MAE $\left(\frac{MAE_{test}}{MAE_{train}}\right)$. The median was used to aggregate values of relative MAE and test pseudo-R^2 across all folds. We considered models where the following criteria were met: median relative MAE ≤2 and median pseudo-R^2 ≥0.1.

Predictions

After the evaluation of model assumptions and predictive model performance, regeneration models for 22 tree species were available to be used for prediction (Table 2). Regeneration density maps across German forests were created using raster layers covering the forest area of Germany for each environmental predictor. The time variable *month and year of NFI measurement* was excluded from the predictions, which results in predictions corresponding to average conditions. Finally, we converted the predicted regeneration counts per 2 m radius plot (approximately 12.6 m^2) to regeneration densities (counts per hectare).

Derived regeneration indicators

We selected three indicators to measure whether regeneration can secure future forests and maintain their multifunctionality in a changing climate. These indicators include sufficient total regeneration density to ensure regrowth of forests e.g. after disturbance, sufficient species richness to distribute the risk of various possible future climate trajectories, and species composition with a low proportion of regeneration at high future cultivation risk.

The total regeneration density was calculated by summing up the densities for all 22 tree species per grid cell. We defined <1,000 ha^{-1} as insufficient, 1,000-2,000 ha^{-1} as intermediate and ≥2,000 ha^{-1} as sufficient evaluation thresholds. Since reports of sufficient regeneration density thresholds vary, e.g. 1,591 ha^{-1} (Kolo et al., 2017) or 2,000 ha^{-1} (Bayerisches Staatsministerium für Ernährung, Landwirtschaft und Forsten, 2023), we chose an intermediate total regeneration density of 1,000-2,000 ha^{-1}.

Tree species richness was calculated as the number of species with at least 5% of the total number of regeneration (Mages et al., 2020). For Central European conditions, a species richness of three or four species has been proposed to be sufficient (Lindner et al., 2025; Mages et al., 2020). Since our analysis included only a part of the available tree species, i.e. 22 out of 43 species, we defined ≤2 species within the regeneration layer as insufficient, 3-4 species as intermediate and ≥5 species as sufficient.

To more precisely assess how the current regeneration fits future conditions, we used Bavaria, a federal state located in southwest Germany, as a case study (see Box 1). We combined our species-specific regeneration density maps with the cultivation risk maps provided by the Bavarian State Institute of Forestry (Falk et al., 2013, 2019). These were developed as an information and planning tool for forest practitioners throughout Bavaria and are actively used to select tree species considering climate projections and local site conditions. The cultivation risk maps are based on predicted occurrence probabilities of adult trees in the year 2100 assuming an average warming of

1.9°C and an average precipitation decrease of 4.4 mm compared to the period of 1971-2000 (for details see: Falk & Mellert, 2011; Falk & Hempelmann, 2013; Thurm et al., 2018). The maps are available for 32 tree species and provide information on cultivation risk in five categories ranging from very low to very high risk. For 17 of these species or species groups, we also obtained regeneration distribution maps (Table 2). In the case of the genus *Tilia* L., the NFI did not differentiate between *Tilia platyphyllos* and *T. cordata*, but cultivation risk maps were available for both. We combined the two maps by transforming the five cultivation risk categories into values ranging from 1 to 5 (from *very low* to *very high risk*), calculating the mean risk for each grid cell, and back transforming the values into the former categories. If the mean was between risk categories, we chose the lower category.

As a next step, we aggregated the cultivation risk assessment per grid cell by calculating the percentage of regeneration density at high cultivation risk. To this end, we combined the risk categories *very high risk* and *high risk* into a *high-risk* category, and the categories *increased risk*, *low risk* and *very low risk* into a *low-risk* category. The percentage of regeneration at high cultivation risk $R_{high\,risk}$ was calculated as:

$$R_{high\,risk}[\%] = \frac{N_{high\,risk}}{N_{total}} * 100$$

Here, $N_{high\,risk}$ is the regeneration density summed up over the species with high cultivation risk and N_{total} the total regeneration density across all species of the grid cell. We defined ≥75% of the total regeneration density at high cultivation risk as problematic.

Box 1: Bavaria (Germany) – A case study for identifying regeneration gaps.

Using Bavaria as an example, we demonstrate the potential use of regeneration indicator maps to identify regeneration gaps and hotspots (Figure 2) and derive recommendations for silvicultural interventions. Bavaria, a federal state in the southeast of Germany, has a forest coverage of 36.9% (Klemmt et al., 2014). This corresponds to 22.8% of Germany's total forest area (Bundesministerium für Ernährung und Landwirtschaft, 2016). Recent climate change induced summer droughts and

subsequent bark beetle outbreaks have led to a loss of tree canopies, especially in Norway spruce (*Picea abies*) dominated areas (Thonfeld et al., 2022). We chose Bavaria as a case study because detailed maps of future cultivation risk are available for many tree species, which allowed us to derive not only the total regeneration density and species richness but also the proportion of regeneration at high future cultivation risk.

For Bavaria, we found a high total regeneration density (≥2,000 ha^{-1}) in the southern part and towards the eastern and northwestern edges of the state (Figure 2A). Only few regions, amounting to 3.5% of the forest area, showed a total regeneration density deficit of <1,000 ha^{-1}. Species richness of the regeneration was generally low (≤2 tree species) to intermediate (3-4 species) throughout Bavaria (Figure 2B). Forests with a deficit in species richness covered 50.0% of the Bavarian forest area, mainly in the low mountain ranges. The proportion of regeneration at high future cultivation risk (Figure 2C) was calculated on the basis of 17 species regeneration density maps (Table 2), covering 74.9% of the Bavarian NFI regeneration data and 76.8% of the Bavarian forest area. The proportion of species at high cultivation risk in the regeneration was heterogeneous across Bavaria (Figure 2C). Half of the analysed forest area had a cultivation risk lower than 37.7% (Figure 2D), for instance in the Bavarian Alps (Figure 2C). Regeneration at high risk (i.e. proportions ≥75%) dominated on 25.2% (489,385 ha) of the forest area, e.g. in the northeast. This pattern was mainly driven by *Picea abies*, amounting to 94.5% of all regeneration densities at high risk (Table S3).

Such spatially resolved results on the quantity and quality of forest regeneration indicate regeneration gaps and allow for targeted silvicultural measures and incentives that can significantly contribute to the adaptation of forests to climate change. For example, regions like the Frankenwald and the Bavarian Alps (Figure 2A) are major hotspots for climate change impacts and adaptation in Bavarian forests. Severe large-scale disturbances are a significant issue in the Frankenwald (Viana-Soto & Senf, 2024), while the Alps are increasingly prone to rockfall due to climate change, making forests especially valuable for protection (e.g. Hillebrand et al., 2023; Moos et al., 2021). Combining

this information with forest regeneration indicators allows priorities to be set for forest management: In the Frankenwald with a notable regeneration gap in species richness and climate-adapted tree species (Figure 2B and C), selective cutting of the existing regeneration and planting of additional climate-adapted tree species should be encouraged to increase species richness and reduce future cultivation risk. In contrast, the few local gaps in total regeneration density (Figure 2A) and species richness (Figure 2B) in the Bavarian Alps should be addressed by promoting natural regeneration and planting. Overall, regions with severe regeneration gaps should be prioritized, e.g. the forest area in the Frankenwald.

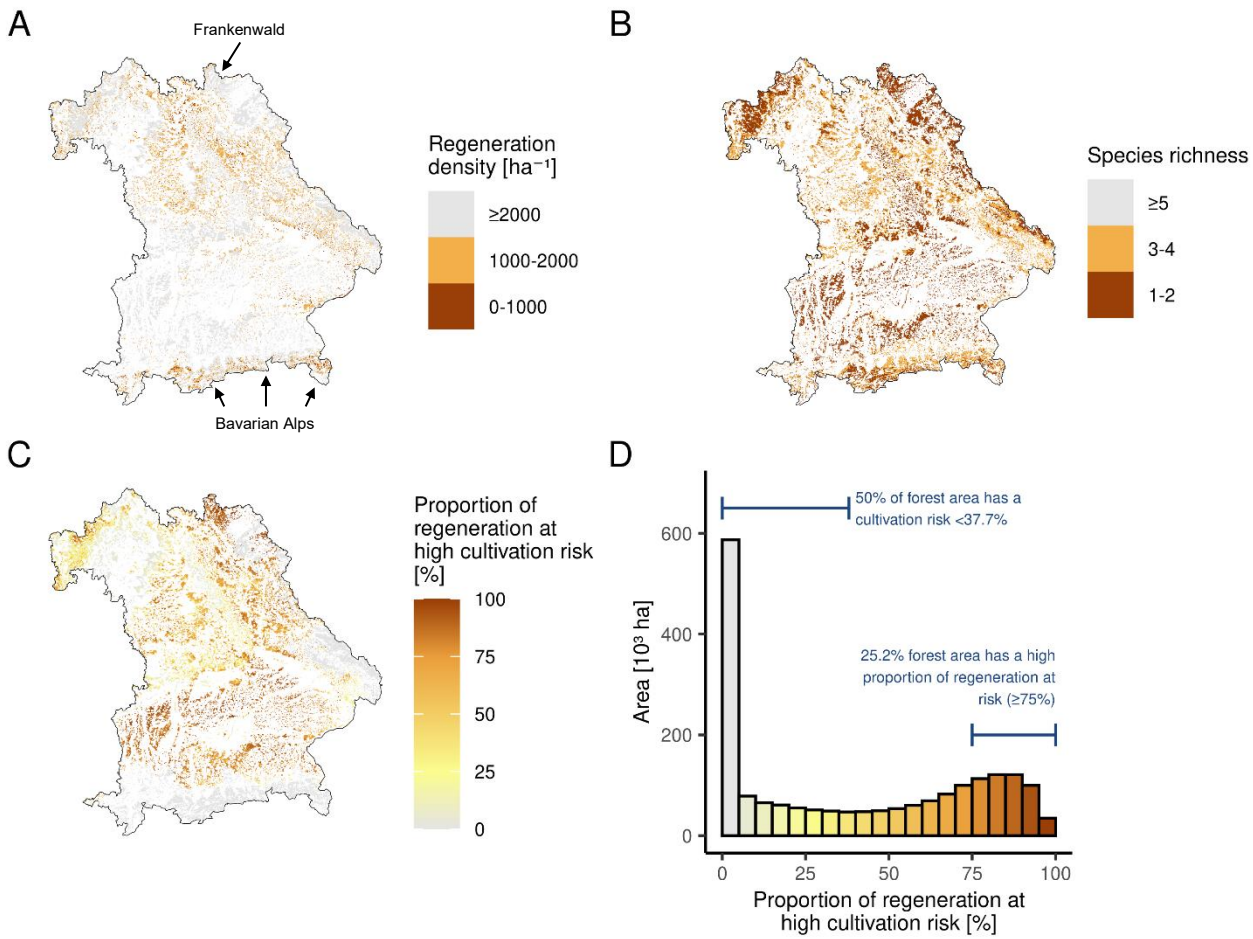

Figure 2: Indicator maps on quantity and quality of forest regeneration for Bavaria: (A) total density, (B) species richness and (C) proportion of regeneration at high cultivation risk. (D) shows the distribution of proportion of regeneration at high cultivation risk. (A) and (B) were derived from regeneration density maps of 22 tree species, while (C) and (D) are based on 17 tree species. Maps are available online at https://easi.users.earthengine.app/view/regeneration-maps and available for

download at https://doi.org/10.5281/zenodo.15550864. Map lines delineate study areas and do not necessarily depict accepted national boundaries.

Programs used

All calculations were conducted in R v.4.4.1 (R Core Team, 2024). Spatial data processing was carried out using the R-package terra (v.1.7.78; Hijmans, 2024) and sf (v.1.0-16; Pebesma et al., 2024).

Results

Regeneration density models

From the 43 calibrated species-specific regeneration density models, 22 met the performance criteria (Table 2), i.e. median pseudo-R^2 ≥0.1 and median relative MAE ≤2 from 10-fold spatially blocked cross-validation. We used these to predict the regeneration density for 78.5% (8,615,918 ha) of the German forest area at a resolution of 1 ha. The 22 species represented 74.9% of the regeneration measured within the NFI. We found that, across Germany, the most common tree species within the regeneration were *Fagus sylvatica, Picea abies* and *Prunus serotina* Ehrh. with mean densities of 1,192, 985 and 349 individuals per hectare, respectively (Table 2). Species with lowest abundance in the regeneration throughout Germany were *Quercus rubra* L., *Sorbus aria* (L.) Crantz and *Pinus strobus* L. with average densities of 5, 2, and 1 individual(s) per hectare.

Of all 43 calibrated regeneration models, five did not converge and 16 did not meet the performance criteria (total 21; Table 2). Out of these, 15 were rare tree species, with total regeneration density <1% within the German NFI (Table S2). The other six were common tree species *Acer pseudoplatanus* L., *Sorbus aucuparia* L., *Betula pendula, Quercus petraea* (Matt.) Liebl., *Populus tremula* L. and *Prunus padus* L. (Table S2), that nevertheless could not be sufficiently modelled with our approach (Table 2). The median pseudo-R^2 criterion was the primary factor in determining the model quality, as the median relative MAE criterion was consistently met (Table 2).

Table 2: Evaluation and summary statistics of regeneration density models for 43 tree species. The availability of regeneration density maps (Germany) or cultivation risk maps (only for Bavaria; Falk et al., 2013, 2019) is indicated by a dot (available) or a circle (not available). Regeneration density maps were predicted when the model performance criteria of median relative MAE ≤2 and median pseudo-R^2 ≥0.1 were met, as determined by 10-fold spatially blocked cross-validation.

Species	**Model performance**		**Regeneration density map availability (Germany)**	**Regeneration density [#/ha]**		**Cultivation risk map availability (Bavaria)**
	Median relative MAE	**Median pseudo-R^2**		**Mean**	**SD**	
Abies alba	1.02	0.48	●	167	819	●
Abies grandis	1.06	0.07	○			●
Acer campestre	0.83	0.31	●	18	345	●
Acer platanoides	0.91	0.12	●	8	154	●
Acer pseudoplatanus	0.99	-0.01	○			●
Alnus glutinosa	1.12	0.16	●	23	324	●
Alnus incana	1.06	0.39	●	84	9122	○
Betula pendula	1.00	-0.12	○			●
Betula pubescens	0.05	0.43	●	25	533	○
Carpinus betulus	0.84	0.20	●	208	1108	●
Castanea sativa	1.01	0.32	●	1	12	●
Fagus sylvatica	1.05	0.26	●	1192	1940	●
Fraxinus excelsior	0.90	0.15	●	329	1900	●
Larix decidua	0.75	0.06	○			●
Larix kaempferi	0.30	0.44	●	7	88	●
Malus sylvestris			○			○
Picea abies	0.75	0.16	●	985	1572	●
Picea sitchensis	0.20	0.09	○			○
Pinus mugo			○			○
Pinus nigra	0.50	-0.28	○			●
Pinus strobus	0.47	-0.01	○			○
Pinus sylvestris	0.33	0.29	●	257	805	●
Populus alba	0.28	0.08	○			○
Populus nigra	0.13	0.20	●	120	12213	○
Populus tremula	0.86	0.07	○			○
Populus trichocarpa x maximoviczii	0.35	-0.98	○			○
Populus x canescens	0.06	-0.09	○			○
Prunus avium	1.00	0.25	●	11	43	●
Prunus padus	0.54	-0.57	○			○
Prunus serotina	0.33	0.11	●	349	5338	○
Pseudotsuga menziesii	0.91	0.21	●	26	101	●
Pyrus communis			○			●
Quercus petraea	0.74	0.02	○			●
Quercus robur	1.06	0.20	●	77	150	●
Quercus rubra	0.84	0.15	●	5	39	●
Robinia pseudoacacia	1.09	0.45	●	75	3850	●
Salix spp.	1.04	0.03	○			○
Sorbus aria	0.89	0.12	●	2	32	○
Sorbus aucuparia	0.99	-0.10	○			●
Sorbus torminalis			○			●
Taxus baccata			○			○
Tilia spp.	0.92	0.29	●	38	582	●
Ulmus spp.	0.60	-0.02	○			●
All species n = 22				4006	17015.5	

Species-specific regeneration maps for Germany

The predicted density maps showed distinct patterns in the availability of regeneration for each tree species (Figure 3, for all other tree species maps see Figure S1). For example, the regeneration of *Fagus sylvatica* was widely distributed with very high abundance in the centre of Germany and lower densities towards the east and the western lowlands (Figure 3). Similarly, the regeneration of *Picea abies* was widely abundant across German forests but showed lower densities (<100 individuals per hectare) towards the northeast. *Abies alba* Mill. - a less common tree species (mean density of 167 ha^{-1}; Table 2) that is considered climate-resilient in low mountain ranges - showed a clear north-south trend with no occurrence in the northern half of Germany and a gradual increase in regeneration from the centre towards the south. In the South, *Abies alba* is particularly abundant in low mountain ranges.

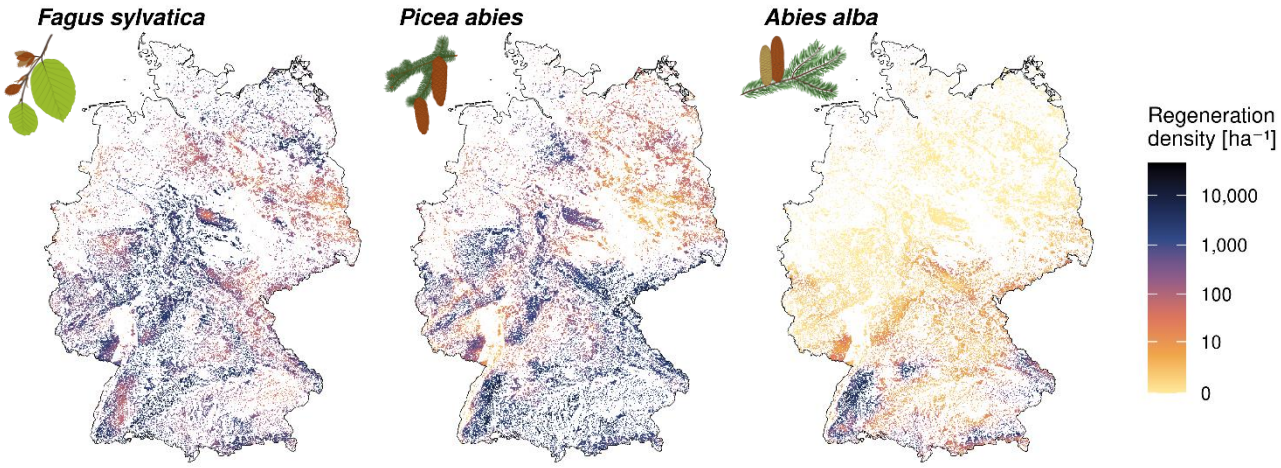

Figure 3: Regeneration densities exemplarily shown for three important tree species in Central Europe, i.e. *Abies alba*, *Fagus sylvatica* and *Picea abies* in 1 ha grid cells for Germany (for remaining tree species maps see Figure S1). All maps are available online at https://easi.users.earthengine.app/view/regeneration-maps and available for download at https://doi.org/10.5281/zenodo.15550864. Map lines delineate study areas and do not necessarily depict accepted national boundaries.

Indicators of total quantity and quality of forest regeneration

The quantity of regeneration, evaluated as the total regeneration density based on 22 tree species, showed an average of 4,006 individuals per hectare (Table 2). A clear trend of insufficient (0-1,000 ha^{-1}) and intermediate (1,000-2,000 ha^{-1}) total regeneration densities in parts of Mid and North Germany was visible (Figure 4, for continuous density colour scale see Figure S2), whereas the South mainly displayed sufficient regeneration (≥2,000 ha^{-1}). Overall, we found 60.1% of the predicted forest area to have sufficient, 26.4% of intermediate and 13.4% of insufficient regeneration densities.

As part of the quality assessment of the regeneration, we evaluated regeneration species richness (Figure 5, for continuous species richness colour scale see Figure S3), which was generally low with an average of 2.8 species per hectare across Germany. A total of 47.1% of the predicted forest area included insufficient (≤2 species) number of tree species in the regeneration (Figure 5B), while 43.5% of the area contained intermediate species numbers (3-4 species) and 9.4% contained sufficient species richness (≥5 species). Forests that are particularly species rich in the regeneration, i.e. ≥5 species, were found towards the northeast (Figure 5A) and are otherwise restricted to local hotspots across Germany. Forests with a species richness ≤2 were particularly common in low mountain ranges.

Regeneration quality was additionally assessed as the future suitability of tree species in the regeneration. We showcase this – and the identification of regeneration gaps and hotspots and potential management strategies more generally – using the example of the German federal state Bavaria (Box 1).

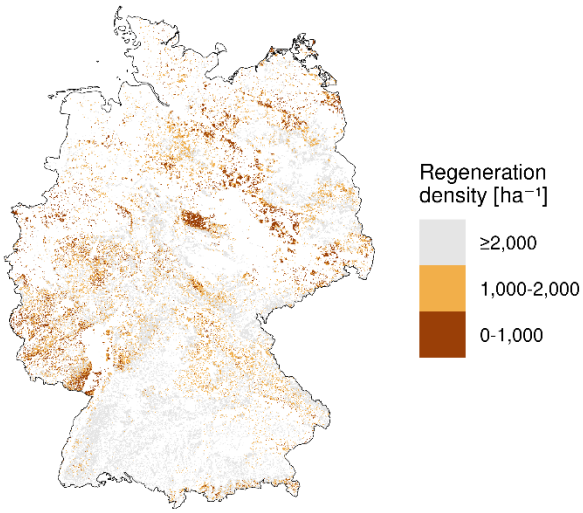

Figure 4: Spatial patterns of total regeneration density (ha^{-1}) for Germany based on 22 tree species. Colour categories describe insufficient (0-1,000 ha^{-1}), intermediate (1,000-2,000 ha^{-1}) and sufficient (≥2,000 ha^{-1}) total regeneration densities (for continuous colour scale see Figure S2). Map is available online at https://easi.users.earthengine.app/view/regeneration-maps and available for download at https://doi.org/10.5281/zenodo.15550864. Map lines delineate study areas and do not necessarily depict accepted national boundaries.

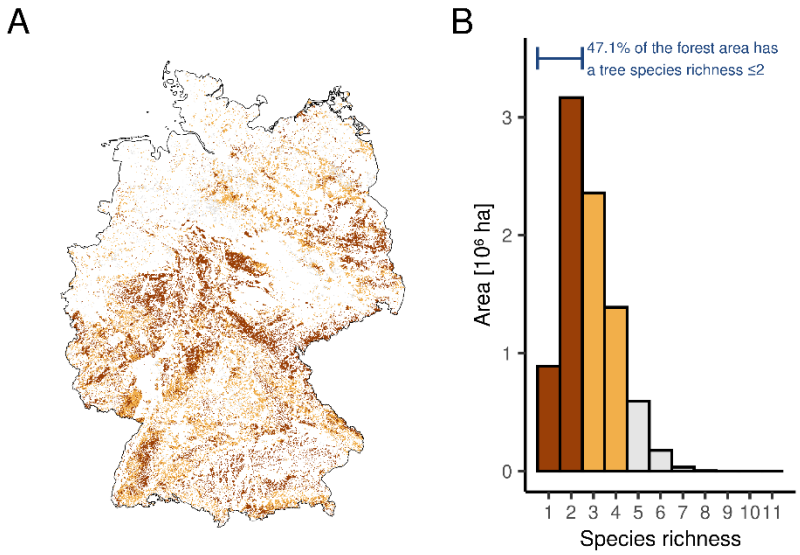

Figure 5: Regeneration tree species richness for the forest area of Germany based on 22 tree species. The map (A) shows spatial patterns, and the histogram (B) describes the distribution of species richness values. Colour categories describe insufficient (1-2), intermediate (3-4) and sufficient (≥5) regeneration species richness (for continuous colour scale see Figure

S3). We considered a species present in a 1 ha-grid cell if its density was at least 5% of the total regeneration density. Map is available online at https://easi.users.earthengine.app/view/regeneration-maps and available for download at https://doi.org/10.5281/zenodo.15550864. Map lines delineate study areas and do not necessarily depict accepted national boundaries.

Discussion

Our results demonstrate the potential to predict forest regeneration density at high spatial resolution from species-specific models calibrated with NFI regeneration data. Using the regeneration density maps predicted for Germany, we evaluated indicators of regeneration quantity and quality, defined here as total regeneration density, species richness and proportion of climate-adapted tree species. The indicators revealed regional gaps and hotspots in forest regeneration.

Predicting forest regeneration at large spatial scale

We successfully predicted forest regeneration density for a large part of the modelled tree species in Central Europe. This contrasts with previous models of forest regeneration. These included only few species (Hasenauer et al., 2000; Kolo et al., 2017), covered only small environmental gradients (Hasenauer et al., 2000) and achieved low predictive accuracy at high spatial resolution because of only few environmental predictors (Zhu et al., 2014). Previous models were therefore not suited to reliably predict community composition and diversity across large environmental gradients. Even more, none of these studies had produced forest regeneration maps at regional or national scales that could be used to assess the quantity and quality of regeneration.

The model approach of our study distinguishes itself by successfully cross-validating 22 of the 43 tree species models (Table 2). This is likely due to the large environmental gradients covered in the NFI data, the large number of environmental predictors (i.e. n = 44), partly at high spatial resolution, and the flexibility of our modelling approach (i.e. GAMs). We conclude that even though forest regeneration is subject to a variety of stochastic processes (Price et al., 2001; Shoemaker et al., 2020) and is measured on small sampling plots (i.e. 12.57 m^2), there is enough signal in local regeneration

densities to successfully model and predict the regional availability of forest regeneration at large spatial scales.

Tree species coverage of the regeneration models

The predicted regeneration density maps (Figure 3 and Figure S2) cover a major part, i.e. 74.9%, of the regeneration sampled within the German NFI. Therefore, our indicators derived from the regeneration maps draw a reliable picture of the dominant forest regeneration state and its gaps. Nevertheless, it would be desirable to expand the range of tree species modelled, especially since a large species pool and rare species will play a greater role as climate change progresses (Huth et al., 2025). In this study, we could not successfully calibrate regeneration models or did not reliably predict observed regeneration densities for 21 tree species (Table 2). Out of these, 15 species are rare and occur at average densities <1% in the German NFI regeneration dataset (Table S2). Because the NFI sample plots for regeneration are small, rare species are not well covered, and the amount of data is not sufficient to uncover the environmental preferences of these tree species and to calibrate predictive regeneration models. To improve data availability for these species, information including regeneration data from previous German NFI surveys, other European NFIs or local inventories could be used in future studies.

In addition to rare species, we could also not reliably predict the regeneration density for more generalist species *Acer pseudoplatanus, Betula pendula*, and *Sorbus aucuparia*. These have wide realized niches and are found across large environmental gradients (Caudullo et al., 2016). This may have made it difficult to relate the regeneration densities of these species to the environmental predictors available to us. As another strategy to predict regeneration density for more species in the future, models could include even more predictors to better reflect environmental niches.

Predictors of forest regeneration

Our regeneration models were calibrated using 44 predictive variables describing the environment with respect to topography, soil, microclimate, macroclimate, stand structure and spatial patterns (Table 1). Previous studies have related forest regeneration to similar environmental variables, such as elevation (Kolo et al., 2017; Kupferschmid et al., 2019; Thom et al., 2023), soil texture (Kolo et al., 2017), mean annual temperature (Harris et al., 2024; Kolo et al., 2017; König et al., 2025; Kupferschmid et al., 2019; Vayreda et al., 2013; Zhu et al., 2014), conspecific basal area (Axer et al., 2021; Martini et al., 2024; Zhu et al., 2014) and microclimatic variables (Caron et al., 2021; Thom et al., 2023). However, it has been shown that forest regeneration density is also related to other predictors such as browsing intensity (Axer et al., 2021; Kupferschmid et al., 2019; Martini et al., 2024; Vayreda et al., 2013), understory light availability (Harris et al., 2024; Martini et al., 2024) or silvicultural management and ownership (Kolo et al., 2017).

We could not account for these additional predictors in our forest regeneration maps because they are not (yet) available as spatial datasets for the entire German forest area (e.g. understory light availability or silvicultural management) or only available at low spatial resolution and not homogenized across federal states (e.g. browsing intensity). We consider it promising to evaluate how much these additional predictors can contribute to the predictability of forest regeneration, and to invest in datasets for these predictors with better spatial coverage in case of considerably improved predictions. Although our approach already accounts for a high level of flexibility (i.e. GAM), the complexity of environmental relationships could be further enhanced by using machine learning algorithms (Pichler & Hartig, 2023), in addition to expanding model predictors (Xu et al., 2025).

Application of regeneration density and indicator maps

Creating species-specific regeneration density maps was motivated by the potential to identify regional gaps and hotspots in regeneration quantity and quality thus to assess the potential

contribution of forest regeneration to a more resilient next forest generation. To this end, we used three indicators that are widely used in forest management and planning: total regeneration density, species richness and proportion of climate-adapted tree species (Cerioni et al., 2024; König et al., 2022). Typically, these indicators are assessed for individual stands by local forest practitioners and managers, but not at larger scales. Our regeneration indicator maps demonstrate the potential to monitor these indicators at national scales and to identify regional differences in forest regeneration.

For Germany, we found that regeneration gaps are small in terms of total regeneration density (Figure 4) but are of concern regarding species richness, with a deficit for almost half of the German forest area (Figure 5). In addition, one quarter of the forest area in Bavaria is affected by a lack of climate-adapted tree species (Figure 2D). While the forest regeneration indicator maps cannot replace a local, on-site assessment of regeneration for stand level silvicultural decisions, they can provide an indication of potential regeneration gaps at the regional scale (Box 1). Such gaps can help forest policymakers identify potential priority areas and target actions to reduce future risks, increase species richness and regeneration density through selective cutting, promoting natural regeneration, or planting climate-adapted tree species. These actions can be implemented through direct hands-on management or through incentives for silvicultural practices that promote regeneration (Huth et al., 2025).

Beyond practical applications, our species-specific regeneration density maps can be used to improve dynamic forest models, where the importance of regeneration processes is increasingly recognized (e.g. Díaz-Yáñez et al., 2024; Hanbury-Brown et al., 2022; König et al., 2025). Incorporating comprehensive information on regeneration availability, especially when including information of species composition and spatial variability, can limit bias and increase the robustness of dynamic models (Díaz-Yáñez et al., 2024). This has a high potential to make more reliable predictions of stand development trajectories and potential future stands, providing valuable information for

policymakers and forest managers. In turn, the incorporation of regeneration data into dynamic forest models also allows for the evaluation of different regeneration management strategies.

Conclusions

This study demonstrates the potential of using NFI regeneration data to predict species-specific regeneration densities at high spatial resolution, from which indicators of regeneration quantity and quality can be derived. The resulting maps of regeneration indicators help to identify regional gaps in total regeneration density, species richness, and climate-adapted species composition. Consequently, our approach allows to estimate whether regeneration can secure future forests and maintain their multifunctionality, which is particularly important in the context of climate change and increased disturbances (Cerioni et al., 2024). We strongly encourage the evaluation of regeneration patterns across Europe and the monitoring of changes in forest regeneration between two consecutive inventories. To achieve such continuous European forest regeneration monitoring, it is essential to prioritize homogenization of forest inventory data and suitable environmental predictor datasets.

Acknowledgements

We would like to express our gratitude to Lukas Heiland whose work set the foundation to work with the German NFI regeneration data. We are thankful for Simon Mayer, who helped with the visualization of the forest regeneration maps on Google Earth Engine and the maintenance of our local environmental predictor database. We also extend our thanks to Lukas Blickensdörfer (Thünen-Institute) for providing predictor information at true NFI plot location and Michael Heym (Bavarian State Institute of Forestry) for valuable help with the German NFI data. We thank Tobias Mette (Bavarian State Institute of Forestry) for the provisioning of the cultivation risk maps of Bavaria. Finally, we want to thank Ottmar Ruppert, Ralph König and Jonas Duscher for their forest practice insights and support.

Funding

Leonie Gass received funding within the Projekt BayForDemo by the Bavarian Ministry of Science and the Arts within the Bavarian Climate Research Network (bayklif).

Author contributions

Leonie Gass: Conceptualization (equal), data curation (lead), formal analysis (lead), methodology (equal), project administration (supporting), visualization (lead), writing – original draft preparation (lead), writing – review & editing (equal).

Lisa Hülsmann: Conceptualization (equal), formal analysis (supporting), funding acquisition (lead), methodology (equal), project administration (lead), resources (lead), supervision (lead), visualization (supporting), writing original draft preparation (supporting), writing – review & editing (equal).

References

Axer, M., Martens, S., Schlicht, R., & Wagner, S. (2021). Modelling natural regeneration of European beech in Saxony, Germany: Identifying factors influencing the occurrence and density of regeneration. *European Journal of Forest Research*, *140*(4), 947–968. https://doi.org/10.1007/s10342-021-01377-w

Ballabio, C., Lugato, E., Fernández-Ugalde, O., Orgiazzi, A., Jones, A., Borrelli, P., Montanarella, L., & Panagos, P. (2019). Mapping LUCAS topsoil chemical properties at European scale using Gaussian process regression. *Geoderma*, *355*, 113912. https://doi.org/10.1016/j.geoderma.2019.113912

Ballabio, C., Panagos, P., & Monatanarella, L. (2016). Mapping topsoil physical properties at European scale using the LUCAS database. *Geoderma*, *261*, 110–123. https://doi.org/10.1016/j.geoderma.2015.07.006

Bayerisches Staatsministerium für Ernährung, Landwirtschaft und Forsten. (2023). *Richtlinie für Zuwendungen zu waldbaulichen Maßnahmen im Rahmen eines forstlichen Förderprogramms (WALDFÖPR 2020)* (Az. F2-7752.1-1/361; pp. 1–21).

Blickensdörfer, L., Oehmichen, K., Pflugmacher, D., Kleinschmit, B., & Hostert, P. (2024). National tree species mapping using Sentinel-1/2 time series and German National Forest Inventory data. *Remote Sensing of Environment*, *304*, 114069. https://doi.org/10.1016/j.rse.2024.114069

Bonannella, C., Hengl, T., Heisig, J., Parente, L., Wright, M. N., Herold, M., & Bruin, S. de. (2022). Forest tree species distribution for Europe 2000–2020: Mapping potential and realized distributions using spatiotemporal machine learning. *PeerJ*, *10*, e13728. https://doi.org/10.7717/peerj.13728

Bundesamt für Kartographie und Geodäsie. (2022). *Verwaltungsgebiete 1: 5 000 000* [Dataset].

Bundesministerium für Ernährung und Landwirtschaft. (2016). *Ergebnisse der Bundeswaldinventur 2012* (Bundesministerium für Ernährung und Landwirtschaft, Ed.).

Bundesministerium für Ernährung und Landwirtschaft. (2024). *Der Wald in Deutschland—Ausgewählte Ergebnisse der vierten Bundeswaldinventur* (p. 60).

Cameron, A. C., & Windmeijer, F. A. G. (1997). An R-squared measure of goodness of fit for some common nonlinear regression models. *Journal of Econometrics*, *77*(2), 329–342. https://doi.org/10.1016/S0304-4076(96)01818-0

Caron, M. M., Zellweger, F., Verheyen, K., Baeten, L., Hédl, R., Bernhardt-Römermann, M., Berki, I., Brunet, J., Decocq, G., Díaz, S., Dirnböck, T., Durak, T., Heinken, T., Jaroszewicz, B., Kopecký, M., Lenoir, J., Macek, M., Malicki, M., Máliš, F., … De Frenne, P. (2021). Thermal differences between juveniles and adults increased over time in European forest trees. *Journal of Ecology*, *109*(11), 3944–3957. https://doi.org/10.1111/1365-2745.13773

Caudullo, G., De Rigo, D., Mauri, A., Houston Durrant, T., & San-Miguel-Ayanz, J. (2016). *European atlas of forest tree species* (G. Caudullo, D. De Rigo, A. Mauri, T. Houston Durrant, & J. San-

Miguel-Ayanz, Eds.). Publications Office of the European Union. https://doi.org/doi/10.2760/776635

Cerioni, M., Brabec, M., Bače, R., Bāders, E., Bončina, A., Brůna, J., Chećko, E., Cordonnier, T., de Koning, J. H. C., Diaci, J., Dobrowolska, D., Dountchev, A., Engelhart, J., Fidej, G., Fuhr, M., Garbarino, M., Jansons, Ā., Keren, S., Kitenberga, M., … Nagel, T. A. (2024). Recovery and resilience of European temperate forests after large and severe disturbances. *Global Change Biology*, *30*(2), e17159. https://doi.org/10.1111/gcb.17159

Chai, T., & Draxler, R. R. (2014). Root mean square error (RMSE) or mean absolute error (MAE)? – Arguments against avoiding RMSE in the literature. *Geoscientific Model Development*, *7*(3), 1247–1250. https://doi.org/10.5194/gmd-7-1247-2014

Díaz-Yáñez, O., Käber, Y., Anders, T., Bohn, F., Braziunas, K. H., Brůna, J., Fischer, R., Fischer, S. M., Hetzer, J., Hickler, T., Hochauer, C., Lexer, M. J., Lischke, H., Mairota, P., Merganič, J., Merganičová, K., Mette, T., Mina, M., Morin, X., … Bugmann, H. (2024). Tree regeneration in models of forest dynamics: A key priority for further research. *Ecosphere*, *15*(3), e4807. https://doi.org/10.1002/ecs2.4807

Duijnisveld, W. (2015). *Available water capacity in the rooting zone of German soils* [Dataset].

Dyderski, M. K., Paź, S., Frelich, L. E., & Jagodziński, A. M. (2018). How much does climate change threaten European forest tree species distributions? *Global Change Biology*, *24*(3), 1150–1163. https://doi.org/10.1111/gcb.13925

Erdozain, M., Alberdi, I., Aszalós, R., Bollmann, K., Detsis, V., Diaci, J., Đodan, M., Efthimiou, G., Gálhidy, L., Haase, M., Hoffmann, J., Jaymond, D., Johann, E., Jørgensen, H., Krumm, F., Kuuluvainen, T., Lachat, T., Lapin, K., Lindner, M., … de-Miguel, S. (2024). The Evolution of Forest Restoration in Europe: A Synthesis for a Step Forward Based on National Expert Knowledge. *Current Forestry Reports*, *11*(1), 4. https://doi.org/10.1007/s40725-024-00235-3

European Environment Agency. (2016). *European Digital Elevation Model (EU-DEM), version 1.1* [Dataset]. European Environment Agency.

European Environment Agency. (2018a). *Tree Cover Density 2012 (raster 20 m), Europe, 3-yearly, Mar. 2018* [Dataset]. European Environment Agency. https://doi.org/10.2909/91687EF2-F907-4F84-81F7-C9C81980C306

European Environment Agency. (2018b). *Water and Wetness 2015 (raster 20 m), Europe, 3-yearly, Nov. 2020* (Version 07.00) [Dataset]. European Environment Agency. https://doi.org/10.2909/25ED7A97-E3A6-42ED-A403-D636D6880E6D

Falk, W., & Hempelmann, N. (2013). Species Favourability Shift in Europe due to Climate Change: A Case Study for Fagus sylvatica L. and Picea abies (L.) Karst. Based on an Ensemble of Climate Models. *Journal of Climatology*, *2013*, 1–18. https://doi.org/10.1155/2013/787250

Falk, W., Mellert, K., Bachmann-Gigl, U., & Kölling, C. (2013). Bäume für die Zukunft: Baumartenwahl auf wissenschaftlicher Grundlage. *LWF aktuell*, *94*, 8–11.

Falk, W., & Mellert, K. H. (2011). Species distribution models as a tool for forest management planning under climate change: Risk evaluation of Abies alba in Bavaria. *Journal of Vegetation Science*, *22*(4), 621–634. https://doi.org/10.1111/j.1654-1103.2011.01294.x

Falk, W., Thurm, E. A., Mette, T., Schuster, O., & Klemmt, H.-J. (2019). Anbaurisiko-Karten für nichtheimische Baumarten. *LWF aktuell*, *123*, 23–27.

Fischer, H., Huth, F., Hagemann, U., & Wagner, S. (2016). Developing restoration strategies for temperate forests using natural regeneration processes. In *Restoration of Boreal and Temperate Forests* (pp. 103–164). CRC Press.

George, J.-P., Bürkner, P.-C., Sanders, T. G. M., Neumann, M., Cammalleri, C., Vogt, J. V., & Lang, M. (2022). Long-term forest monitoring reveals constant mortality rise in European forests. *Plant Biology*, *24*(7), 1108–1119. https://doi.org/10.1111/plb.13469

Gschwantner, T., Alberdi, I., Bauwens, S., Bender, S., Borota, D., Bosela, M., Bouriaud, O., Breidenbach, J., Donis, J., Fischer, C., Gasparini, P., Heffernan, L., Hervé, J.-C., Kolozs, L., Korhonen, K. T., Koutsias, N., Kovácsevics, P., Kučera, M., Kulbokas, G., … Tomter, S. M. (2022). Growing stock monitoring by European National Forest Inventories: Historical origins, current

methods and harmonisation. *Forest Ecology and Management*, *505*, 119868. https://doi.org/10.1016/j.foreco.2021.119868

Gschwantner, T., Schodterer, H., Kainz, C., & Freudenschuß, A. (2024). Regeneration of the Austrian forests and browsing impact – Insights from the latest National Forest Inventory. *Central European Forestry Journal*, *70*(4), 235–247. https://doi.org/10.2478/forj-2024-0010

Haesen, S., Lembrechts, J. J., De Frenne, P., Lenoir, J., Aalto, J., Ashcroft, M. B., Kopecký, M., Luoto, M., Maclean, I., Nijs, I., Niittynen, P., Van Den Hoogen, J., Arriga, N., Brůna, J., Buchmann, N., Čiliak, M., Collalti, A., De Lombaerde, E., Descombes, P., … Van Meerbeek, K. (2023). ForestClim—Bioclimatic variables for microclimate temperatures of European forests. *Global Change Biology*, *29*(11), 2886–2892. https://doi.org/10.1111/gcb.16678

Hanbury-Brown, A. R., Ward, R. E., & Kueppers, L. M. (2022). Forest regeneration within Earth system models: Current process representations and ways forward. *The New Phytologist*, *235*(1), 20–40. https://doi.org/10.1111/nph.18131

Hanewinkel, M., Cullmann, D. A., Schelhaas, M.-J., Nabuurs, G.-J., & Zimmermann, N. E. (2013). Climate change may cause severe loss in the economic value of European forest land. *Nature Climate Change*, *3*(3), 203–207. https://doi.org/10.1038/nclimate1687

Harris, L. B., Woodall, C. W., & D'Amato, A. W. (2024). Relationships between juvenile tree survival and tree density, shrub cover and temperature vary by size class based on ratios of abundance. *Canadian Journal of Forest Research*, *54*(2), 122–133. https://doi.org/10.1139/cjfr-2023-0097

Hartig, F. (2022). *DHARMa: Residual Diagnostics for Hierarchical (Multi-Level / Mixed) Regression Models* (Version 0.4.6) [Computer software]. https://CRAN.R-project.org/package=DHARMa

Hasenauer, H., Kindermann, G., & Merkl, D. (2000). Zur Schätzung der Verjüngungssituation in Mischbeständen mit Hilfe Neuraler Netze. *Forstwissenschaftliches Centralblatt vereinigt mit Tharandter forstliches Jahrbuch*, *119*(1), 350–366. https://doi.org/10.1007/BF02769149

Heiland, L., Kunstler, G., Ruiz–Benito, P., Buras, A., Dahlgren, J., & Hülsmann, L. (2022). Divergent occurrences of juvenile and adult trees are explained by both environmental change and ontogenetic effects. *Ecography*, *2022*(3). https://doi.org/10.1111/ecog.06042

Hennig, P. (2022). *Informationen zur Nutzung / Weitergabe anonymisierter Trakt-Koordinaten der Bundeswaldinventur*. Thünen-Institut. https://bwi.info/Download/de/BWI-Basisdaten/_Hinweise_BWI-Koordinaten.pdf

Hernández, L., Cañellas, I., Alberdi, I., Torres, I., & Montes, F. (2014). Assessing changes in species distribution from sequential large-scale forest inventories. *Annals of Forest Science*, *71*(2), Article 2. https://doi.org/10.1007/s13595-013-0308-6

Hijmans, R. J. (2024). *terra: Spatial Data Analysis* (Version 1.7.78) [Computer software]. https://CRAN.R-project.org/package=terra

Hillebrand, L., Marzini, S., Crespi, A., Hiltner, U., & Mina, M. (2023). Contrasting impacts of climate change on protection forests of the Italian Alps. *Frontiers in Forests and Global Change*, *6*. https://doi.org/10.3389/ffgc.2023.1240235

Huth, F., Tischer, A., Nikolova, P., Feldhaar, H., Wehnert, A., Hülsmann, L., Bauhus, J., Heer, K., Vogt, J., Ammer, C., Berger, U., Bernhardt-Römermann, M., Böhme, M., Bugmann, H., Buse, J., Demant, L., Dörfler, I., Ewald, J., Feldmann, E., … Schuldt, B. (2025). Ecological assessment of forest management approaches to develop resilient forests in the face of global change in Central Europe. *Basic and Applied Ecology*. https://doi.org/10.1016/j.baae.2025.05.001

Jactel, H., Bauhus, J., Boberg, J., Bonal, D., Castagneyrol, B., Gardiner, B., Gonzalez-Olabarria, J. R., Koricheva, J., Meurisse, N., & Brockerhoff, E. G. (2017). Tree Diversity Drives Forest Stand Resistance to Natural Disturbances. *Current Forestry Reports*, *3*(3), 223–243. https://doi.org/10.1007/s40725-017-0064-1

Jones, R. J. A., Hiederer, R., Rusco, E., & Montanarella, L. (2005). Estimating organic carbon in the soils of Europe for policy support. *European Journal of Soil Science*, *56*(5), 655–671. https://doi.org/10.1111/j.1365-2389.2005.00728.x

Karger, D. N., Conrad, O., Böhner, J., Kawohl, T., Kreft, H., Soria-Auza, R. W., Zimmermann, N. E., Linder, H. P., & Kessler, M. (2017). Climatologies at high resolution for the earth's land surface areas. *Scientific Data*, *4*(1), 170122. https://doi.org/10.1038/sdata.2017.122

Karger, D. N., Conrad, O., Böhner, J., Kawohl, T., Kreft, H., Soria-Auza, R. W., Zimmermann, N. E., Linder, H. P., & Kessler, M. (2018). *Data from: Climatologies at high resolution for the earth's land surface areas* (Version 1, p. 7266970904 bytes) [Dataset]. Dryad. https://doi.org/10.5061/DRYAD.KD1D4

Klemmt, H.-J., Neubert, M., & Mößnang, M. (2014). *Nachhaltig und naturnah: Wald und Forstwirtschaft in Bayern Ergebnisse der dritten Bundeswaldinventur Eine Broschüre* (Bayerische Landesanstalt für Wald und Forstwirtschaft, Ed.).

Kolo, H., Ankerst, D., & Knoke, T. (2017). Predicting natural forest regeneration: A statistical model based on inventory data. *European Journal of Forest Research*, *136*(5–6), 923–938. https://doi.org/10.1007/s10342-017-1080-1

König, L. A., Mohren, F., Schelhaas, M.-J., Astigarraga, J., Cienciala, E., Flury, R., Fridman, J., Govaere, L., Lehtonen, A., Muelbert, A. E., Pugh, T. A. M., Rohner, B., Ruiz-Benito, P., Suvanto, S., Talarczyk, A., Zavala, M. A., Vega, J. M., Staritsky, I., Hengeveld, G., & Nabuurs, G.-J. (2025). Combining national forest inventories reveals distinct role of climate on tree recruitment in European forests. *Ecological Modelling*, *505*, 111112. https://doi.org/10.1016/j.ecolmodel.2025.111112

König, L. A., Mohren, F., Schelhaas, M.-J., Bugmann, H., & Nabuurs, G.-J. (2022). Tree regeneration in models of forest dynamics – Suitability to assess climate change impacts on European forests. *Forest Ecology and Management*, *520*, 120390. https://doi.org/10.1016/j.foreco.2022.120390

Kupferschmid, A. D., Bütikofer, L., Hothorn, T., Schwyzer, A., & Brang, P. (2019). Quantifying the relative influence of terminal shoot browsing by ungulates on tree regeneration. *Forest Ecology and Management*, *446*, 331–344. https://doi.org/10.1016/j.foreco.2019.05.009

Lackner, C., Schreck, M., & Walli. (2023). *Österreichischer Waldbericht 2023*. Bundesministerium für Land- und Forstwitschaft, Regionen und Wasserwirtschaft.

Langner, N., Oehmichen, K., Henning, L., Blickensdörfer, L., & Riedel, T. (2022). *Bestockte Holzbodenkarte 2018*. Johann Heinrich von Thünen-Institut. https://doi.org/10.3220/DATA20221205151218

Lima, J. S., Lenoir, J., & Hylander, K. (2024). Potential migration pathways of broadleaved trees across the receding boreal biome under future climate change. *Global Change Biology*, *30*(8), e17471. https://doi.org/10.1111/gcb.17471

Lindner, M., Seidl, R., Grünig, M., Bauhus, J., Willig, J., Hlásny, T., Nabuurs, G.-J., Patacca, M., Peltoniemi, M., Espelta, J.-M., Picos, J., Hoeben, A., Cantarello, E., & Schifferdecker, G. (2025). *Managing Forest Disturbances in a Changing Climate*. European Forest Institute. https://doi.org/10.36333/rs9

Löf, M., Ammer, C., Coll, L., Drössler, L., Huth, F., Madsen, P., & Wagner, S. (2018). Regeneration Patterns in Mixed-Species Stands. In A. Bravo-Oviedo, H. Pretzsch, & M. del Río (Eds.), *Dynamics, Silviculture and Management of Mixed Forests* (pp. 103–130). Springer International Publishing. https://doi.org/10.1007/978-3-319-91953-9_4

Löf, M., Madsen, P., Metslaid, M., Witzell, J., & Jacobs, D. F. (2019). Restoring forests: Regeneration and ecosystem function for the future. *New Forests*, *50*(2), 139–151. https://doi.org/10.1007/s11056-019-09713-0

Mages, M., Müller, K., & Schwarz, D. (2020). *Waldbauhandbuch Bayerische Staatsforsten, Richtlinie zur Baumartenwahl.* (WNJF-RL-007; p. 9). Bayerische Staatsforsten.

Martinez del Castillo, E., Zang, C. S., Buras, A., Hacket-Pain, A., Esper, J., Serrano-Notivoli, R., Hartl, C., Weigel, R., Klesse, S., Resco de Dios, V., Scharnweber, T., Dorado-Liñán, I., van der Maaten-Theunissen, M., van der Maaten, E., Jump, A., Mikac, S., Banzragch, B.-E., Beck, W., Cavin, L., … de Luis, M. (2022). Climate-change-driven growth decline of European beech forests. *Communications Biology*, *5*(1), 1–9. https://doi.org/10.1038/s42003-022-03107-3

Martini, F., Buechling, A., Bače, R., Hofmeister, J., Janda, P., Matula, R., & Svoboda, M. (2024). Biotic and abiotic effects on tree regeneration vary by life stage in European primary forests. *Oikos*. https://doi.org/10.1111/oik.10755

McRoberts, R. E., Chirici, G., Winter, S., Barbati, A., Corona, P., Marchetti, M., Hauk, E., Brändli, U.-B., Beranova, J., Rondeux, J., Sanchez, C., Bertini, R., Barsoum, N., Asensio, I. A., Condés, S., Saura, S., Neagu, S., Cluzeau, C., & Hamza, N. (2011). Prospects for Harmonized Biodiversity Assessments Using National Forest Inventory Data. In G. Chirici, S. Winter, & R. E. McRoberts (Eds.), *National Forest Inventories: Contributions to Forest Biodiversity Assessments* (pp. 41–97). Springer Netherlands. https://doi.org/10.1007/978-94-007-0482-4_3

Moos, C., Guisan, A., Randin, C. F., & Lischke, H. (2021). Climate Change Impacts the Protective Effect of Forests: A Case Study in Switzerland. *Frontiers in Forests and Global Change*, *4*. https://doi.org/10.3389/ffgc.2021.682923

Mori, A. S., Dee, L. E., Gonzalez, A., Ohashi, H., Cowles, J., Wright, A. J., Loreau, M., Hautier, Y., Newbold, T., Reich, P. B., Matsui, T., Takeuchi, W., Okada, K., Seidl, R., & Isbell, F. (2021). Biodiversity–productivity relationships are key to nature-based climate solutions. *Nature Climate Change*, *11*(6), 543–550. https://doi.org/10.1038/s41558-021-01062-1

Pebesma, E., Bivand, R., Racine, E., Sumner, M., Cook, I., Keitt, T., Lovelace, R., Wickham, H., Ooms, J., Müller, K., Pedersen, T. L., Baston, D., & Dunnington, D. (2024). *sf: Simple Features for R* (Version 1.0-16) [Computer software]. https://cran.r-project.org/web/packages/sf/index.html

Pichler, M., & Hartig, F. (2023). Machine learning and deep learning—A review for ecologists. *Methods in Ecology and Evolution*, *14*(4), 994–1016. https://doi.org/10.1111/2041-210X.14061

Potočić, N., Timmermann, V., Ognjenović, M., Kirchner, T., Prescher, A.-K., & Ferretti, M. (2021). *Tree health is deteriorating in the European forests*. Johann Heinrich von Thünen-Institut. https://doi.org/10.3220/ICP1638780772000

Price, D. T., Zimmermann, N. E., van der Meer, P. J., Lexer, M. J., Leadley, P., Jorritsma, I. T. M., Schaber, J., Clark, D. F., Lasch, P., McNulty, S., Wu, J., & Smith, B. (2001). Regeneration in Gap Models: Priority Issues for Studying Forest Responses to Climate Change. *Climatic Change*, *51*(3), 475–508. https://doi.org/10.1023/A:1012579107129

R Core Team. (2024). *R: A Language and Environment for Statistical Computing* (Version 4.4.1) [Computer software]. R Foundation for Statistical Computing. https://www.R-project.org/

Riedel, T., Hennig, P., Kroiher, F., Polley, H., Schmitz, F., & Schwitzgebel, F. (2017). *Die dritte Bundeswaldinventur (BWI 2012): Inventur- und Auswertungsmethoden*. Johann Heinrich von Thünen-Institut.

Rigling, A., & Schaffer, H. P. (2015). *Waldbericht 2015. Zustand und Nutzung des Schweizer Waldes.* Bundesamt für Umwelt.

Royo, A., & Carson, W. P. (2006). On the formation of dense understory layers in forests worldwide: Consequences and implications for forest dynamics, biodiversity, and succession. *Canadian Journal of Forest Research*, *36*, 1345–1362. https://doi.org/10.1139/X06-025

Schaap, M., Hendriks, C., Kranenburg, R., Kuenen, J., Segers, A., Schlutow, A., Nagel, H.-D., Ritter, A., & Banzhaf, S. (2018). *PINETI-3: Modellierung atmosphärischer Stoffeinträge von 2000 bis 2015 zur Bewertung der ökosystem-spezifischen Gefährdung von Biodiversität durch Luftschadstoffe in Deutschland*. Umweltbundesamt.

Sebald, J., Thrippleton, T., Rammer, W., Bugmann, H., & Seidl, R. (2021). Mixing tree species at different spatial scales: The effect of alpha, beta and gamma diversity on disturbance impacts under climate change. *Journal of Applied Ecology*, *58*(8), 1749–1763. https://doi.org/10.1111/1365-2664.13912

Seidl, R., Potterf, M., Müller, J., Turner, M. G., & Rammer, W. (2024). Patterns of early post-disturbance reorganization in Central European forests. *Proceedings of the Royal Society B: Biological Sciences*, *291*(2031), 20240625. https://doi.org/10.1098/rspb.2024.0625

Seidl, R., & Turner, M. G. (2022). Post-disturbance reorganization of forest ecosystems in a changing world. *Proceedings of the National Academy of Sciences of the United States of America*, *119*(28), e2202190119. https://doi.org/10.1073/pnas.2202190119

Senf, C., Buras, A., Zang, C. S., Rammig, A., & Seidl, R. (2020). Excess forest mortality is consistently linked to drought across Europe. *Nature Communications*, *11*(1), 6200. https://doi.org/10.1038/s41467-020-19924-1

Senf, C., & Seidl, R. (2021). Persistent impacts of the 2018 drought on forest disturbance regimes in Europe. *Biogeosciences*, *18*(18), 5223–5230. https://doi.org/10.5194/bg-18-5223-2021

Shoemaker, L. G., Sullivan, L. L., Donohue, I., Cabral, J. S., Williams, R. J., Mayfield, M. M., Chase, J. M., Chu, C., Harpole, W. S., Huth, A., HilleRisLambers, J., James, A. R. M., Kraft, N. J. B., May, F., Muthukrishnan, R., Satterlee, S., Taubert, F., Wang, X., Wiegand, T., … Abbott, K. C. (2020). Integrating the underlying structure of stochasticity into community ecology. *Ecology*, *101*(2), e02922. https://doi.org/10.1002/ecy.2922

Thom, D., Ammer, C., Annighöfer, P., Aszalós, R., Dittrich, S., Hagge, J., Keeton, W. S., Kovacs, B., Krautkrämer, O., Müller, J., von Oheimb, G., & Seidl, R. (2023). Regeneration in European beech forests after drought: The effects of microclimate, deadwood and browsing. *European Journal of Forest Research*, *142*(2), 259–273. https://doi.org/10.1007/s10342-022-01520-1

Thonfeld, F., Gessner, U., Holzwarth, S., Kriese, J., Da Ponte, E., Huth, J., & Kuenzer, C. (2022). A First Assessment of Canopy Cover Loss in Germany's Forests after the 2018–2020 Drought Years. *Remote Sensing*, *14*(3), 562. https://doi.org/10.3390/rs14030562

Thünen-Institut. (2015). *Dritte Bundeswaldinventur—Basisdaten* (Version Stand 20.03.2015) [Dataset].

Thurm, E. A., Hernandez, L., Baltensweiler, A., Ayan, S., Rasztovits, E., Bielak, K., Zlatanov, T. M., Hladnik, D., Balic, B., Freudenschuss, A., Büchsenmeister, R., & Falk, W. (2018). Alternative tree species under climate warming in managed European forests. *Forest Ecology and Management*, *430*, 485–497. https://doi.org/10.1016/j.foreco.2018.08.028

Trabucco, A., & Zomer, R. (2019). *Global Aridity Index and Potential Evapotranspiration (ET0) Climate Database v2* [Dataset]. figshare. https://doi.org/10.6084/M9.FIGSHARE.7504448.V2

Valavi, R., Elith, J., Lahoz-Monfort, J., Flint, I., & Guillera-Arroita, G. (2024). *blockCV: Spatial and Environmental Blocking for K-Fold and LOO Cross-Validation* (Version 3.1.4) [Computer software]. https://cran.r-project.org/web/packages/blockCV/

Valavi, R., Elith, J., Lahoz-Monfort, J. J., & Guillera-Arroita, G. (2019). blockCV: An R package for generating spatially or environmentally separated folds for k-fold cross-validation of species distribution models. *Methods in Ecology and Evolution*, *10*(2), 225–232. https://doi.org/10.1111/2041-210X.13107

Vayreda, J., Gracia, M., Martinez-Vilalta, J., & Retana, J. (2013). Patterns and drivers of regeneration of tree species in forests of peninsular Spain. *Journal of Biogeography*, *40*(7), 1252–1265. https://doi.org/10.1111/jbi.12105

Viana-Soto, A., & Senf, C. (2024). The European Forest Disturbance Atlas: A forest disturbance monitoring system using the Landsat archive. *Earth System Science Data Discussions*, 1–42. https://doi.org/10.5194/essd-2024-361

Wood, S. N. (2017). *Generalized Additive Models: An Introduction with R, Second Edition* (2nd ed.). Chapman and Hall/CRC. https://doi.org/10.1201/9781315370279

Wood, S. N. (2023). *mgcv: Mixed GAM Computation Vehicle with Automatic Smoothness Estimation* (Version 1.9.1, p. 1.9-1) [Computer software]. https://CRAN.R-project.org/package=mgcv

Wood, S. N., Goude, Y., & Shaw, S. (2015). Generalized Additive Models for Large Data Sets. *Journal of the Royal Statistical Society Series C: Applied Statistics*, *64*(1), 139–155. https://doi.org/10.1111/rssc.12068

Wood, S. N., Pya, N., & Säfken, B. (2016). Smoothing Parameter and Model Selection for General Smooth Models. *Journal of the American Statistical Association*, *111*(516), 1548–1563. https://doi.org/10.1080/01621459.2016.1180986

Xu, W., Luo, D., Peterson, K., Zhao, Y., Yu, Y., Ye, Z., Sun, J., Yan, K., & Wang, T. (2025). Advancements in ecological niche models for forest adaptation to climate change: A comprehensive review. *Biological Reviews*. https://doi.org/10.1111/brv.70023

Zhu, K., Woodall, C. W., Ghosh, S., Gelfand, A. E., & Clark, J. S. (2014). Dual impacts of climate change: Forest migration and turnover through life history. *Global Change Biology*, *20*(1), 251–264. https://doi.org/10.1111/gcb.12382

Supplementary Material

Table S1: Spatial autocorrelation of each calibrated model and set up for spatially blocked cross-validation. Spatial autocorrelation of the model was assessed by using the R-package DHARMa (Hartig, 2022) and spatial autocorrelation range of the response was calculated with the package blockCV (Valavi et al., 2019, 2024).

Species	**Model spatial autocorrelation**			**Spatially blocked cross-validation**		
	Observed Morans I	**p-value**		**Spatial autocorrelation range [m]**	**Used spatial range [m]**	**Block number**
Abies alba	-0.00019	0.32	n.s.	2,502	2,502	16,616
Abies grandis	-0.00030	0.08	n.s.	5,682	5,683	8,645
Acer campestre	-0.00013	0.60	n.s.	39,754	39,754	303
Acer platanoides	-0.00028	0.10	n.s.	71,751	71,752	108
Acer pseudoplatanus	-0.00017	0.42	n.s.	24,913	24,914	732
Alnus glutinosa	-0.00012	0.66	n.s.	41,710	41,710	279
Alnus incana	-0.00021	0.25	n.s.	9,450	9,450	4,163
Betula pendula	-0.00035	0.03	*	13,295,247	300,000	11
Betula pubescens	-0.00035	0.03	*	3,078,096	300,000	11
Carpinus betulus	0.00003	0.54	n.s.	31,648	31,649	465
Castanea sativa	-0.00014	0.53	n.s.	531	532	18,181
Fagus sylvatica	-0.00003	0.87	n.s.	51,183	51,184	191
Fraxinus excelsior	-0.00030	0.07	n.s.	50,850	50,851	193
Larix decidua	-0.00032	0.05	n.s.	224,055	224,056	16
Larix kaempferi	-0.00009	0.80	n.s.	20,003,371	300,000	11
Malus sylvestris						
Picea abies	-0.00004	0.92	n.s.	104,926	104,927	58
Picea sitchensis	-0.00029	0.08	n.s.	466,836	300,000	11
Pinus mugo						
Pinus nigra	-0.00015	0.50	n.s.	15,141	15,142	1,822
Pinus strobus	-0.00024	0.18	n.s.	6,477,058	300,000	11
Pinus sylvestris	-0.00007	0.89	n.s.	110,621	110,621	52
Populus alba	0.00006	0.42	n.s.	10,705	10,706	3,368
Populus nigra	-0.00017	0.41	n.s.	42,140	42,141	269
Populus tremula	-0.00015	0.50	n.s.	74,889	74,890	99
Populus trichocarpa x maximoviczii	-0.00011	0.66	n.s.	1,854,565	300,000	11
Populus x canescens	-0.00008	0.88	n.s.	47,026	47,026	220
Prunus avium	-0.00002	0.82	n.s.	29,395	29,395	535
Prunus padus	-0.00020	0.29	n.s.	17,820	17,821	1,367
Prunus serotina	-0.00011	0.67	n.s.	103,071	103,072	59
Pseudotsuga menziesii	-0.00012	0.63	n.s.	104,926	104,927	58
Pyrus communis						
Quercus petraea	-0.00035	0.03	*	240,624	240,625	15
Quercus robur	-0.00014	0.53	n.s.	77,579	77,580	94
Quercus rubra	-0.00018	0.36	n.s.	10,775	10,776	3,348
Robinia pseudoacacia	-0.00017	0.39	n.s.	105,582	105,583	56
Salix spp.	-0.00024	0.18	n.s.	26,742	26,742	640
Sorbus aria	-0.00012	0.64	n.s.	10,119	10,120	3,721
Sorbus aucuparia	-0.00012	0.63	n.s.	15,991,026	300,000	11
Sorbus torminalis						
Taxus baccata						
Tilia spp.	-0.00038	0.02	*	30,387	30,388	500
Ulmus spp.	-0.00007	0.94	n.s.	27,193	27,193	616

Table S2: Forest regeneration densities per tree species from the German national forest inventory of 2012. The availability of predicted regeneration density maps is indicated by a dot (available) or a circle (not available).

Species	**Density proportion [%]**	**Mean [#/ha]**	**SD [#/ha]**	**Map availability**
Fagus sylvatica	29.9	1052	5085	●
Picea abies	16.9	594	3546	●
Acer pseudoplatanus	8.7	305	2481	○
Fraxinus excelsior	7.0	245	2121	●
Sorbus aucuparia	6.8	240	1617	○
Carpinus betulus	4.2	148	1686	●
Betula pendula	4.0	140	1668	○
Pinus sylvestris	3.8	132	1380	●
Prunus serotina	3.5	124	1467	●
Abies alba	2.3	81	931	●
Quercus robur	1.6	56	582	●
Quercus petraea	1.4	48	1022	○
Populus tremula	1.2	41	804	○
Prunus padus	1.1	40	849	○
Tilia spp.	0.9	32	511	●
Salix spp.	0.8	29	637	○
Acer campestre	0.6	22	407	●
Acer platanoides	0.6	22	593	●
Pseudotsuga menziesii	0.6	21	569	●
Alnus glutinosa	0.6	20	477	●
Alnus incana	0.6	19	651	●
Ulmus spp.	0.5	19	366	○
Prunus avium	0.5	19	341	●
Betula pubescens	0.4	15	437	●
Quercus rubra	0.4	13	364	●
Robinia pseudoacacia	0.3	9	243	●
Larix decidua	0.1	5	126	○
Sorbus aria	0.1	4	143	●
Pinus strobus	<0.1	3	131	○
Larix kaempferi	<0.1	3	108	●
Picea sitchensis	<0.1	2	126	○
Pinus mugo	<0.1	2	147	○
Populus nigra	<0.1	2	164	●
Populus trichocarpa x maximoviczii	<0.1	2	226	○
Castanea sativa	<0.1	2	94	●
Sorbus torminalis	<0.1	2	76	○
Pinus nigra	<0.1	1	77	○
Populus x canescens	<0.1	1	70	○
Pyrus communis	<0.1	1	38	○
Malus sylvestris	<0.1	0	24	○
Abies grandis	<0.1	0	30	○
Taxus baccata	<0.1	0	19	○
Populus alba	<0.1	0	37	○
Sorbus domestica	0.0	0	0	○

Table S3: Proportion of regeneration in Bavaria at high cultivation risk for 17 tree species.

Species	**Regeneration at high cultivation risk [%]**
Abies alba	0.49
Acer campestre	<0.01
Acer platanoides	<0.01
Alnus glutinosa	0.26
Carpinus betulus	<0.01
Castanea sativa	<0.01
Fagus sylvatica	<0.01
Fraxinus excelsior	<0.01
Larix kaempferi	<0.01
Picea abies	94.48
Pinus sylvestris	4.52
Prunus avium	0.19
Pseudotsuga menziesii	0.01
Quercus robur	<0.01
Quercus rubra	0.02
Robinia pseudoacacia	<0.01
Tilia spp.	<0.01

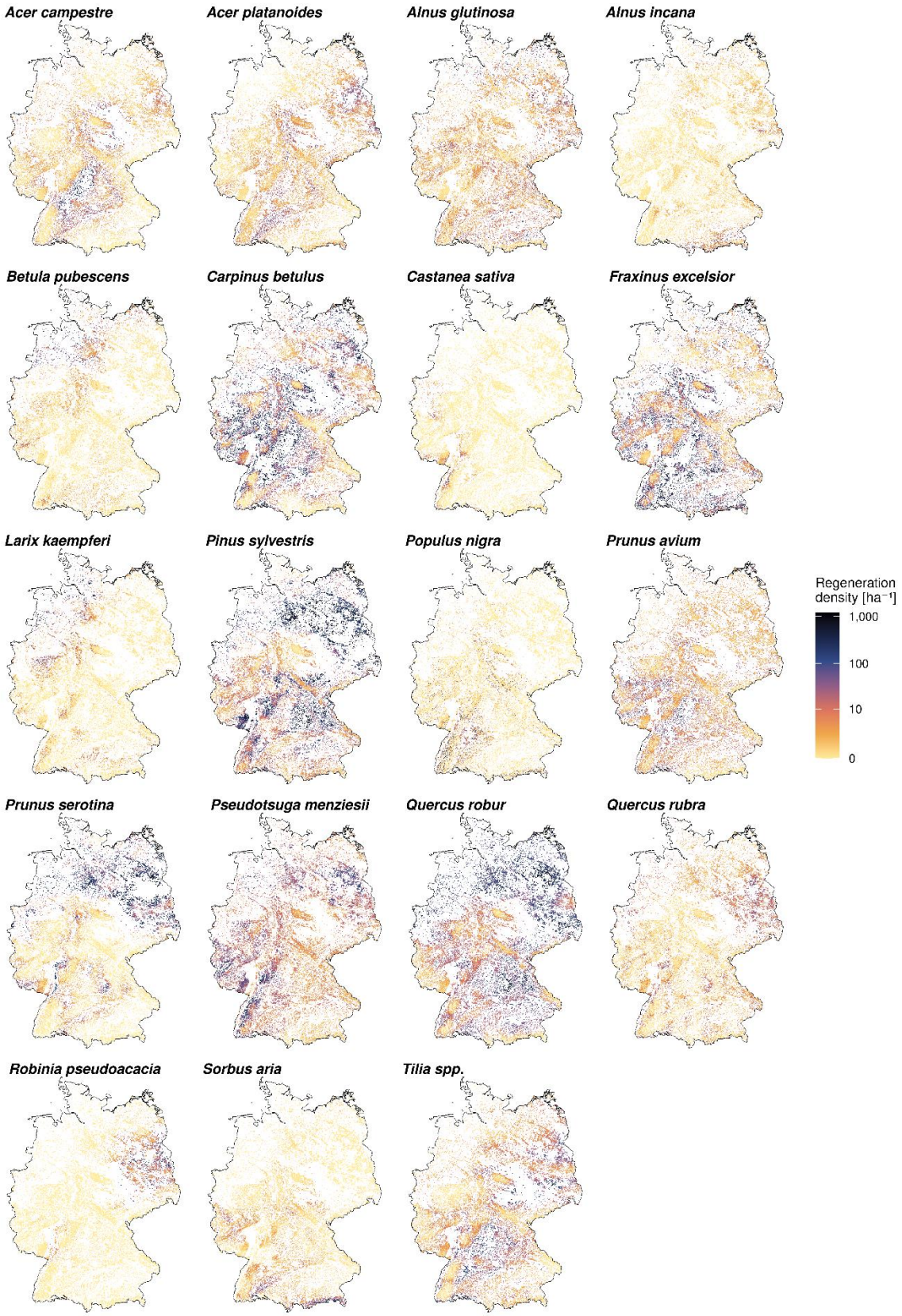

Figure S1: Total regeneration density maps of remaining tree species not displayed in **Error! Reference source not found.**. Regeneration density scale was cut off at the 99% percentile across all species map values (1,186 ha^{-1}). All maps are available online at https://easi.users.earthengine.app/view/regeneration-maps and available for download at https://doi.org/10.5281/zenodo.15550864. Map lines delineate study areas and do not necessarily depict accepted national boundaries.

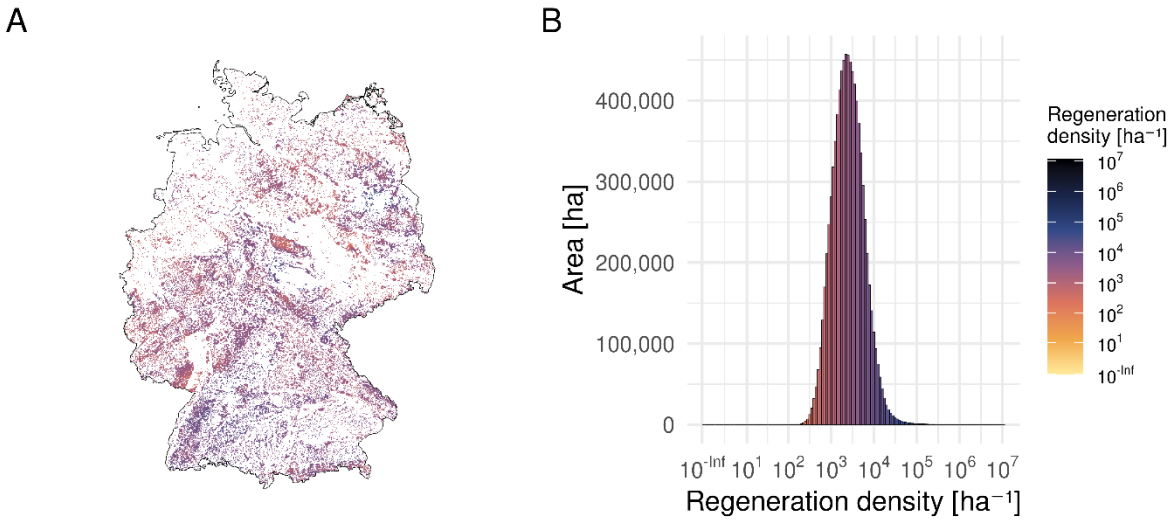

Figure S2: Spatial patterns of total regeneration density (ha^{-1}) for Germany based on 22 tree species. Map lines delineate study areas and do not necessarily depict accepted national boundaries.

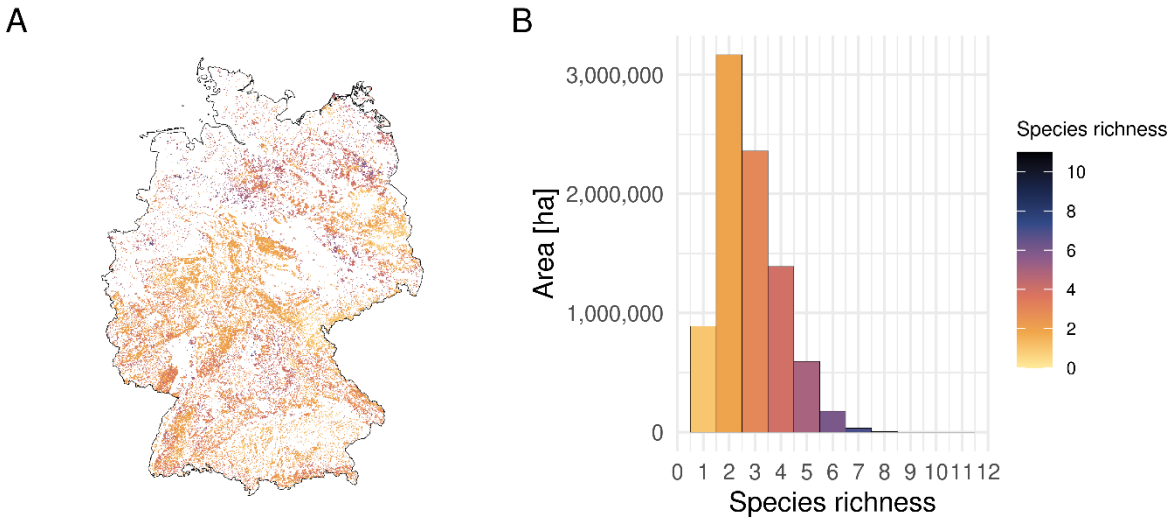

Figure S3: Regeneration tree species richness for the forest area of Germany based on 22 tree species. The map (A) shows spatial patterns, and the histogram (B) describes the distribution of species richness occurrence. We considered a species present in a 1 ha-grid cell if its density was at least 5% of the total regeneration density. Map lines delineate study areas and do not necessarily depict accepted national boundaries.

DHARMa residual

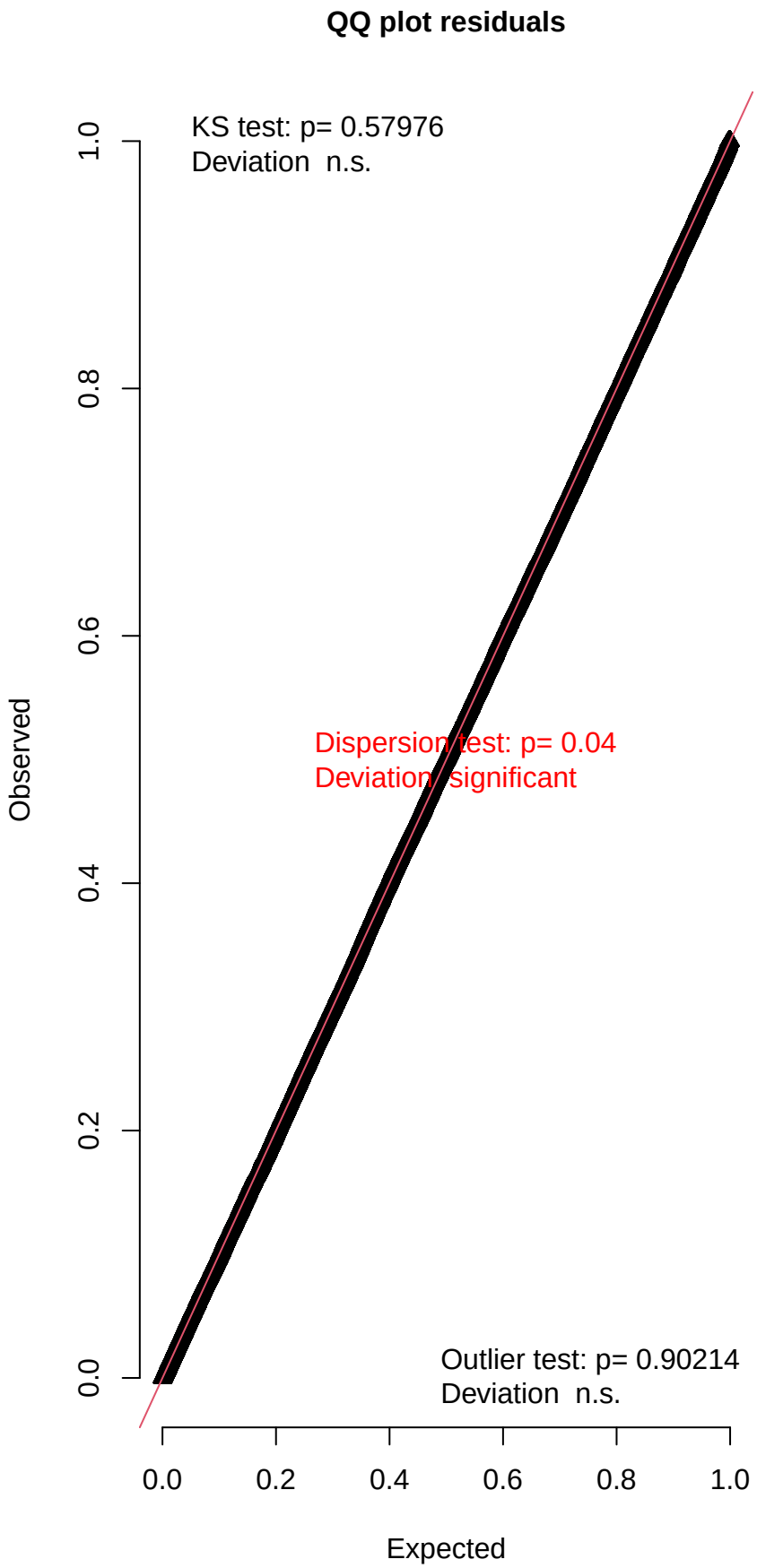

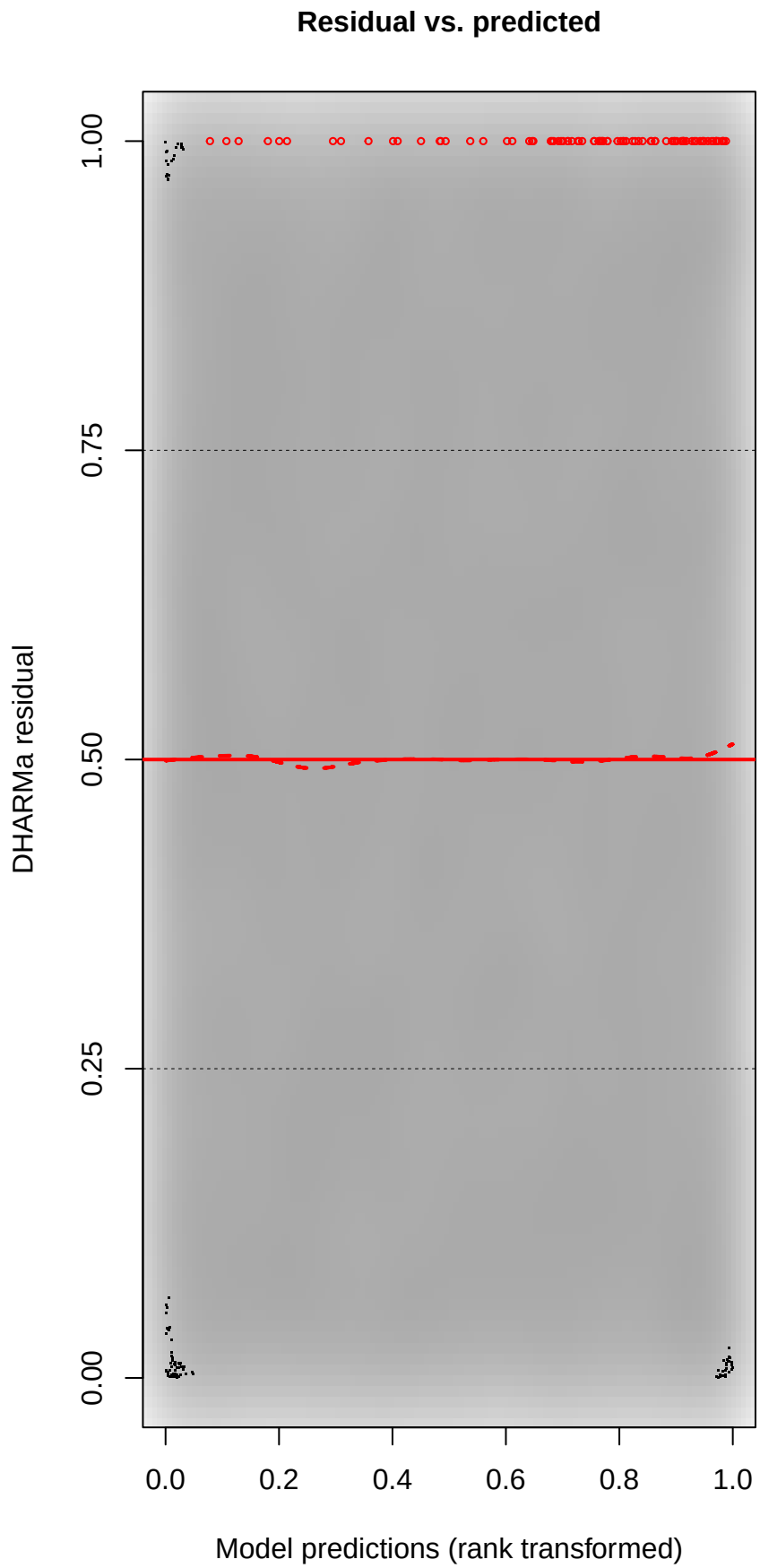

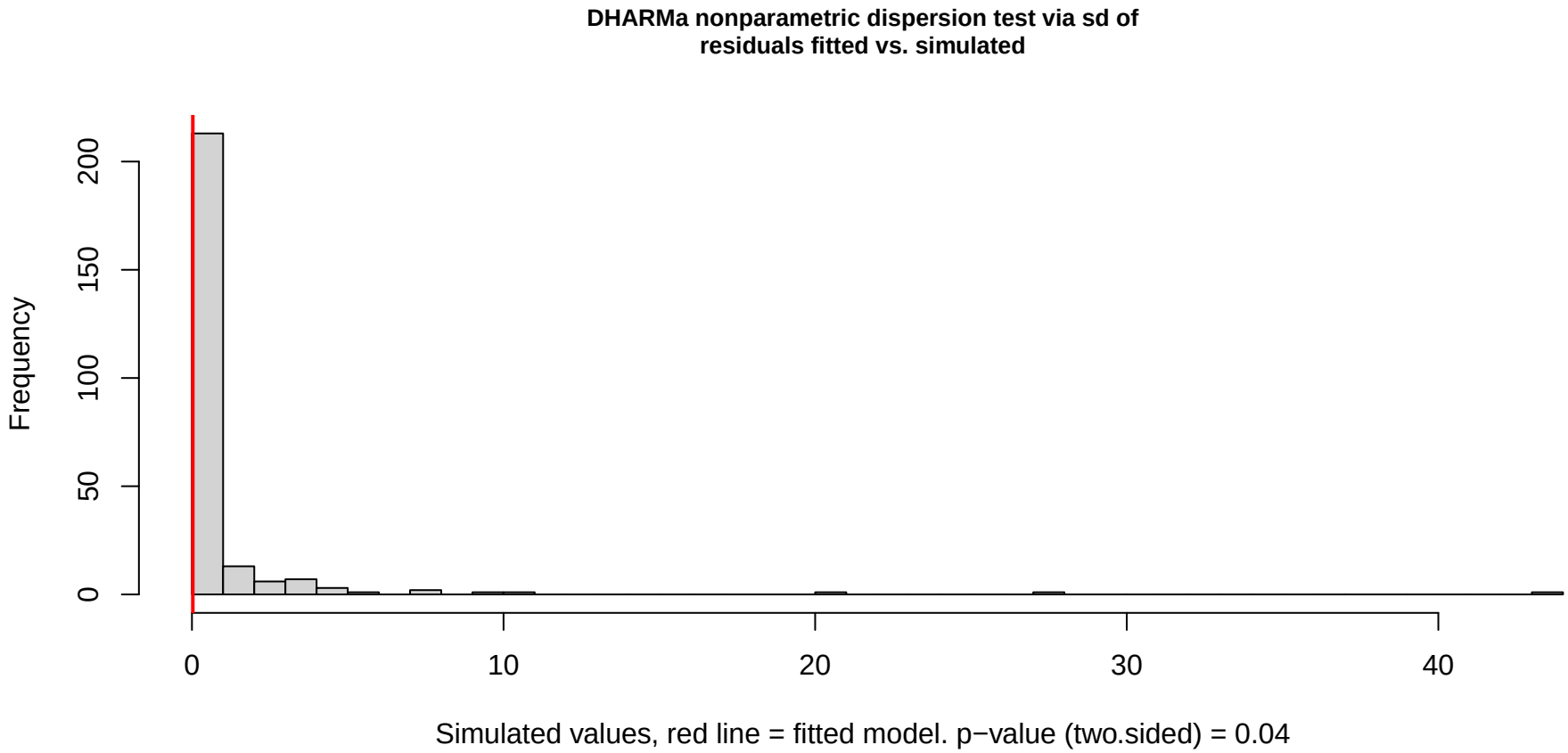
DHARMa nonparametric dispersion test via sd of residuals fitted vs. simulated
Frequency
0
50
100
150
200
0
10
20
30
40
Simulated values, red line = fitted model. p−value (two.sided) = 0.04

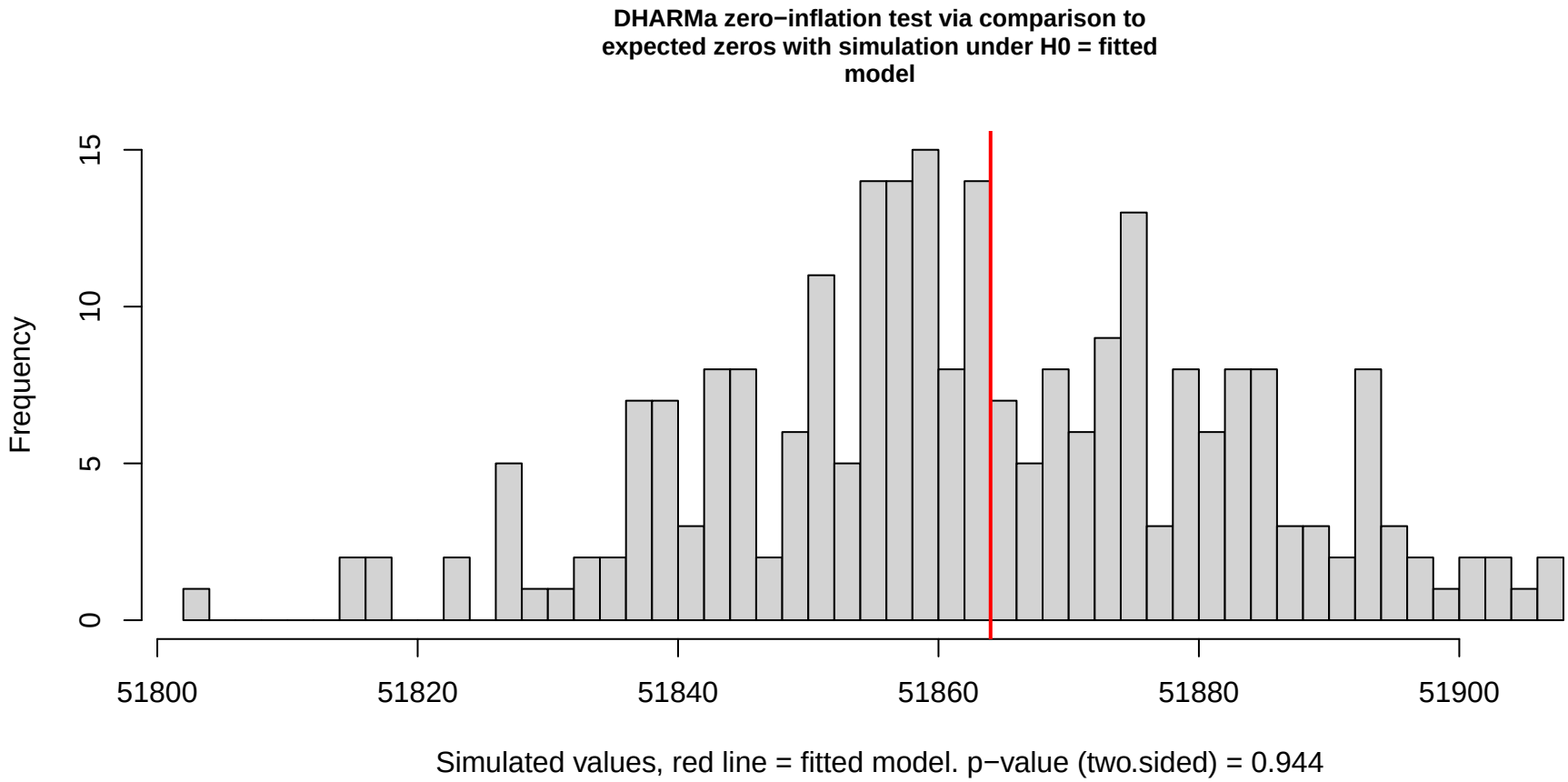
DHARMa zero−inflation test via comparison to expected zeros with simulation under H0 = fitted model
Frequency
0
5
10
15
51800
51820
51840
51860
51880
51900
Simulated values, red line = fitted model. p−value (two.sided) = 0.944

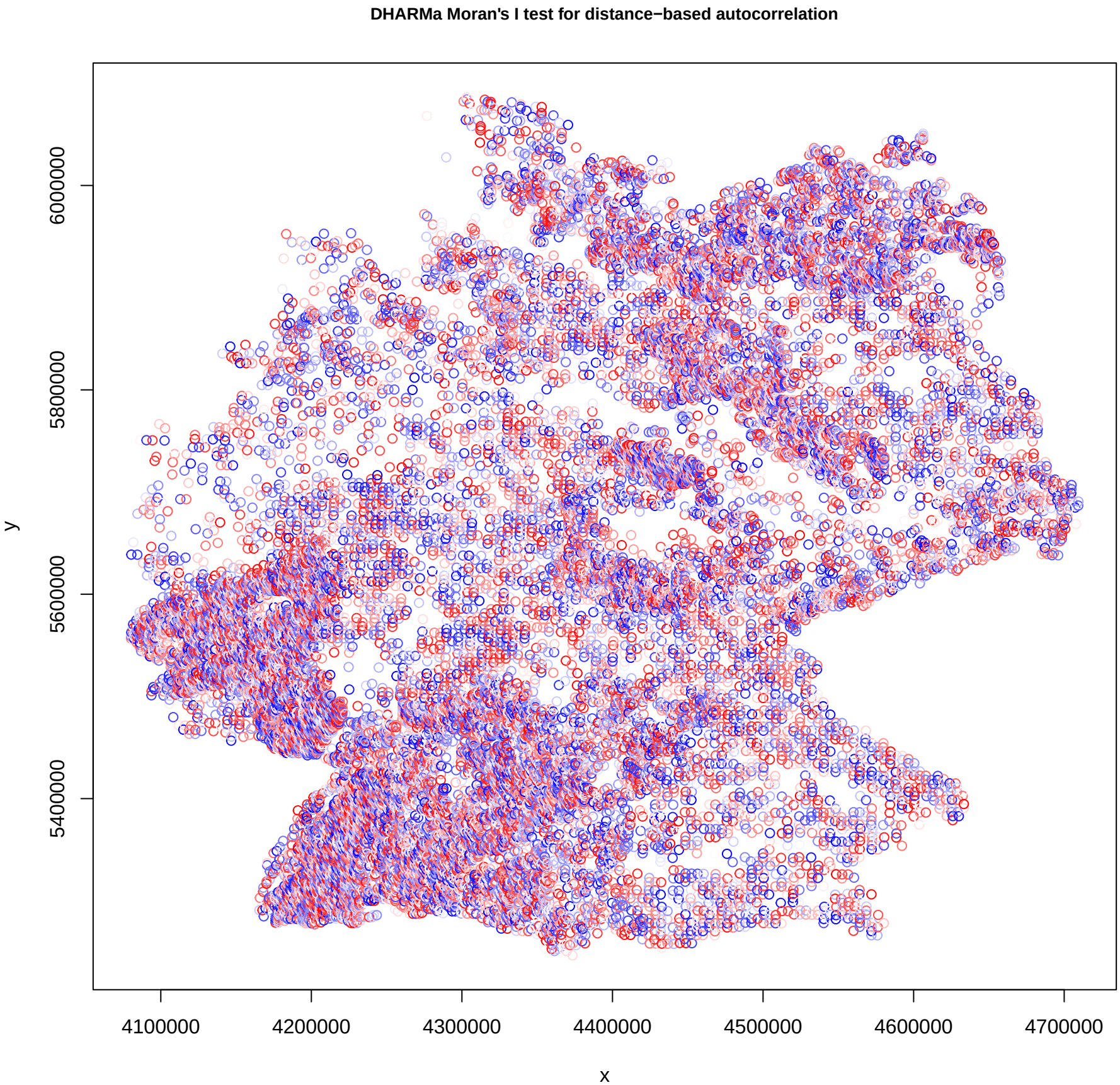
DHARMa Moran's I test for distance−based autocorrelation
6000000
5800000
5600000
5400000
y
4100000
4200000
4300000
4400000
4500000
4600000
4700000
x

DHARMa residual

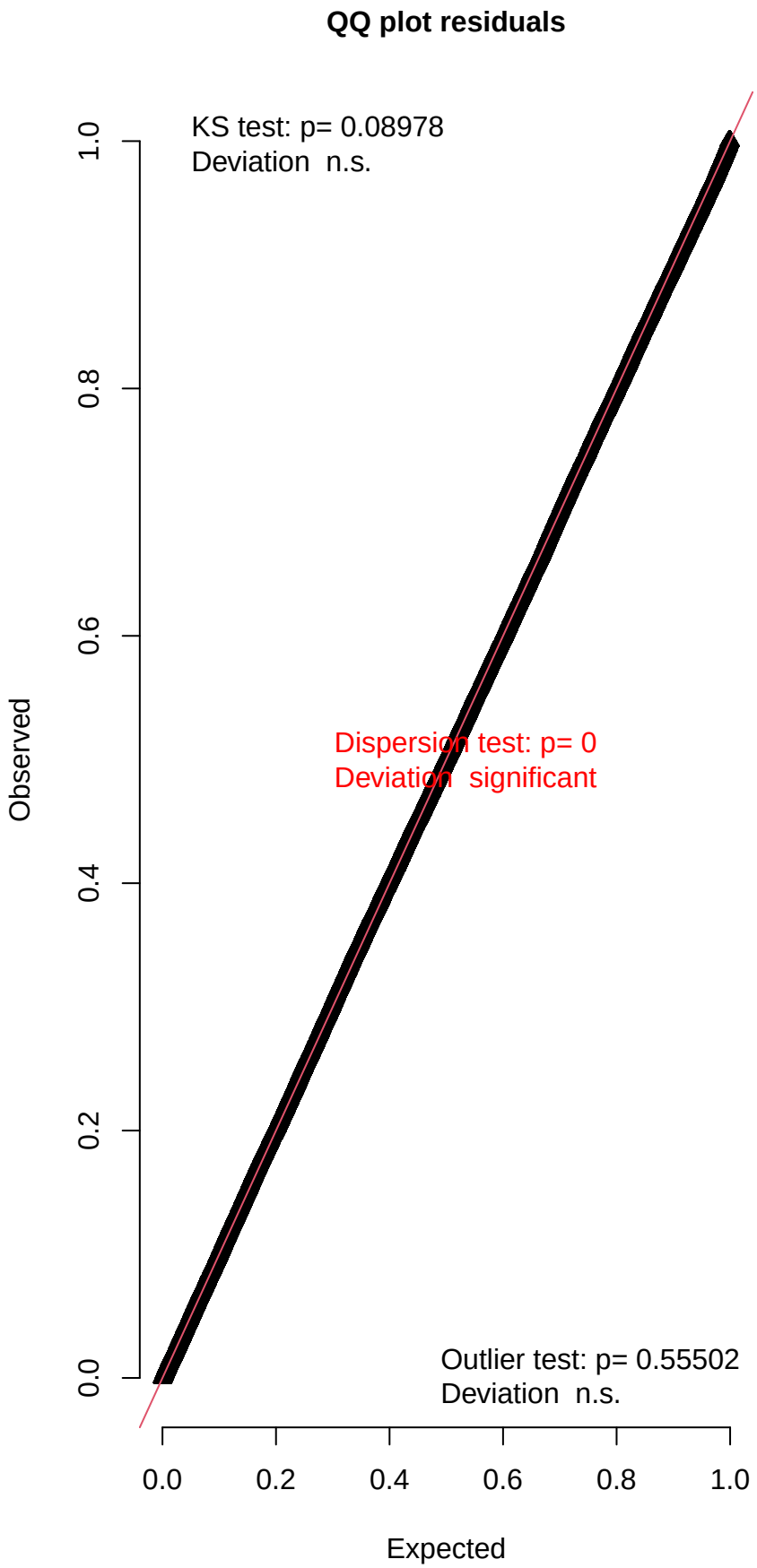

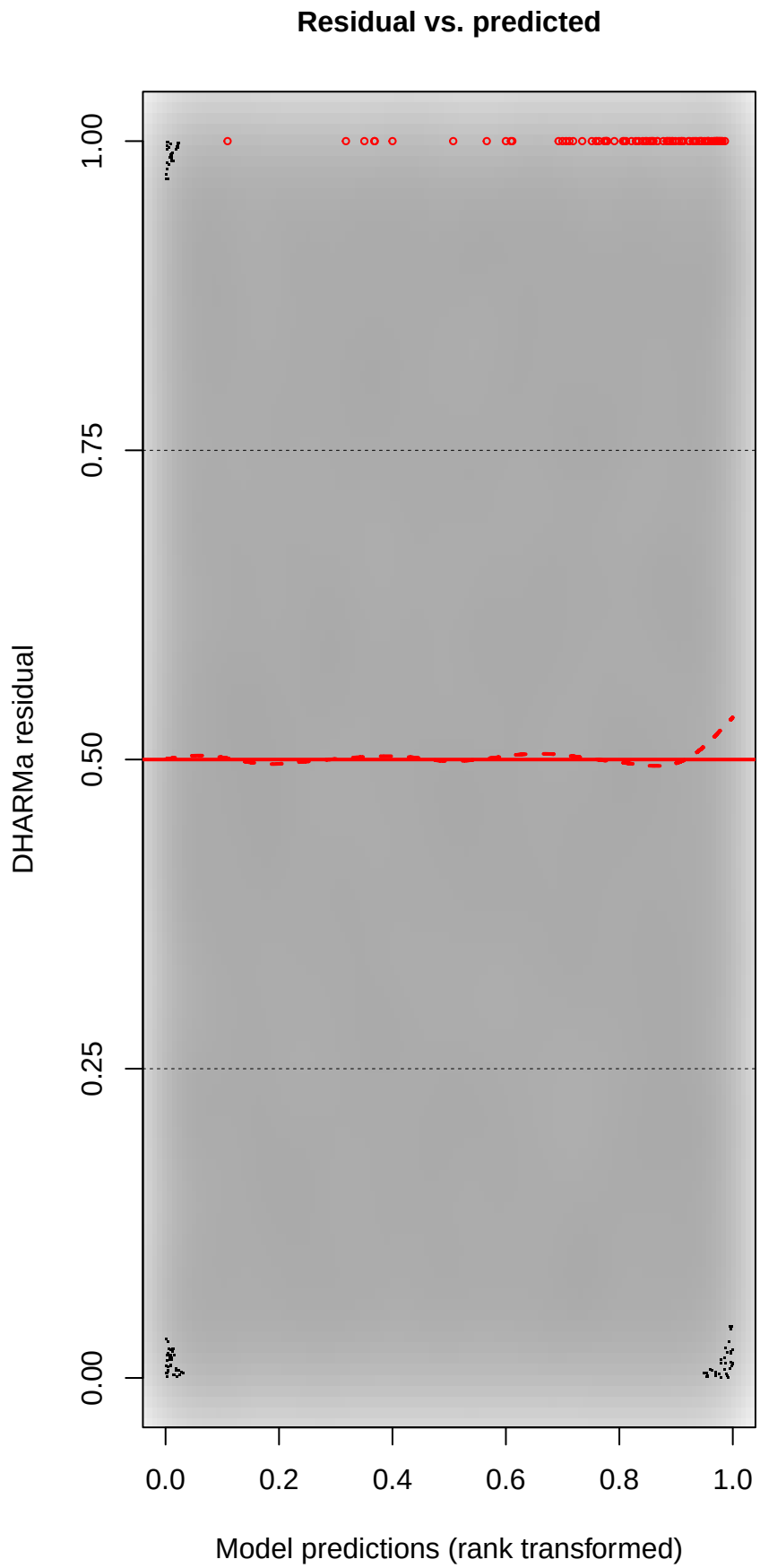

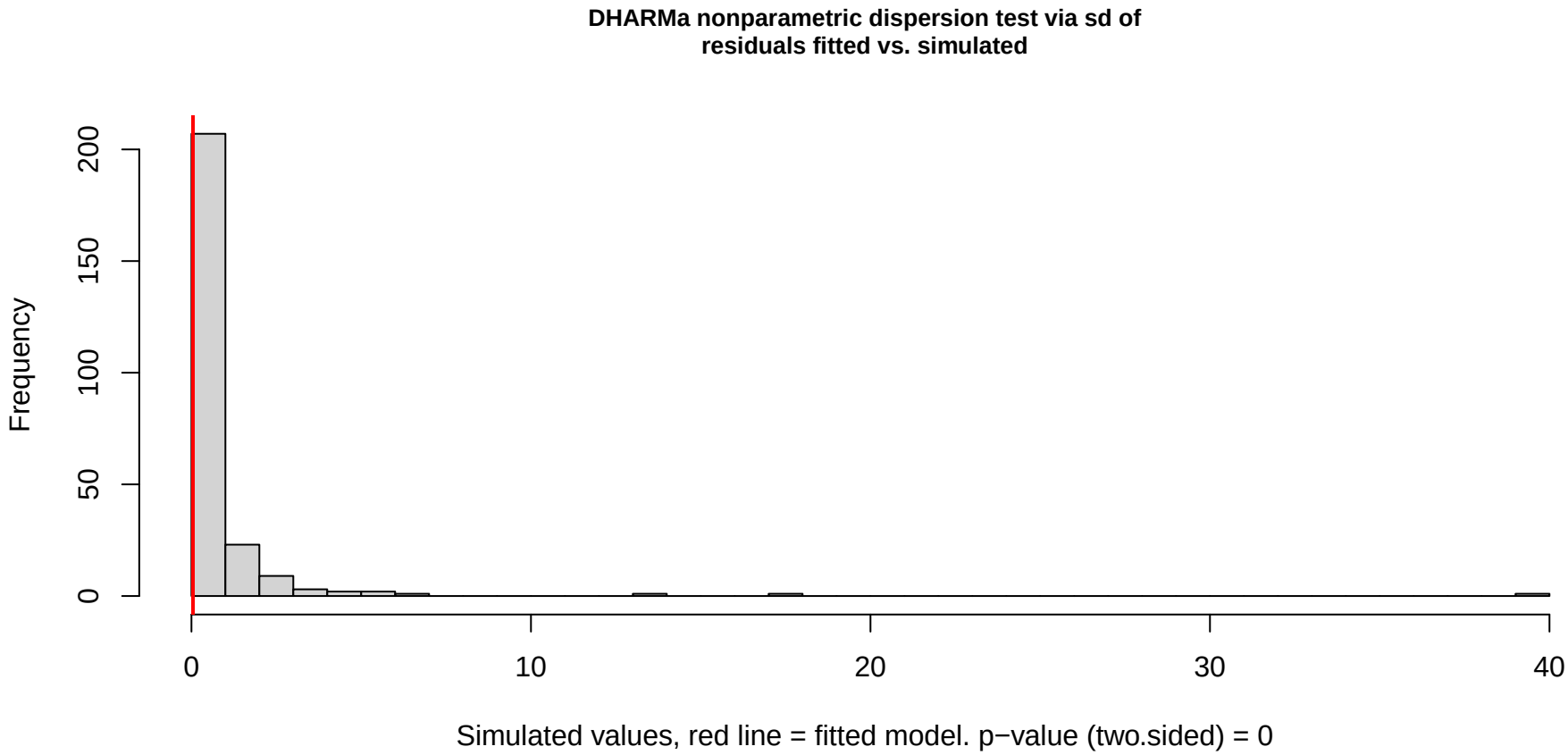
DHARMa nonparametric dispersion test via sd of residuals fitted vs. simulated
Frequency
0
50
100
150
200
0
10
20
30
40
Simulated values, red line = fitted model. p−value (two.sided) = 0

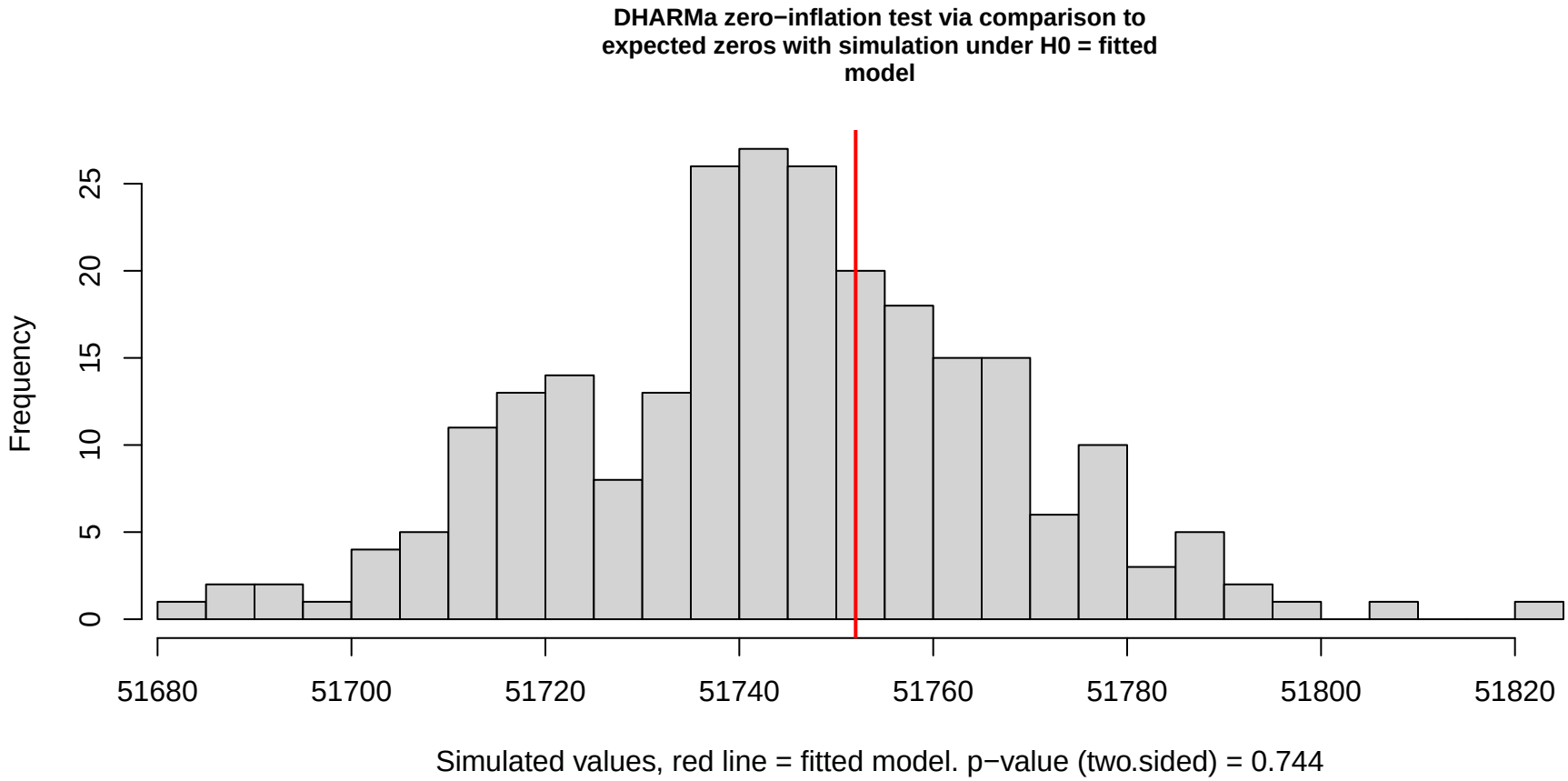
DHARMa zero−inflation test via comparison to expected zeros with simulation under H0 = fitted model
Frequency
0
5
10
15
20
25
51680
51700
51720
51740
51760
51780
51800
51820
Simulated values, red line = fitted model. p−value (two.sided) = 0.744

Tilia


DHARMa Moran's I test for distance−based autocorrelation
y
6000000
5800000
5600000
5400000
x
4100000
4200000
4300000
4400000
4500000
4600000
4700000

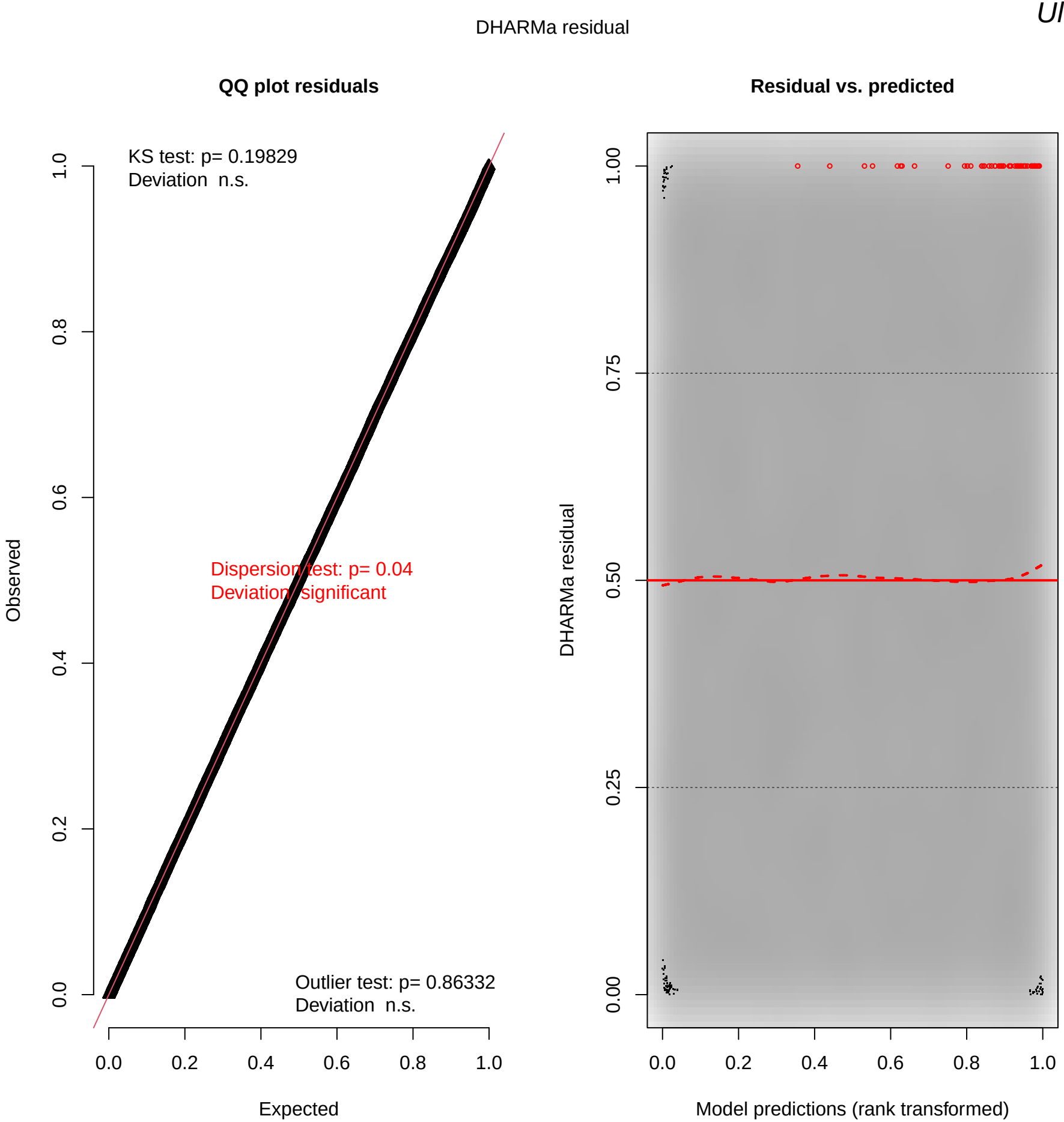
DHARMa residual
QQ plot residuals
KS test: p= 0.19829
Deviation n.s.
Dispersion test: p= 0.04
Deviation significant
Outlier test: p= 0.86332
Deviation n.s.
Observed
Expected
0.0
0.2
0.4
0.6
0.8
1.0
Residual vs. predicted
DHARMa residual
Model predictions (rank transformed)
0.00
0.25
0.50
0.75
1.00

Ulmus

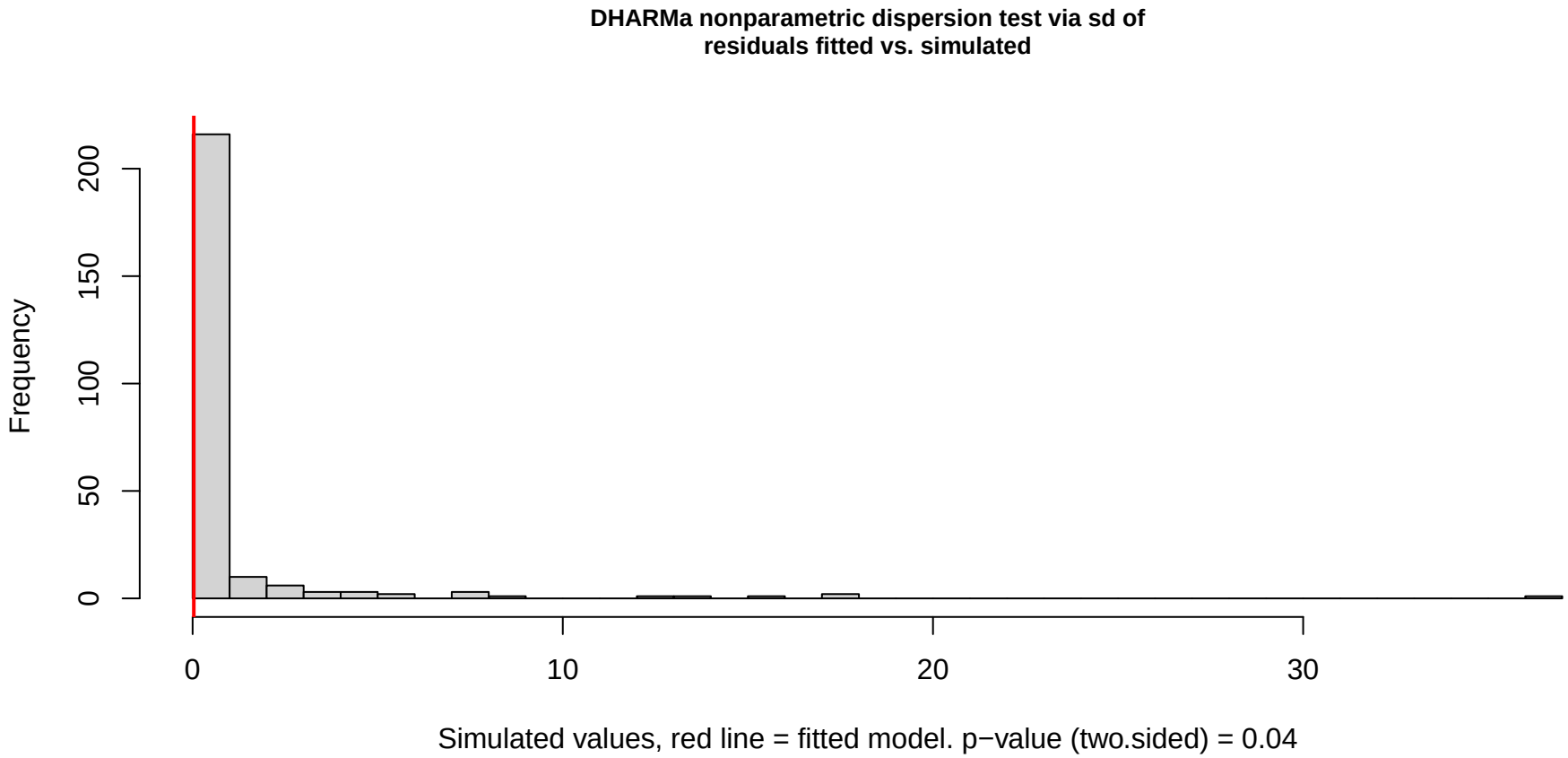
DHARMa nonparametric dispersion test via sd of residuals fitted vs. simulated
Frequency
0
50
100
150
200
0
10
20
30
Simulated values, red line = fitted model. p−value (two.sided) = 0.04

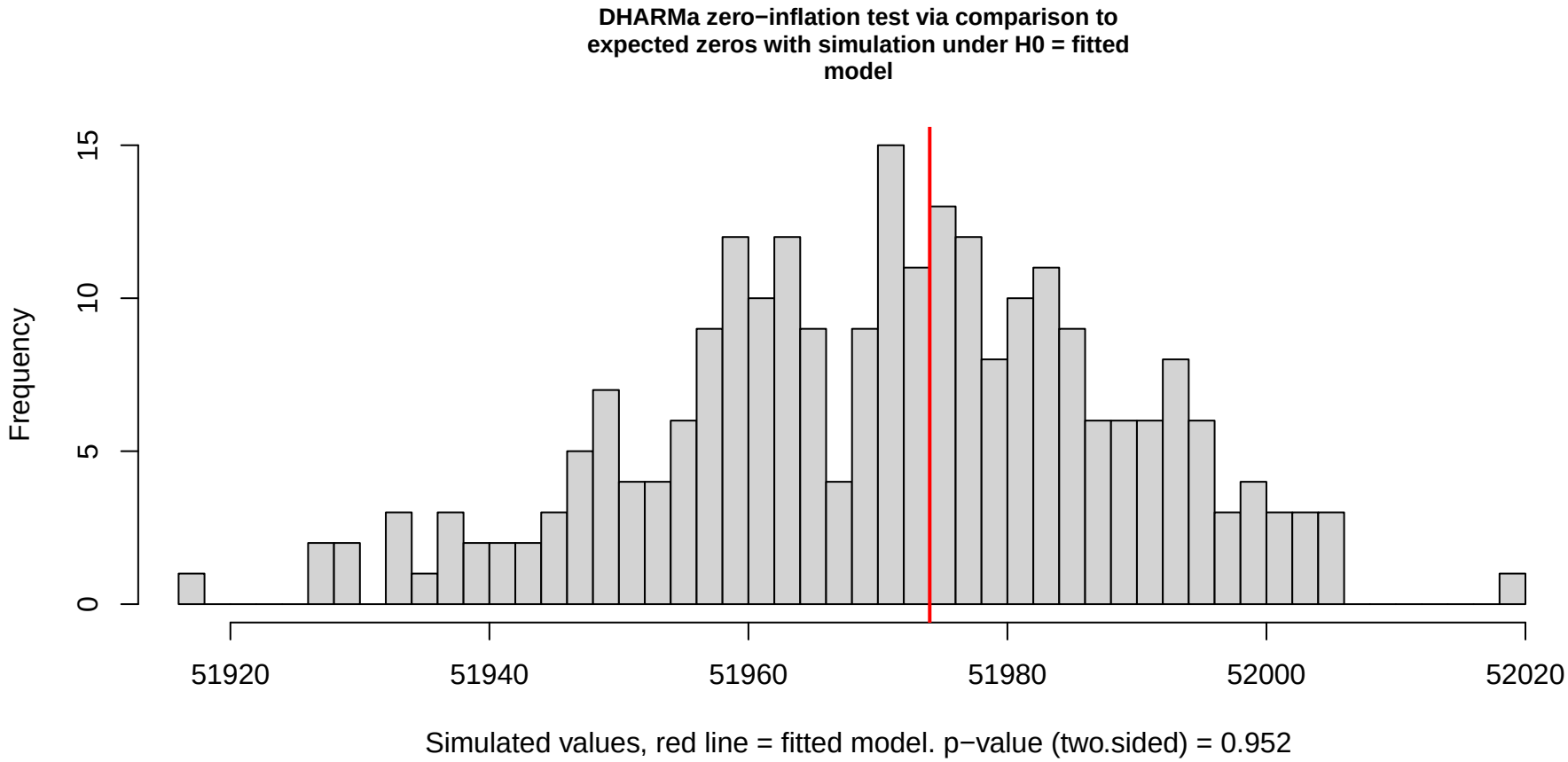
DHARMa zero−inflation test via comparison to expected zeros with simulation under H0 = fitted model
Frequency
0
5
10
15
51920
51940
51960
51980
52000
52020
Simulated values, red line = fitted model. p−value (two.sided) = 0.952

Ulmus

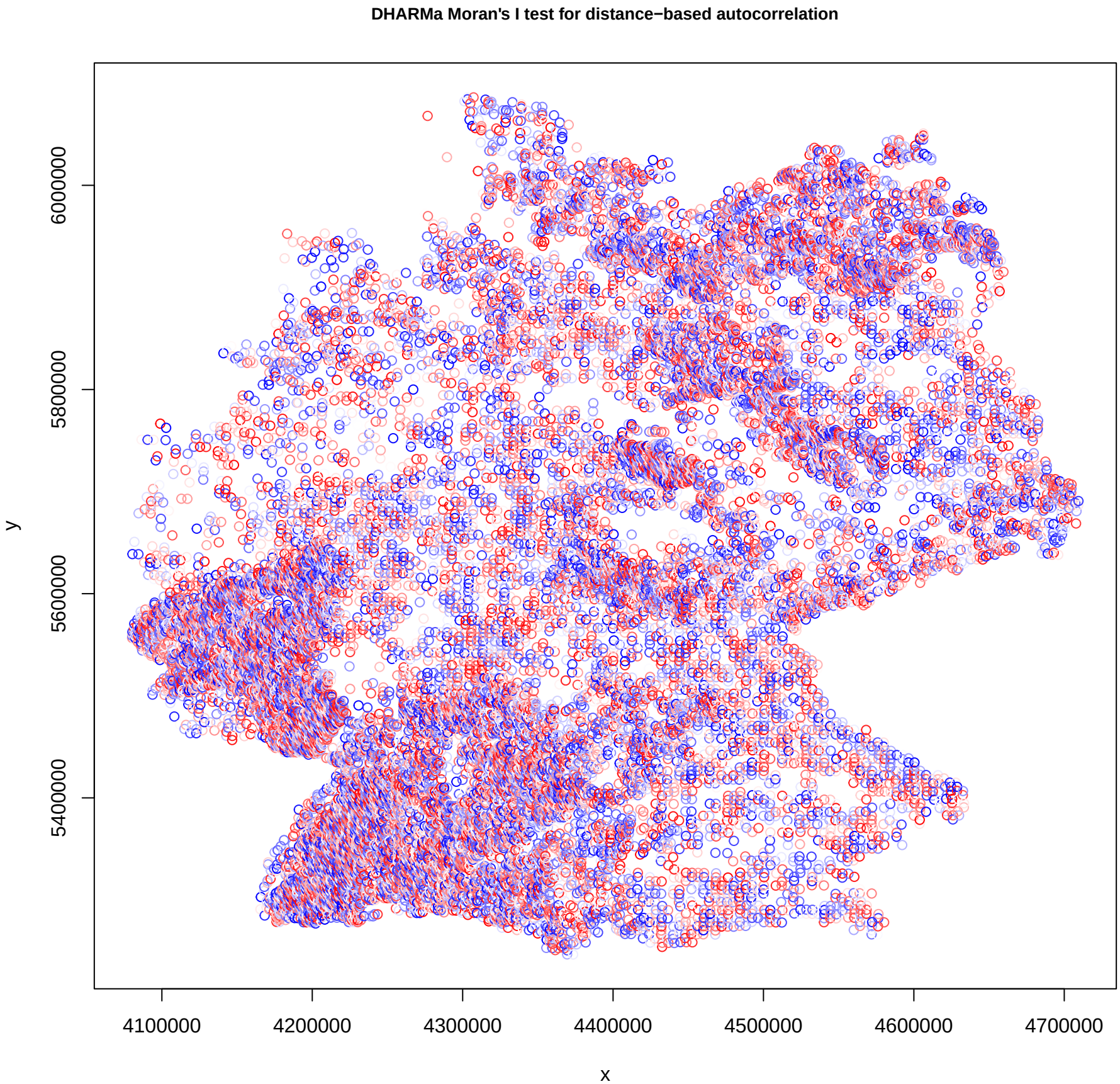
DHARMa Moran's I test for distance−based autocorrelation
6000000
5800000
5600000
5400000
y
4100000
4200000
4300000
4400000
4500000
4600000
4700000
x

Robinia pseudoacacia

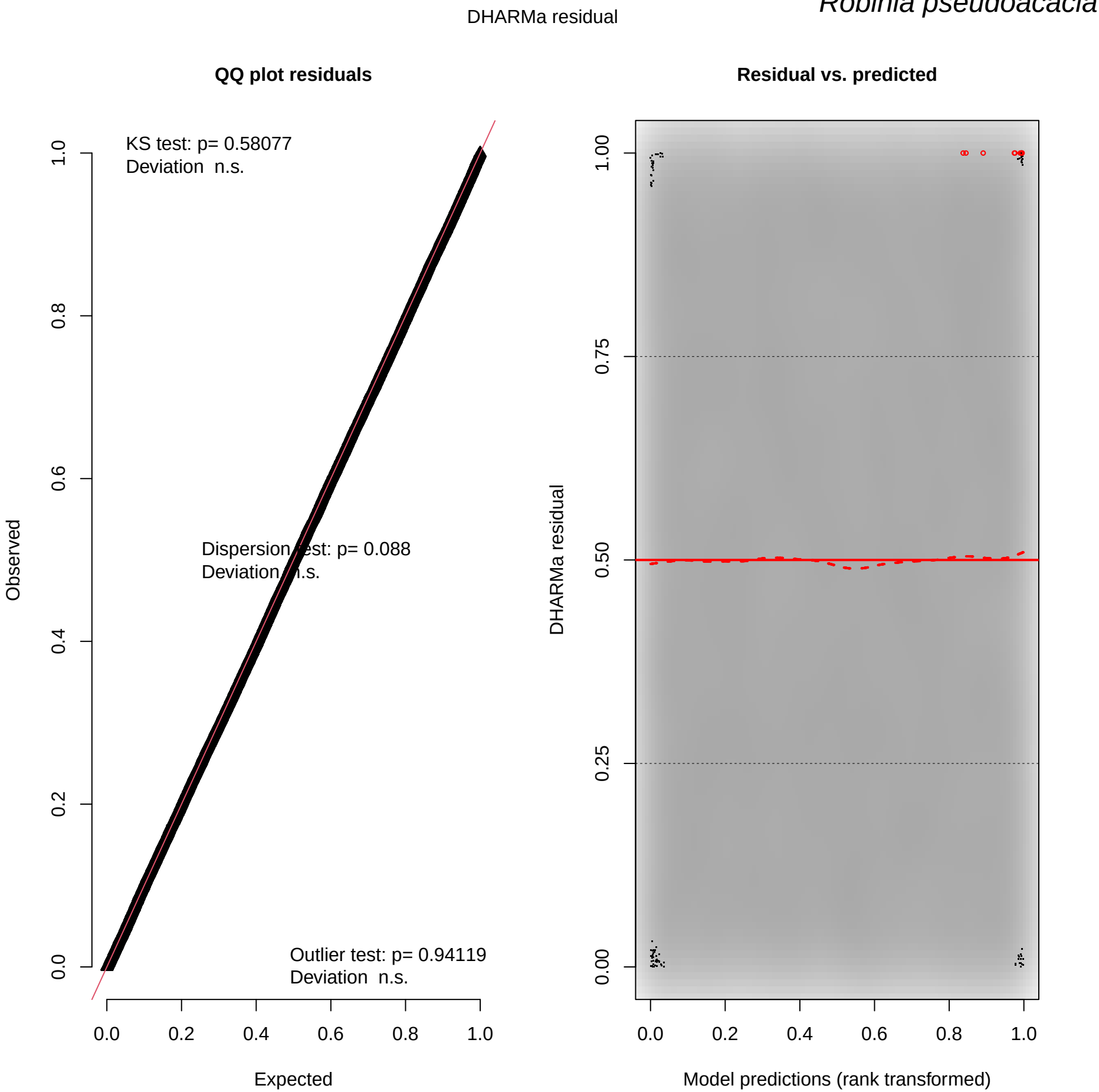

Robinia pseudoacacia

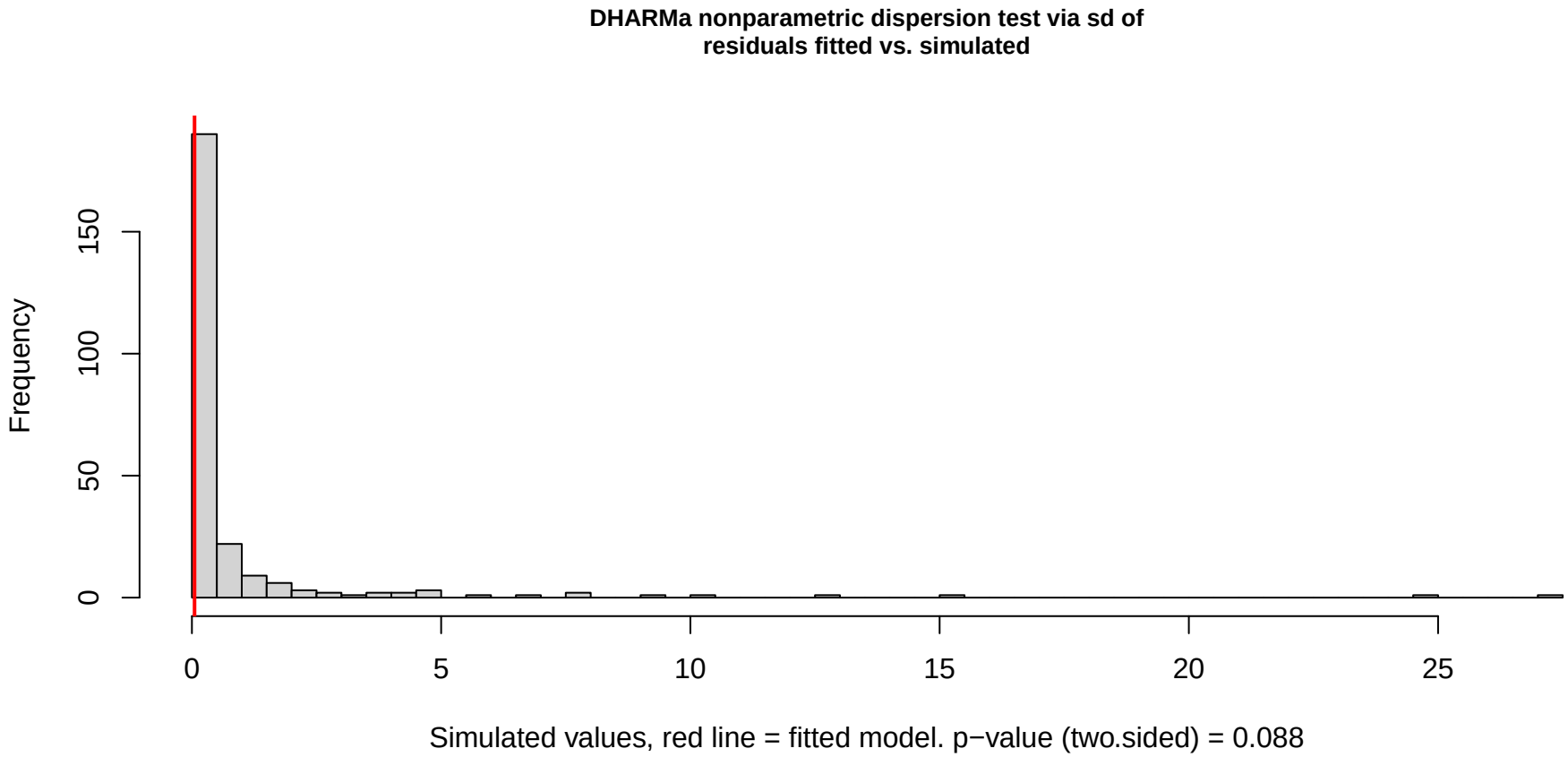

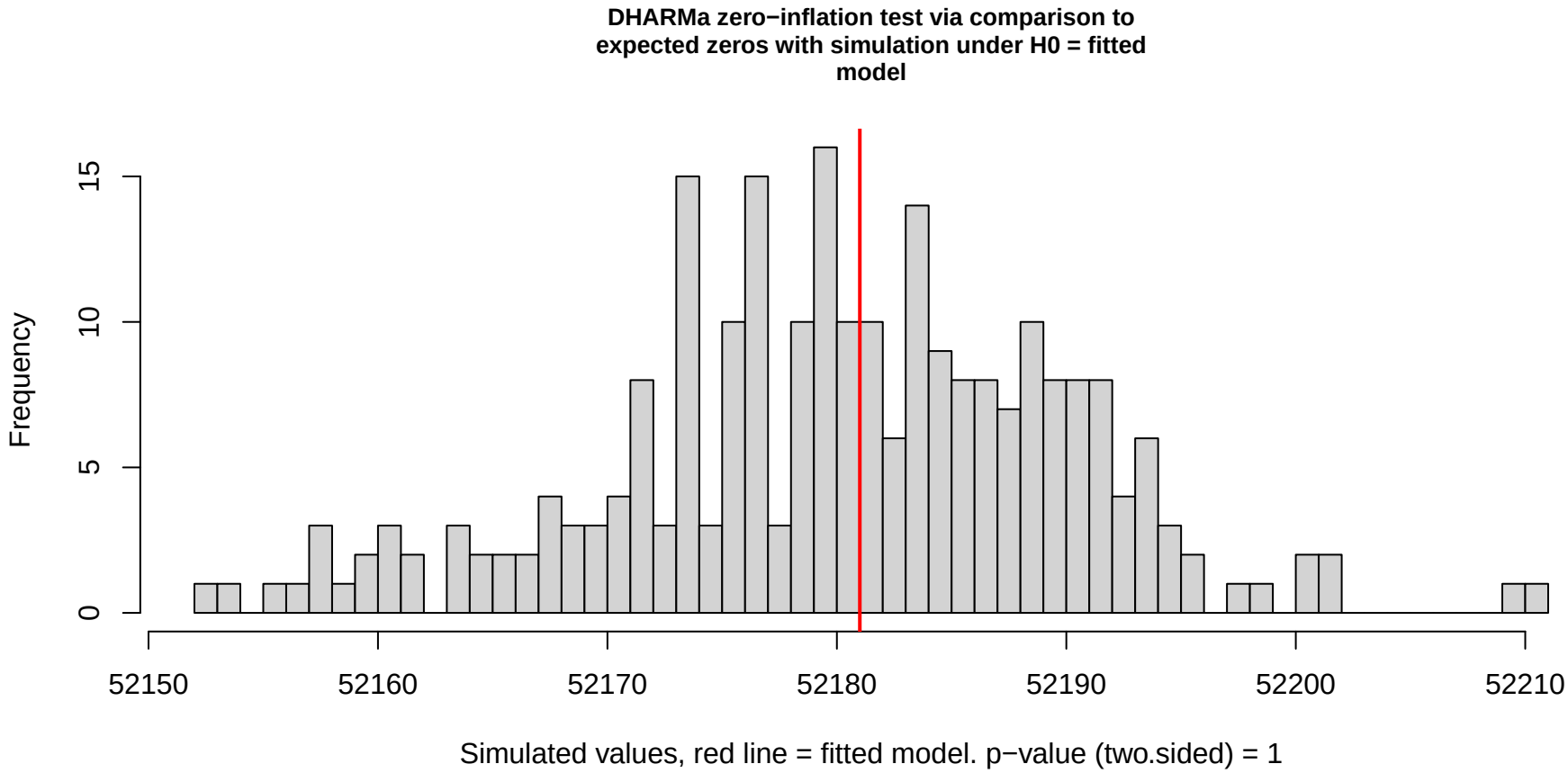

Robinia pseudoacacia

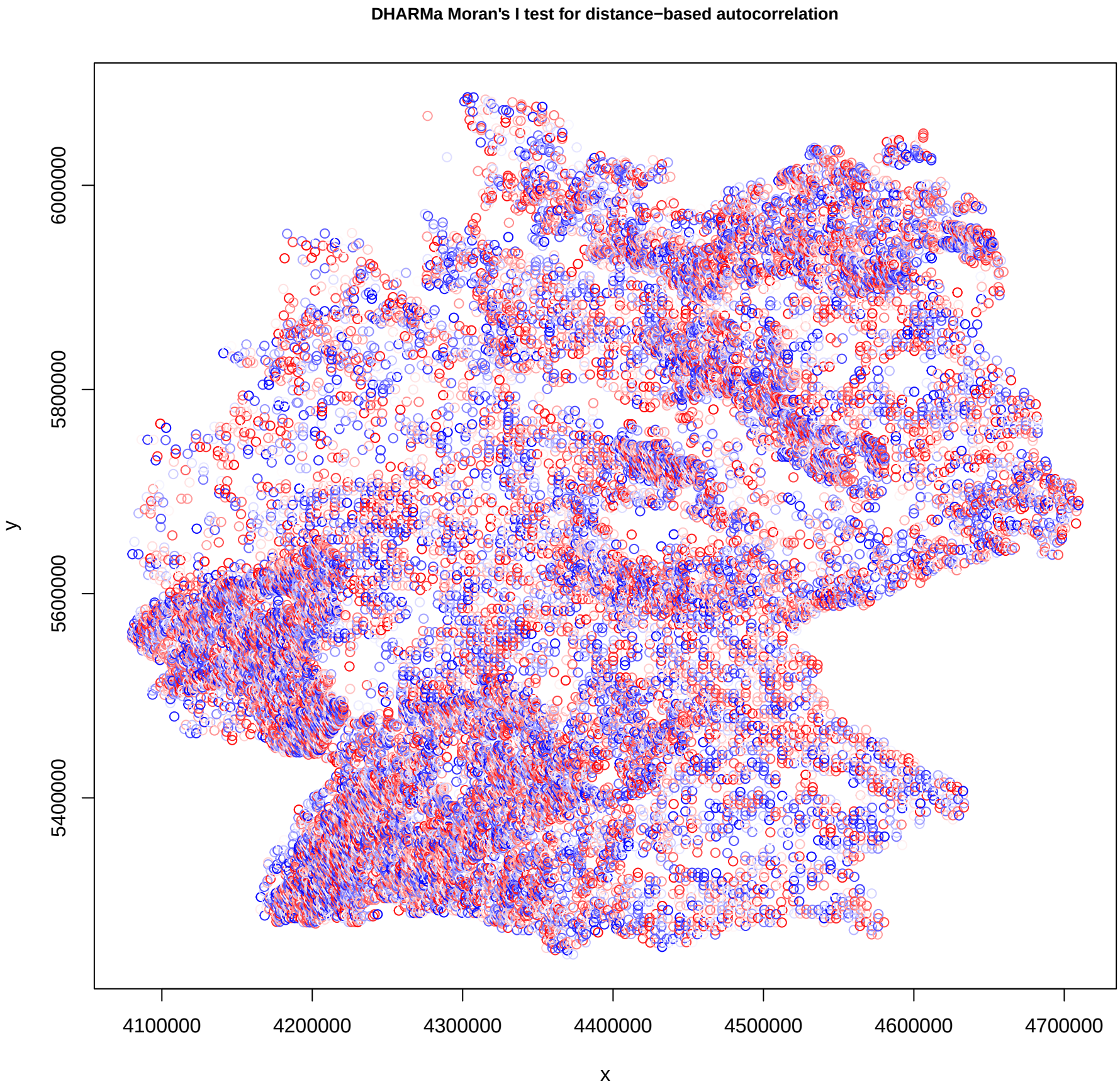

Quercus petraea

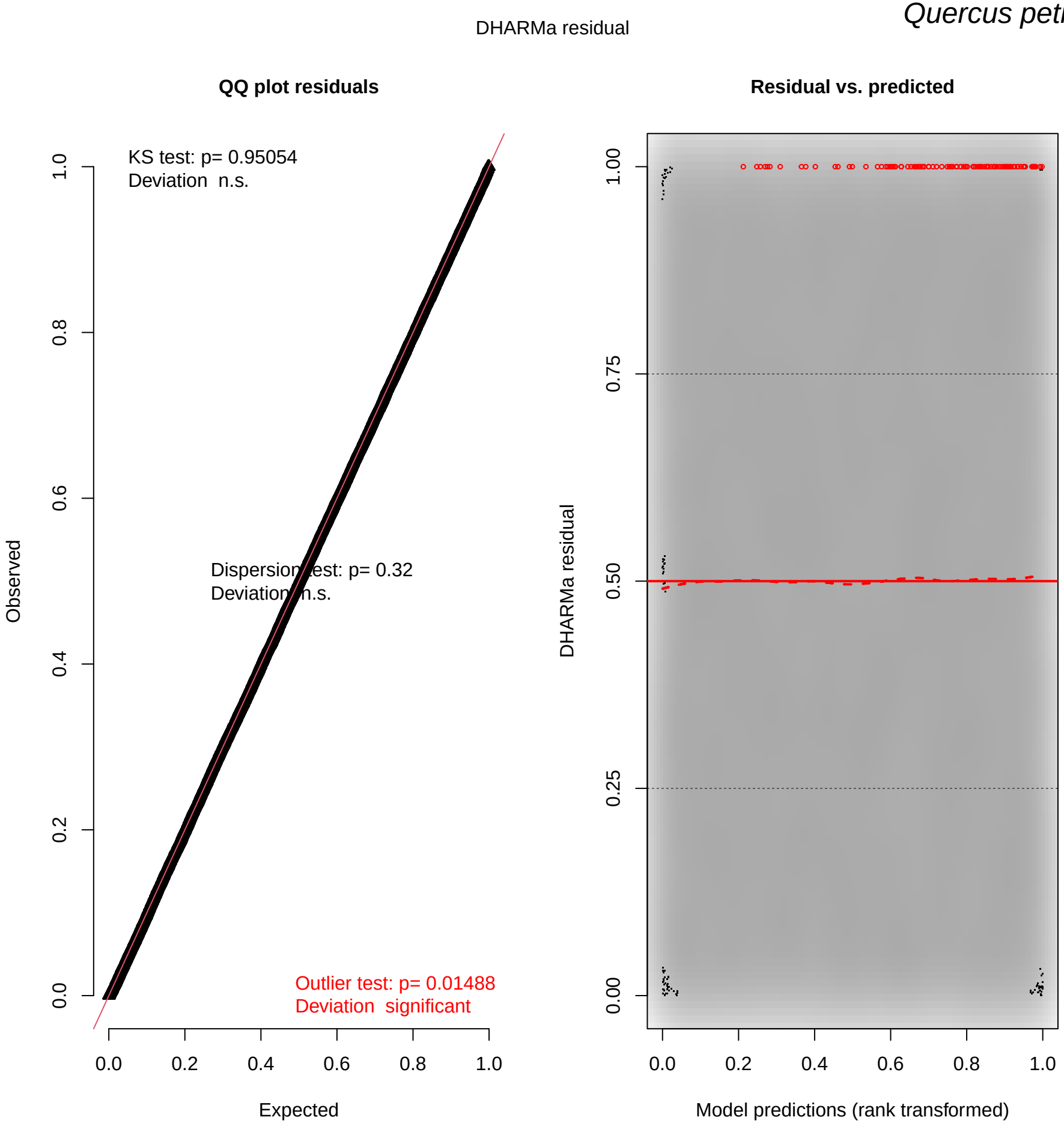

Quercus petraea

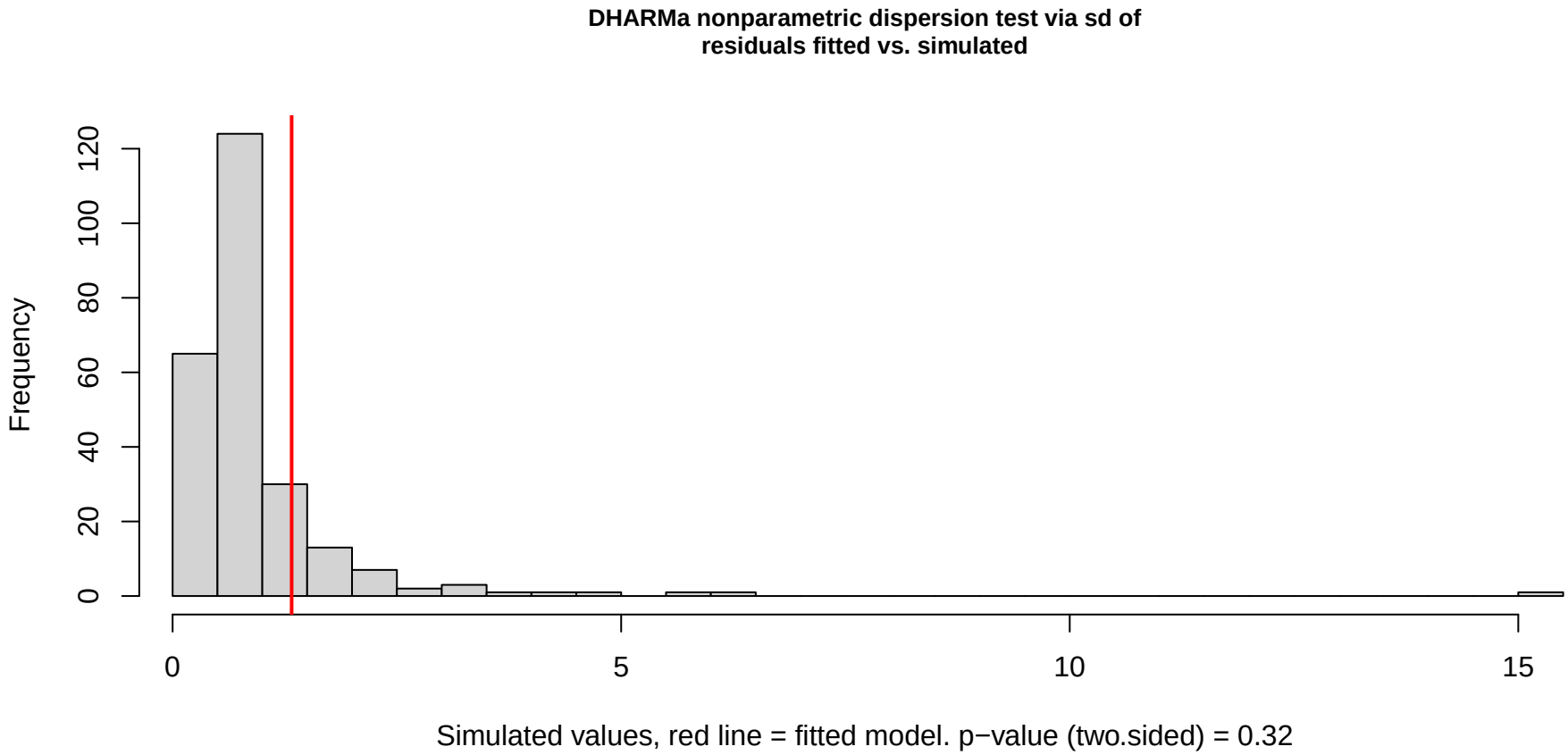

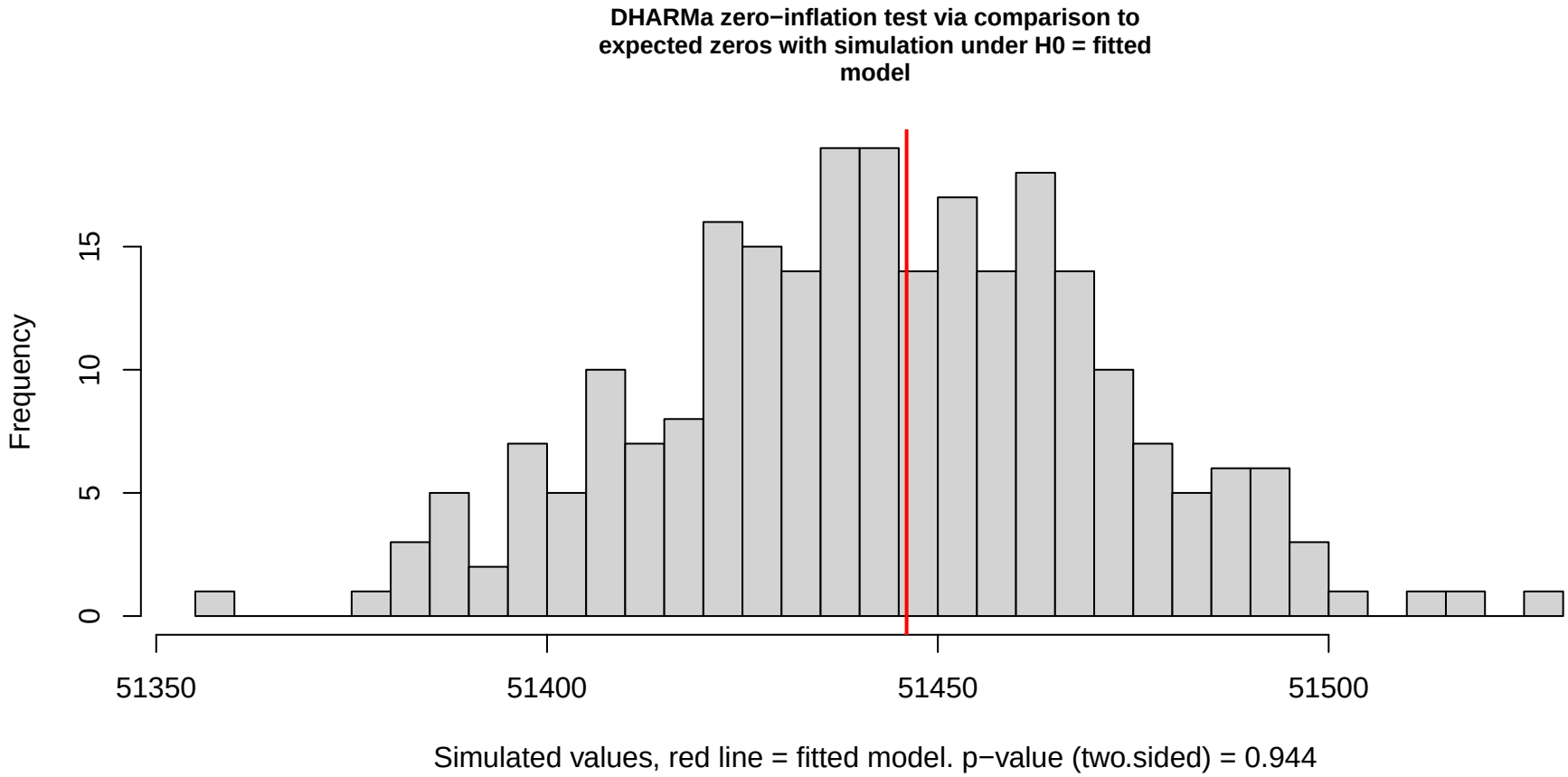

Quercus petraea

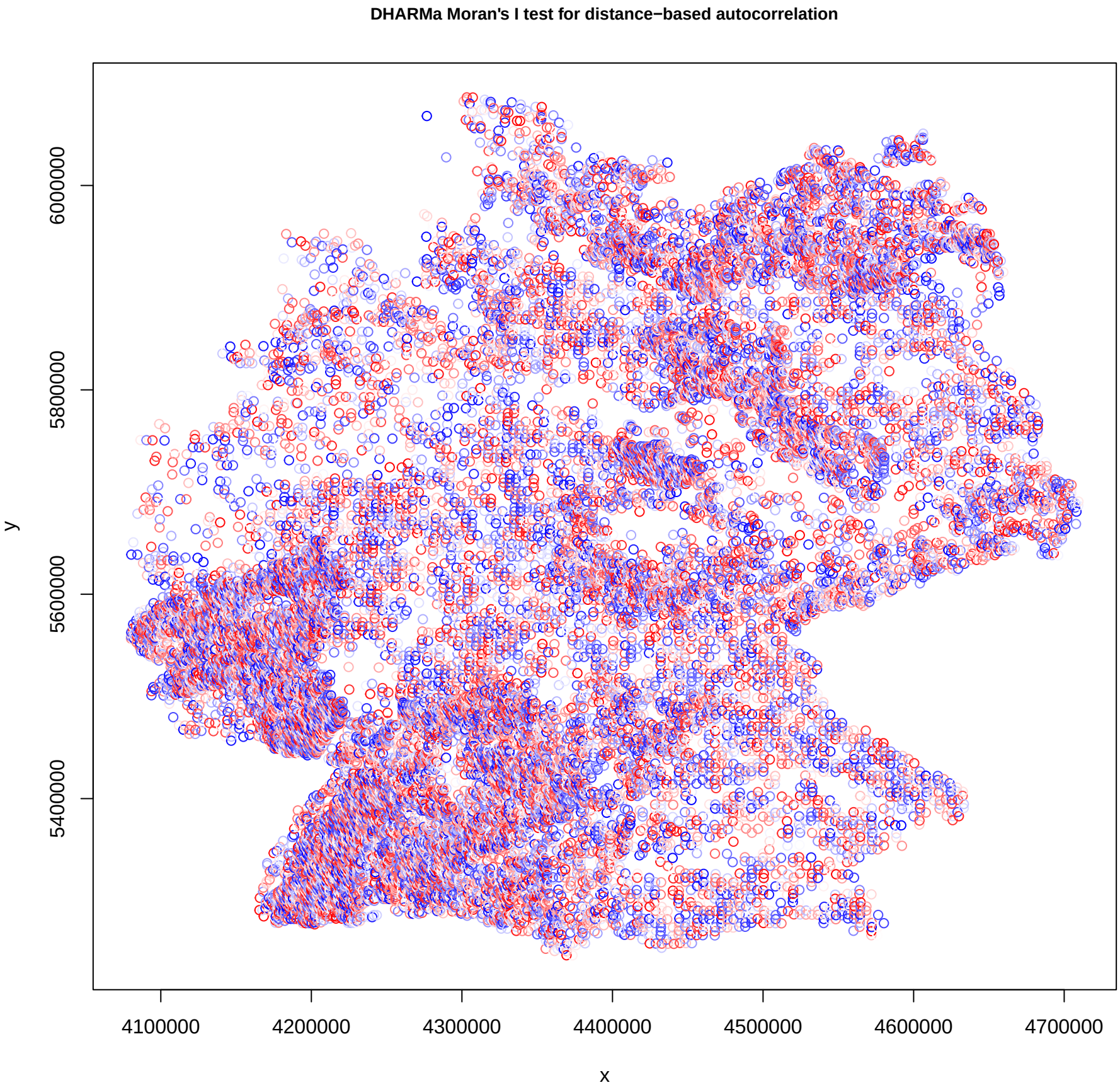

Quercus robur

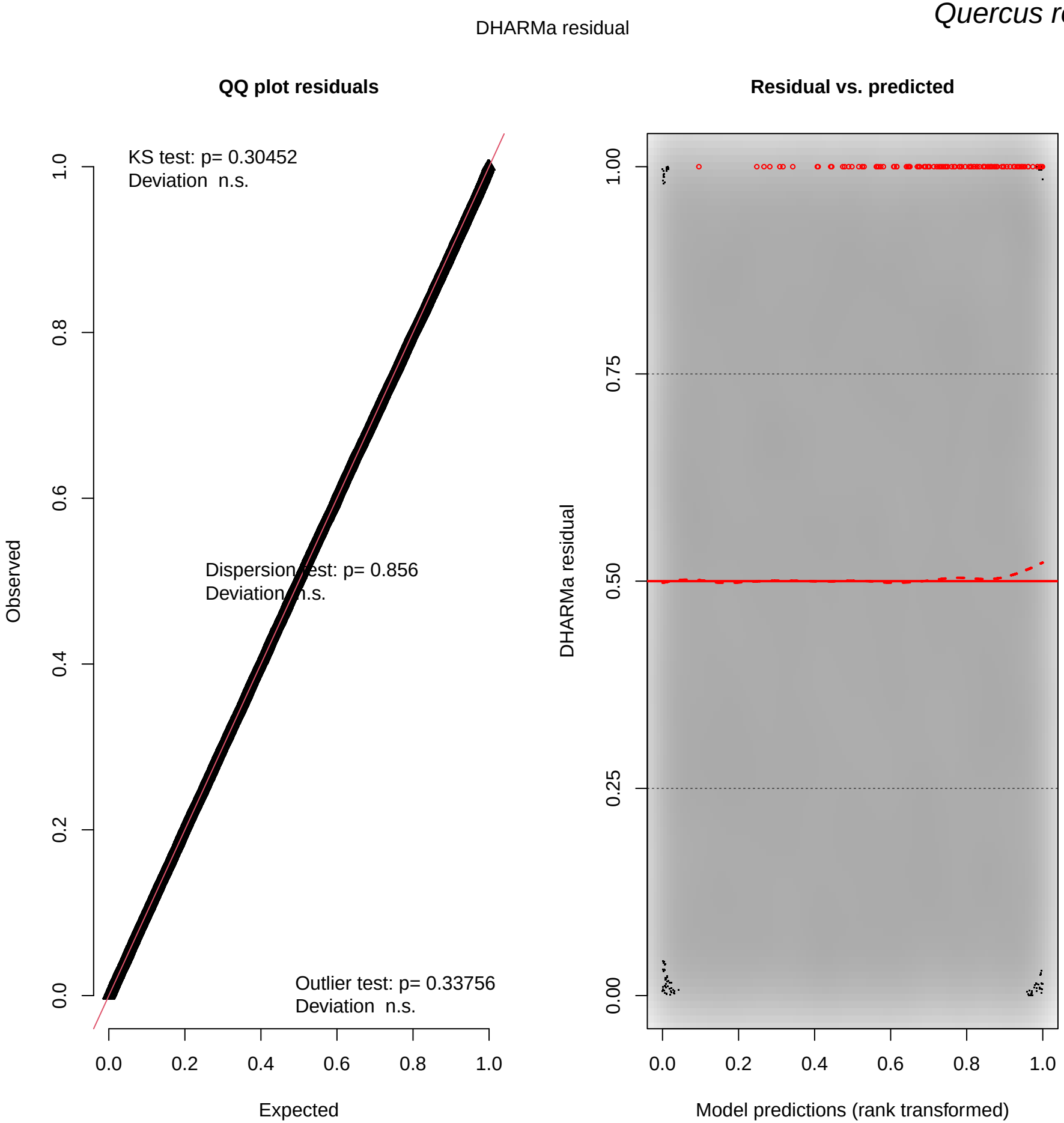

Quercus robur

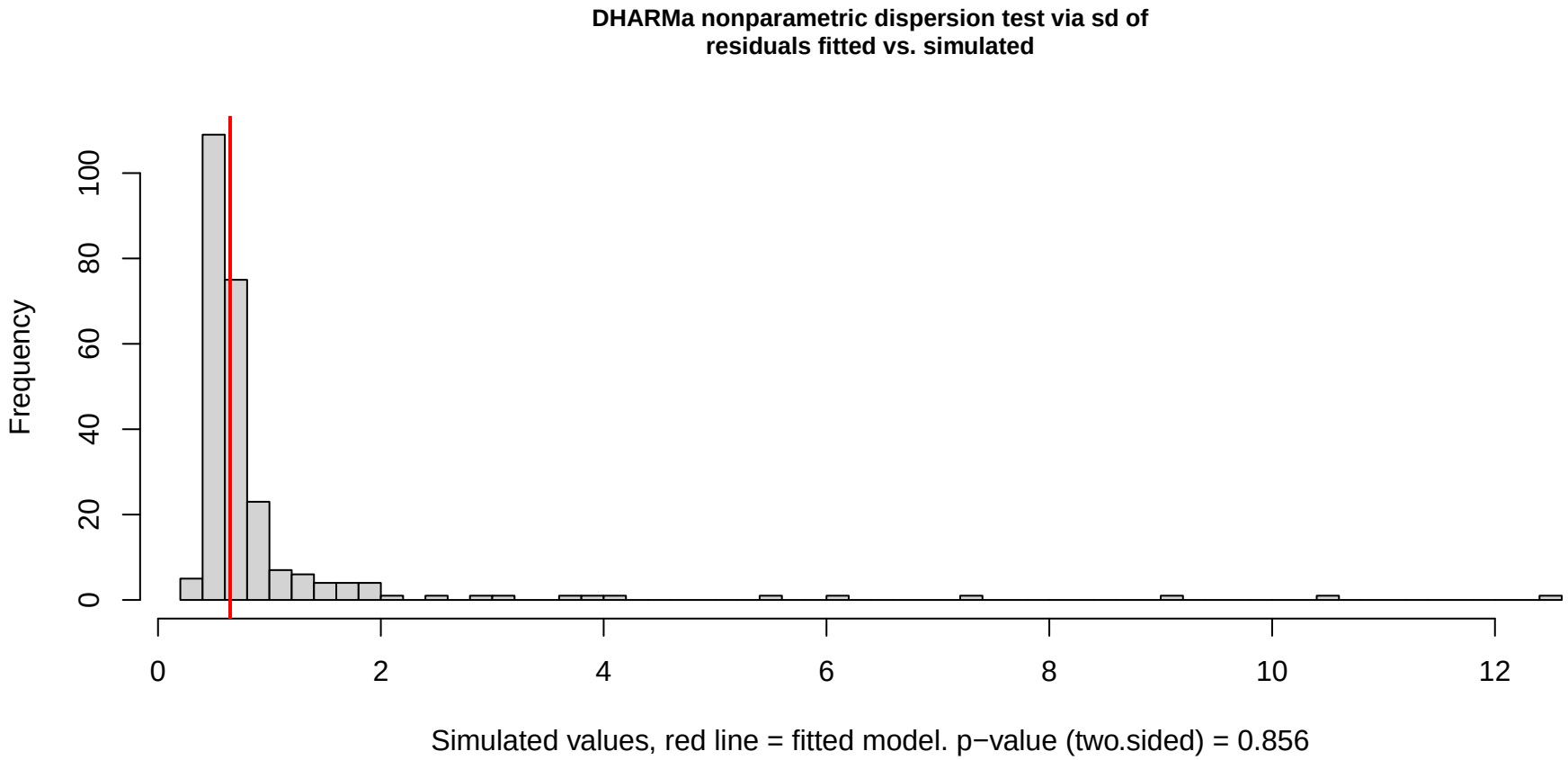

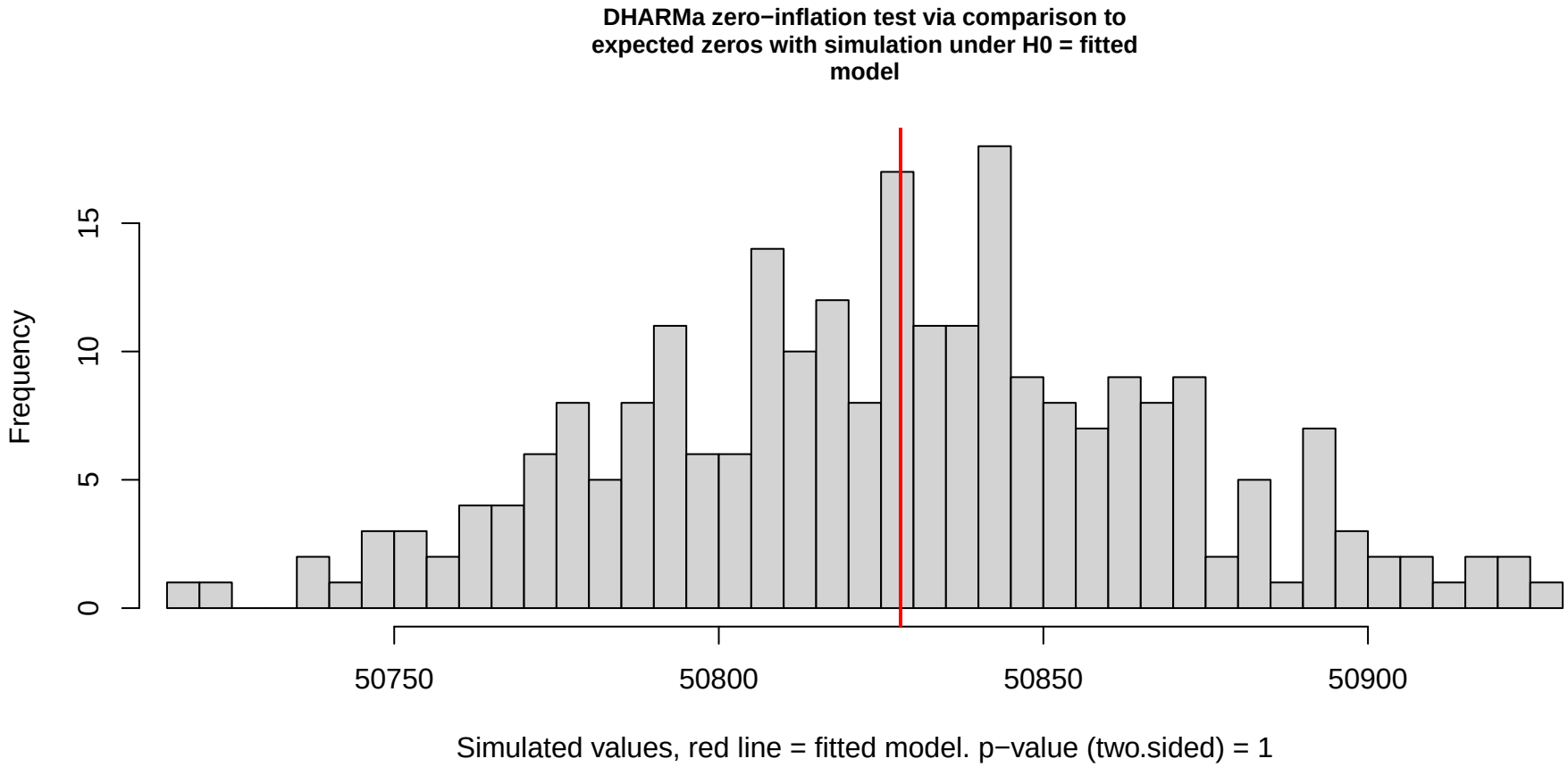

Quercus robur

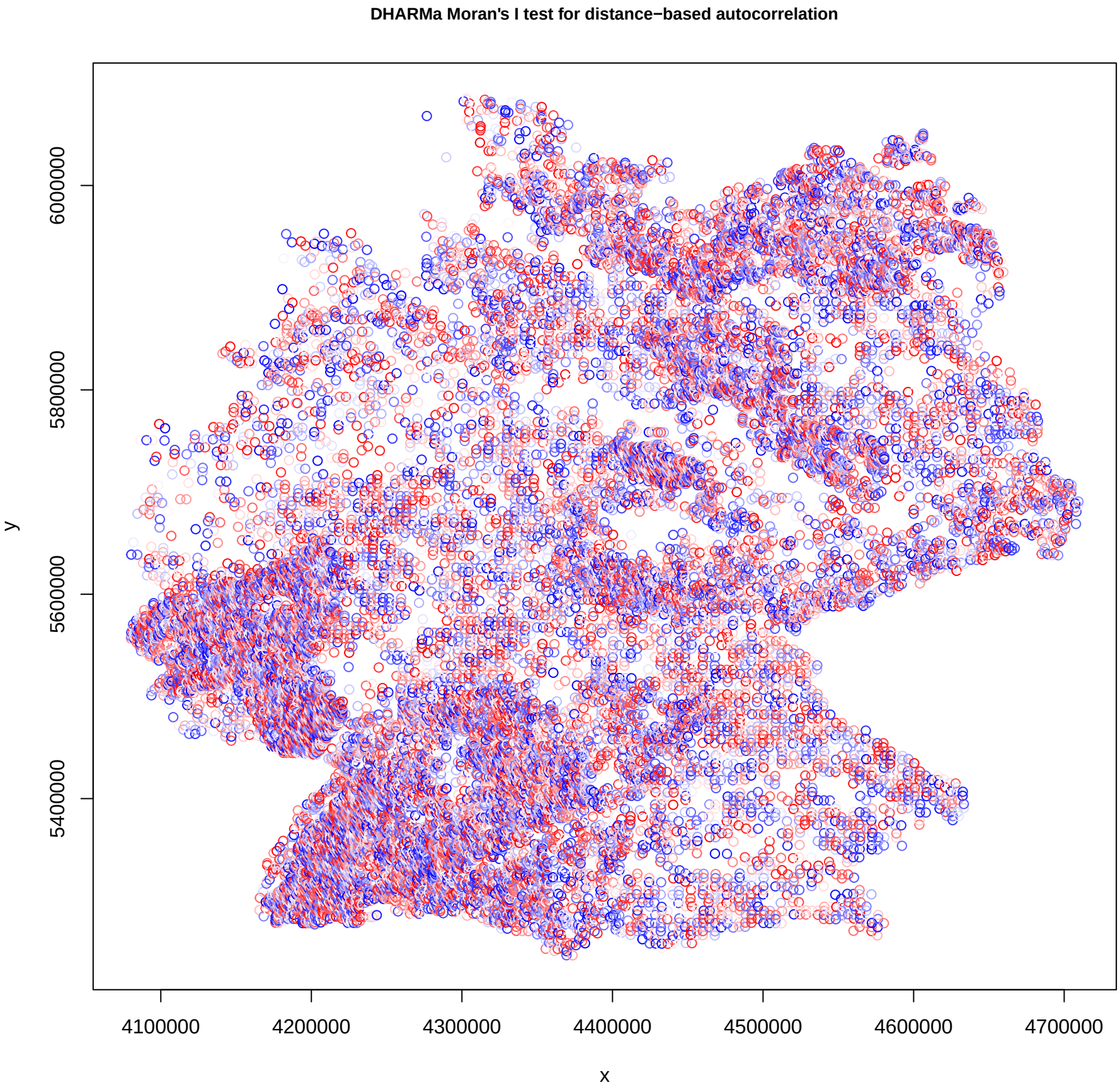

Quercus rubra

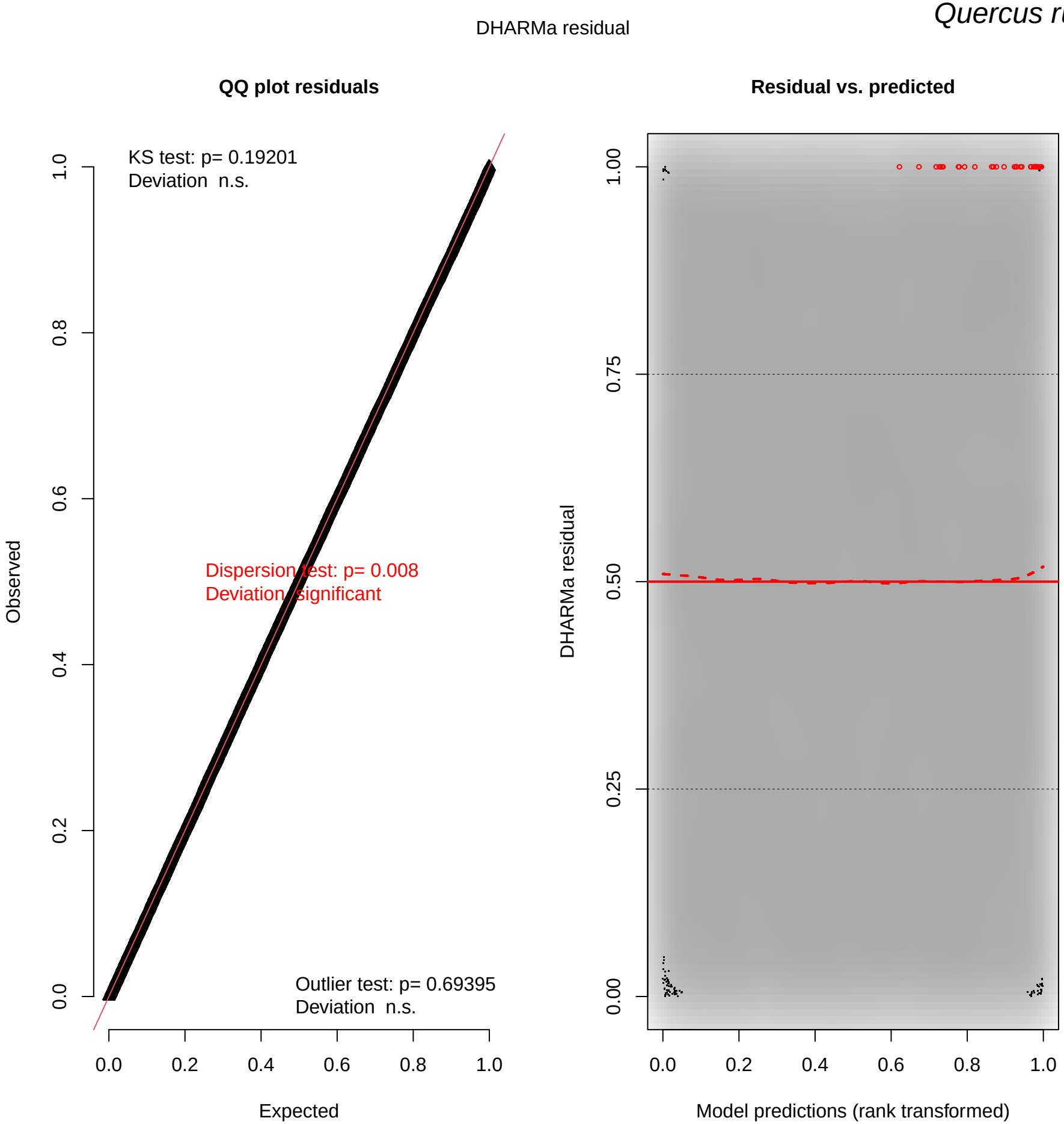

Quercus rubra

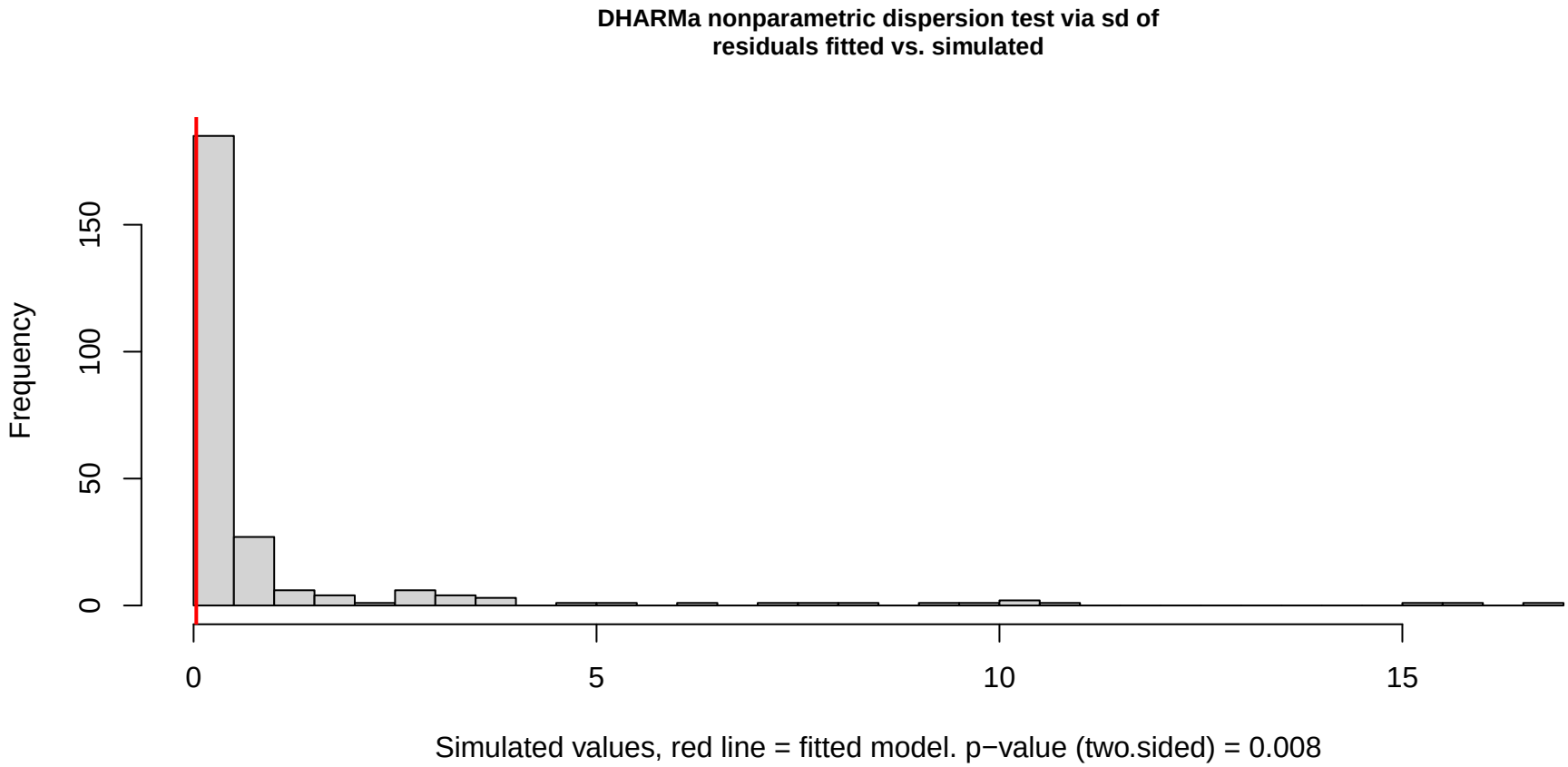

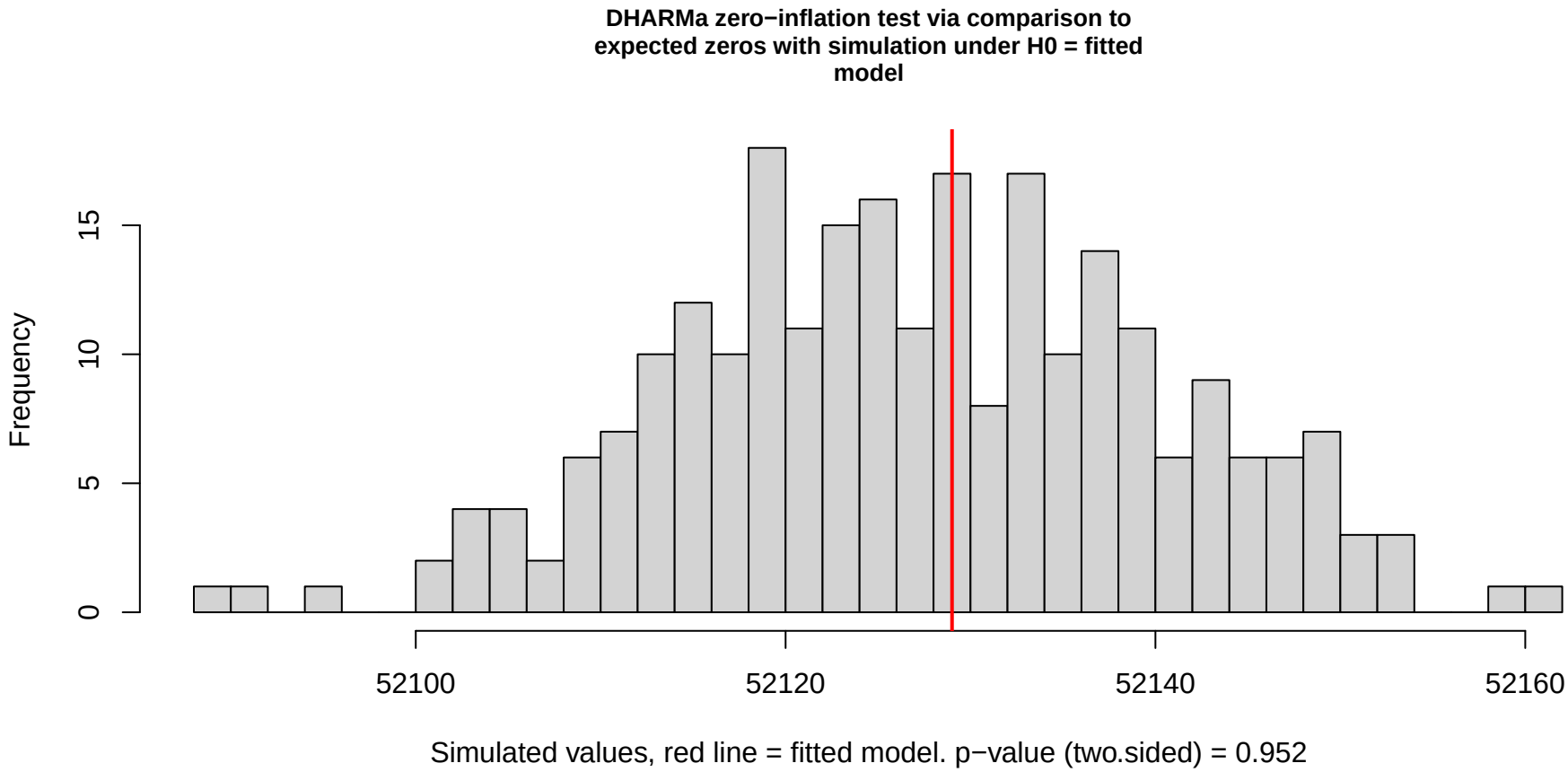

Quercus rubra

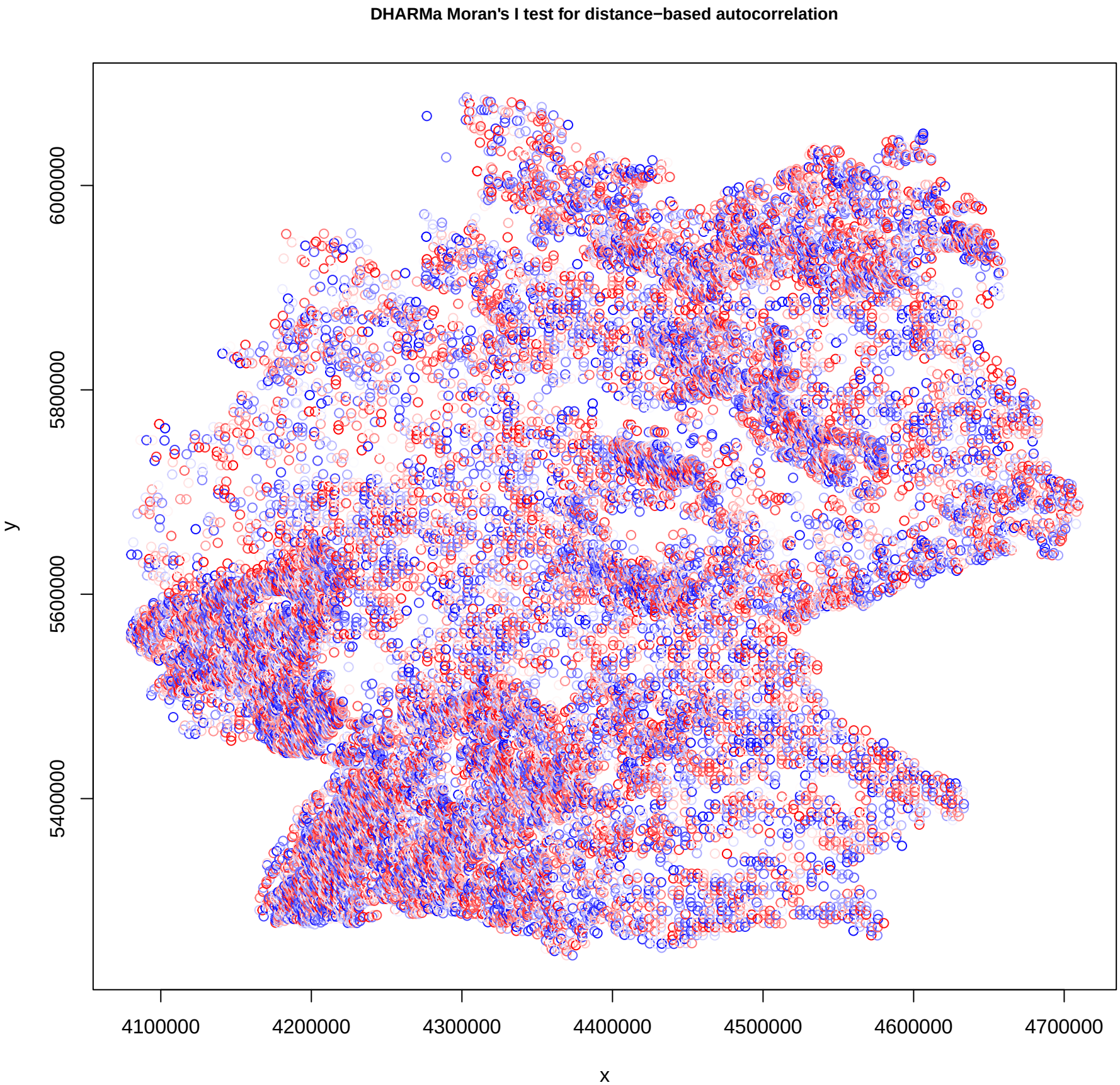

Betula pendula

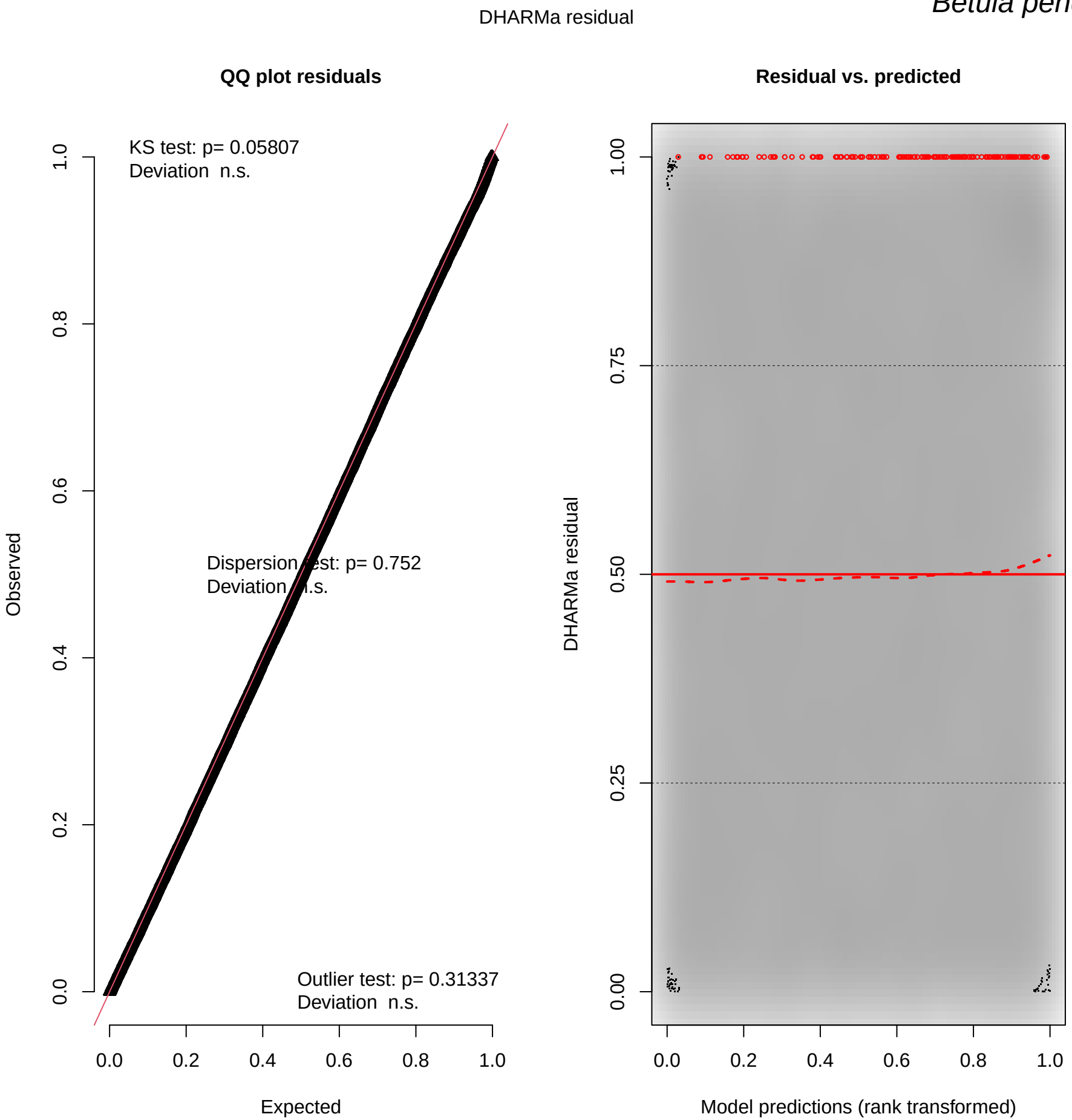

Betula pendula

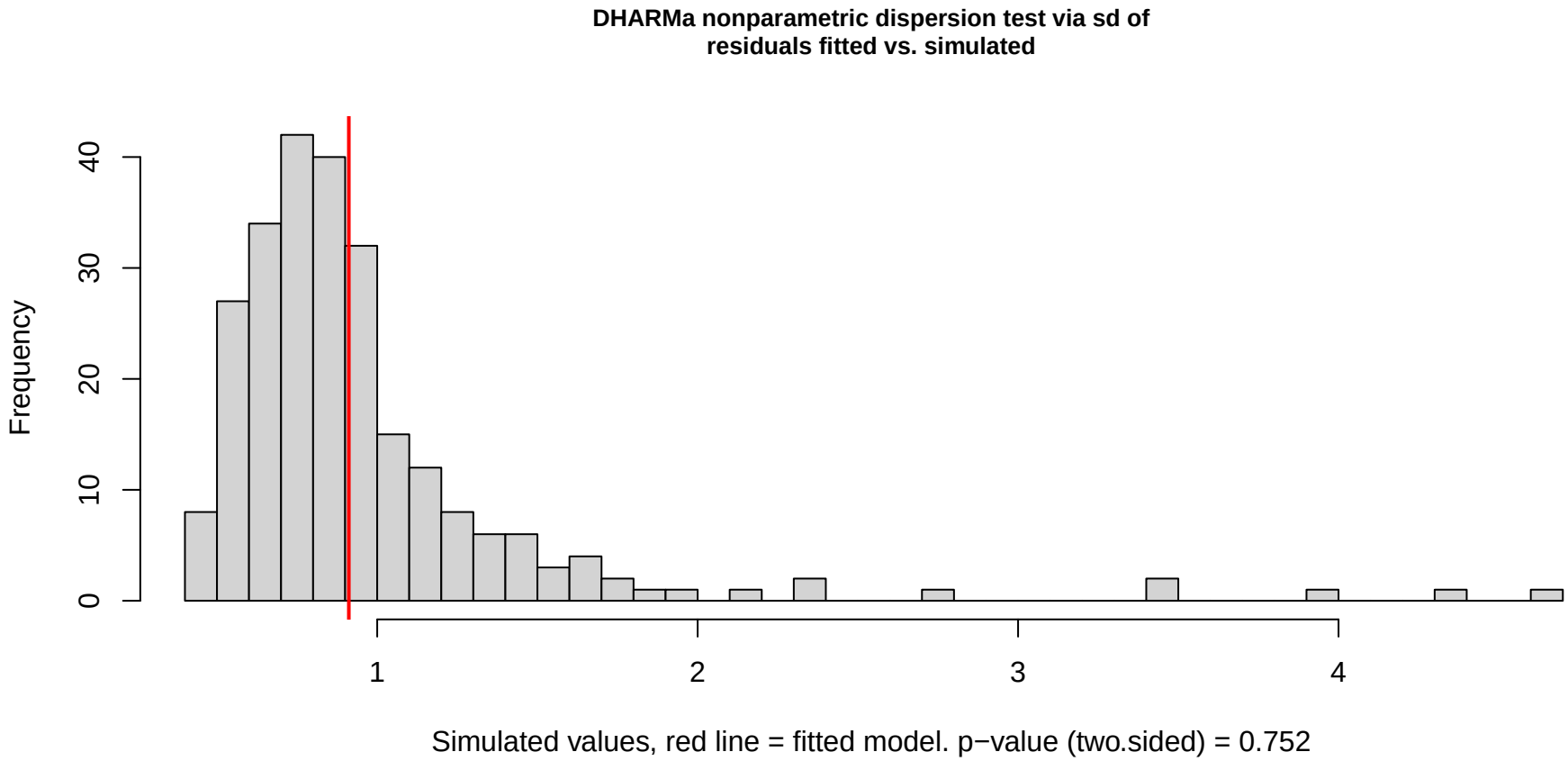

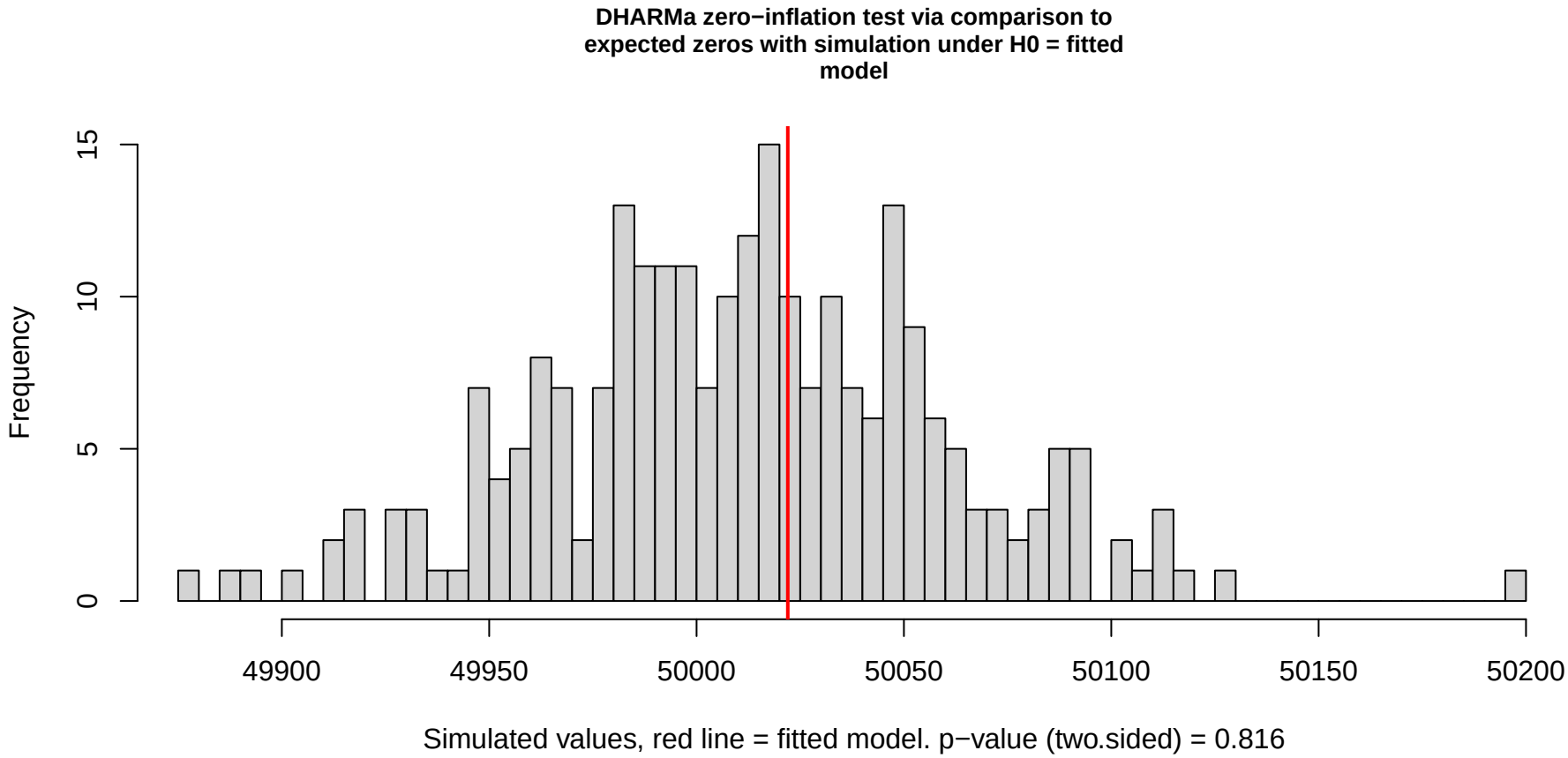

Betula pendula

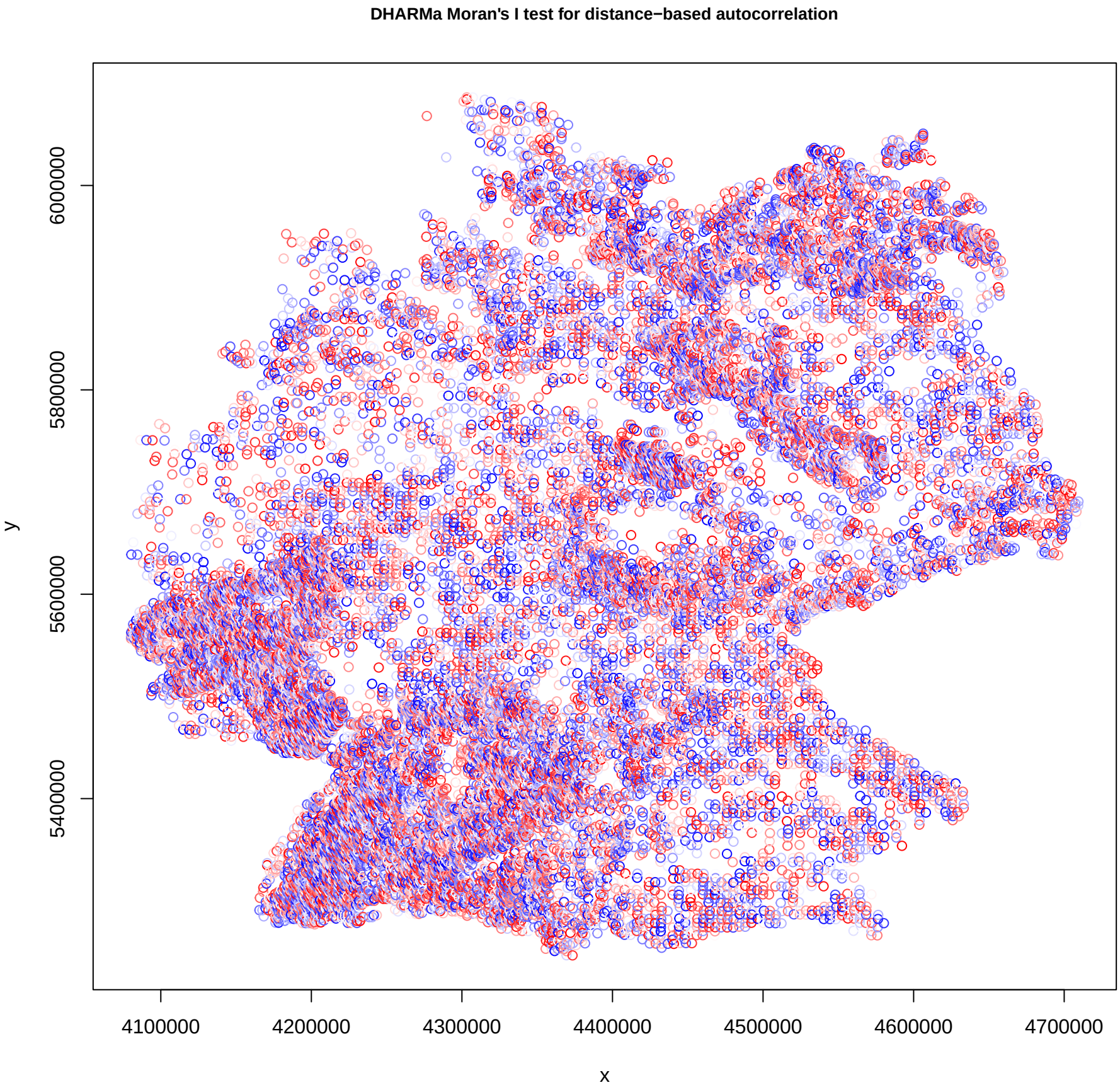

Betula pubescens

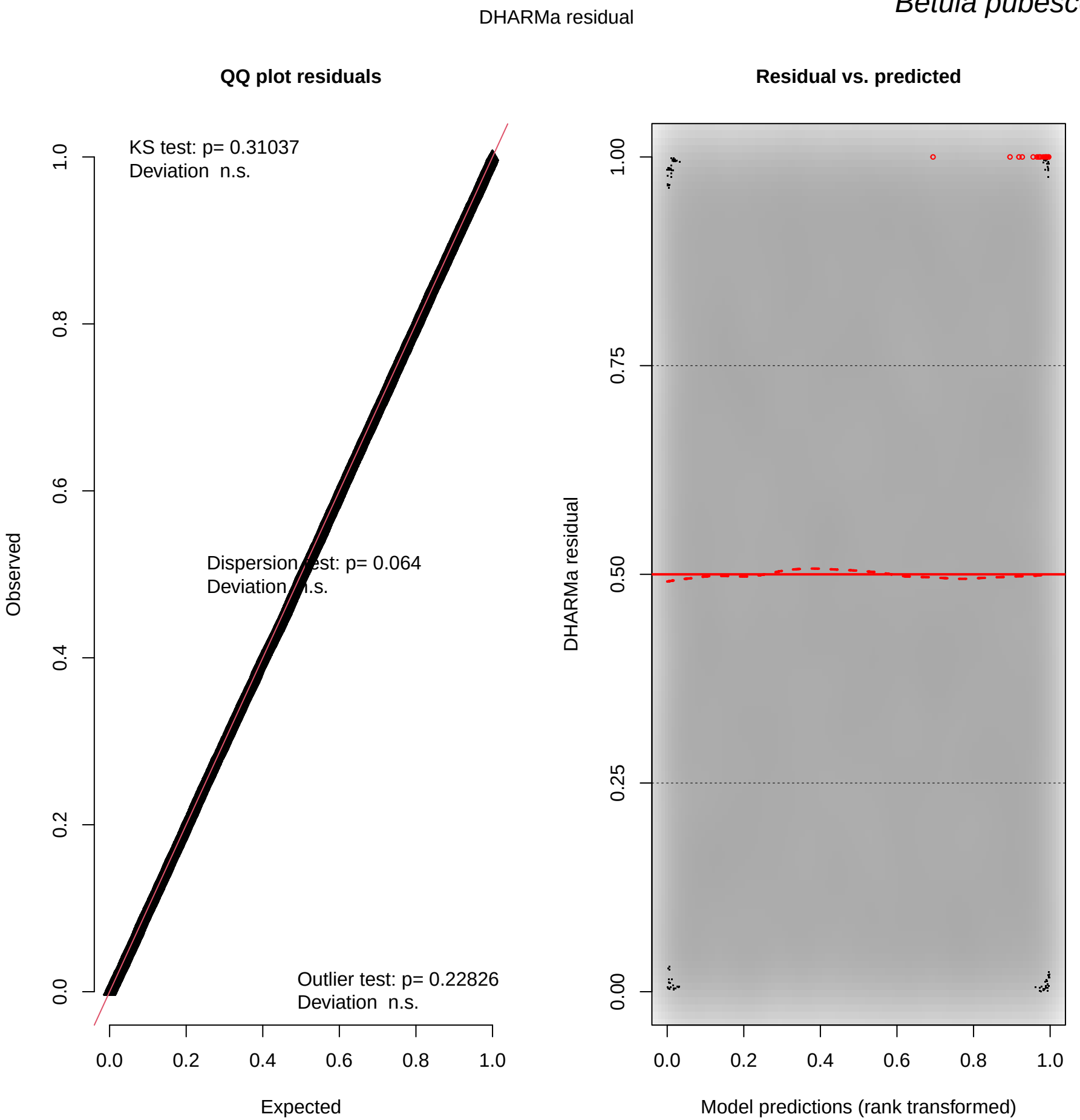

Betula pubescens

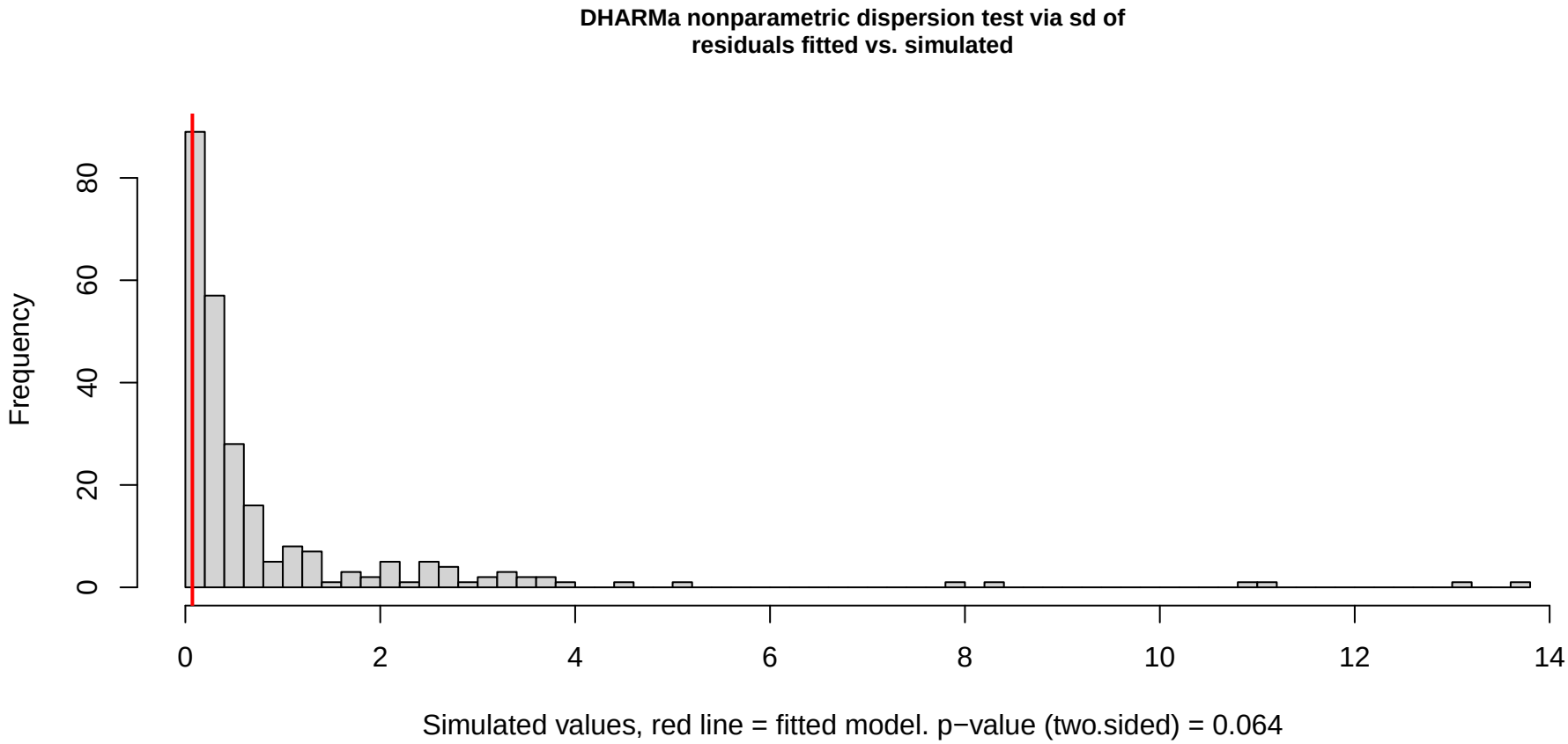

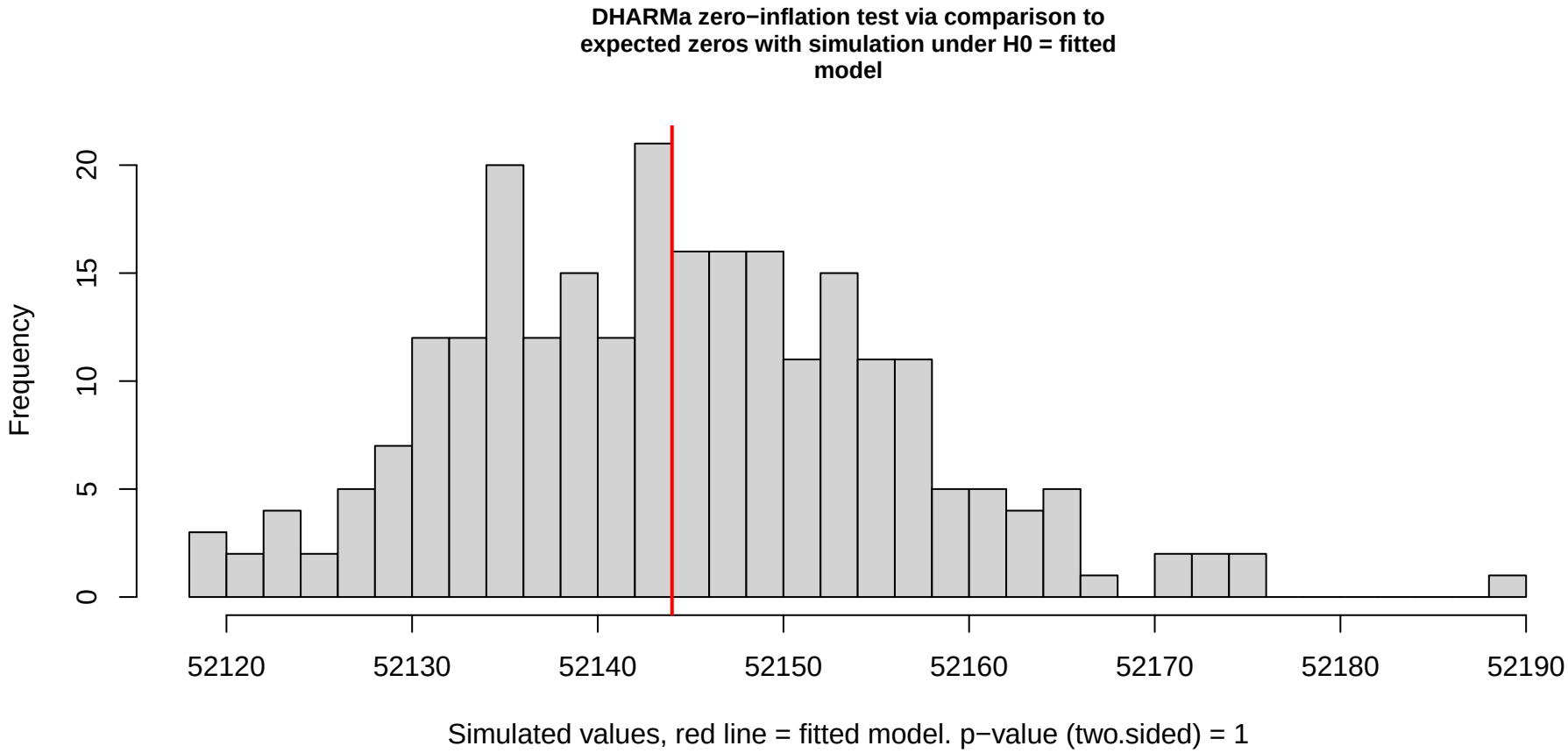

Betula pubescens

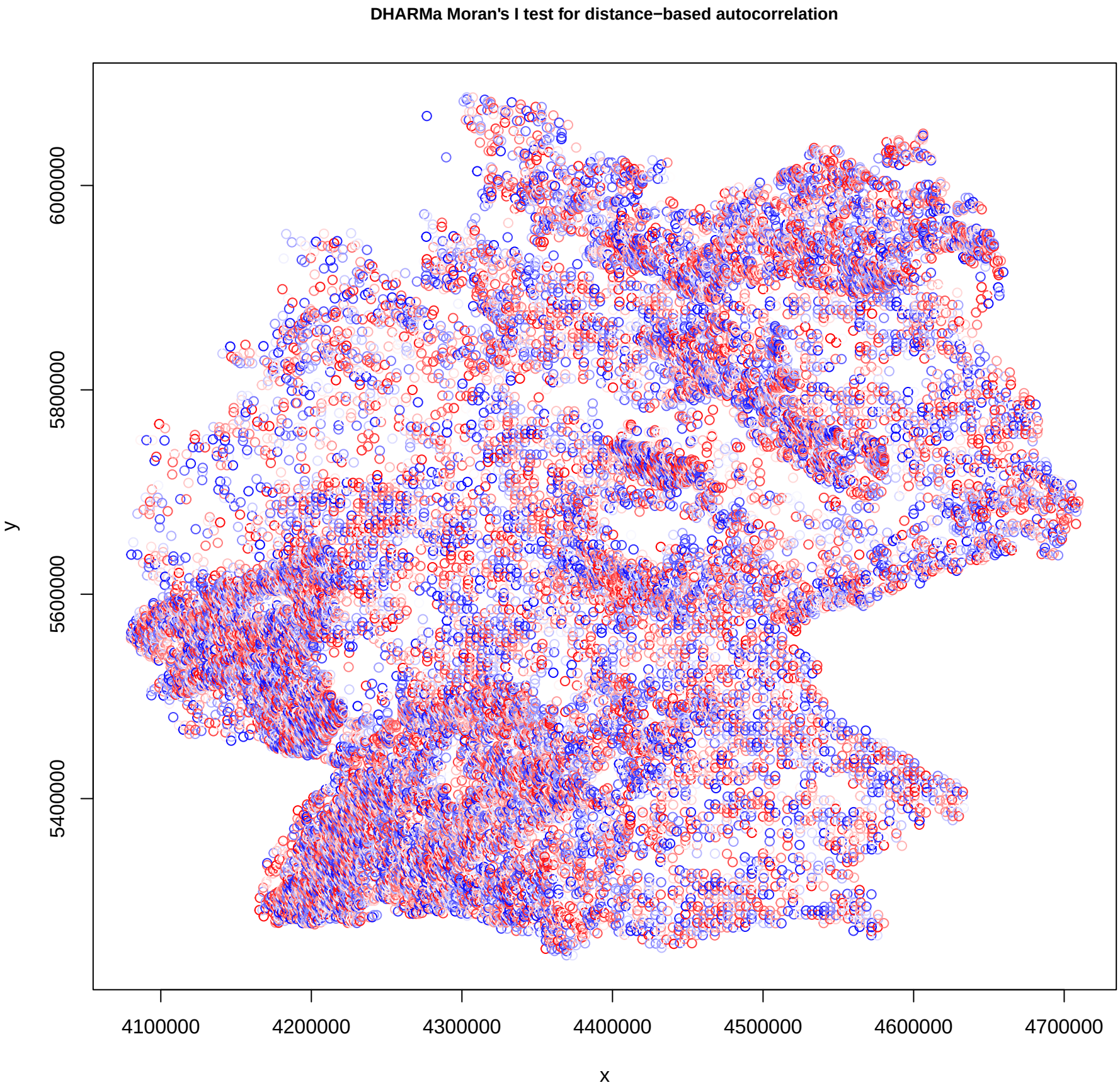

Larix decidua

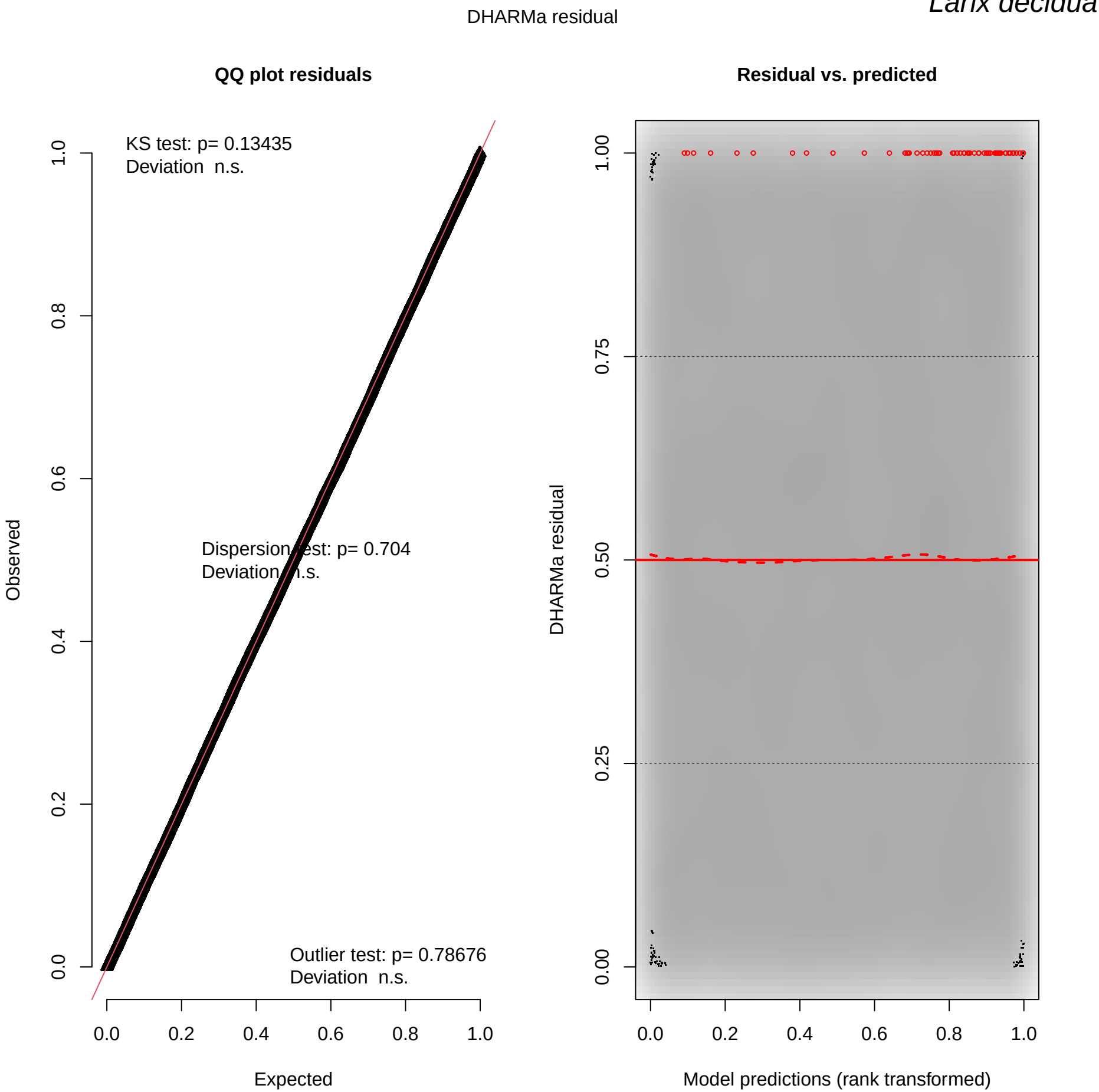

Larix decidua

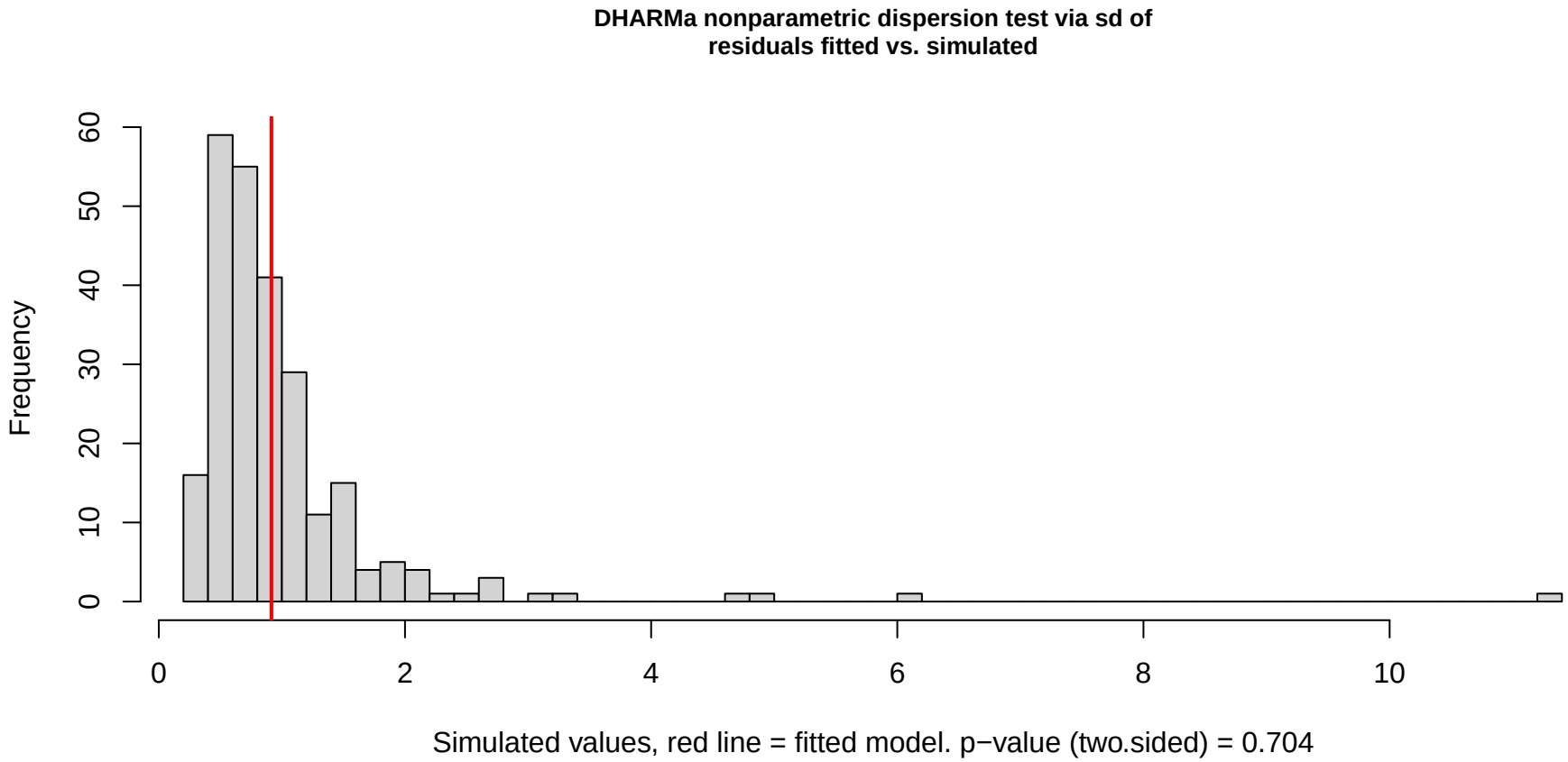

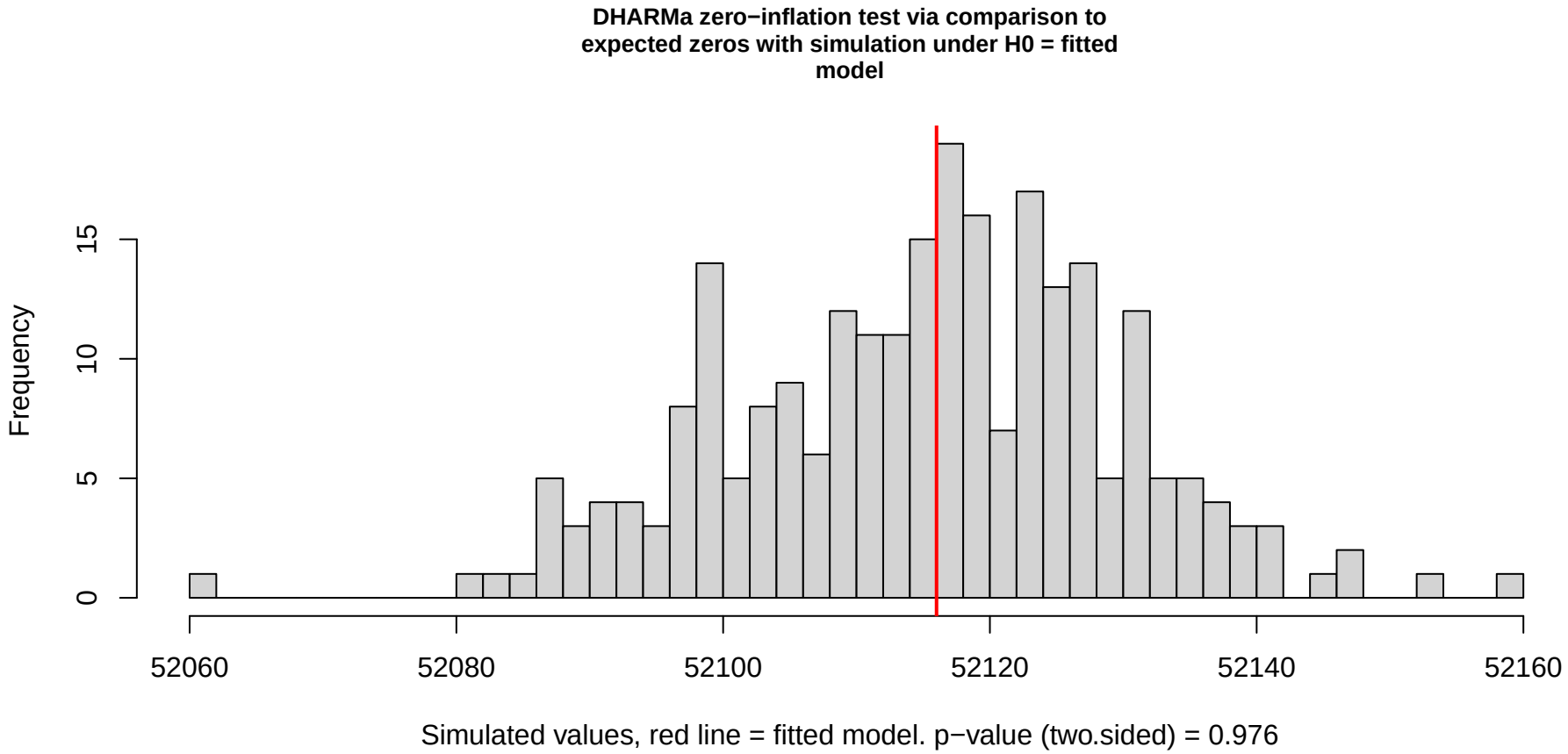

Larix decidua

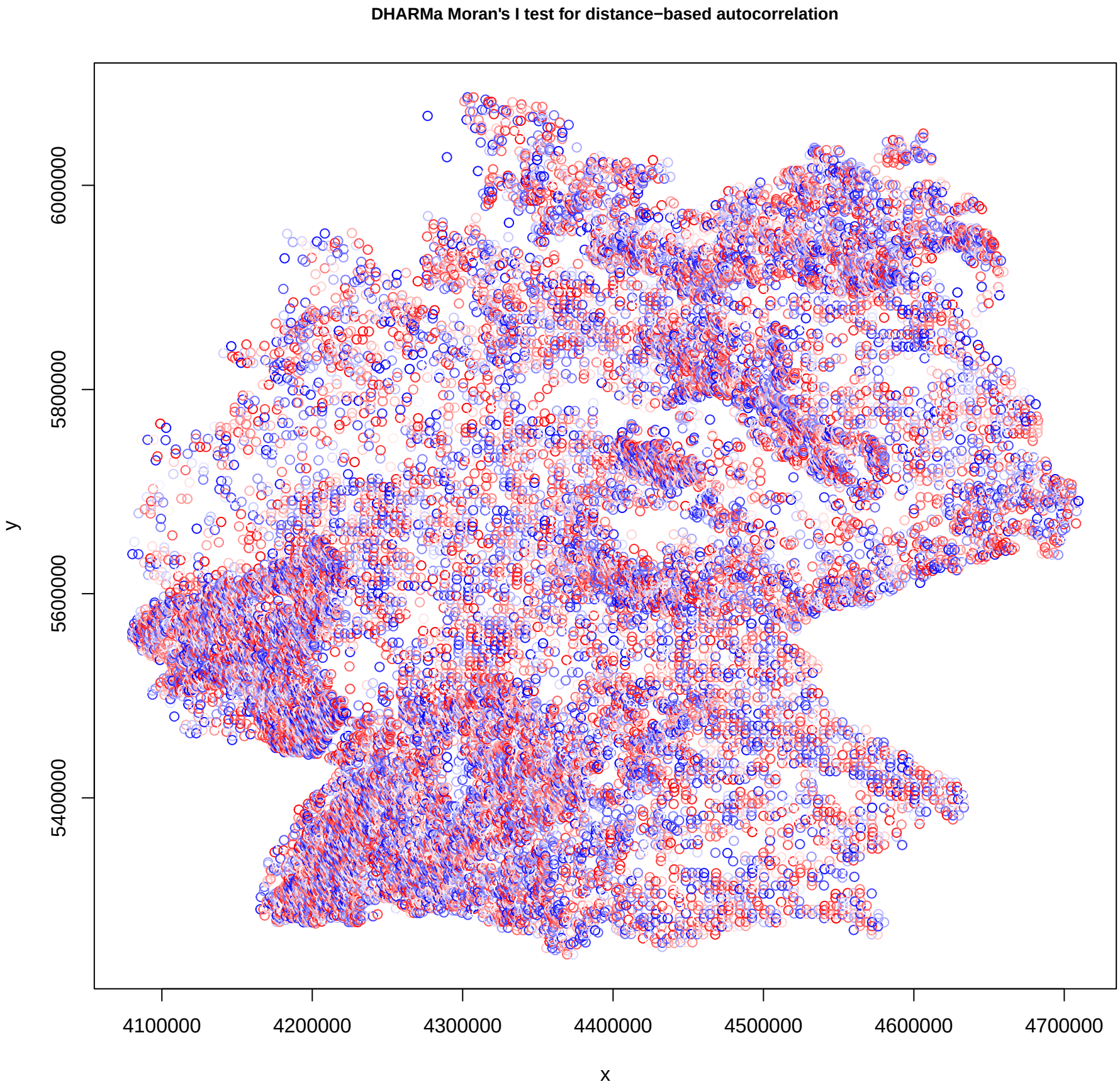

Larix kaempferi

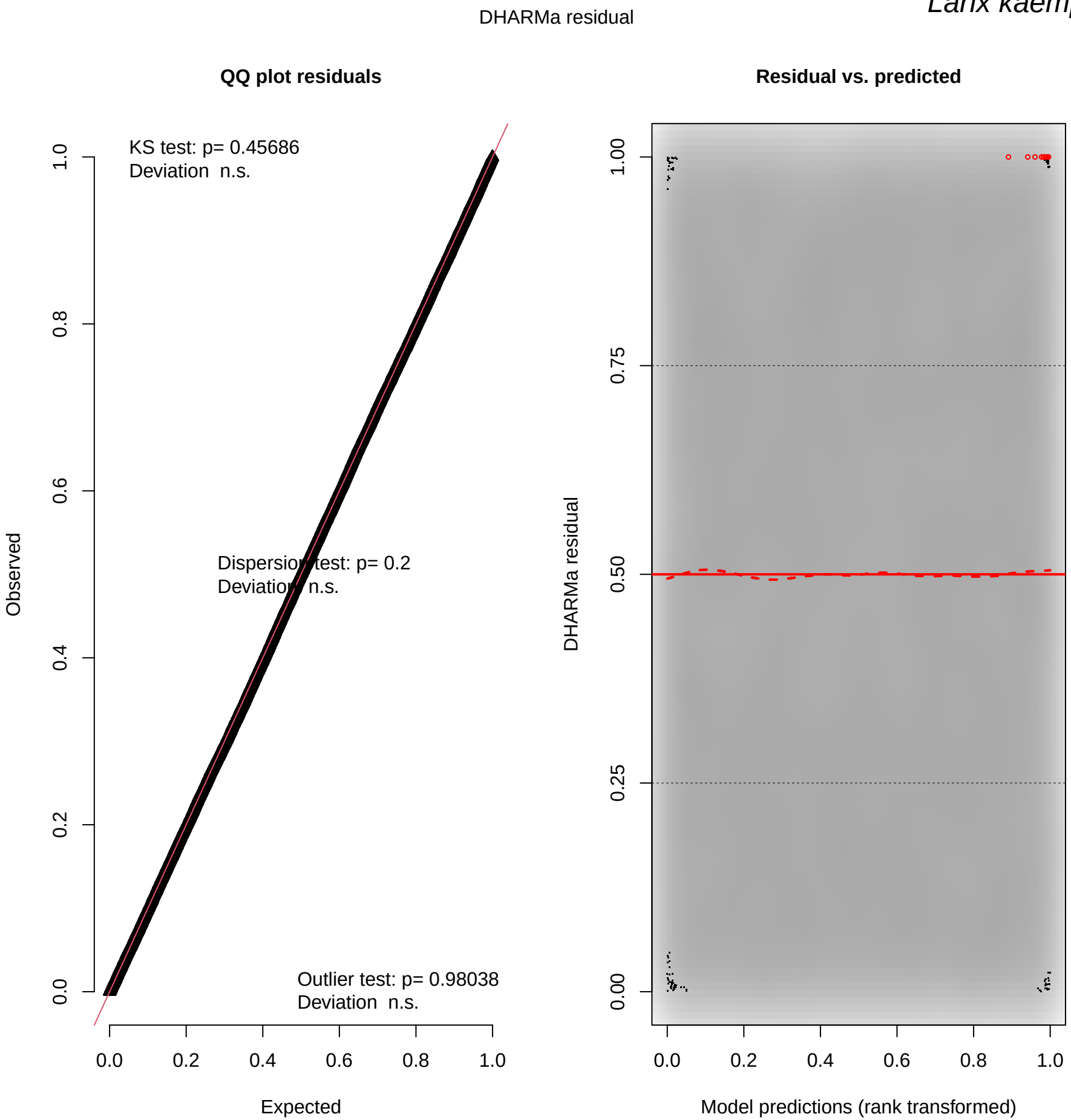

Larix kaempferi

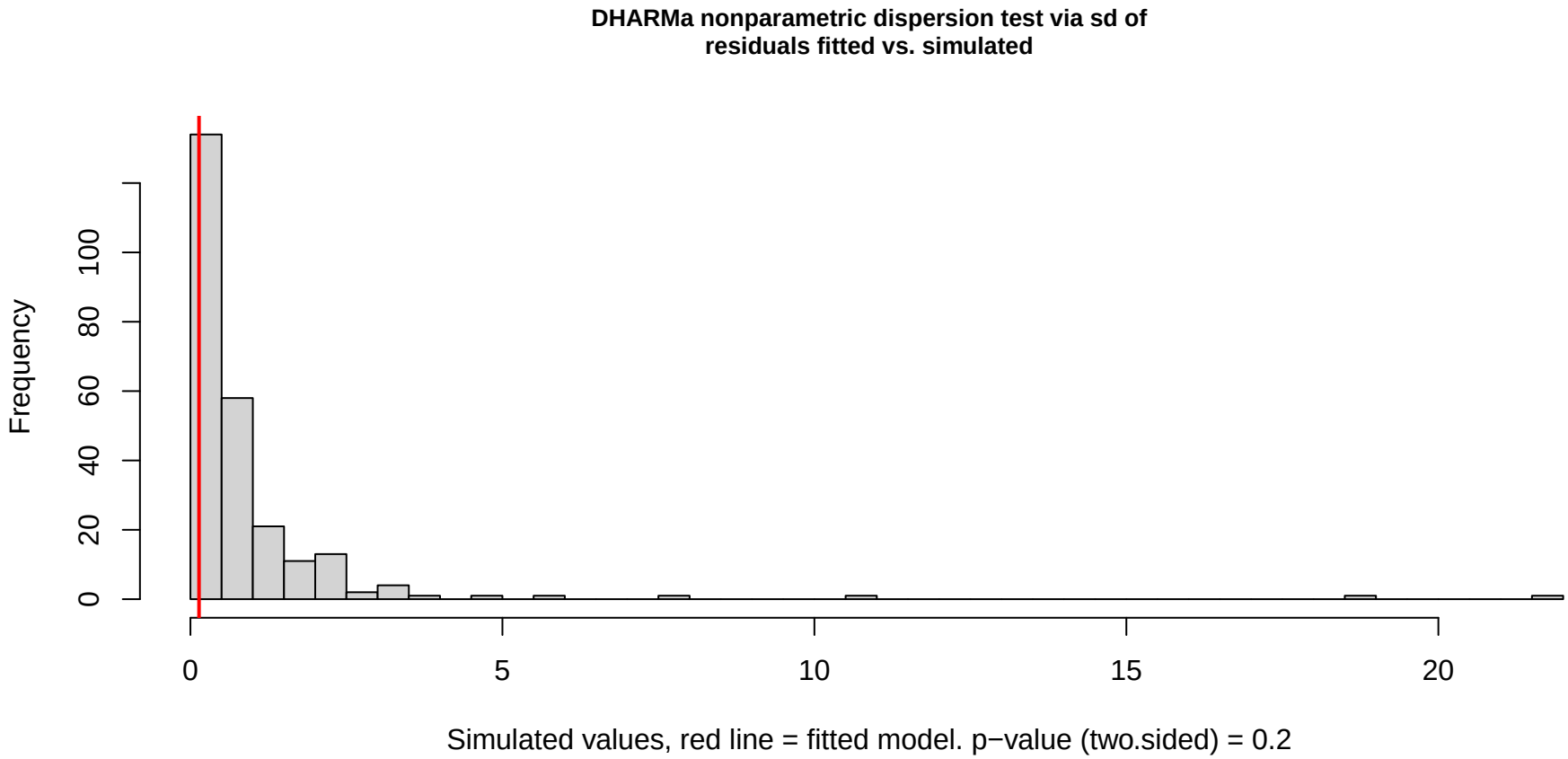

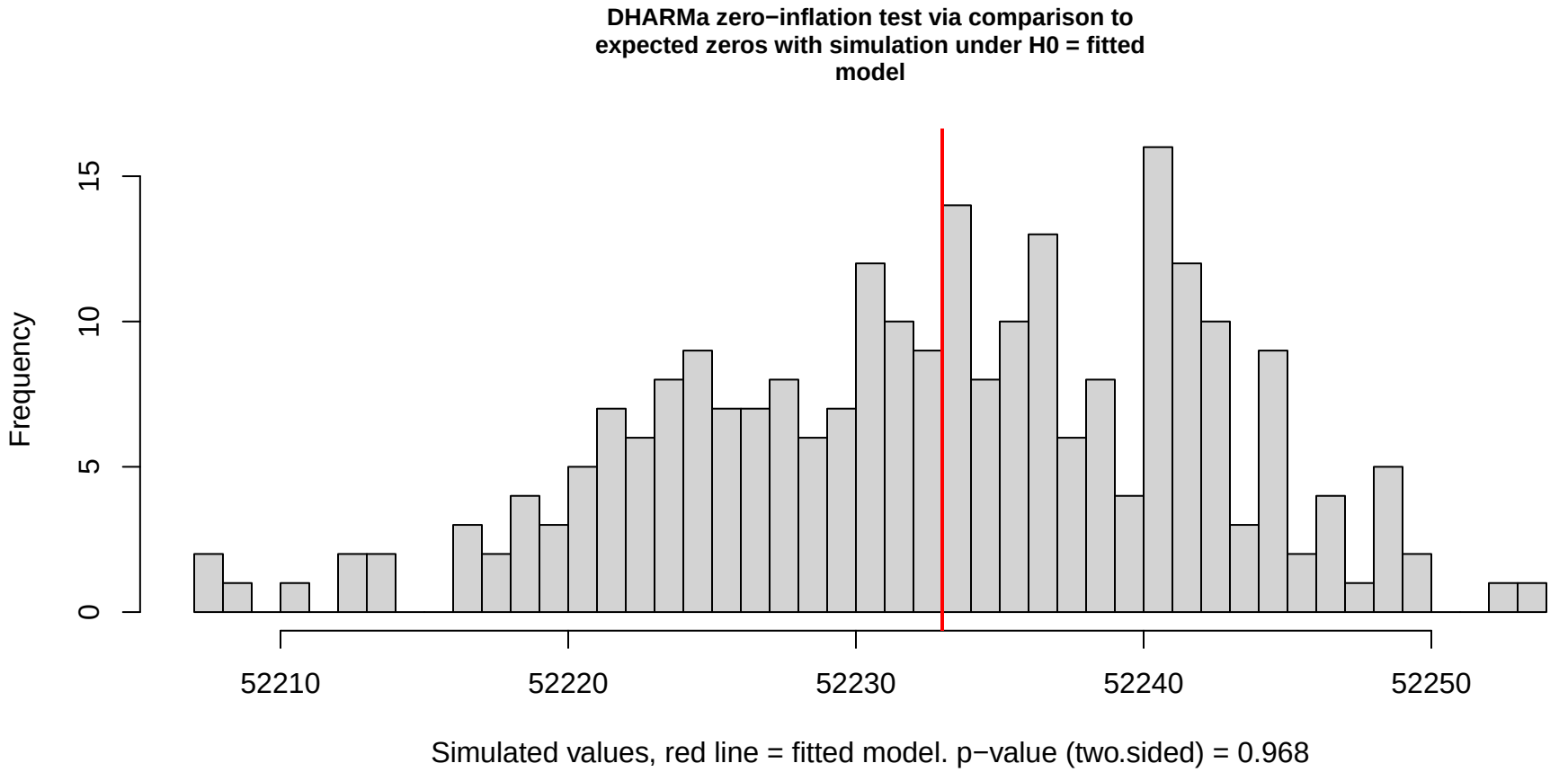

Larix kaempferi

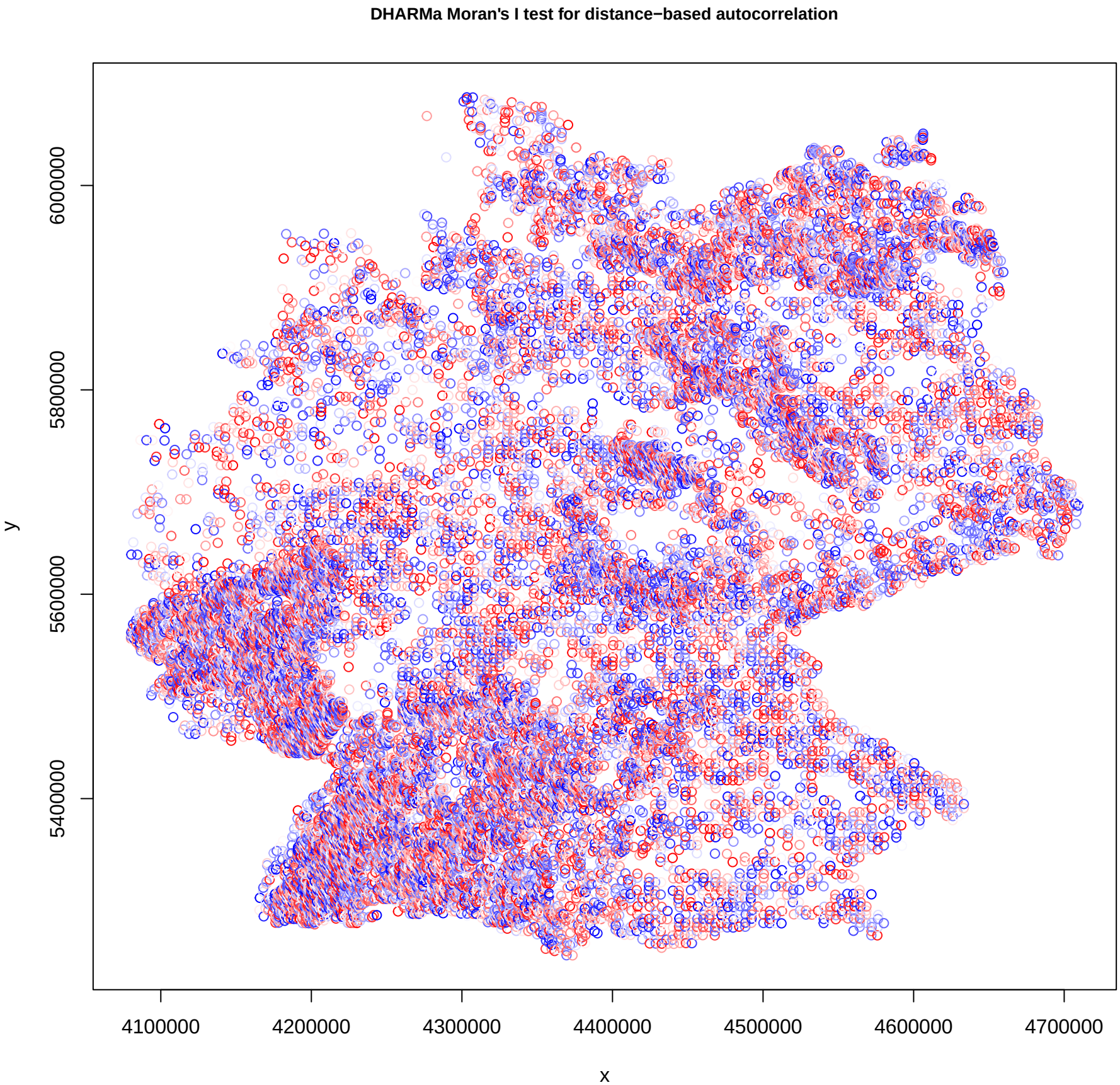

Pseudotsuga menziesii

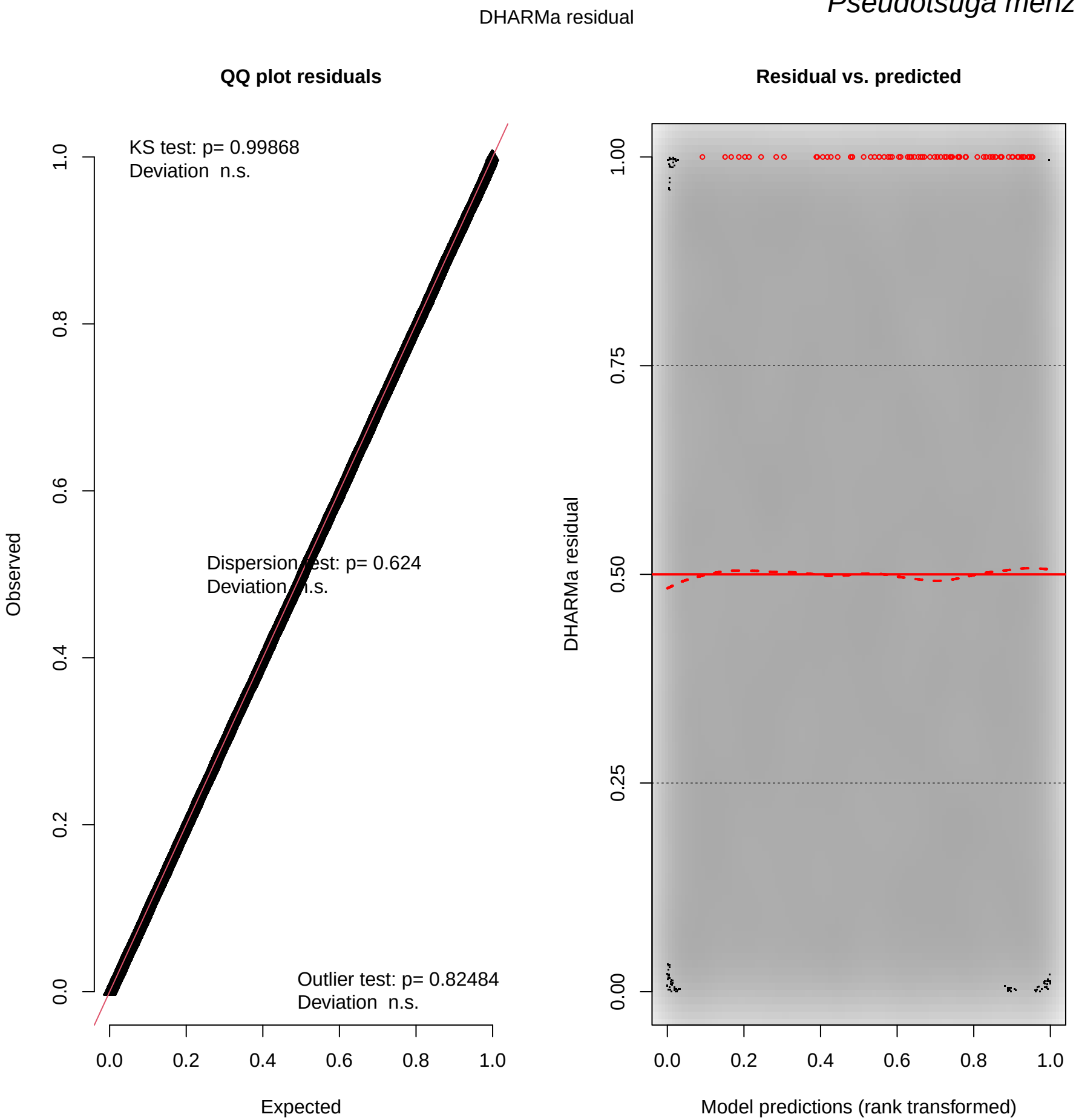

Pseudotsuga menziesii

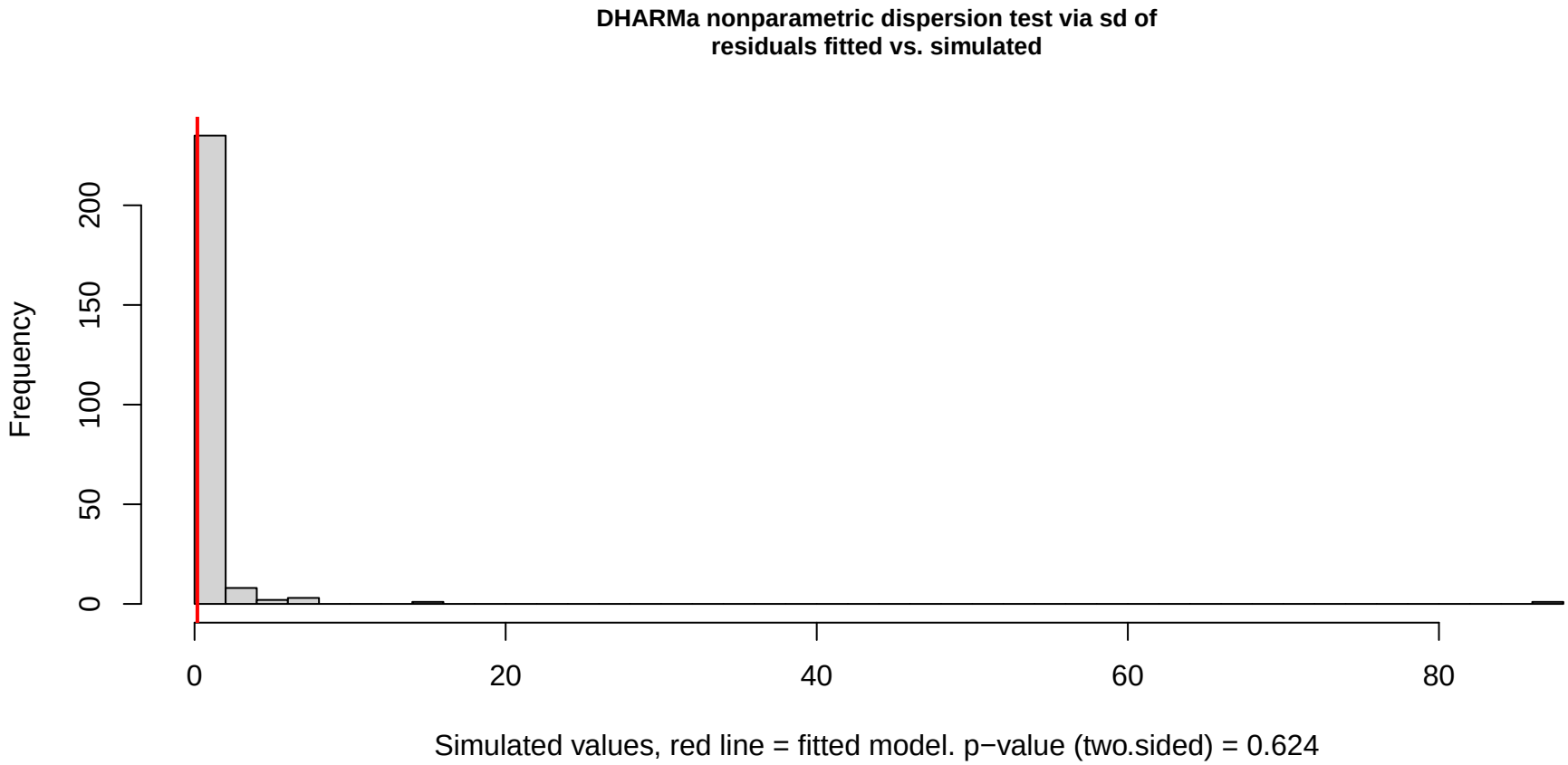

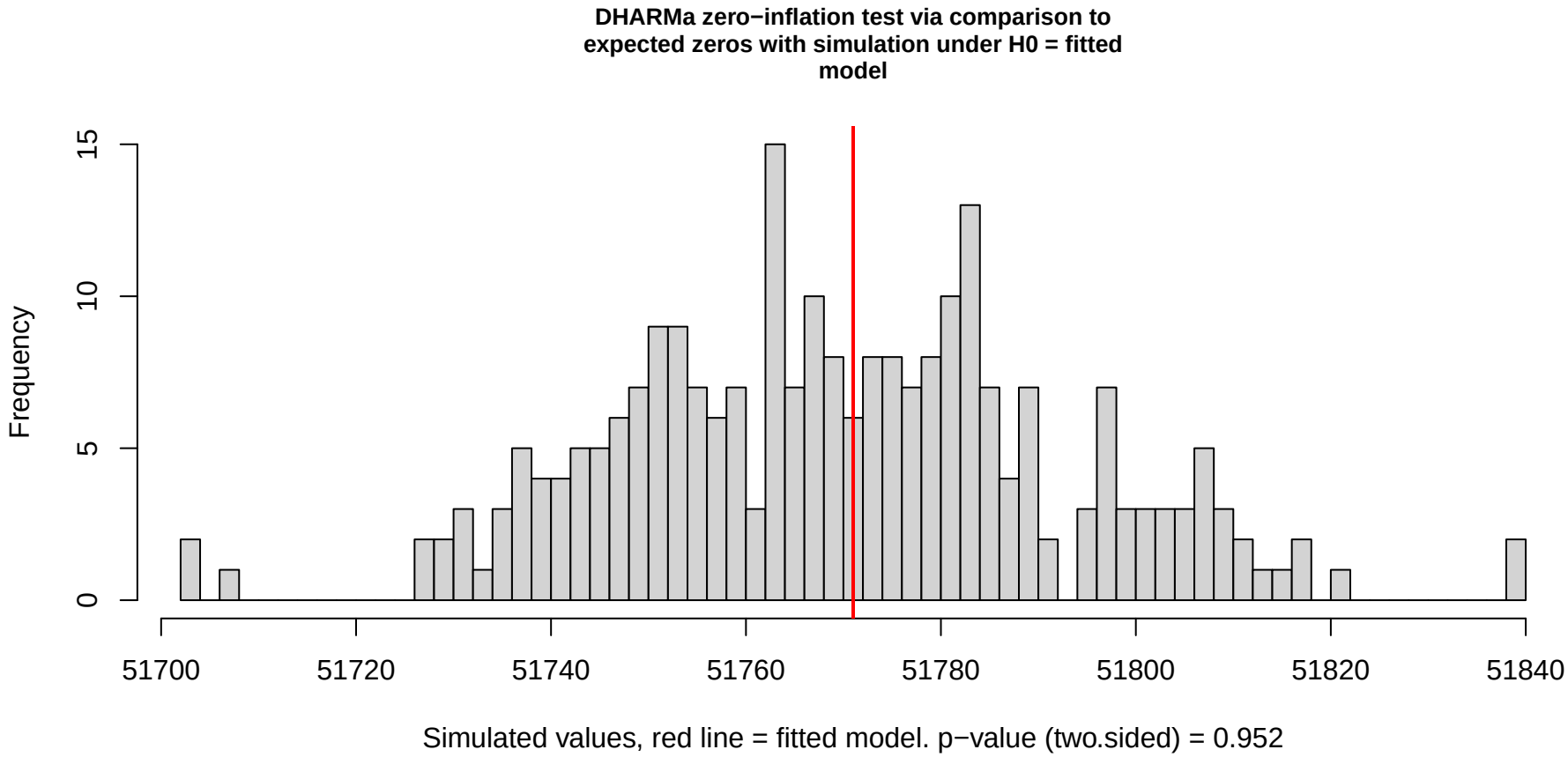

Pseudotsuga menziesii

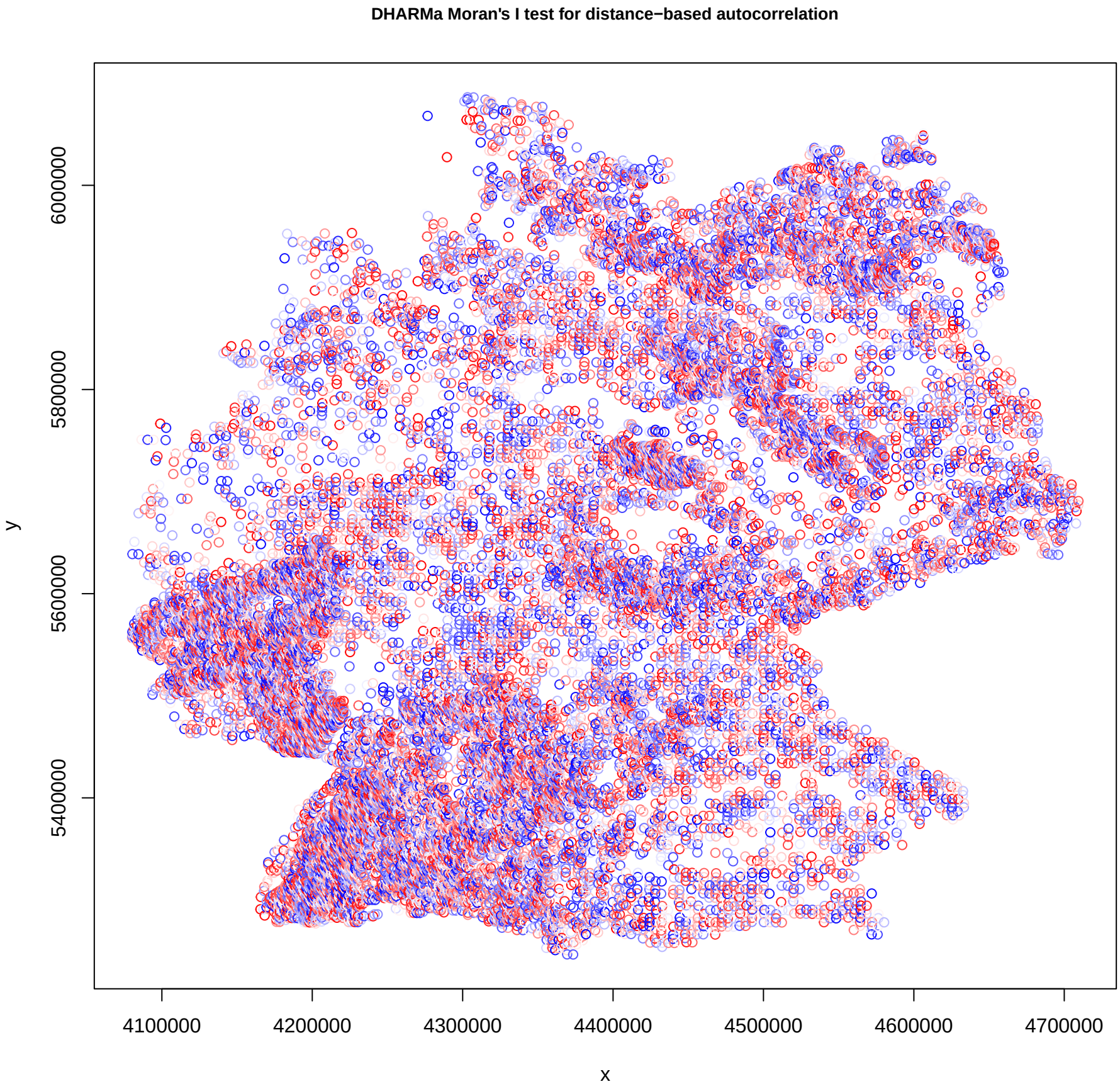

Pinus strobus

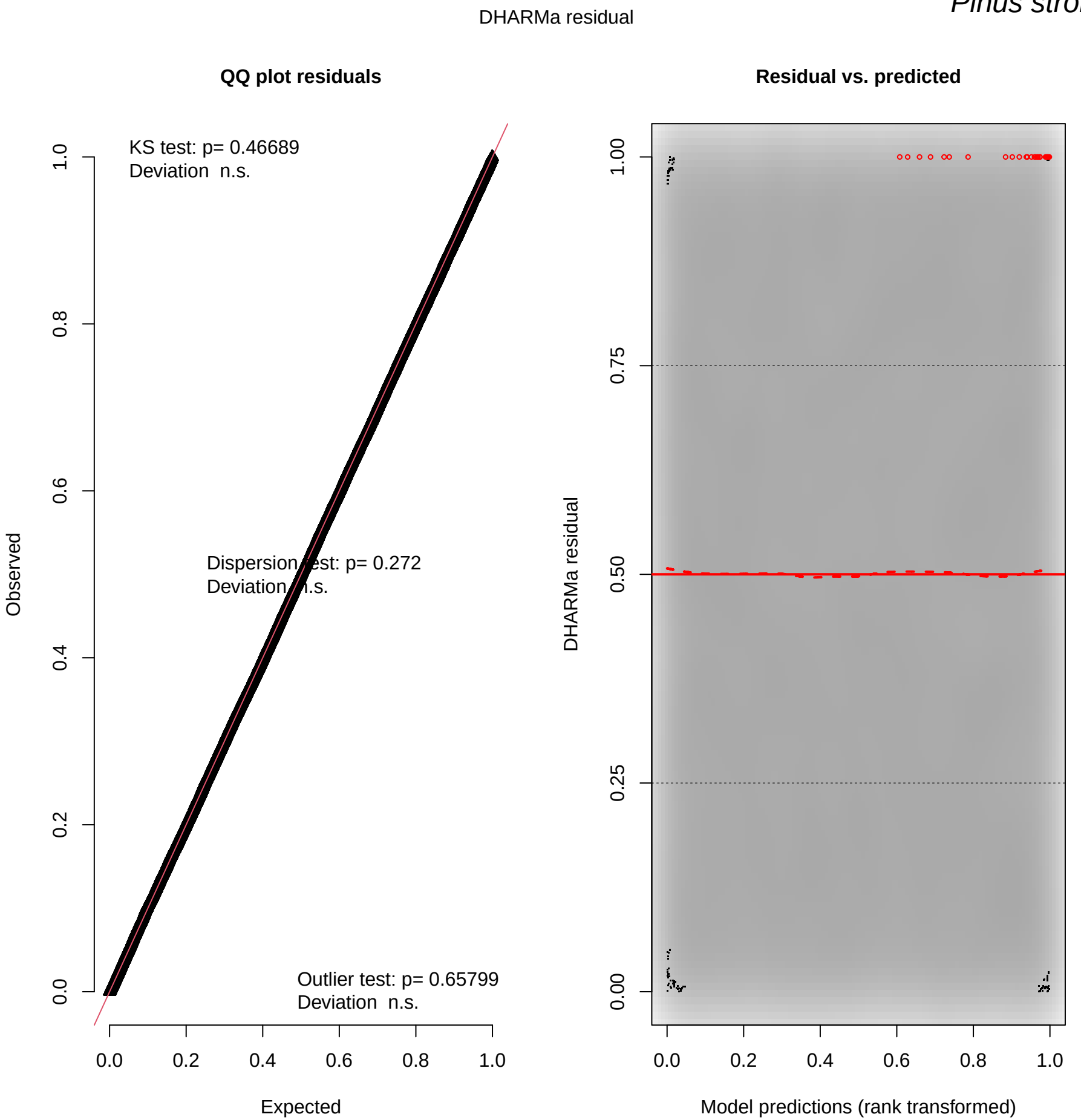

Pinus strobus

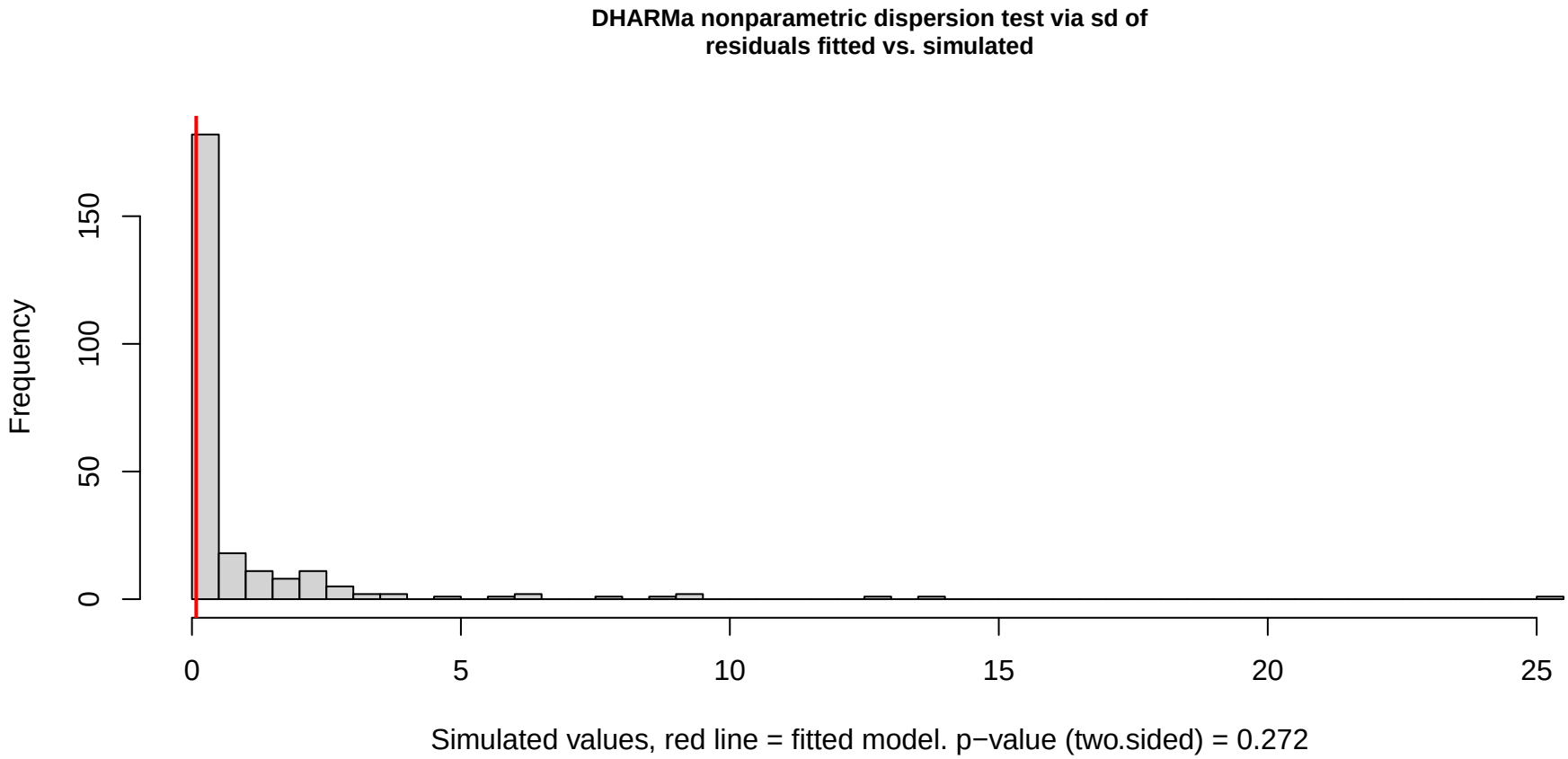

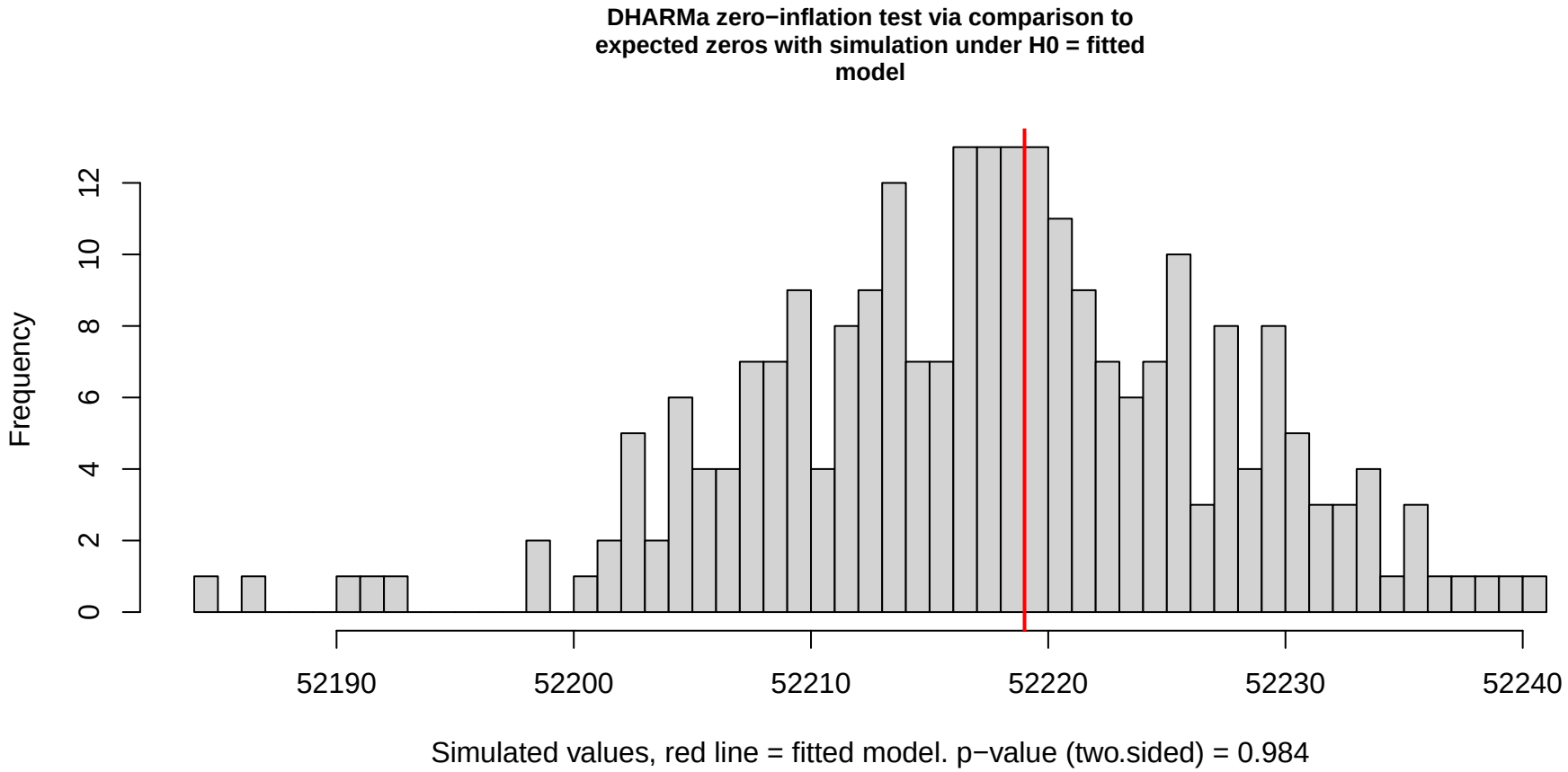

Pinus strobus

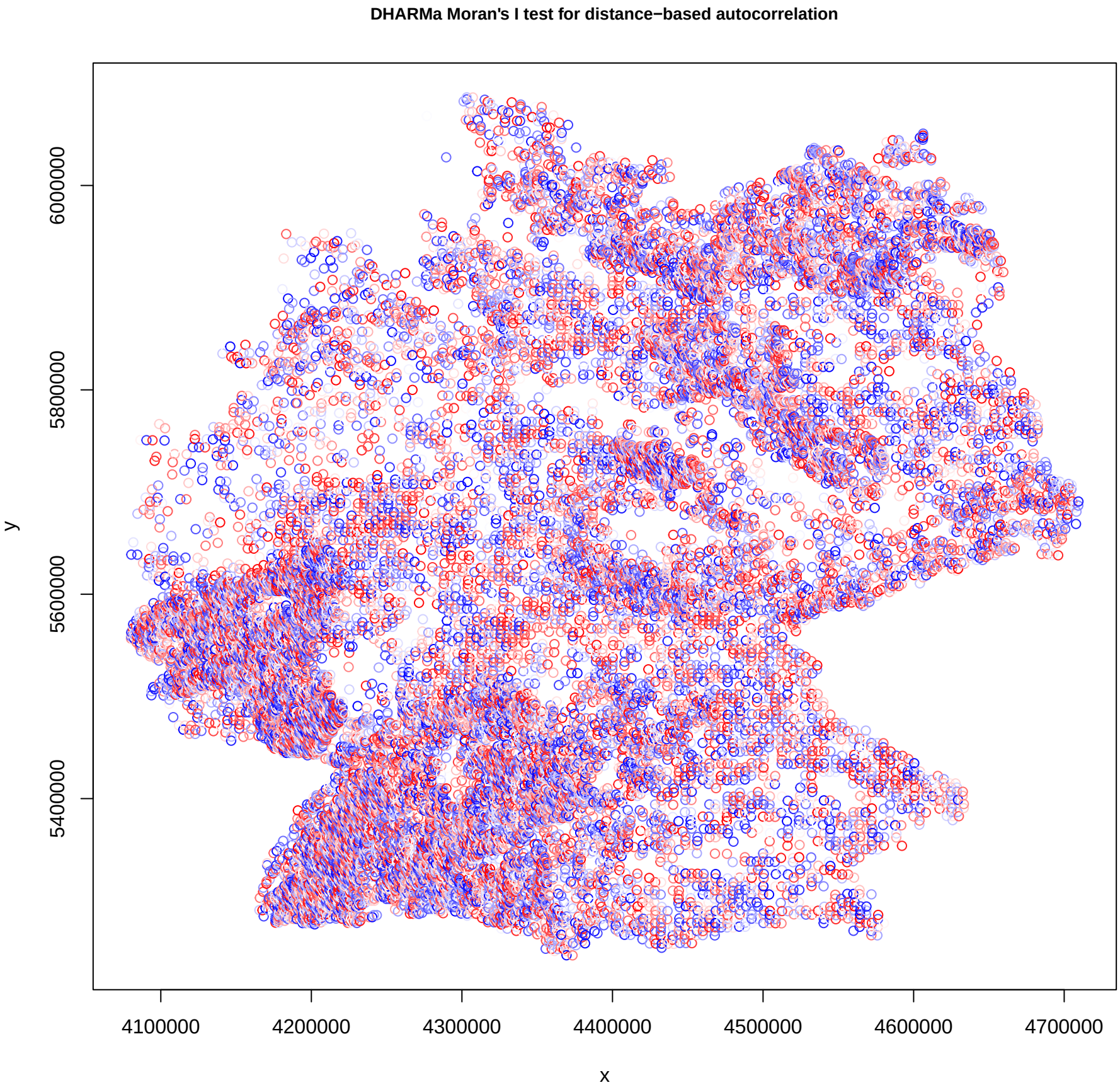

Pinus sylvestris

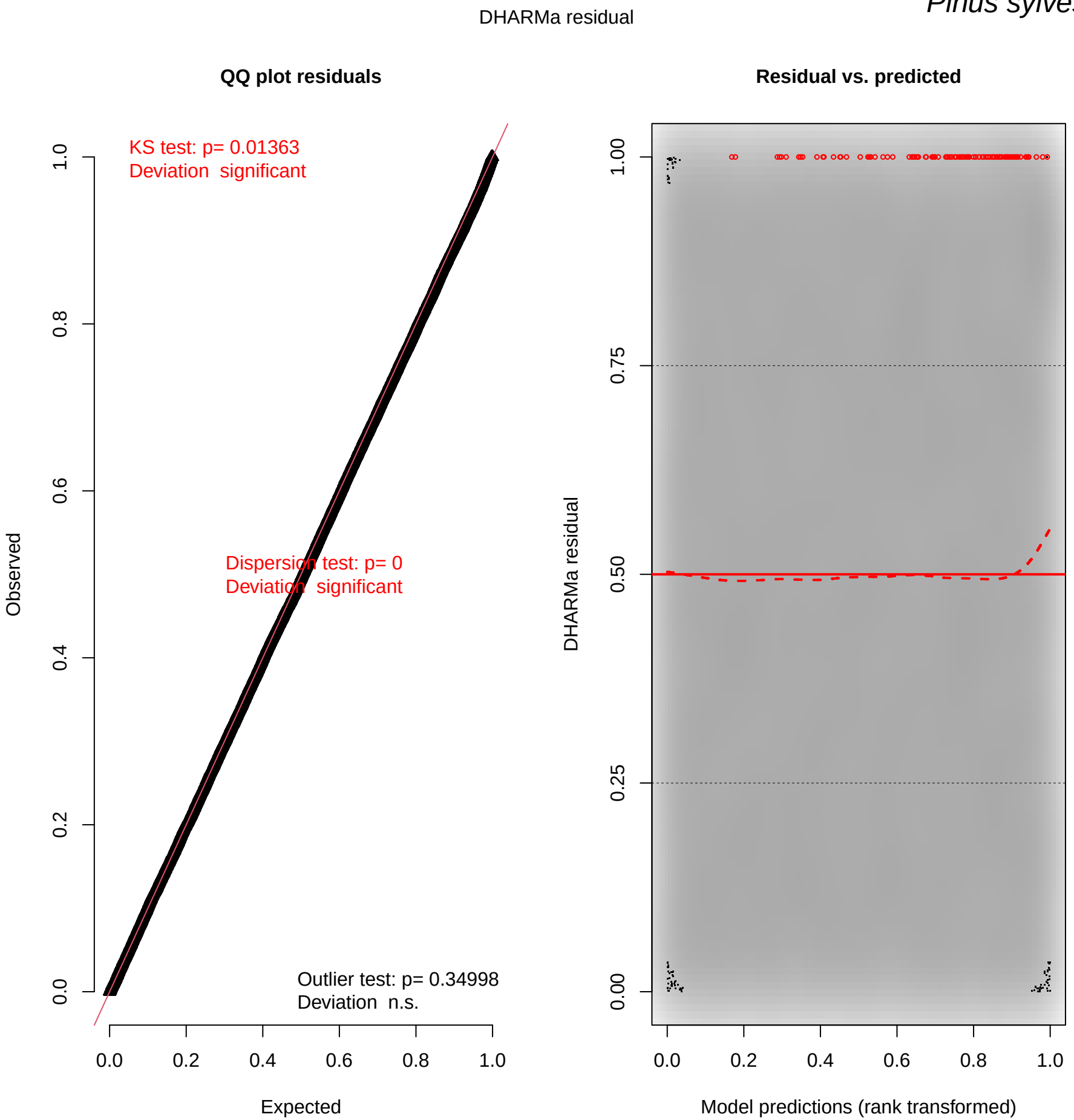

Pinus sylvestris

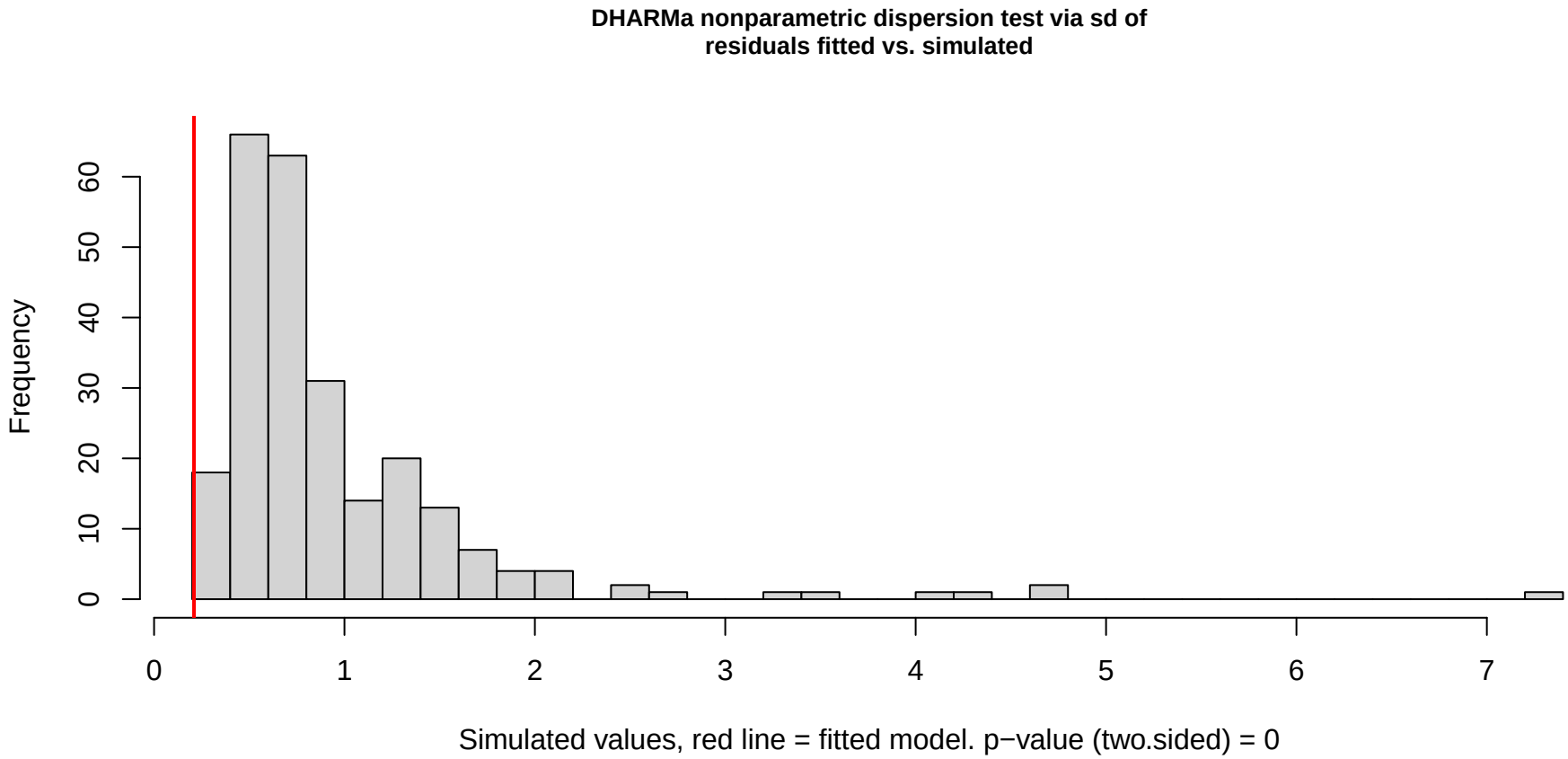

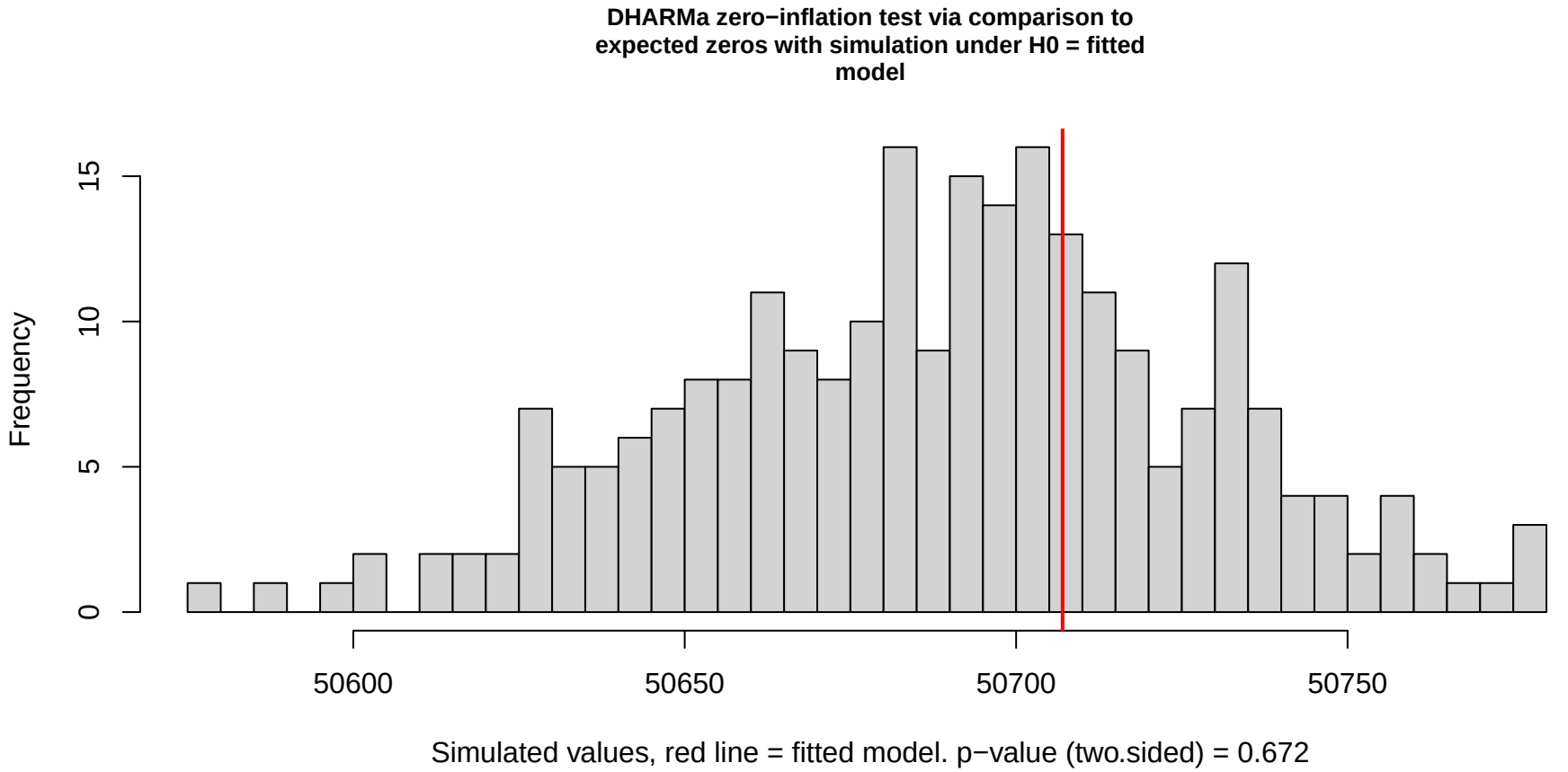

Pinus sylvestris

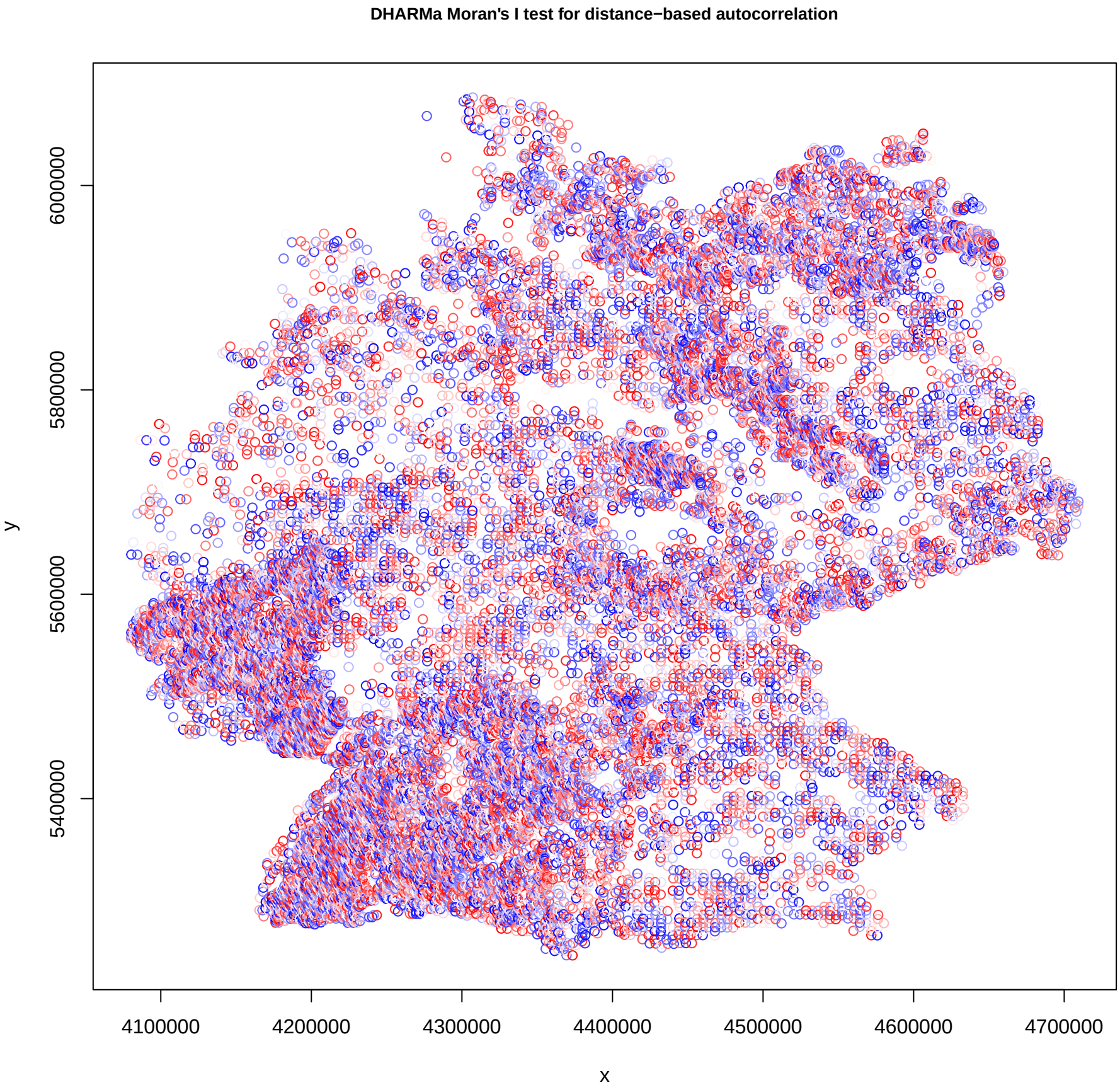

Pinus nigra

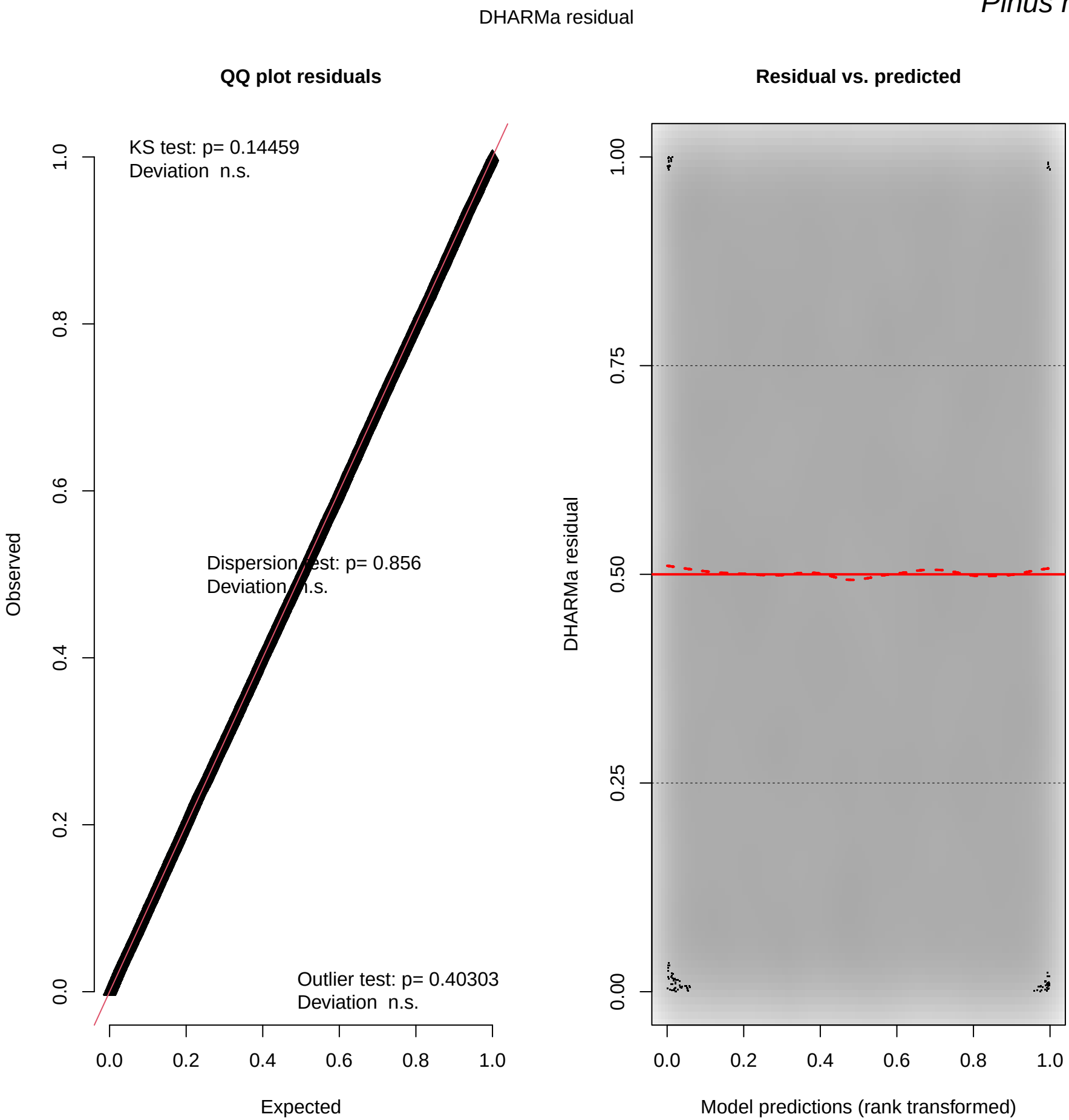
DHARMa residual
QQ plot residuals
KS test: p= 0.14459
Deviation n.s.
Dispersion test: p= 0.856
Deviation n.s.
Outlier test: p= 0.40303
Deviation n.s.
Observed
Expected
0.0
0.2
0.4
0.6
0.8
1.0
Residual vs. predicted
DHARMa residual
Model predictions (rank transformed)
0.00
0.25
0.50
0.75
1.00

Pinus nigra

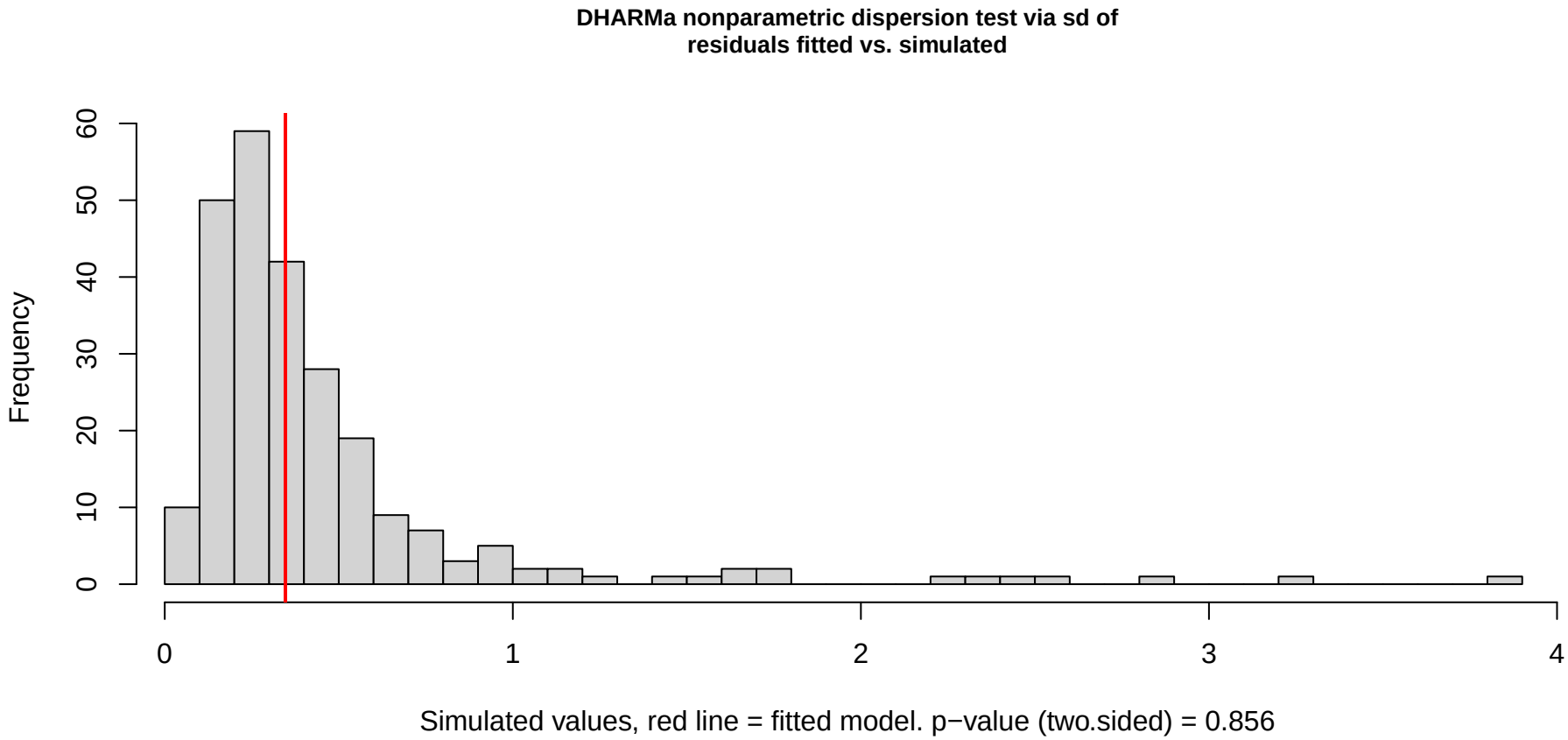
DHARMa nonparametric dispersion test via sd of residuals fitted vs. simulated
Frequency
0
10
20
30
40
50
60
0
1
2
3
4
Simulated values, red line = fitted model. p−value (two.sided) = 0.856

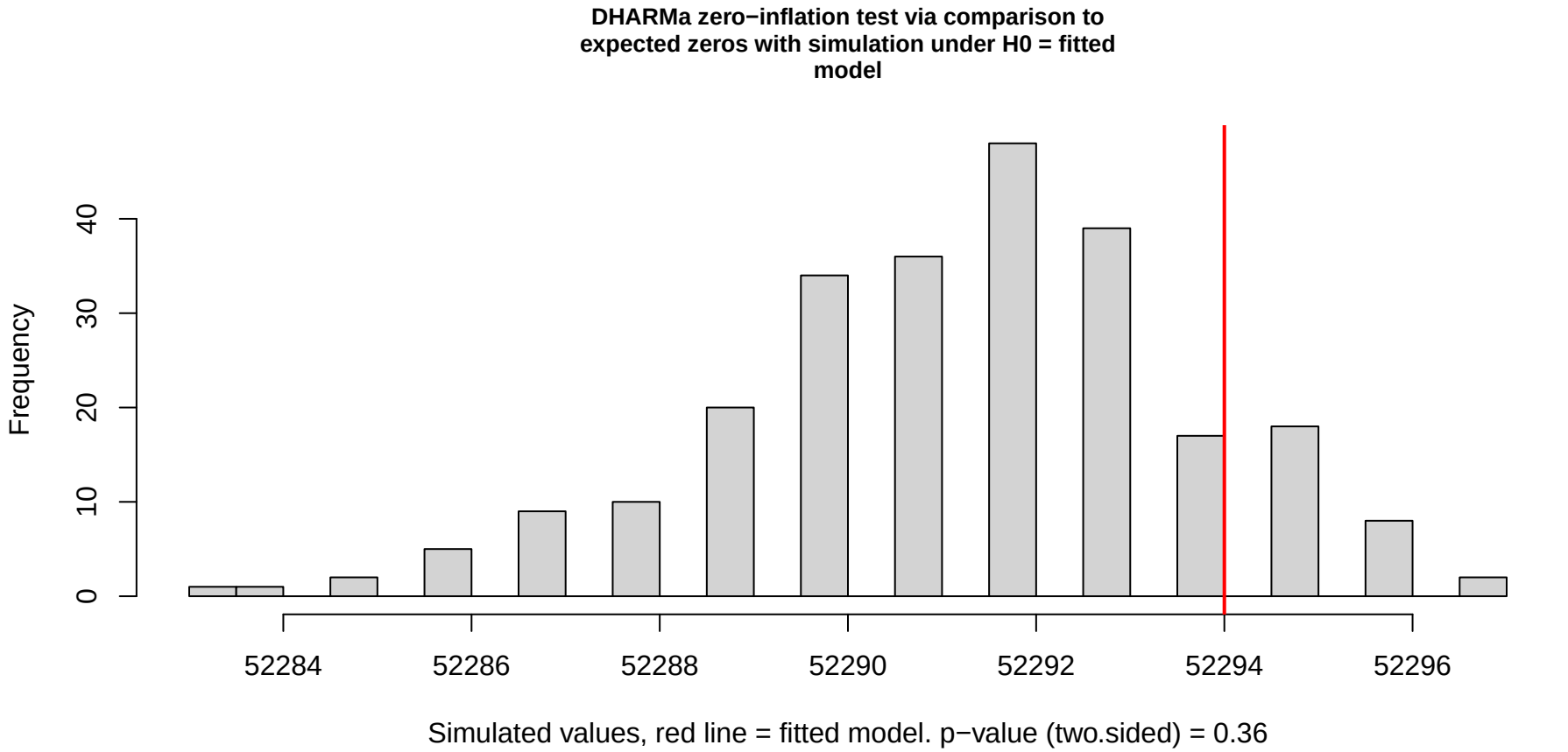
DHARMa zero−inflation test via comparison to expected zeros with simulation under H0 = fitted model
Frequency
0
10
20
30
40
52284
52286
52288
52290
52292
52294
52296
Simulated values, red line = fitted model. p−value (two.sided) = 0.36

Pinus nigra

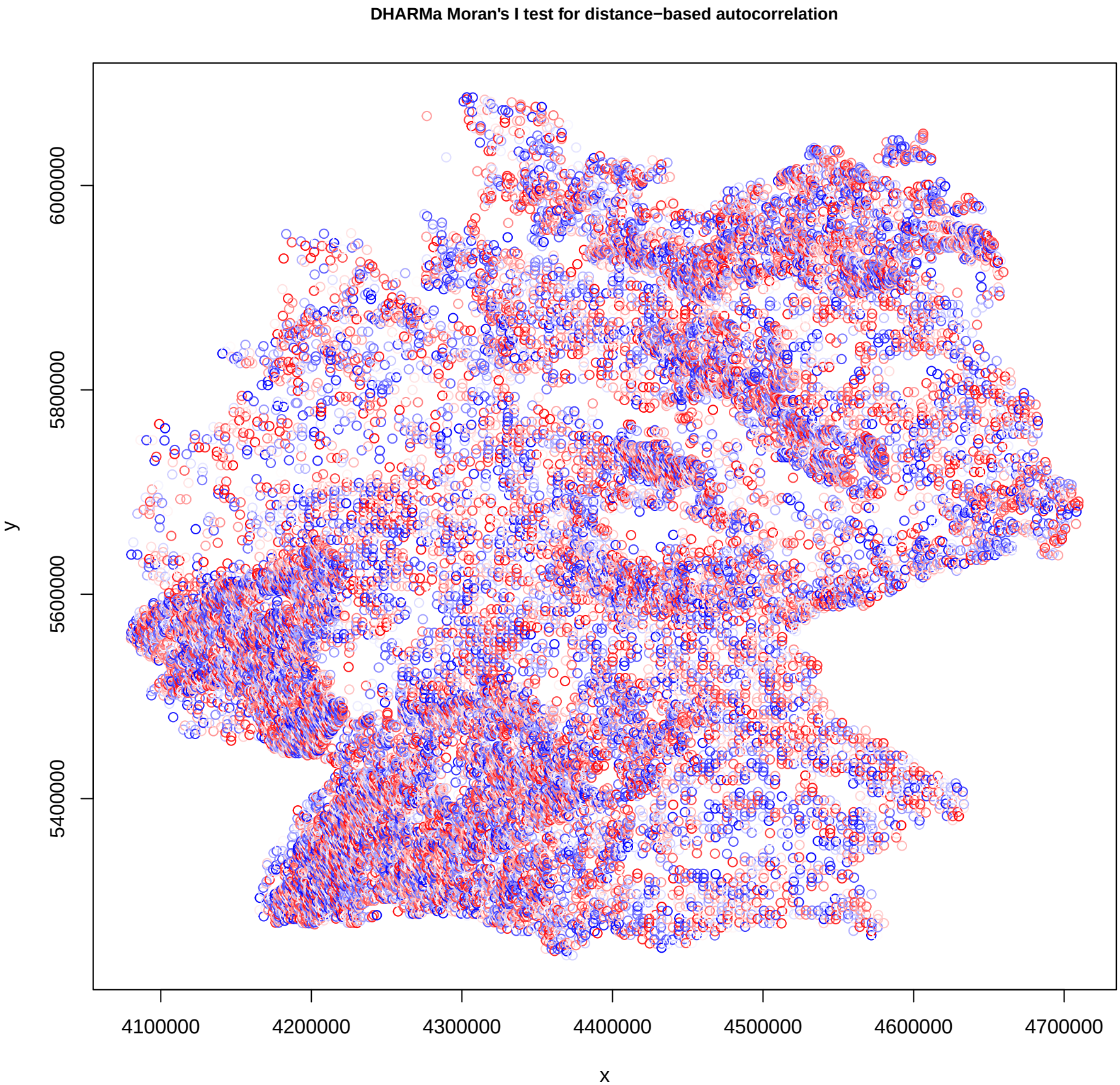
DHARMa Moran's I test for distance−based autocorrelation
y
6000000
5800000
5600000
5400000
x
4100000
4200000
4300000
4400000
4500000
4600000
4700000

Picea abies

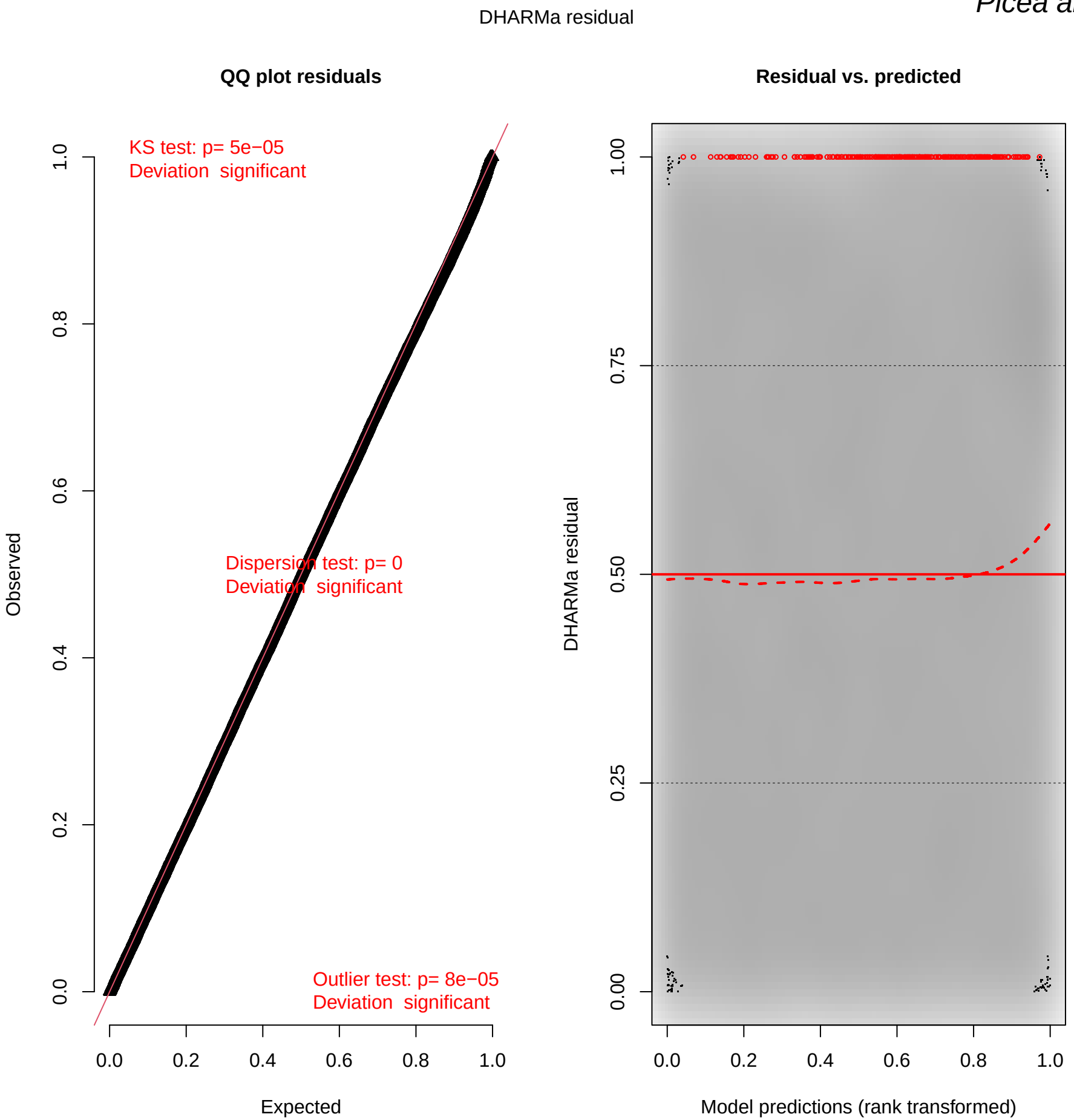
DHARMa residual
QQ plot residuals
KS test: p= 5e−05
Deviation significant
Dispersion test: p= 0
Deviation significant
Outlier test: p= 8e−05
Deviation significant
Observed
Expected
0.0
0.2
0.4
0.6
0.8
1.0
Residual vs. predicted
DHARMa residual
Model predictions (rank transformed)
0.00
0.25
0.50
0.75
1.00

Picea abies

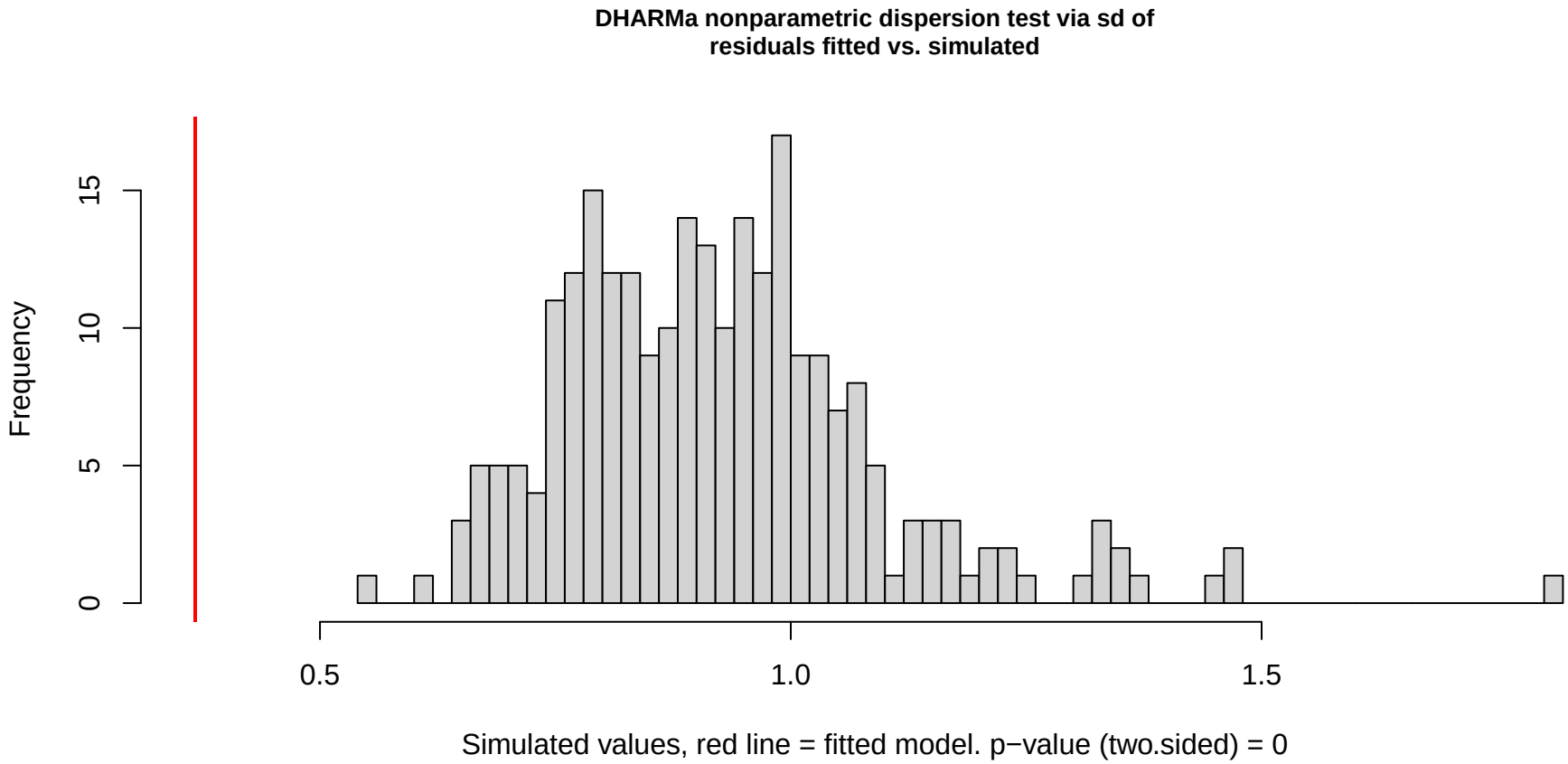
DHARMa nonparametric dispersion test via sd of residuals fitted vs. simulated
Frequency
0
5
10
15
0.5
1.0
1.5
Simulated values, red line = fitted model. p−value (two.sided) = 0

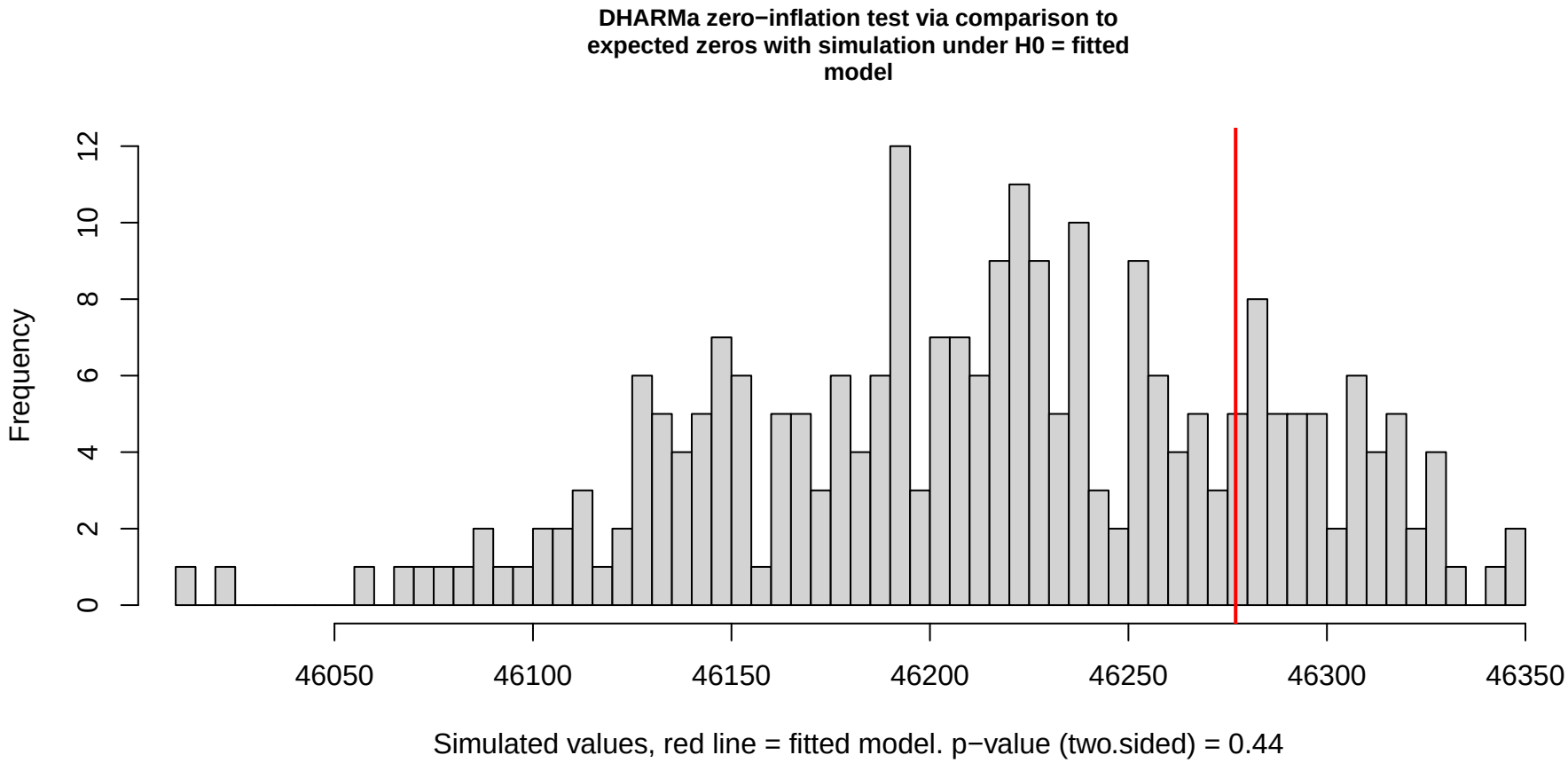
DHARMa zero−inflation test via comparison to expected zeros with simulation under H0 = fitted model
Frequency
0
2
4
6
8
10
12
46050
46100
46150
46200
46250
46300
46350
Simulated values, red line = fitted model. p−value (two.sided) = 0.44

Picea abies

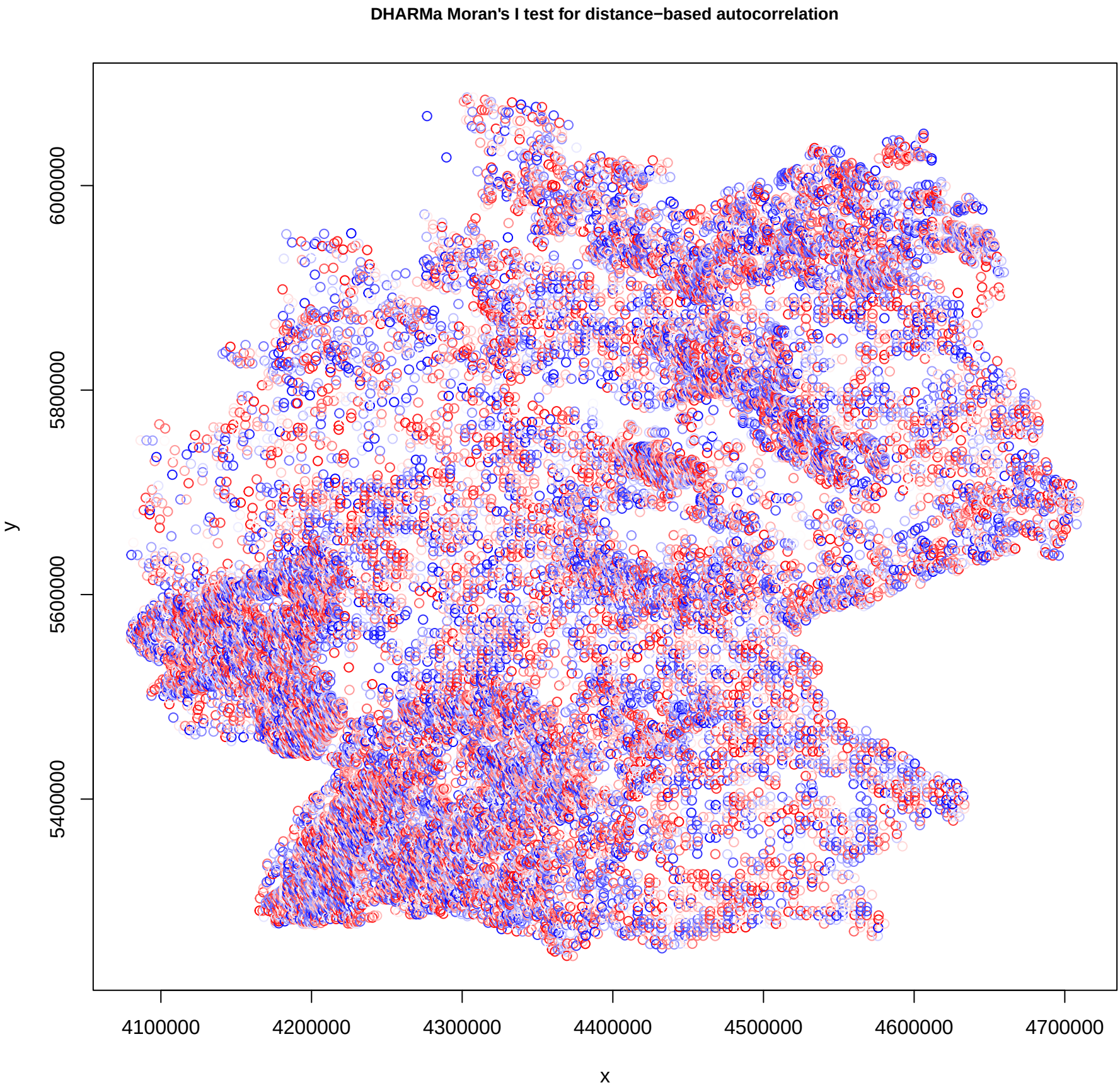
DHARMa Moran's I test for distance−based autocorrelation
y
6000000
5800000
5600000
5400000
x
4100000
4200000
4300000
4400000
4500000
4600000
4700000

Picea sitchensis

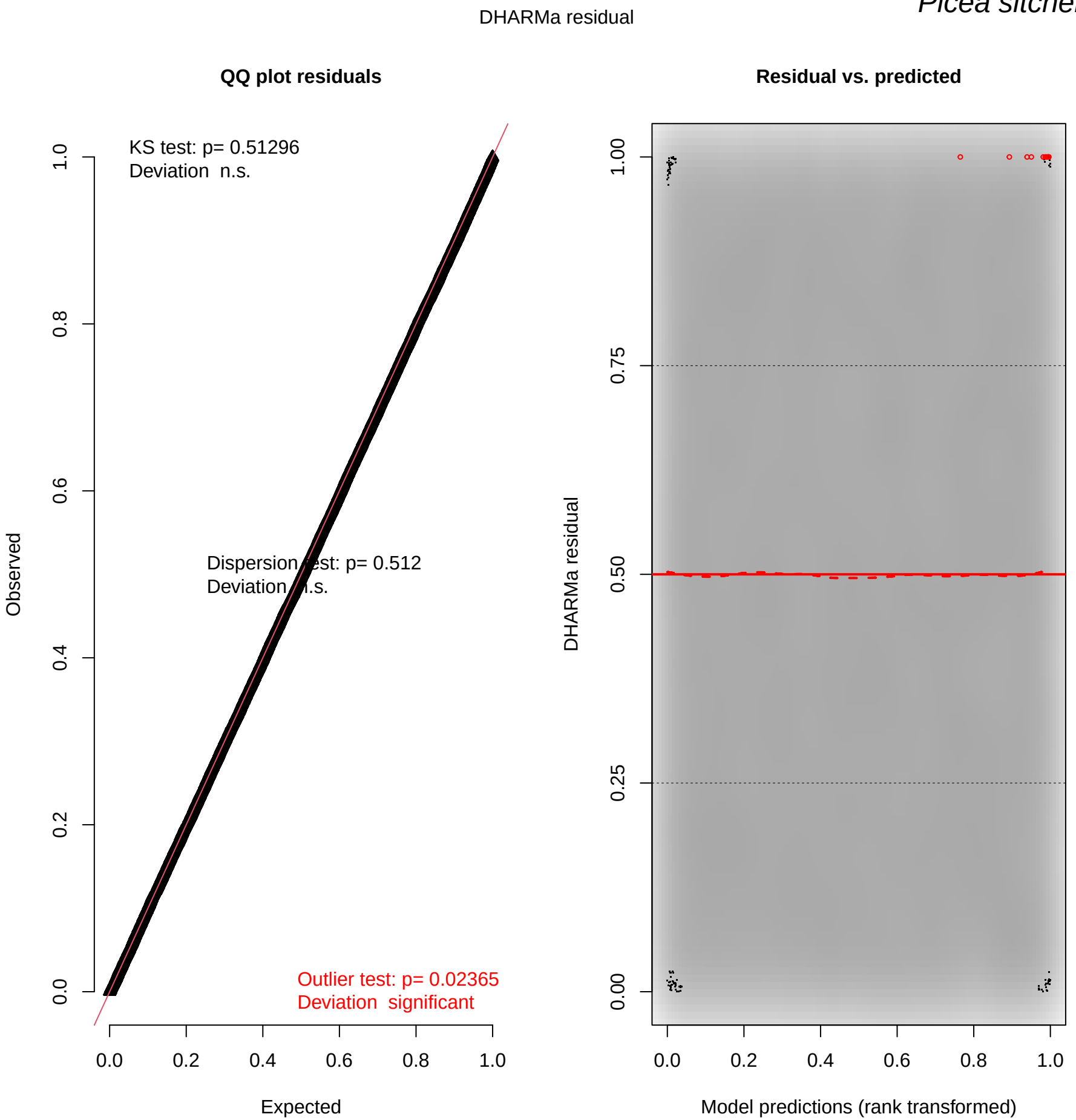

Picea sitchensis

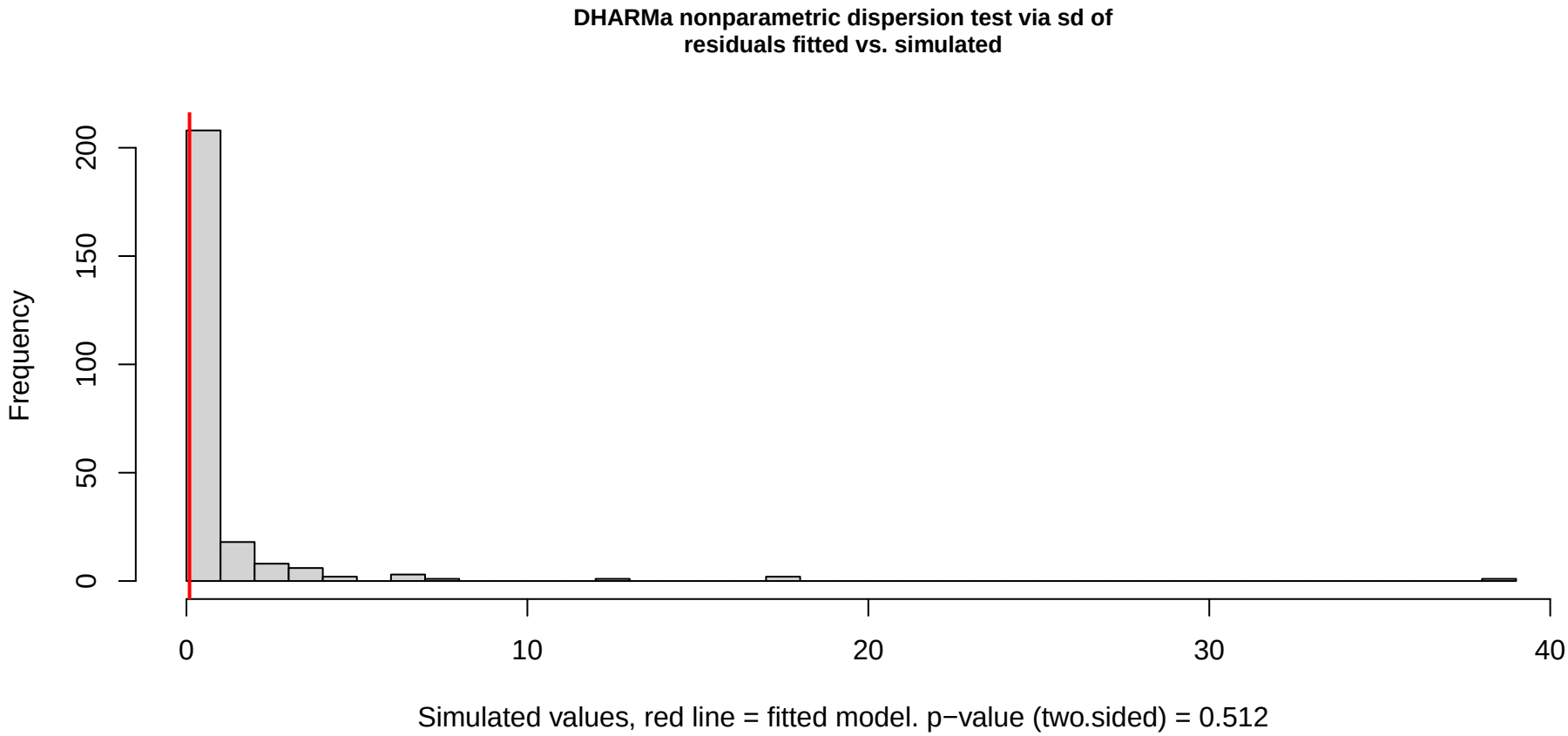

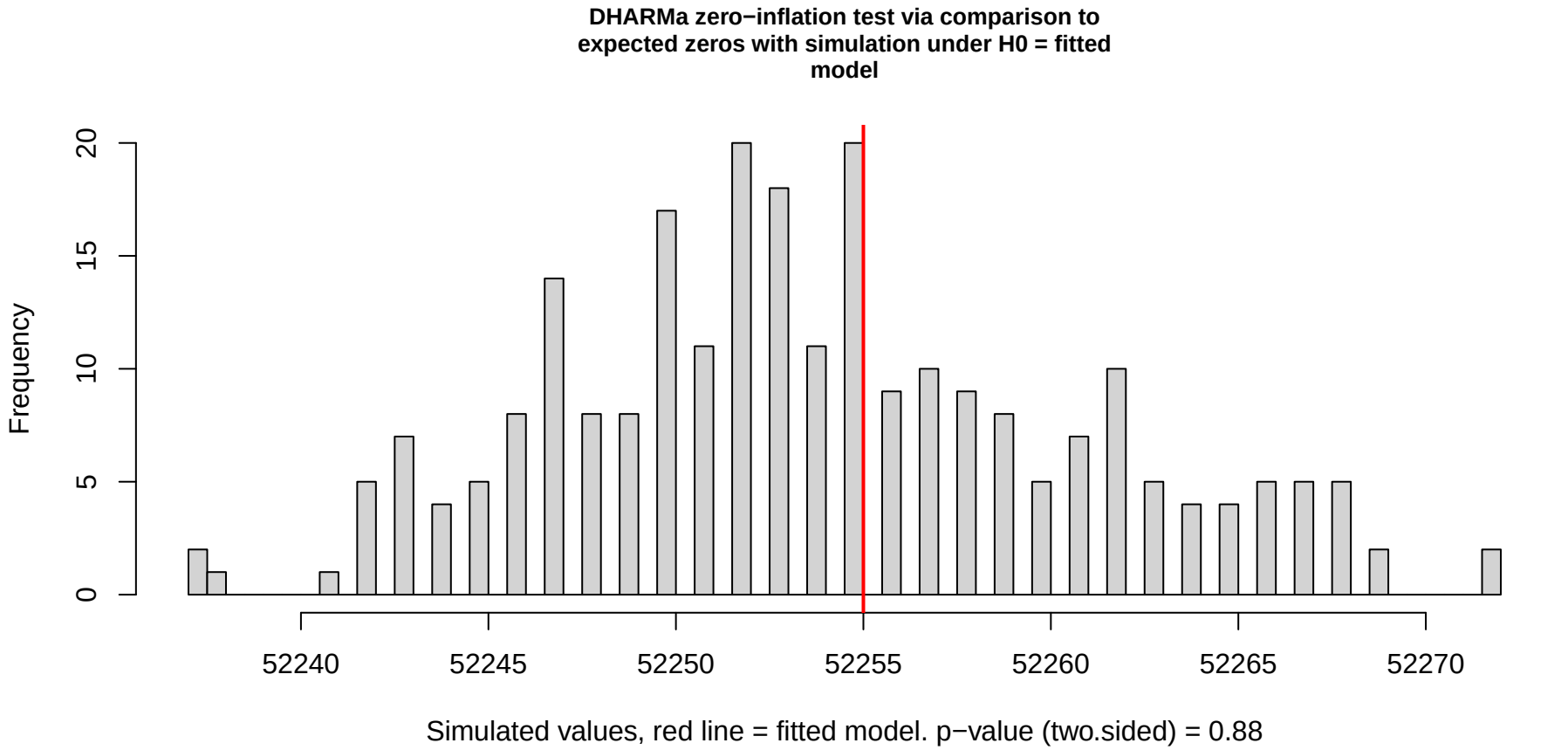

Picea sitchensis

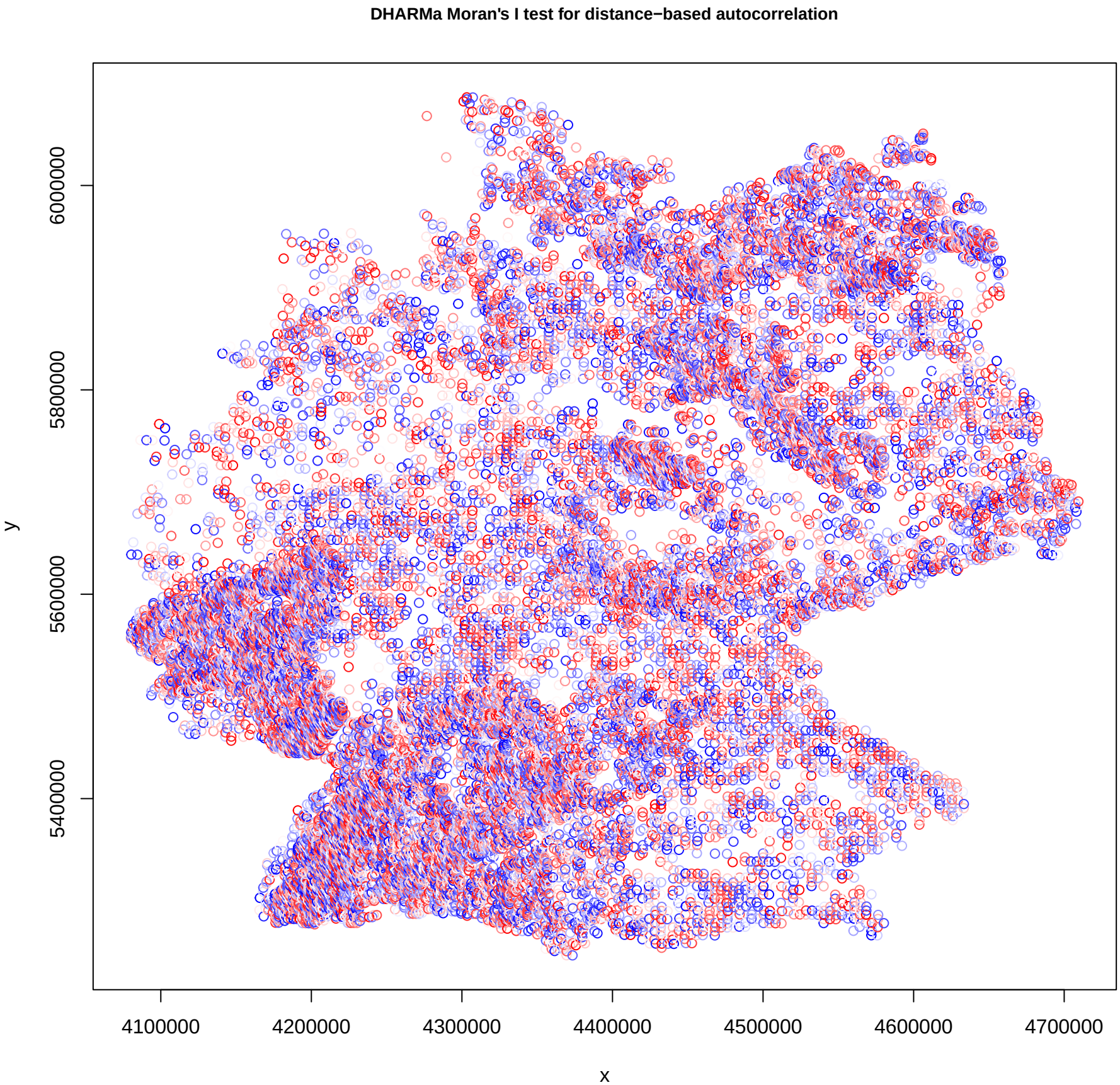

Abies alba

DHARMa residual

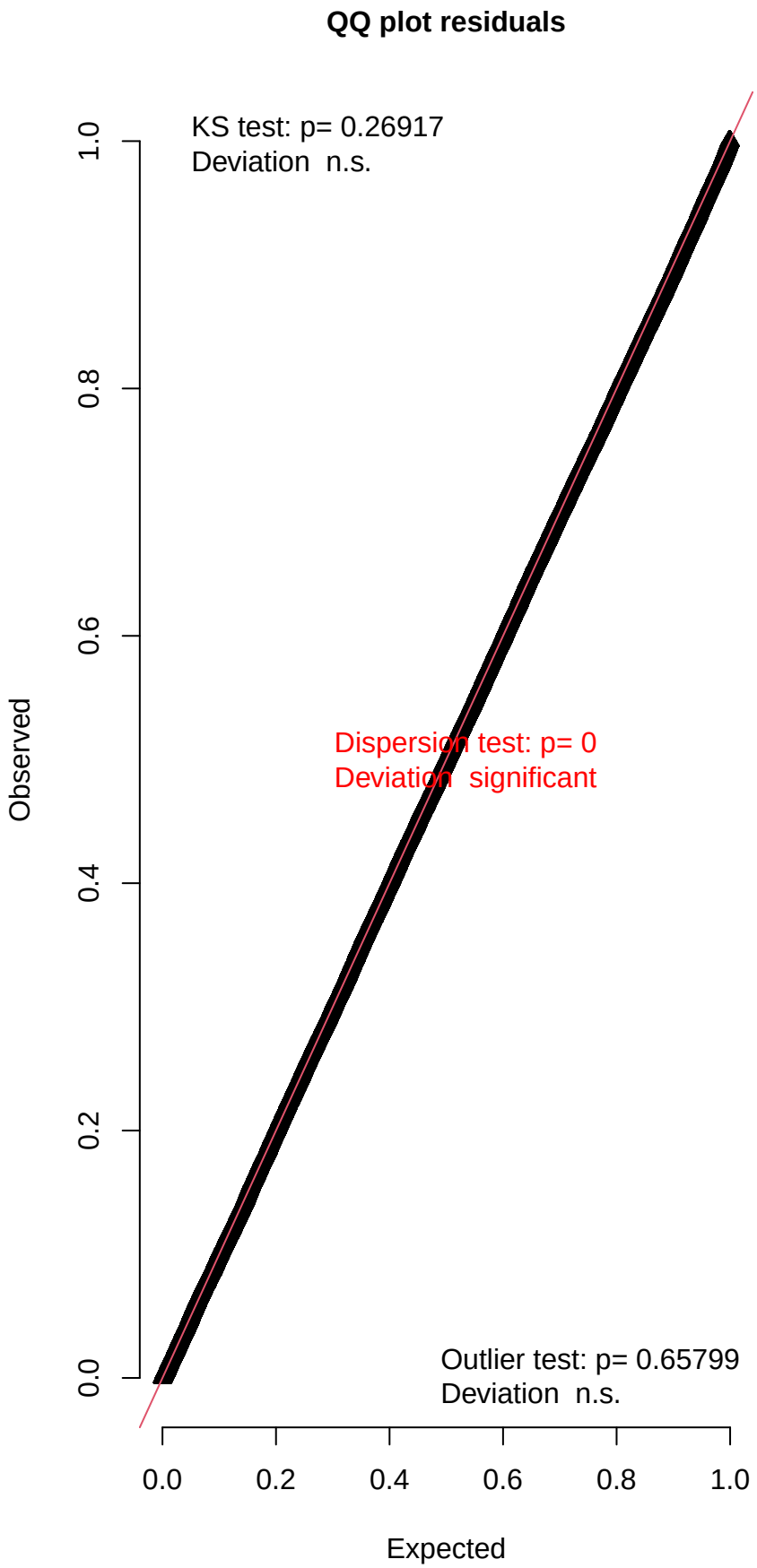

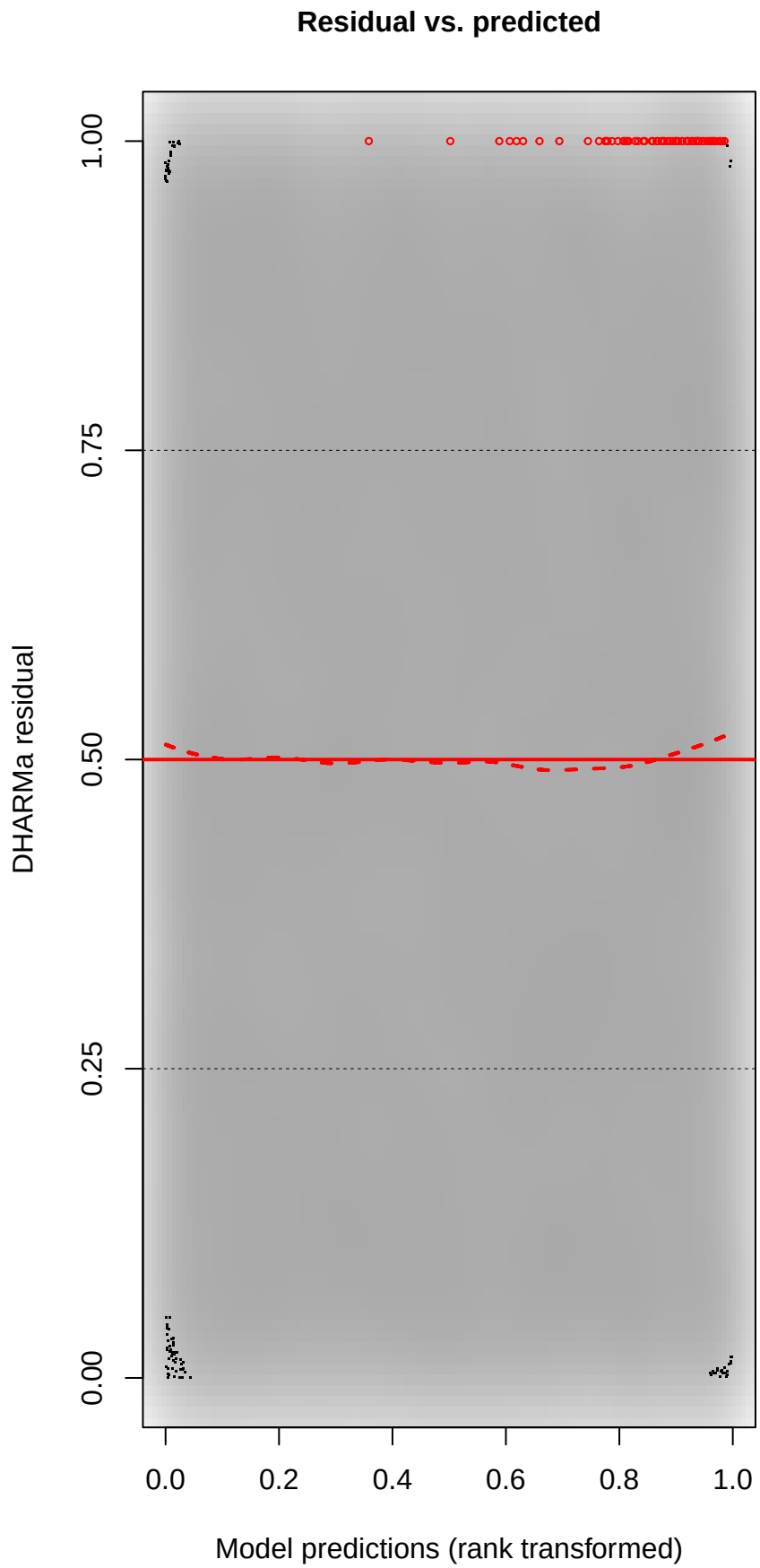

Abies alba

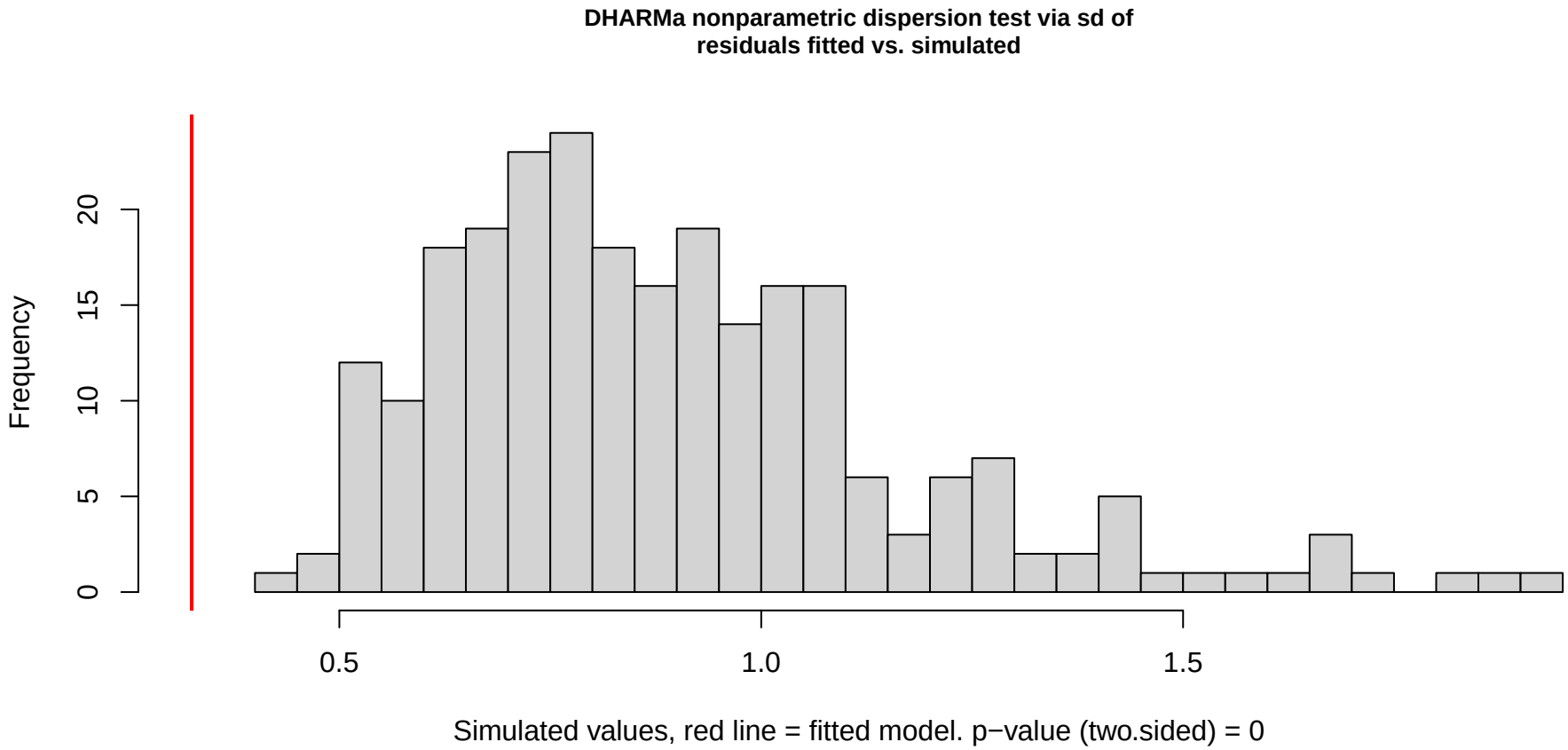
DHARMa nonparametric dispersion test via sd of residuals fitted vs. simulated
Frequency
0
5
10
15
20
0.5
1.0
1.5
Simulated values, red line = fitted model. p−value (two.sided) = 0

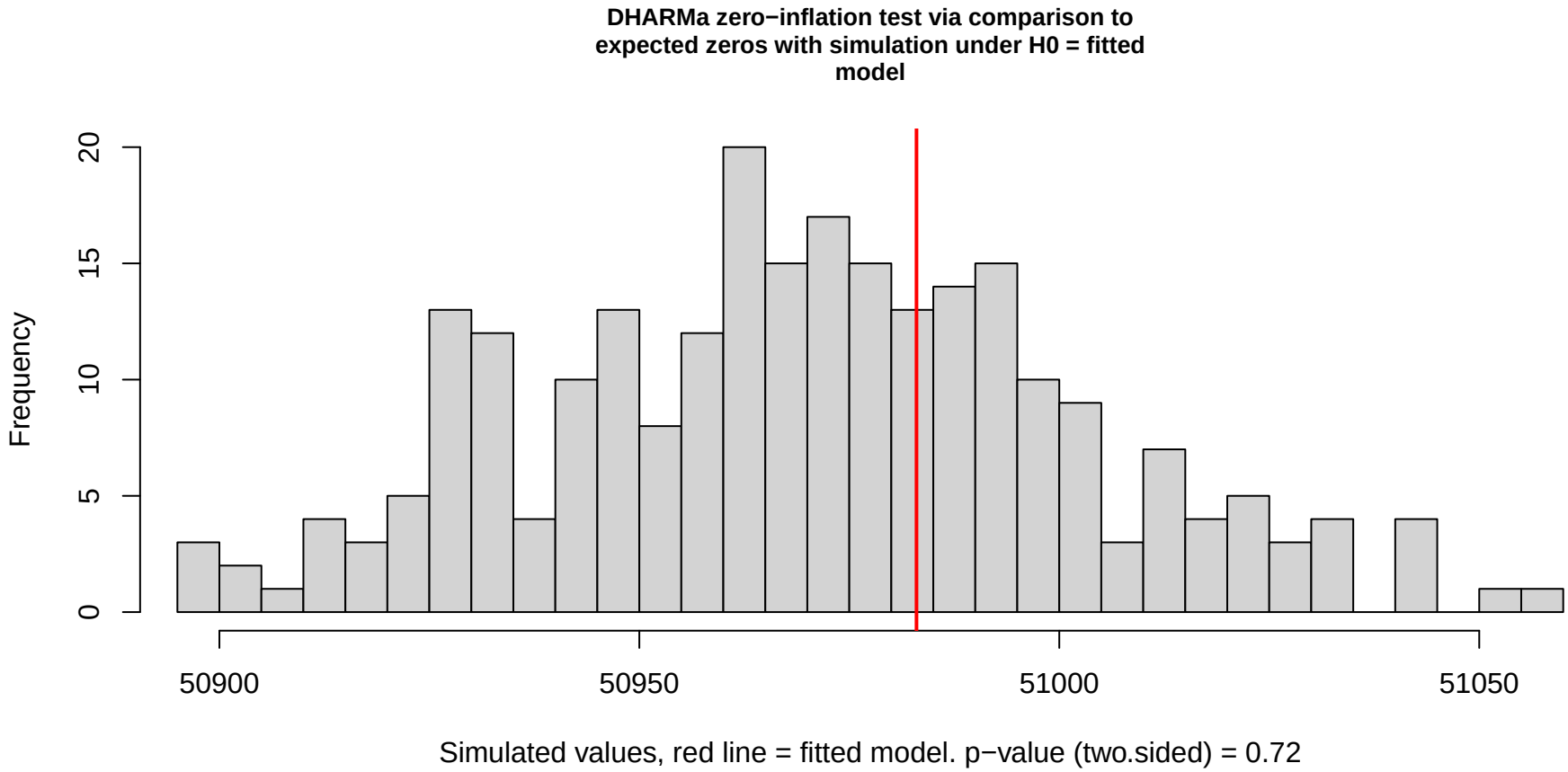
DHARMa zero−inflation test via comparison to expected zeros with simulation under H0 = fitted model
Frequency
0
5
10
15
20
50900
50950
51000
51050
Simulated values, red line = fitted model. p−value (two.sided) = 0.72

Abies alba


DHARMa Moran's I test for distance−based autocorrelation
6000000
5800000
5600000
5400000
y
4100000
4200000
4300000
4400000
4500000
4600000
4700000
x

Abies grandis

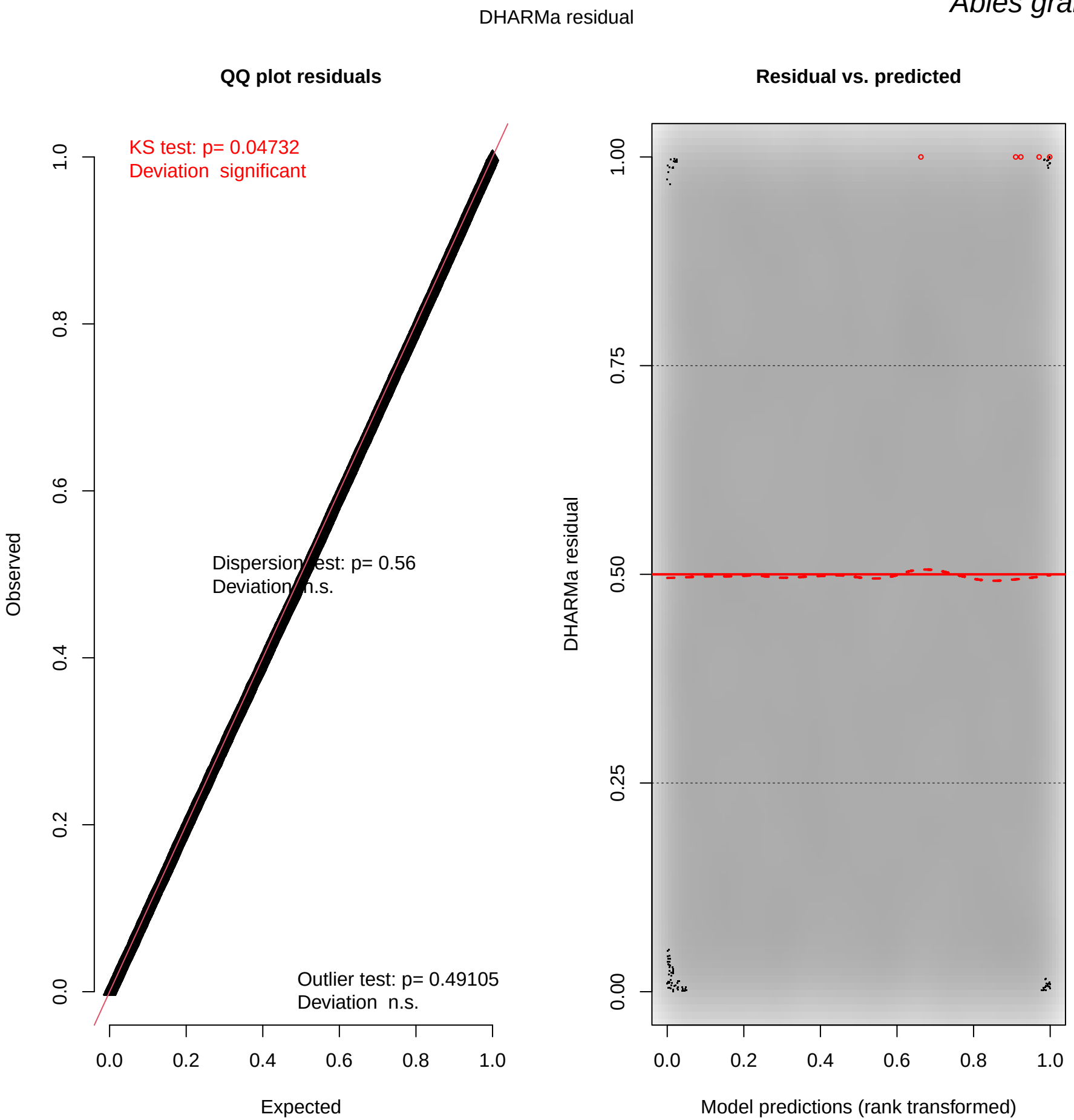

Abies grandis

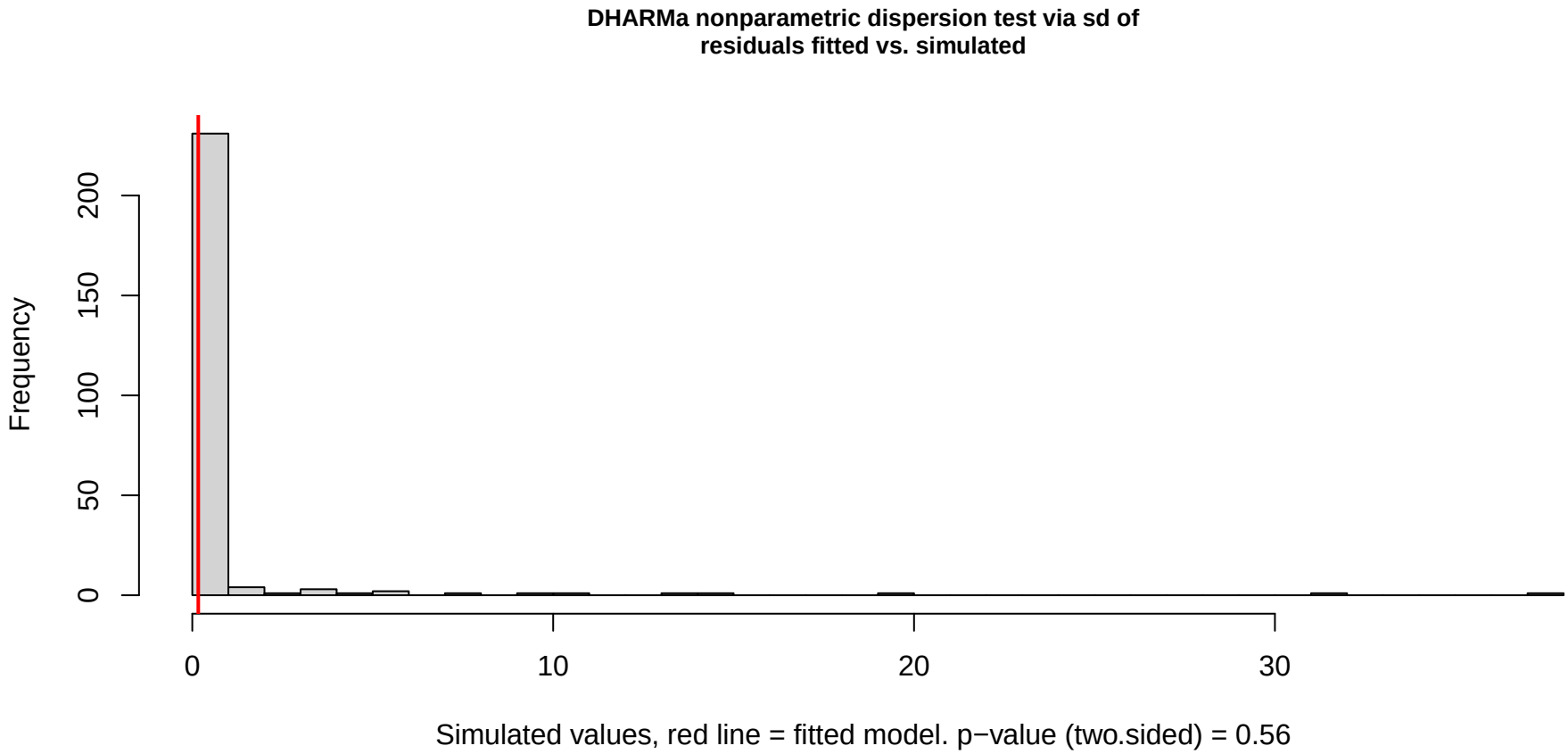

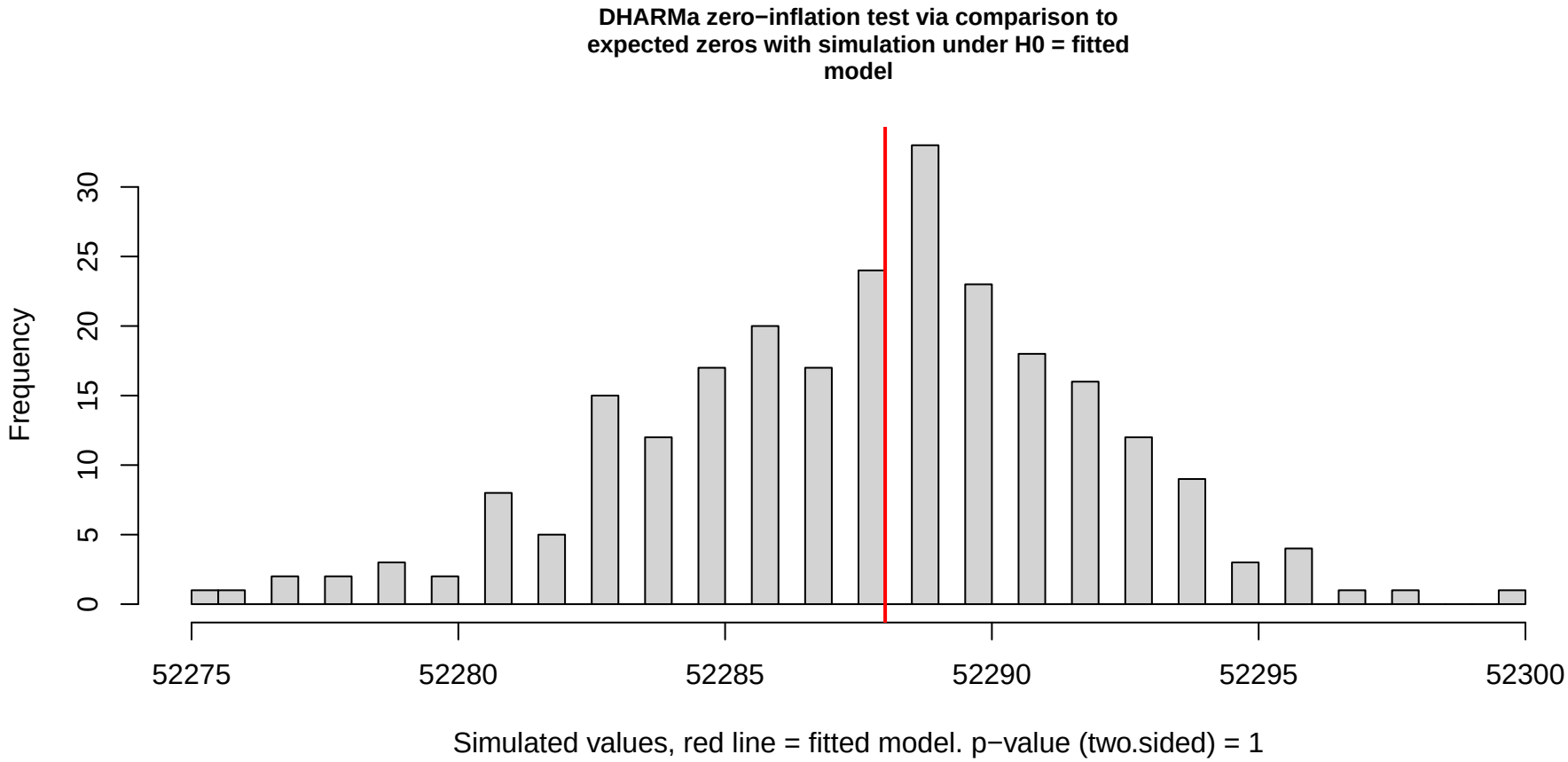

Abies grandis

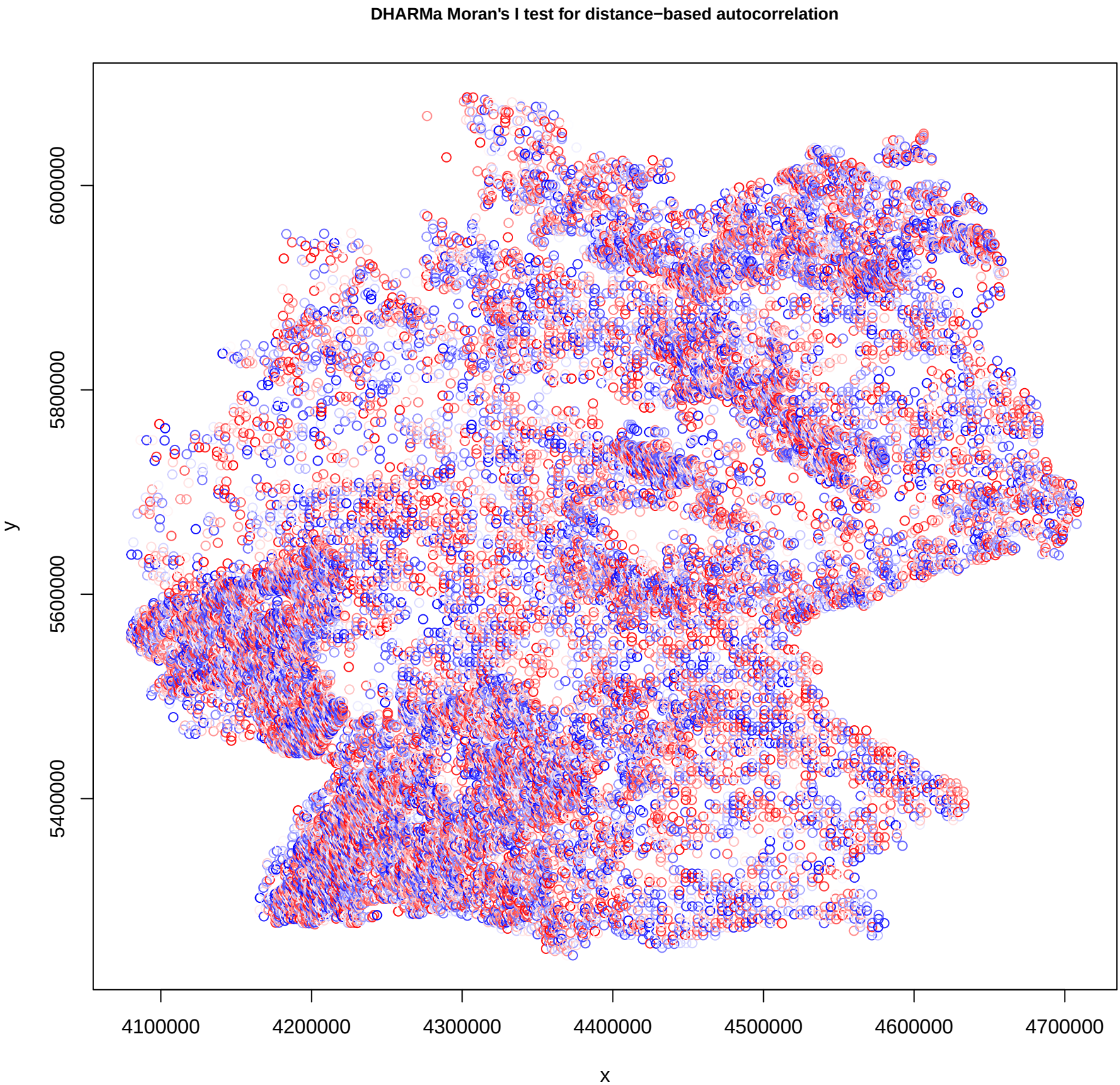

Acer campestre

DHARMa residual

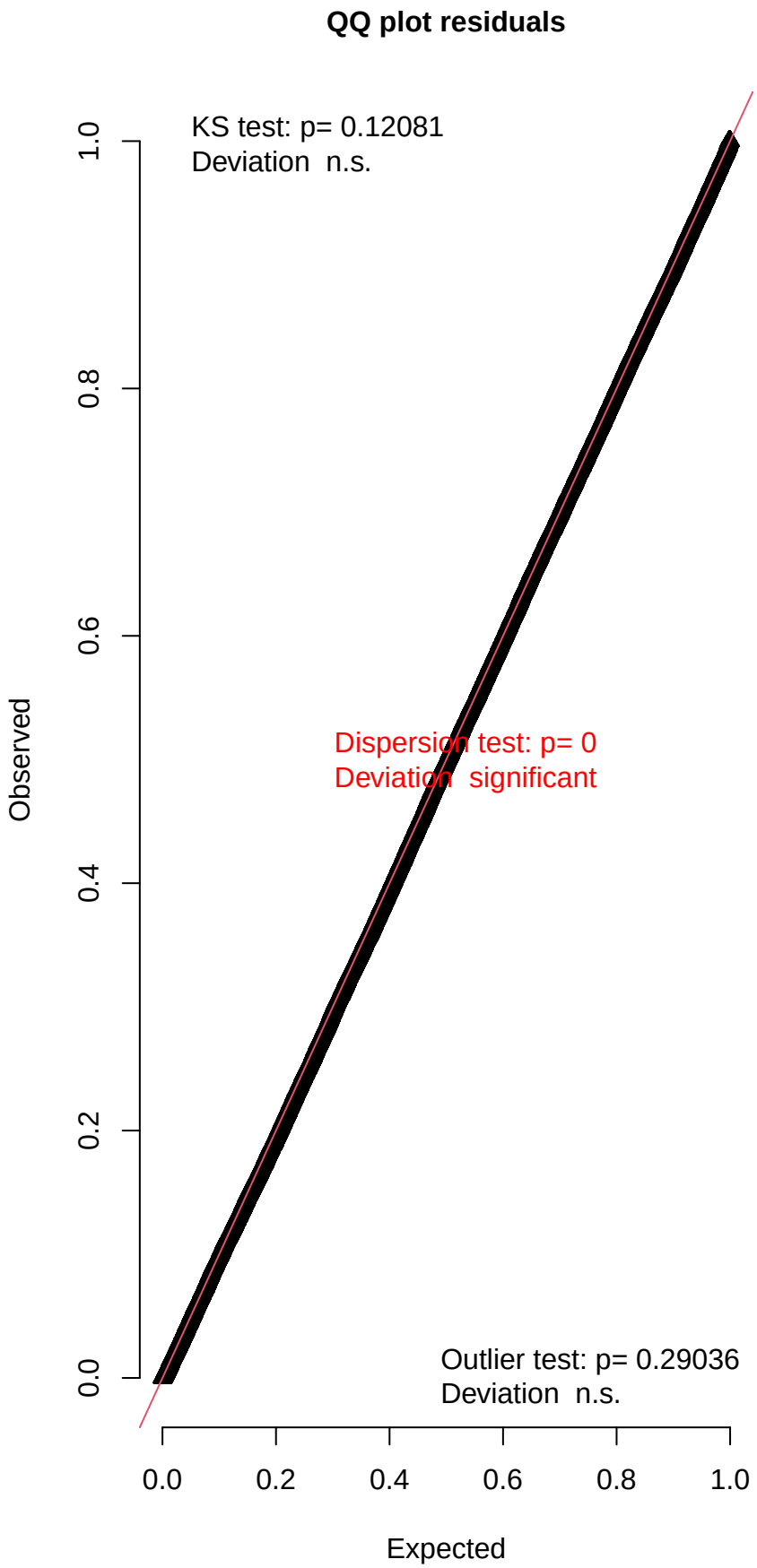

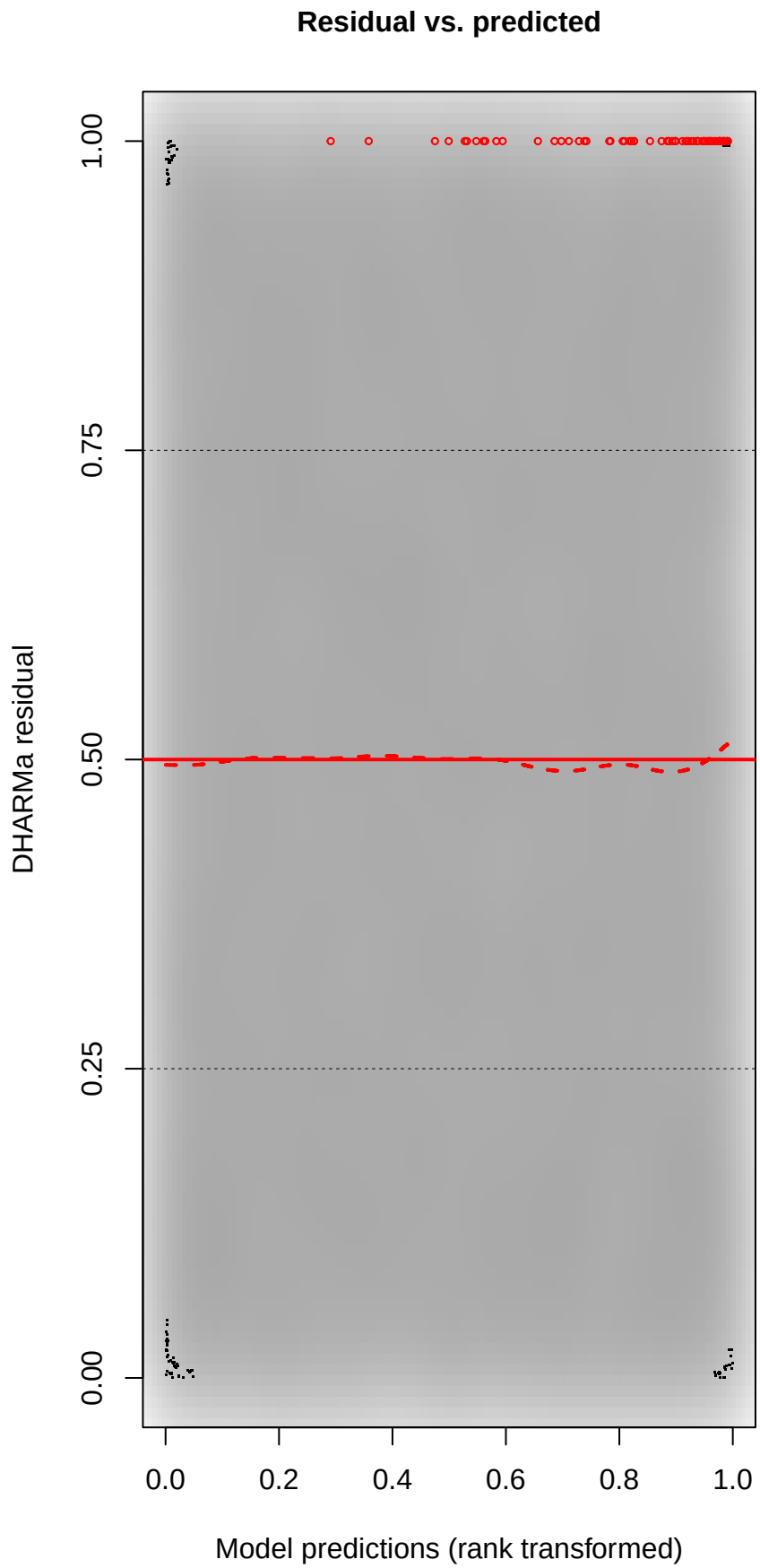

Acer campestre

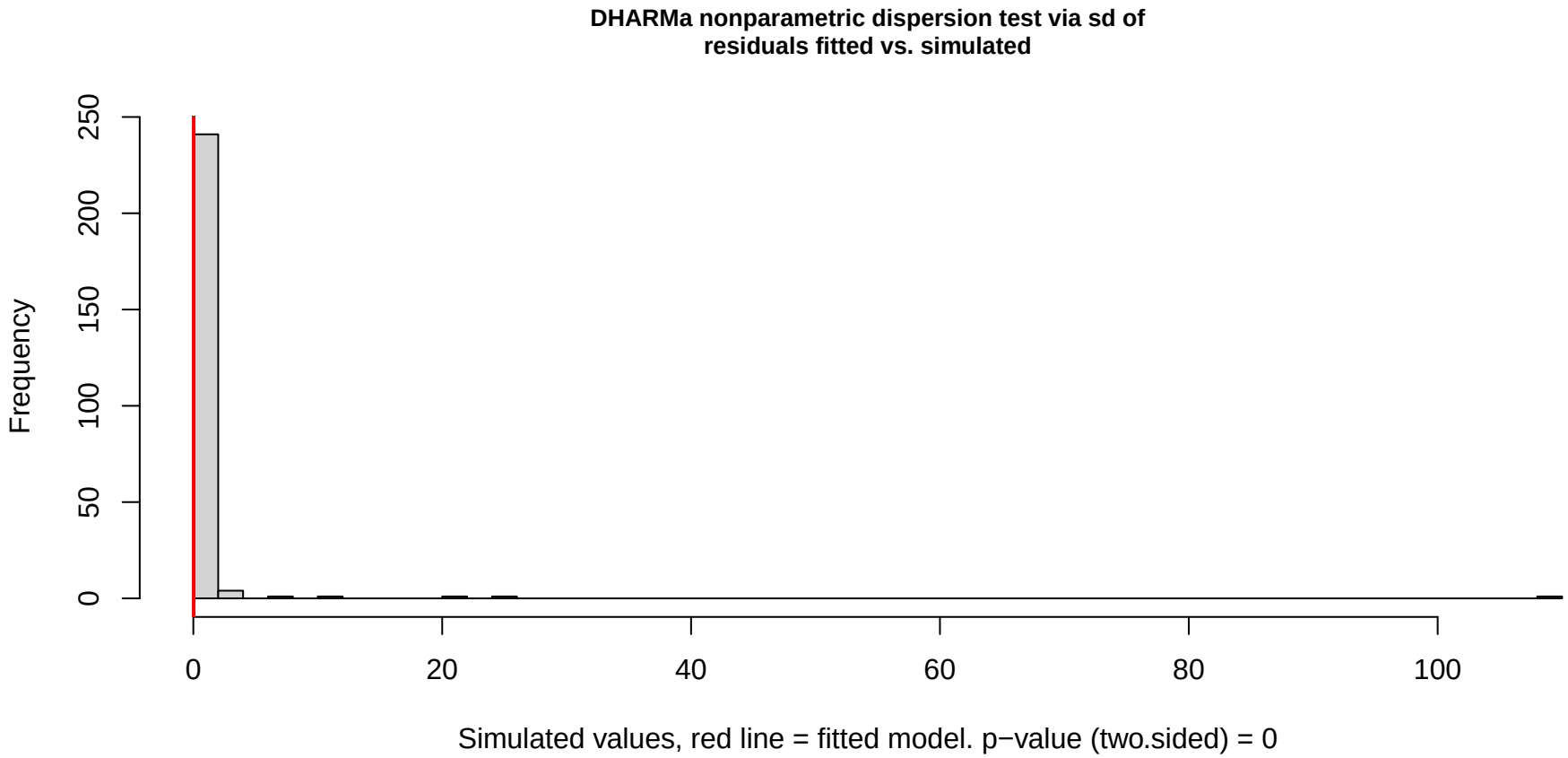

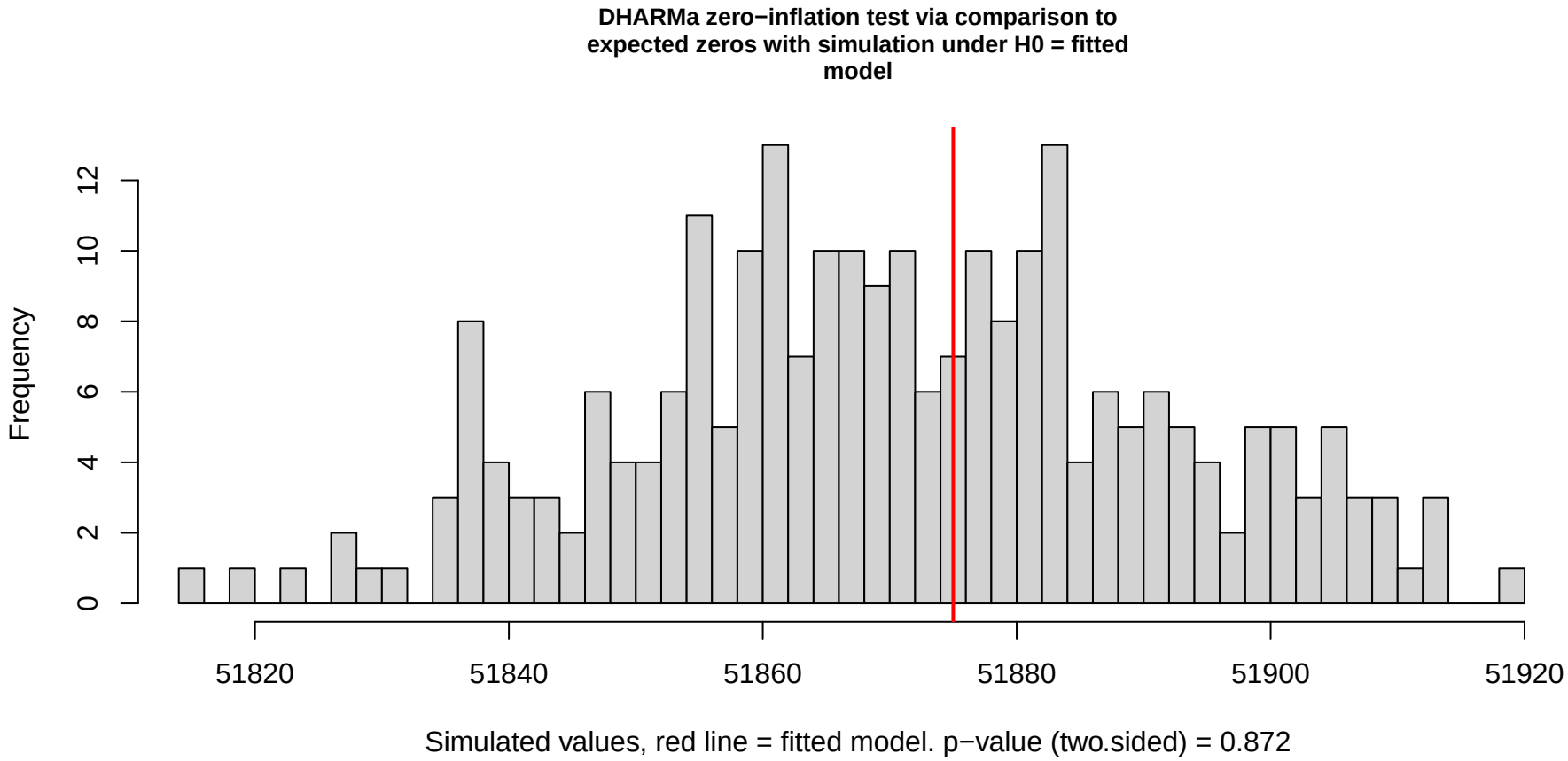

Acer campestre

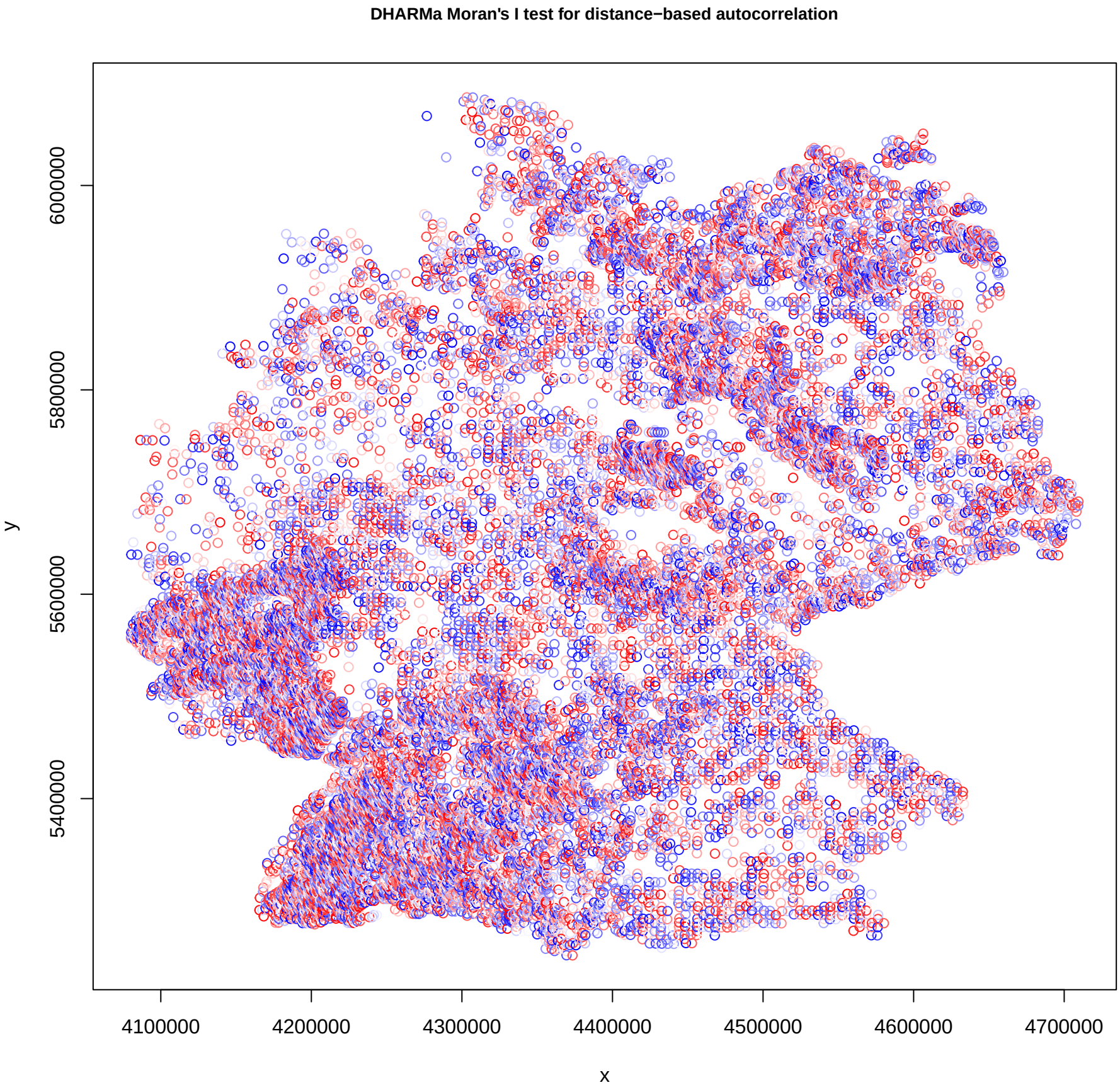

Acer platanoides

DHARMa residual

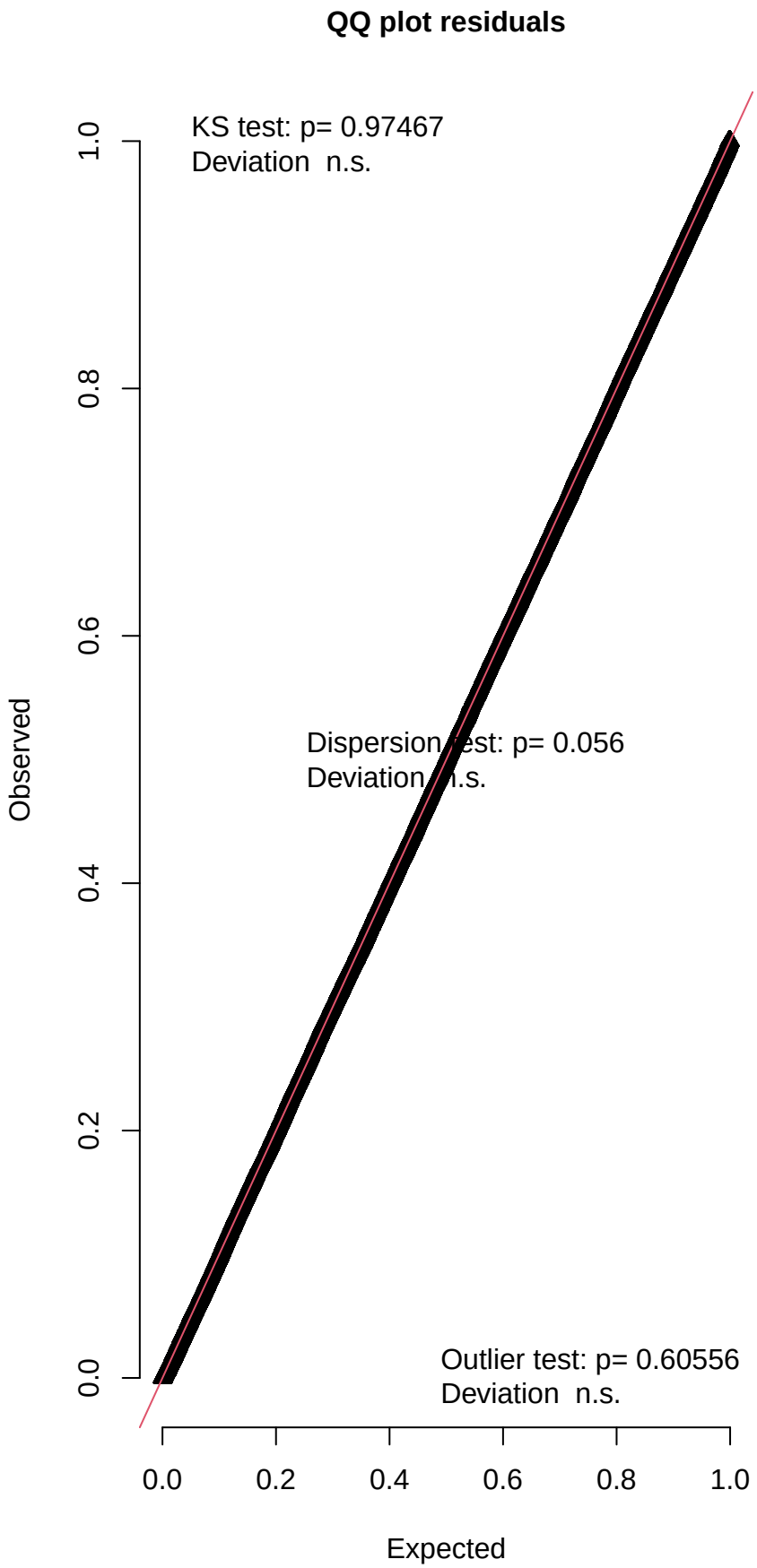

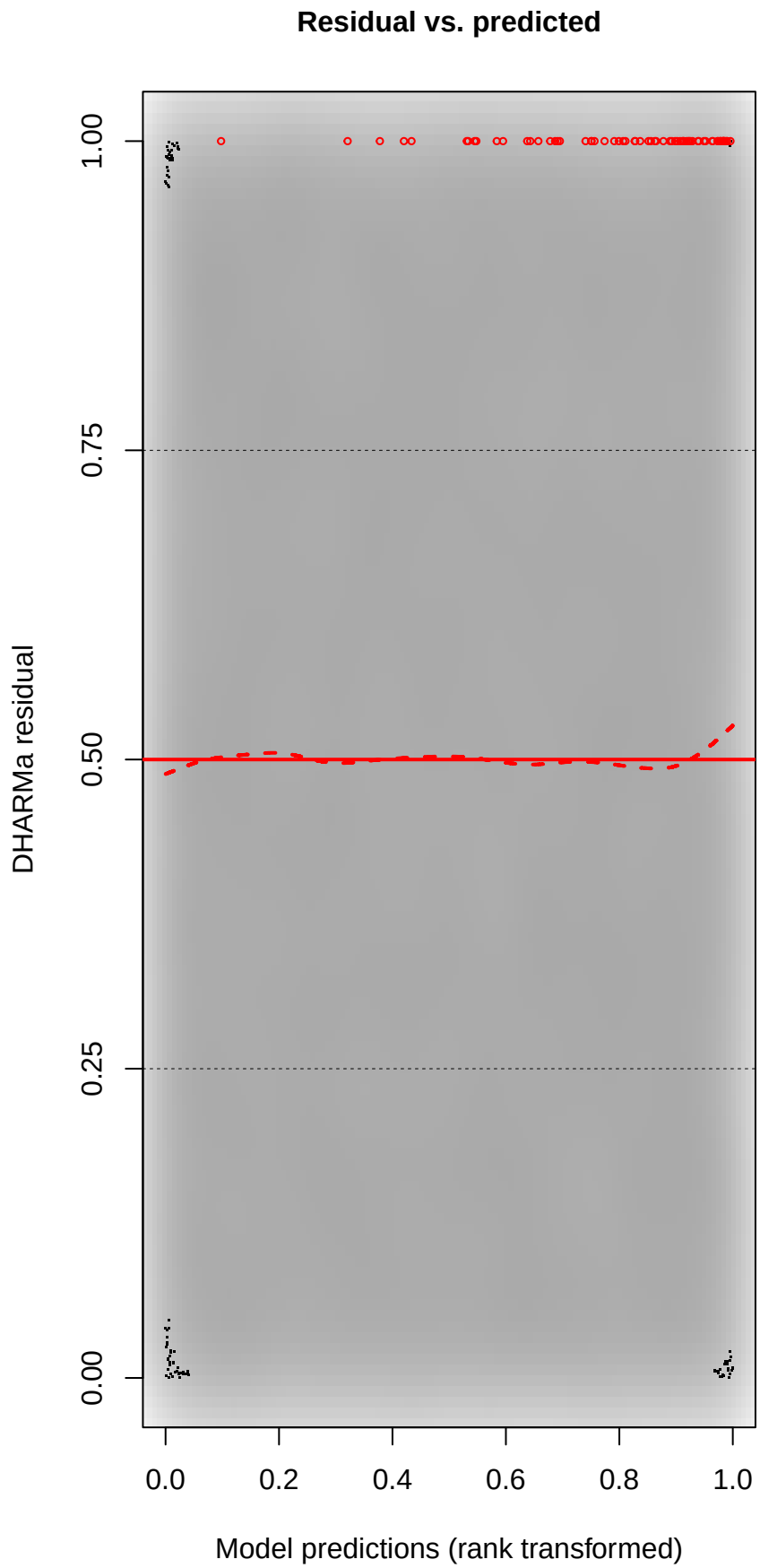

Acer platanoides

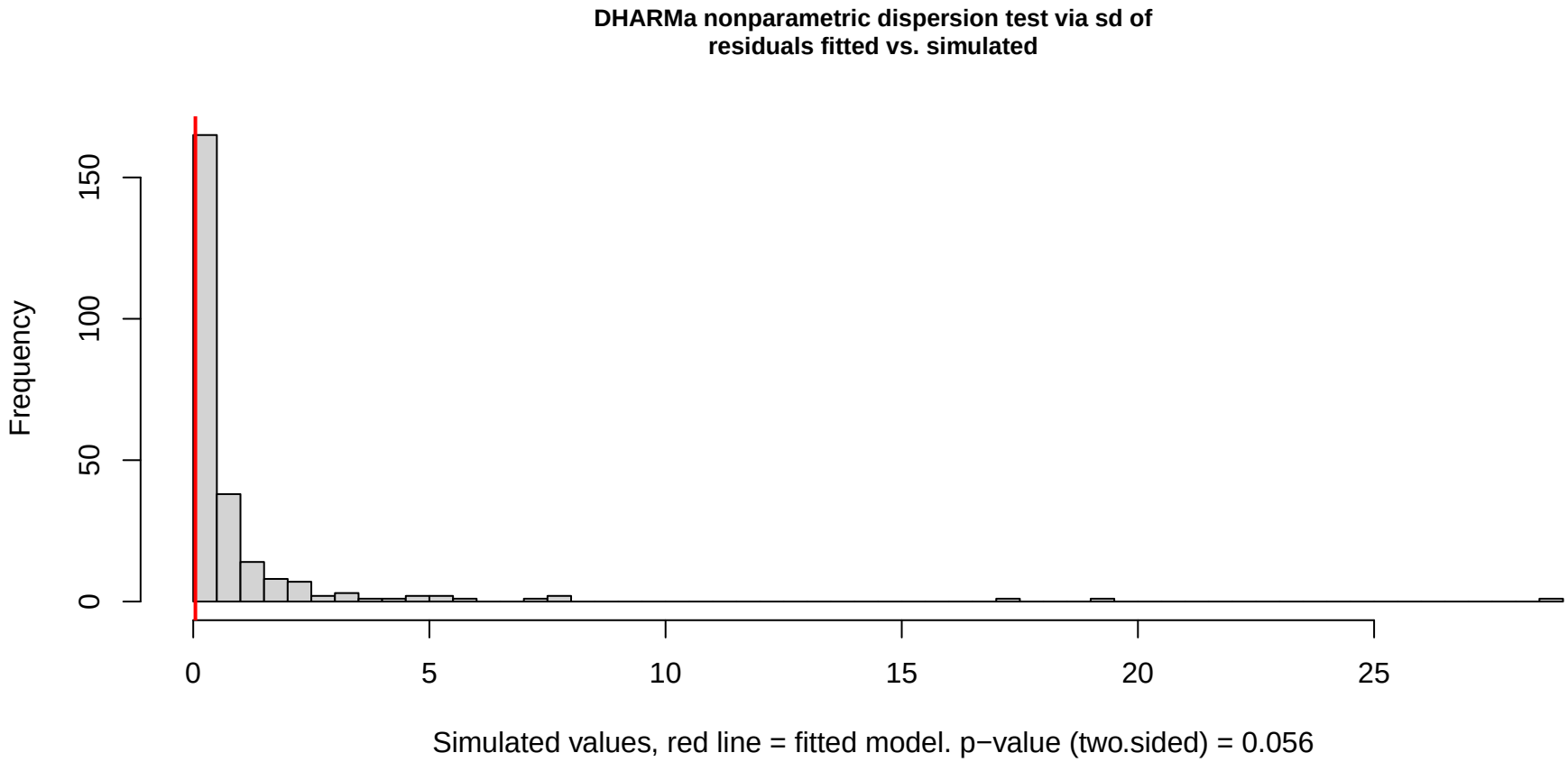

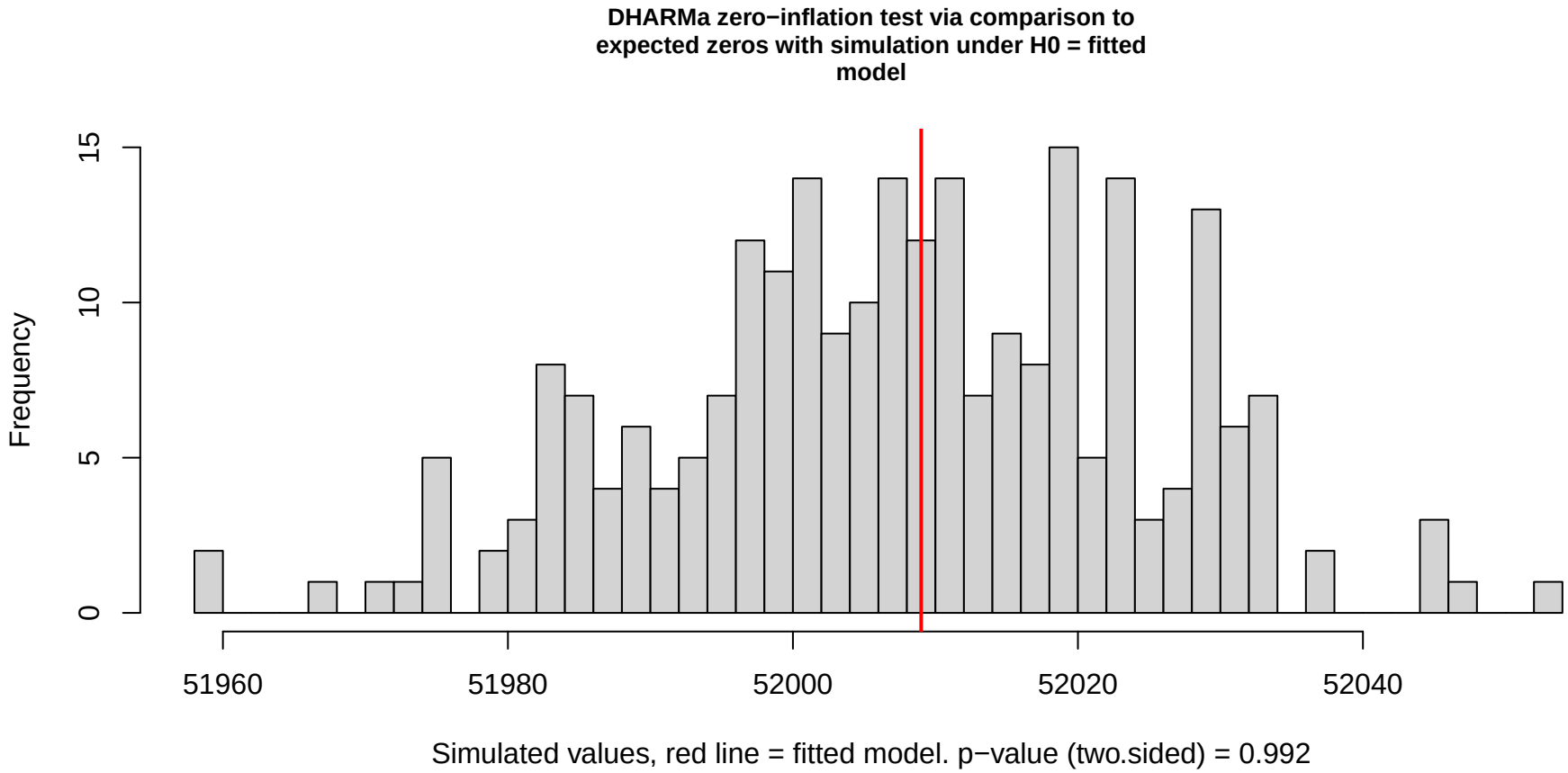

Acer platanoides

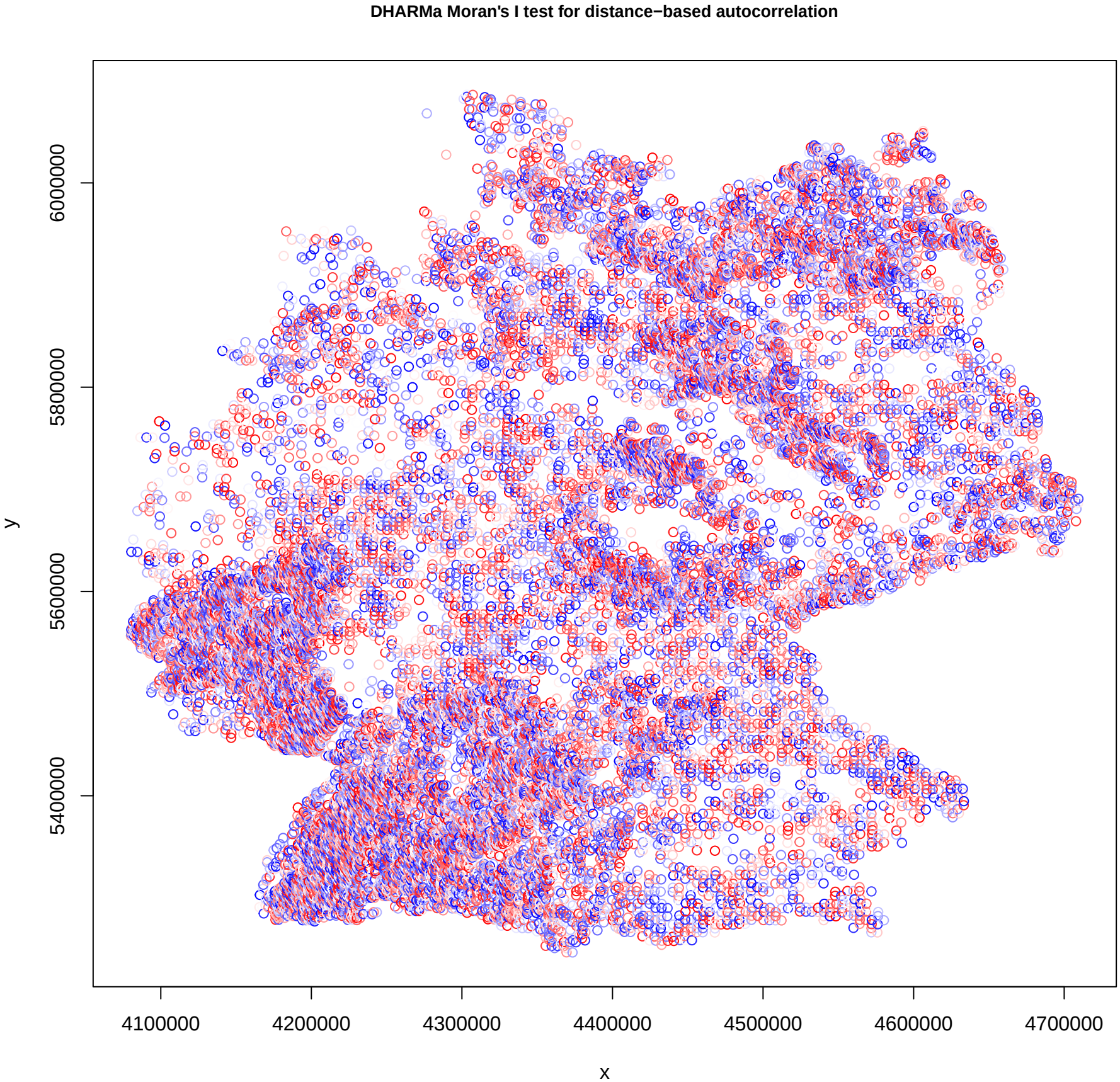

Acer pseudoplatanus

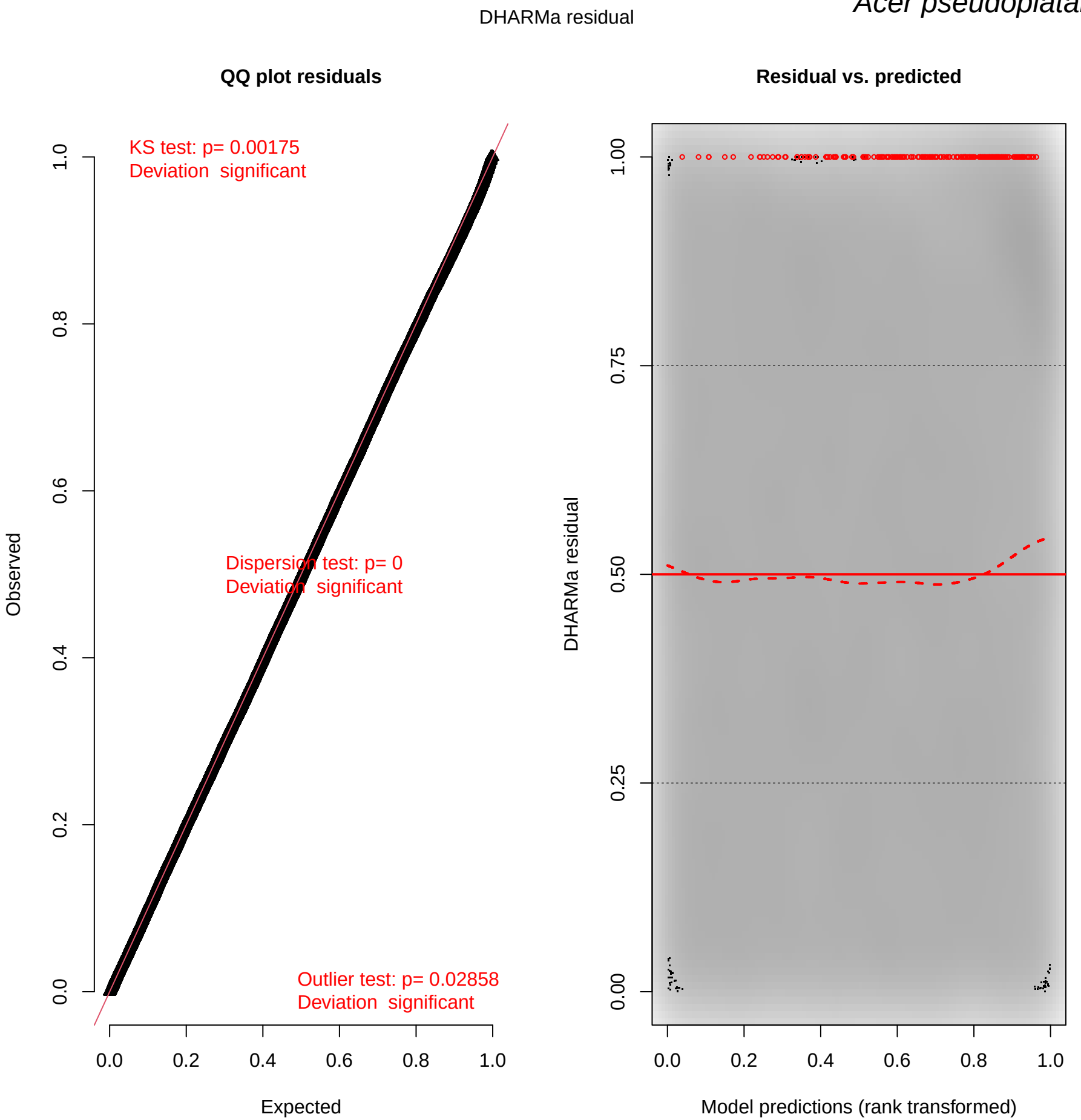

Acer pseudoplatanus

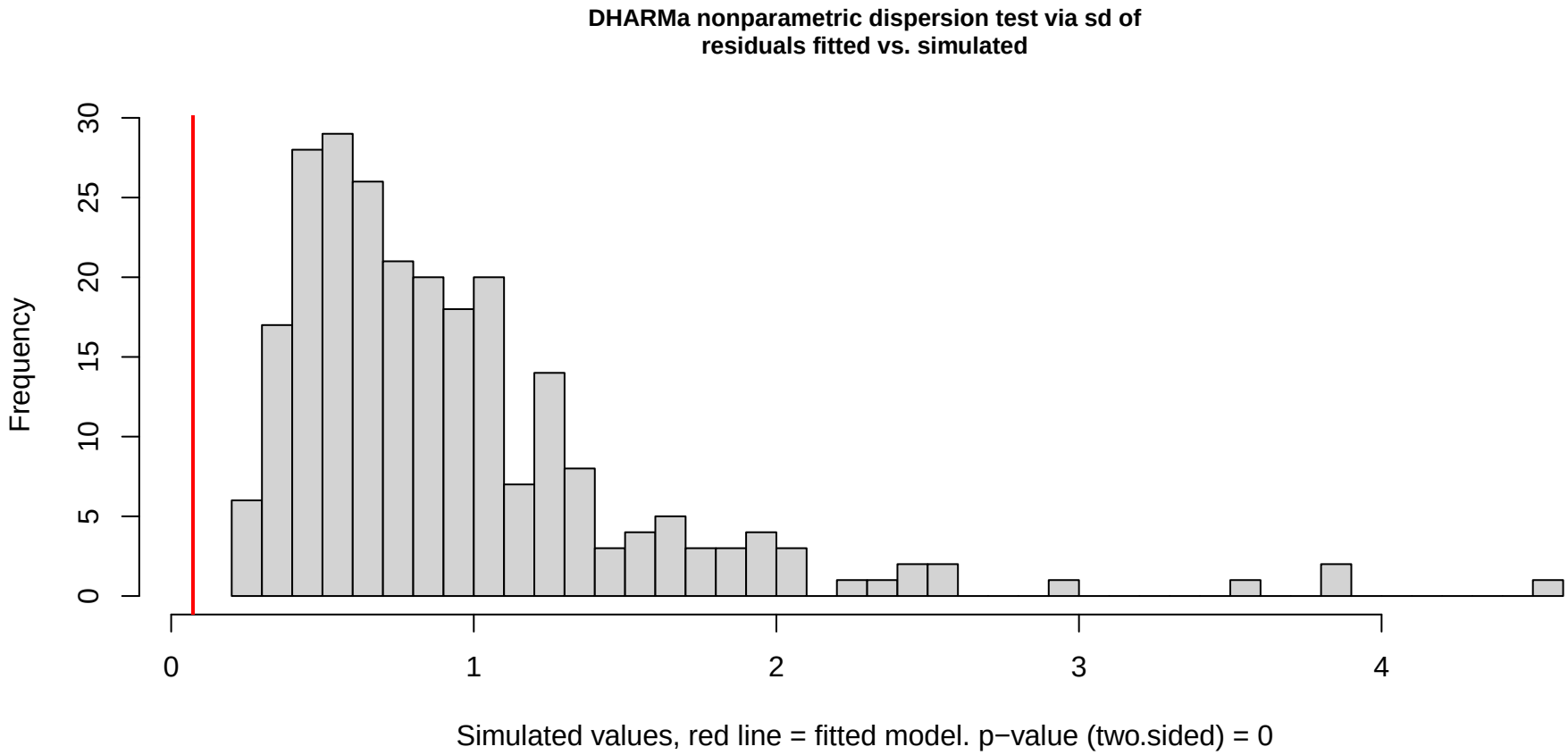

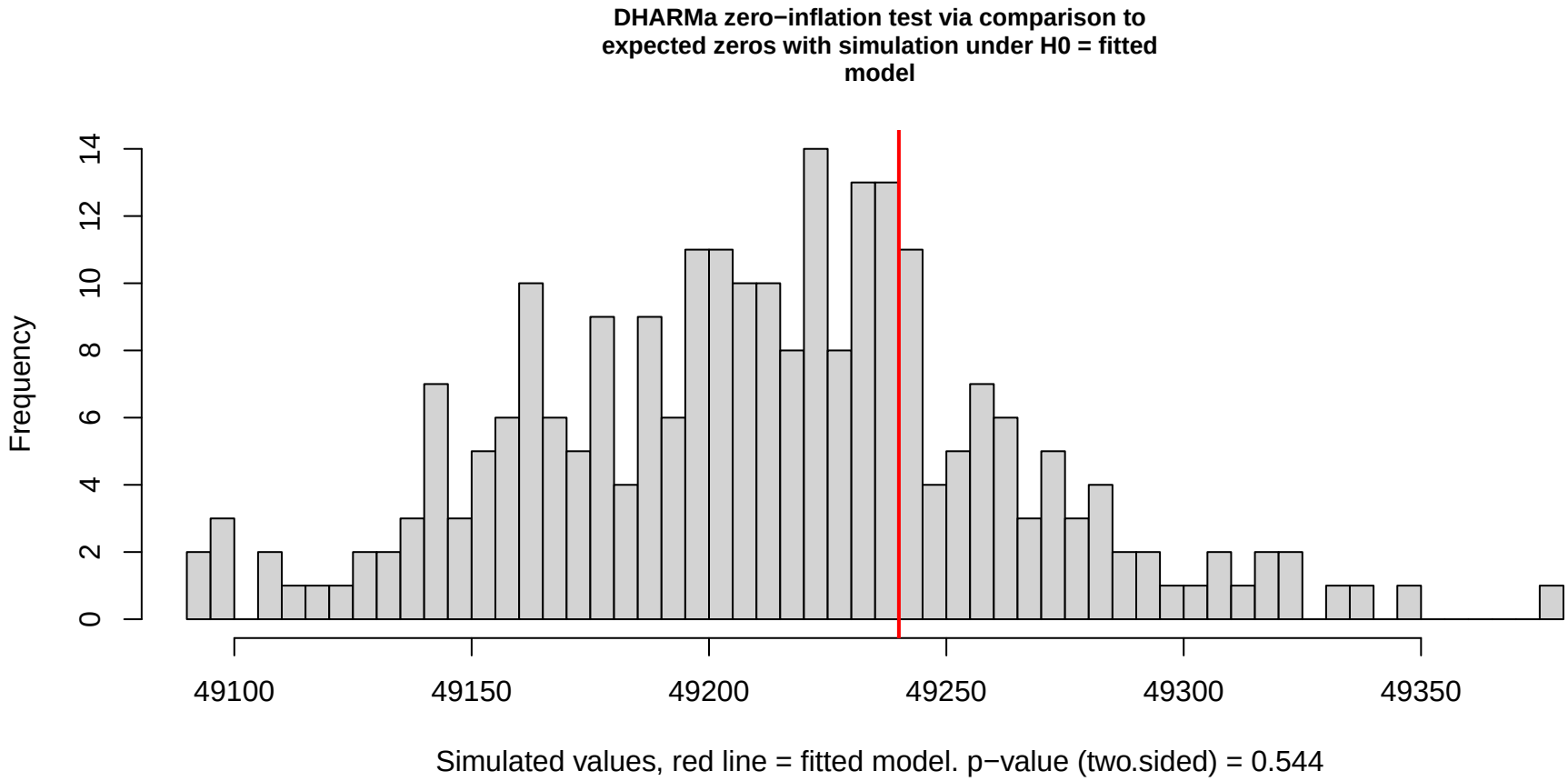

Acer pseudoplatanus

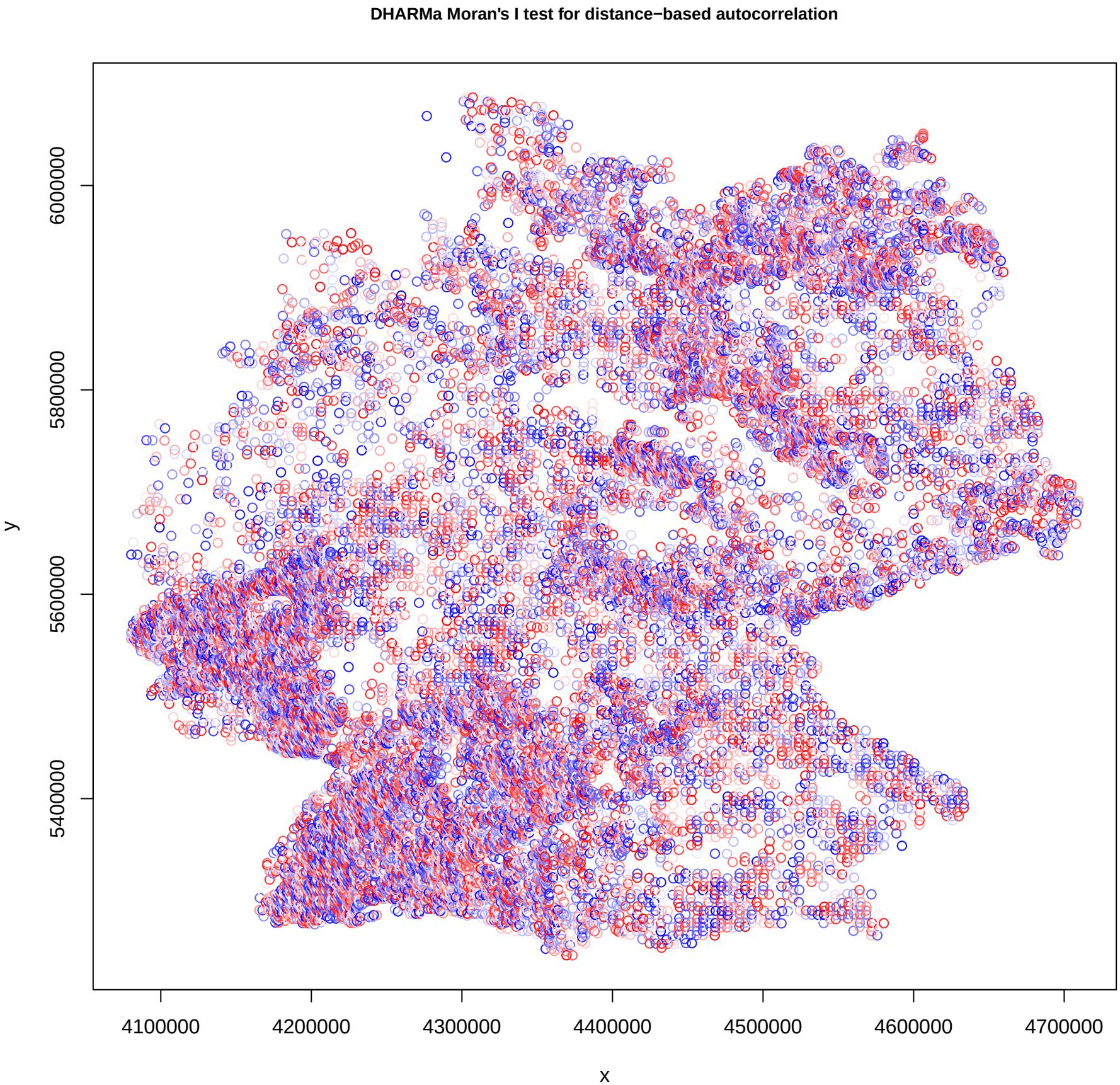

Carpinus betulus

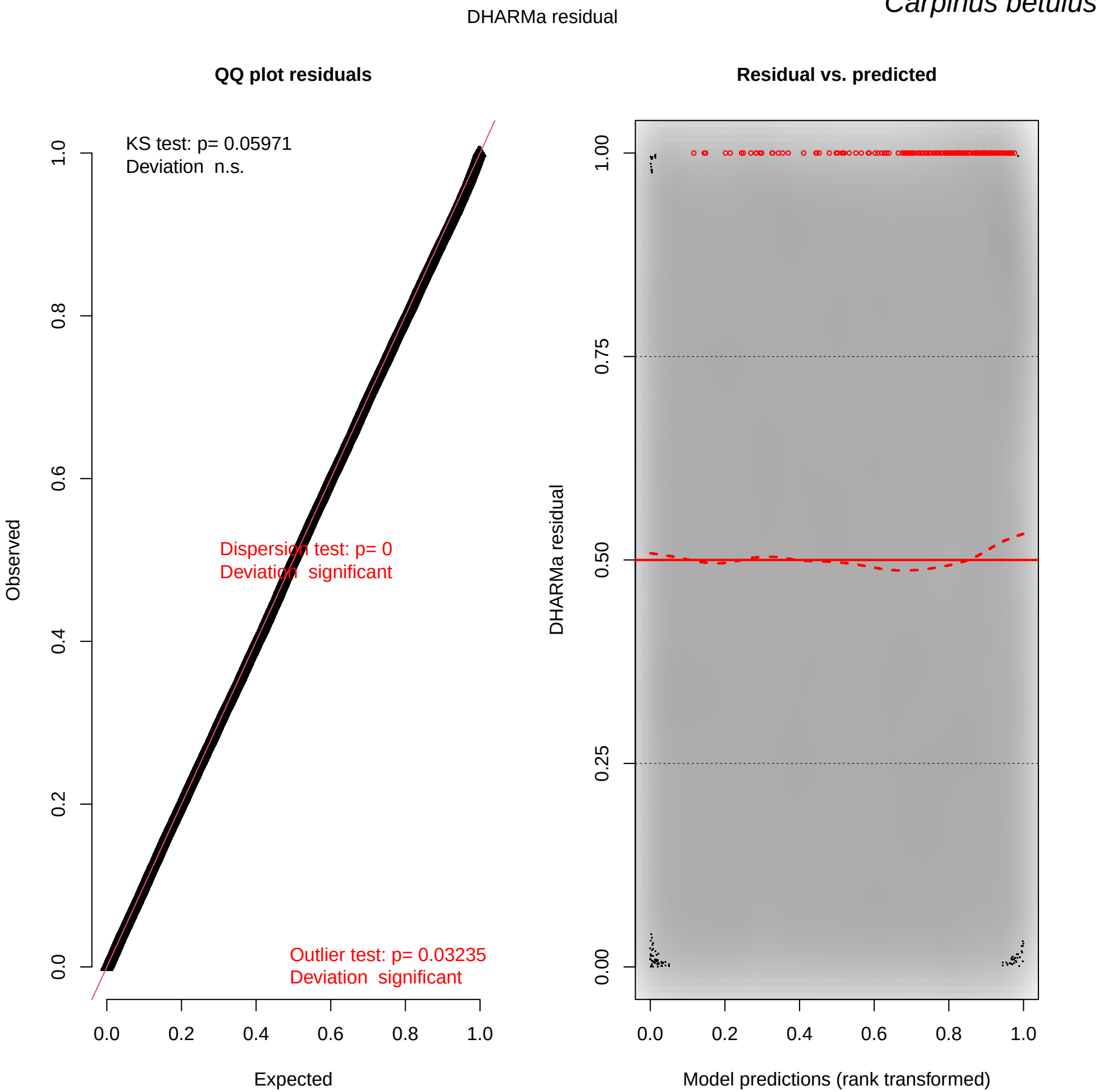

Carpinus betulus

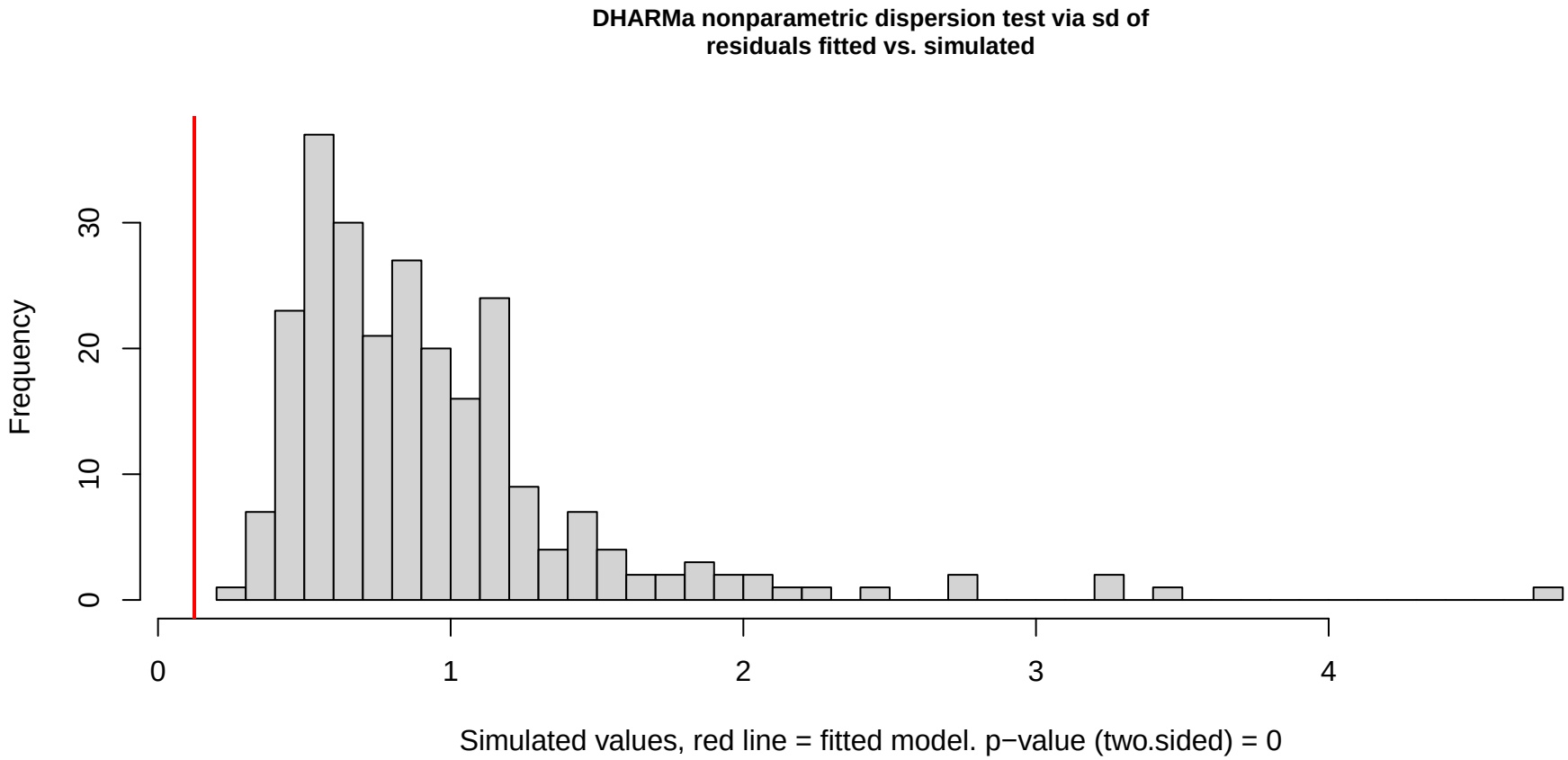

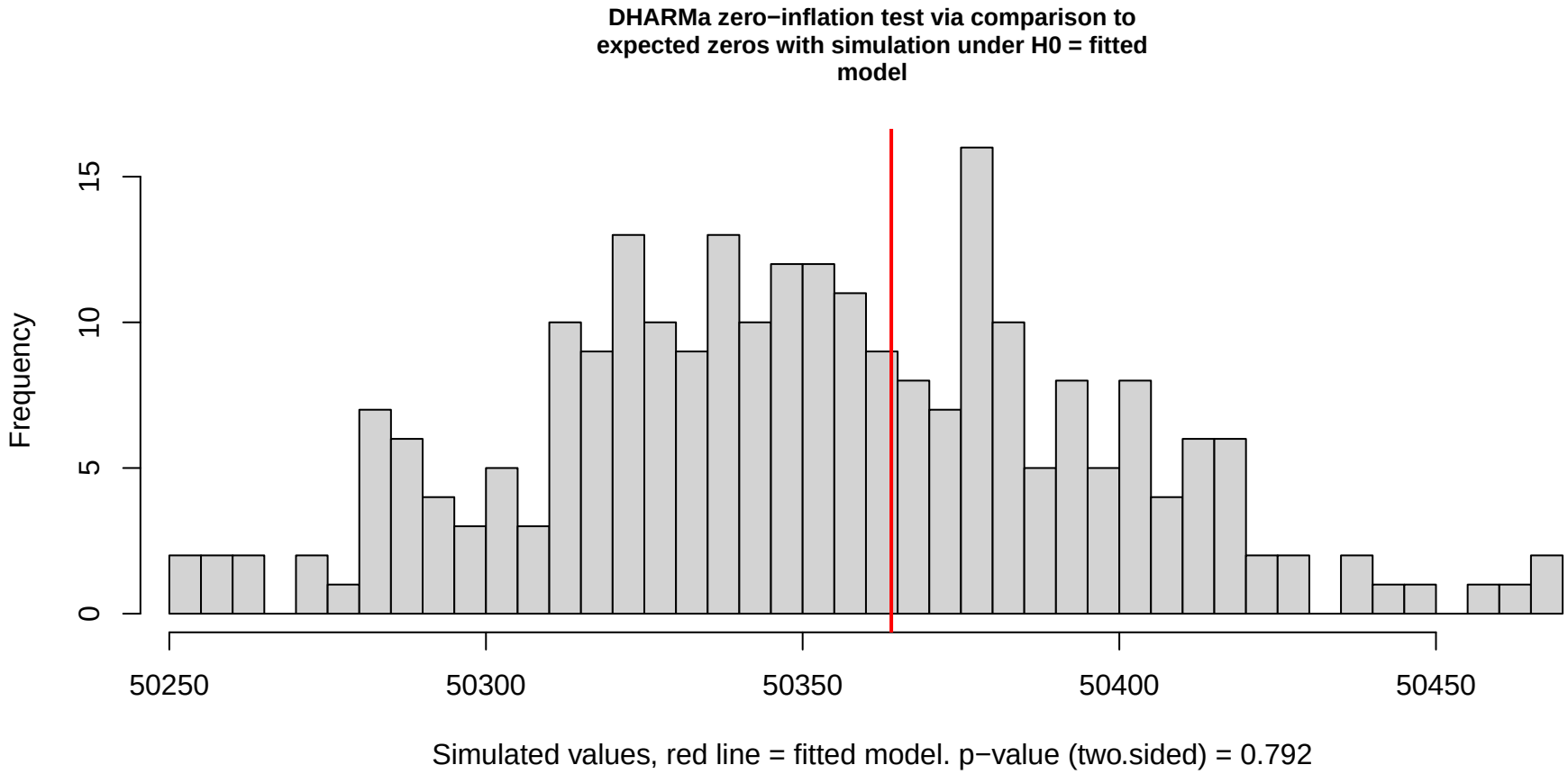

Carpinus betulus

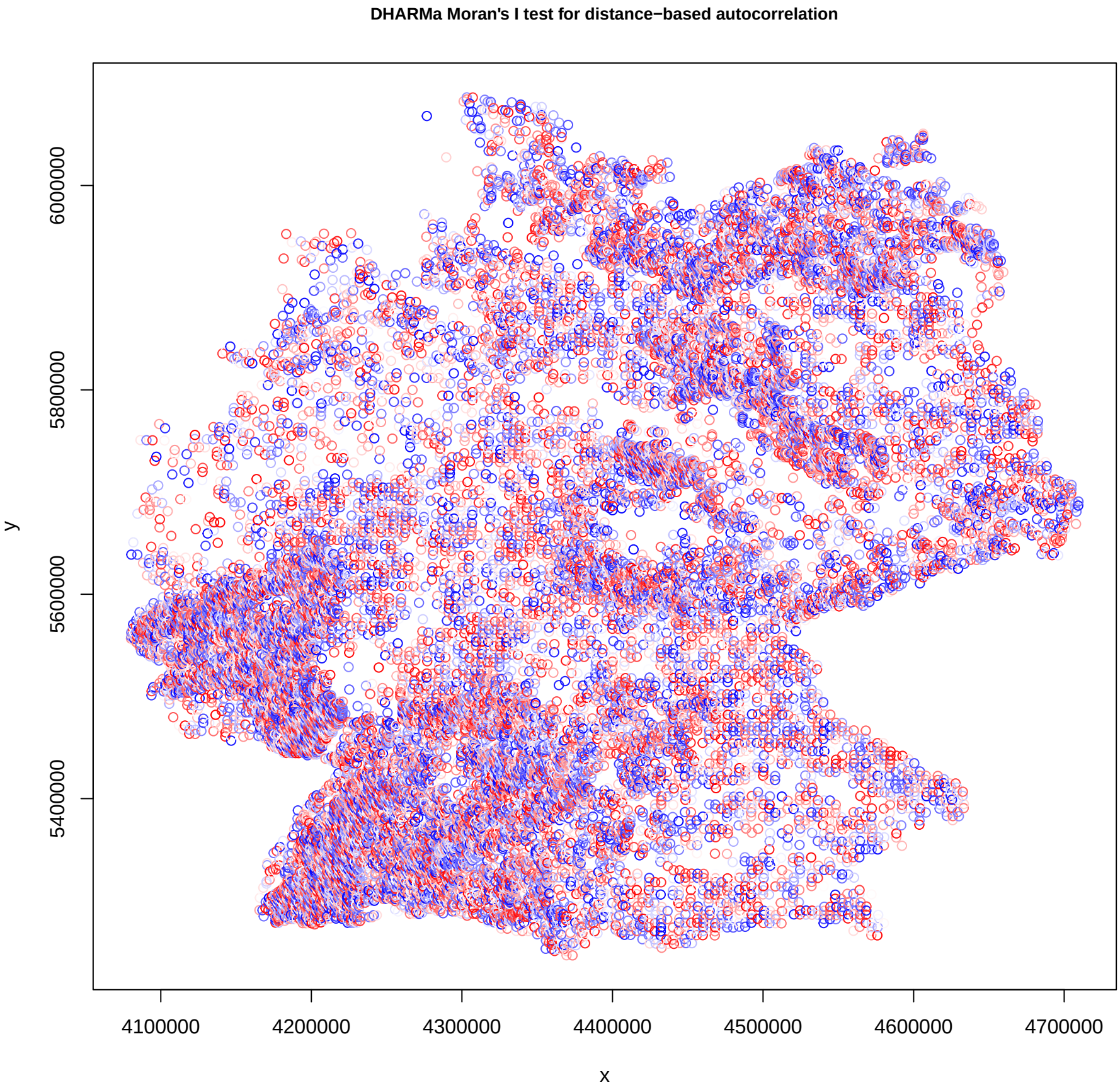

Castanea sativa

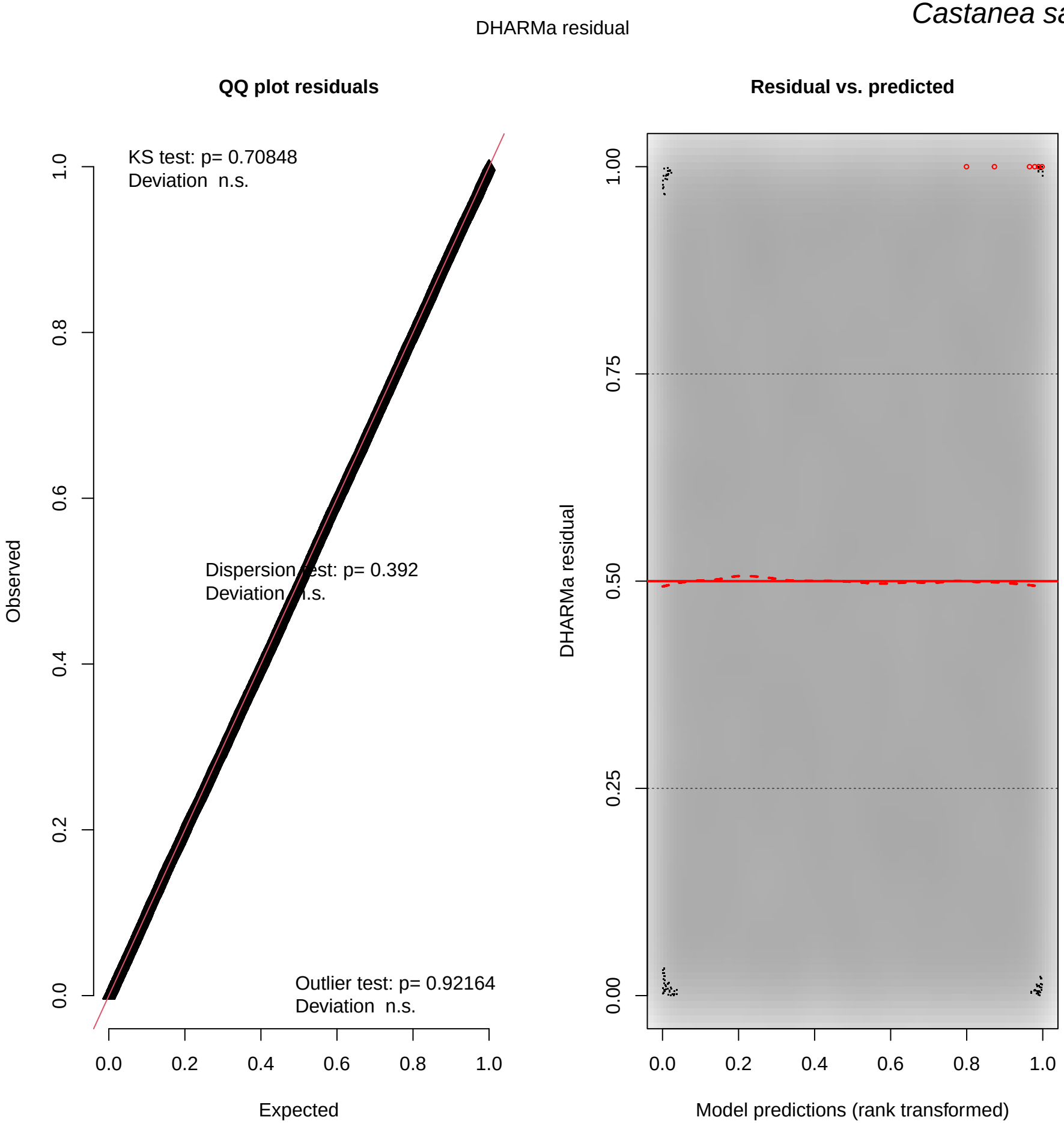

Castanea sativa

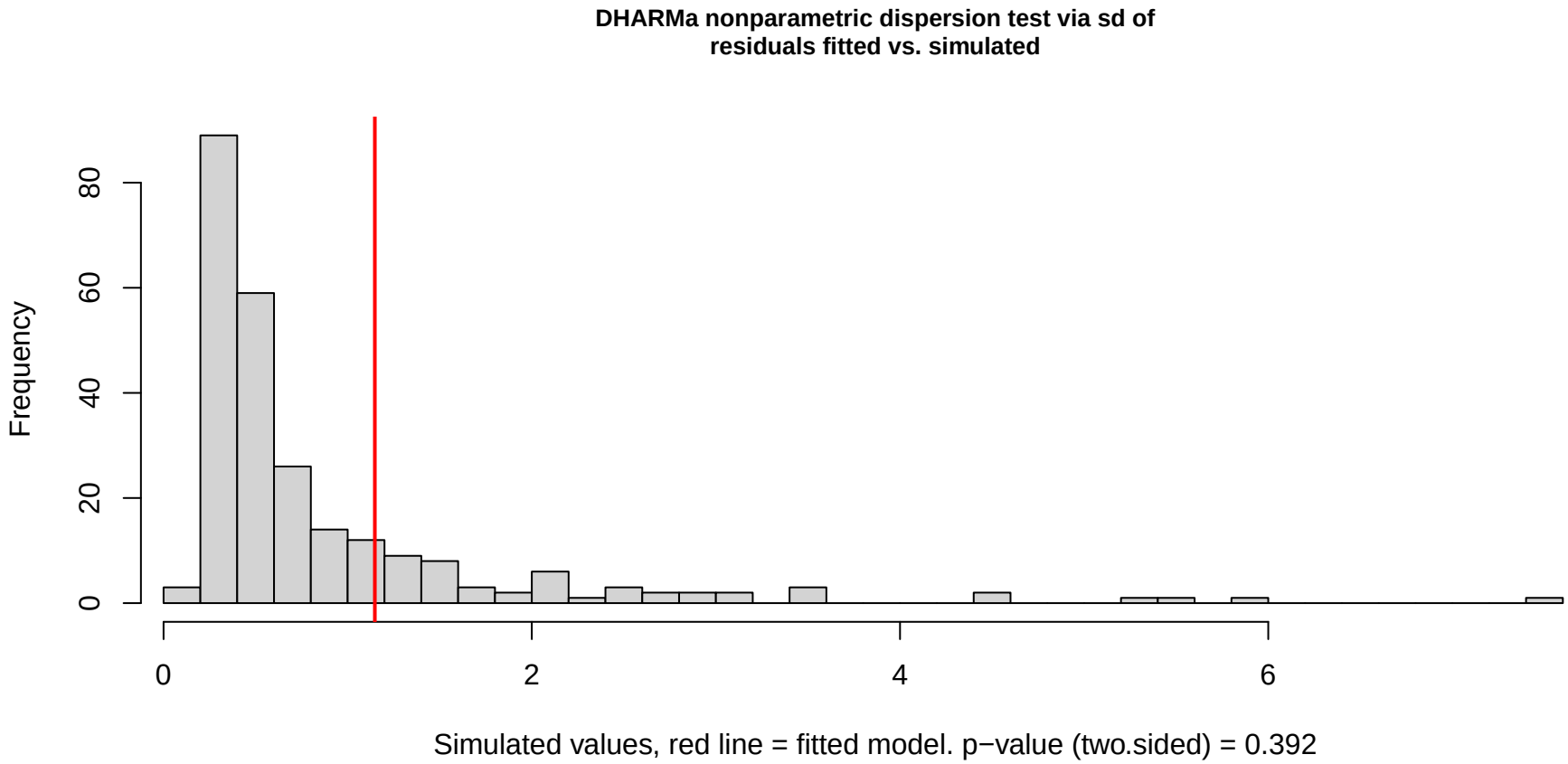

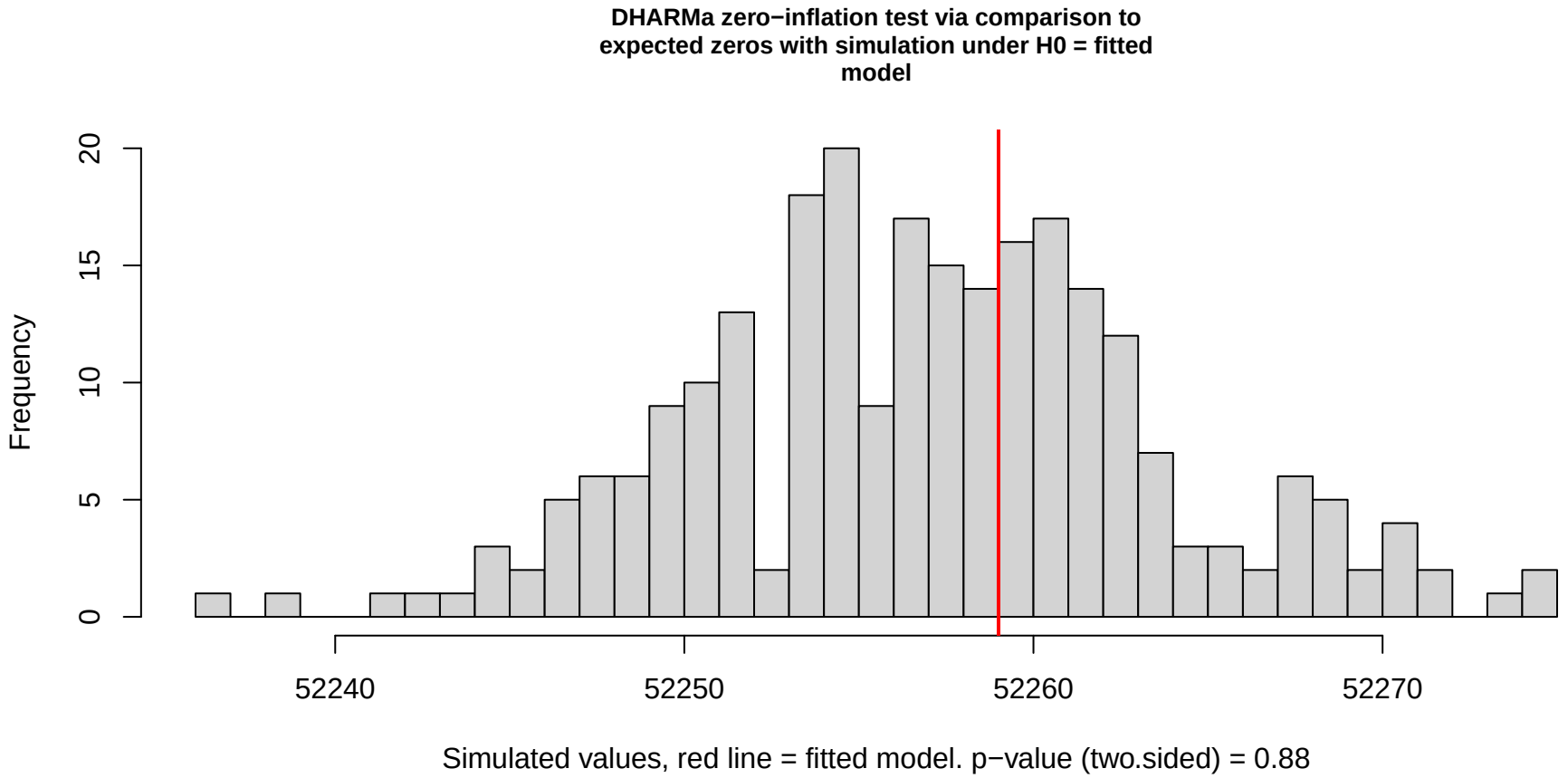

Castanea sativa

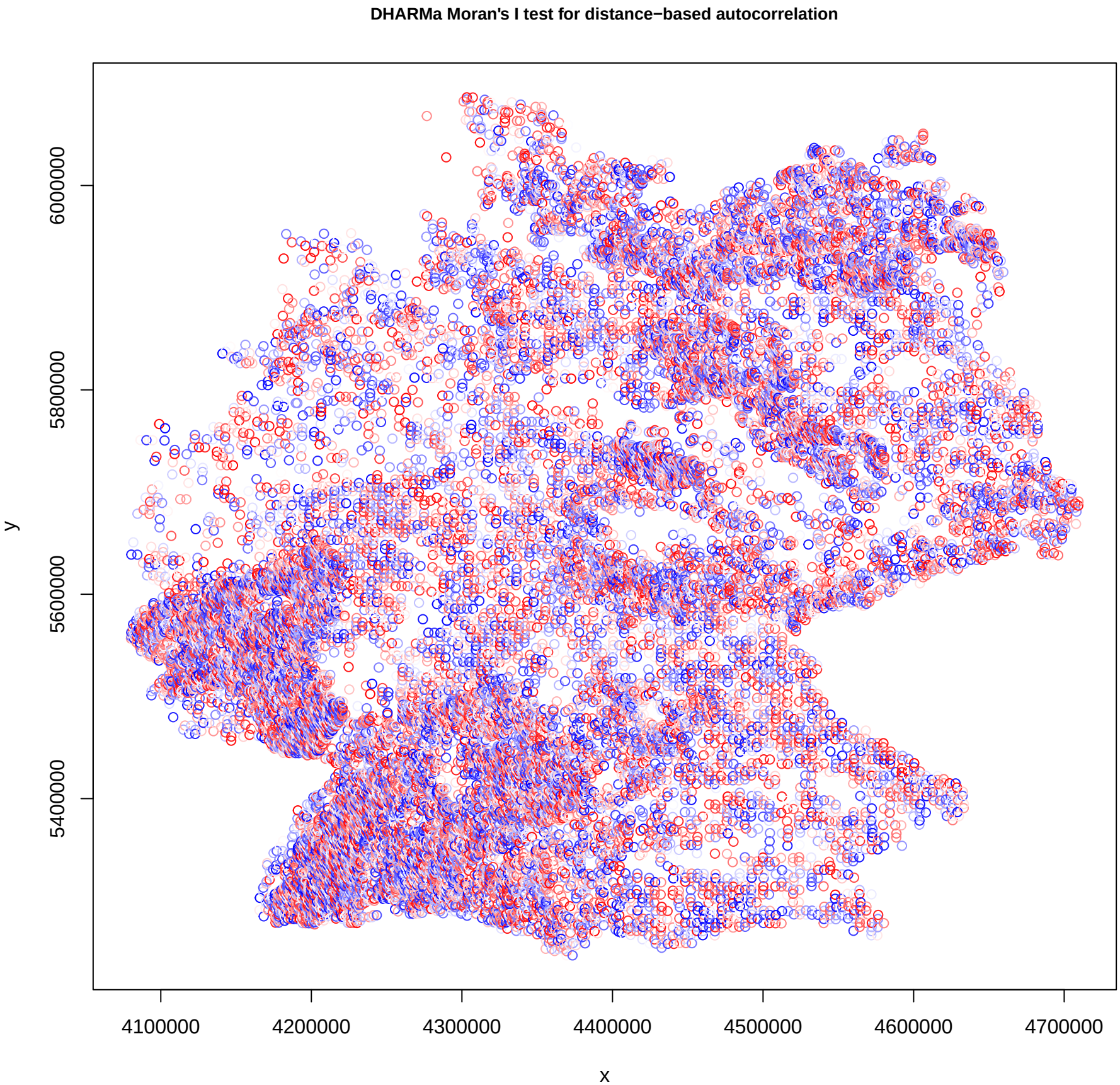

Fraxinus excelsior

DHARMa residual

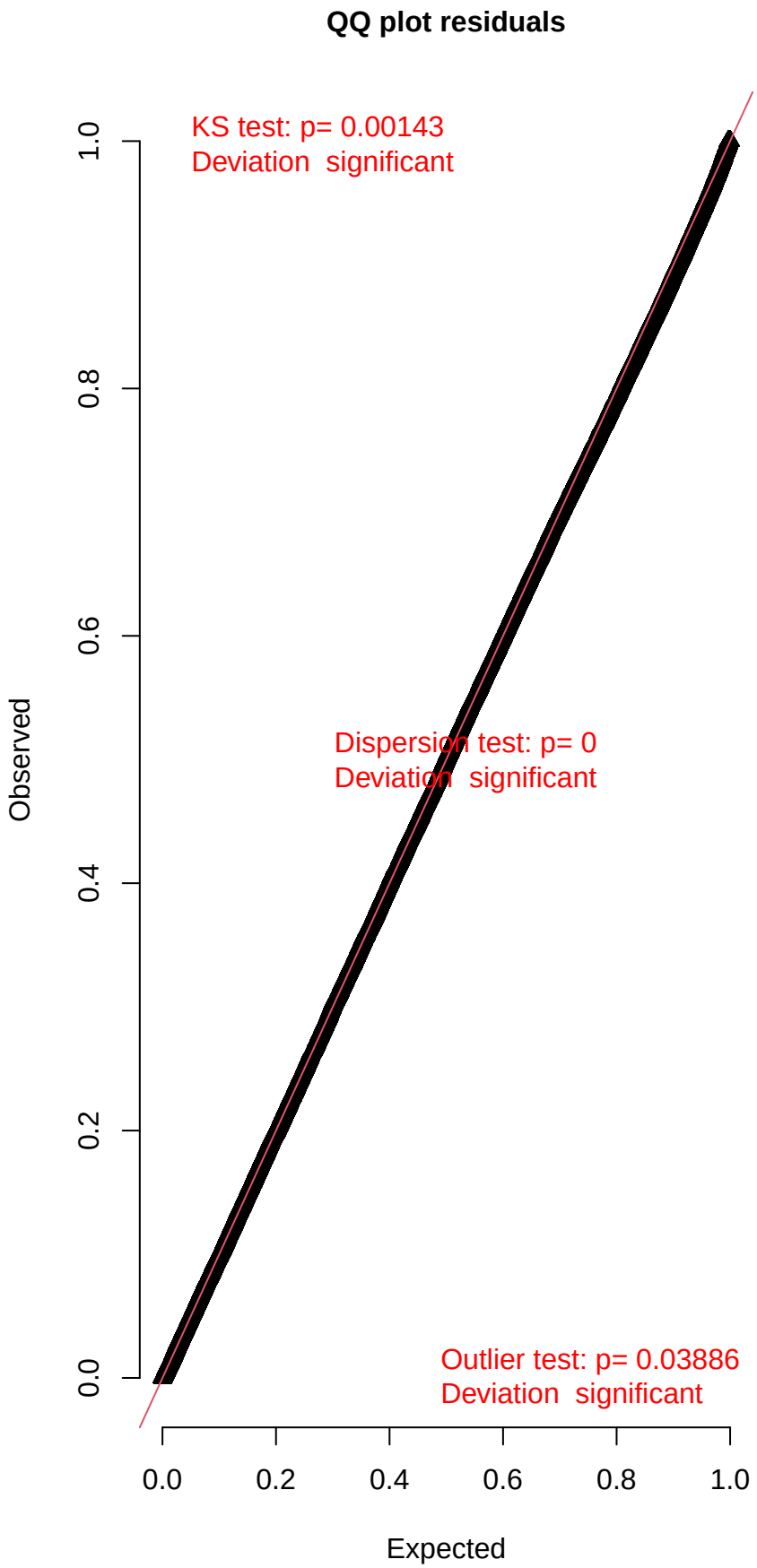

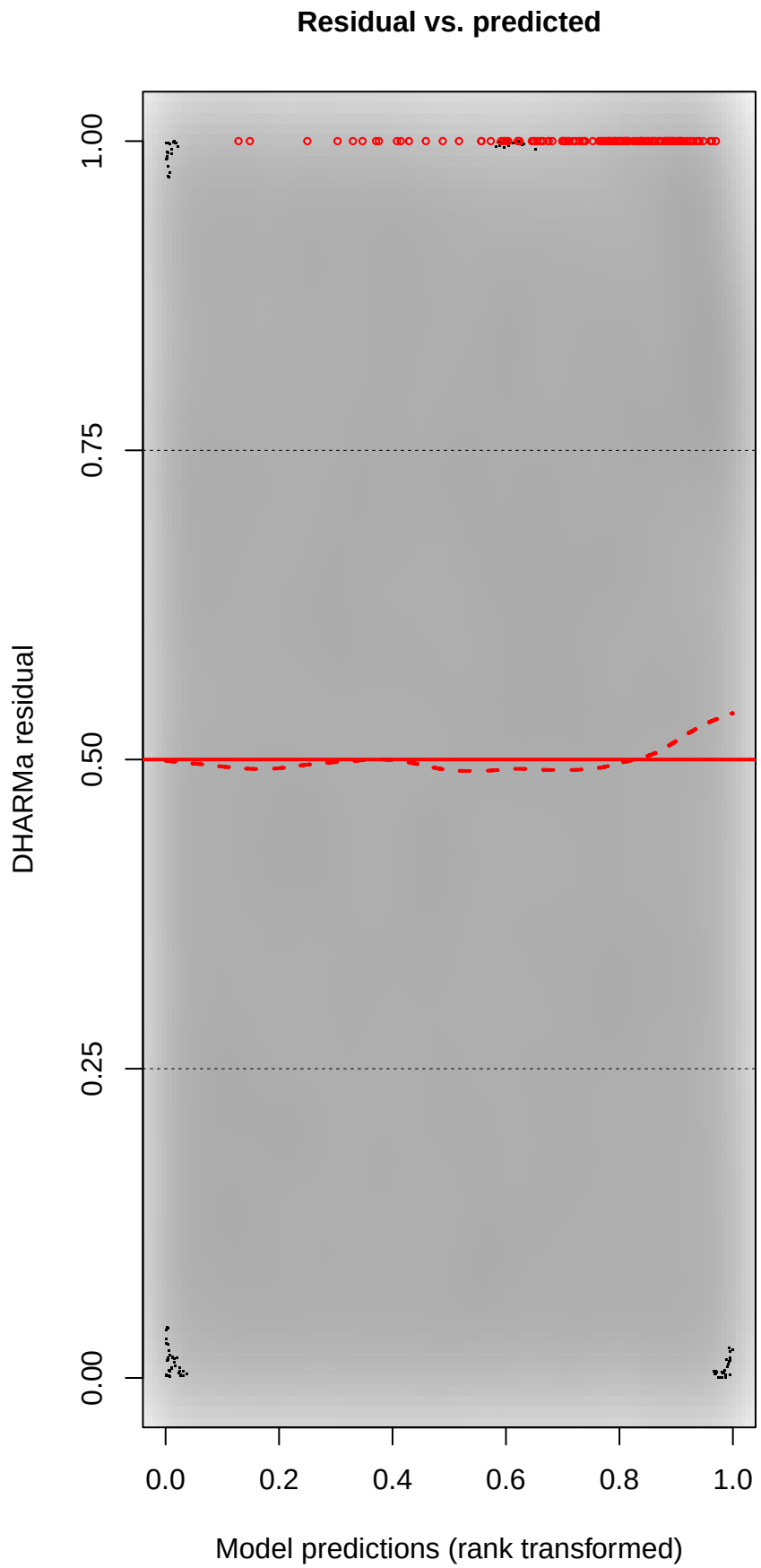

Fraxinus excelsior

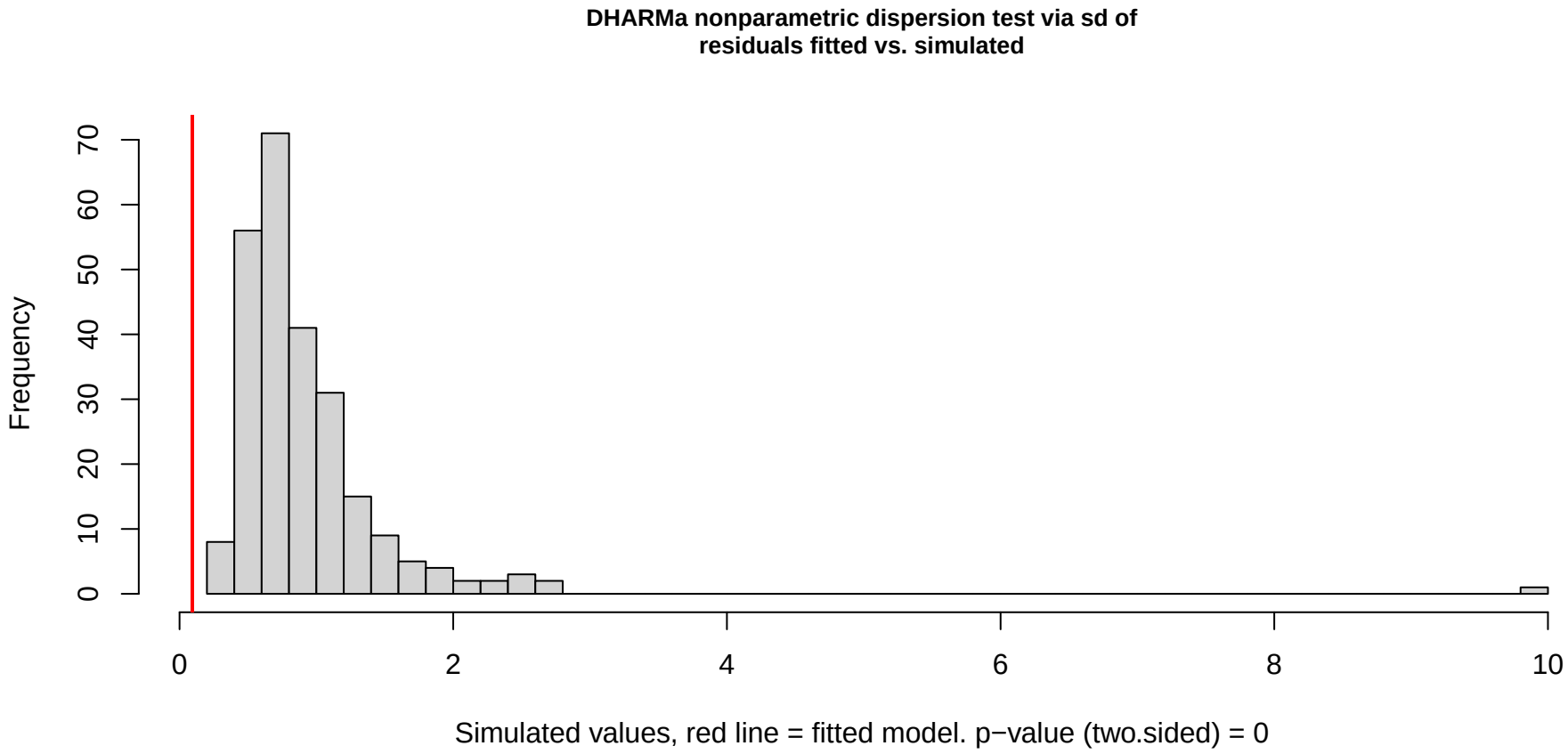

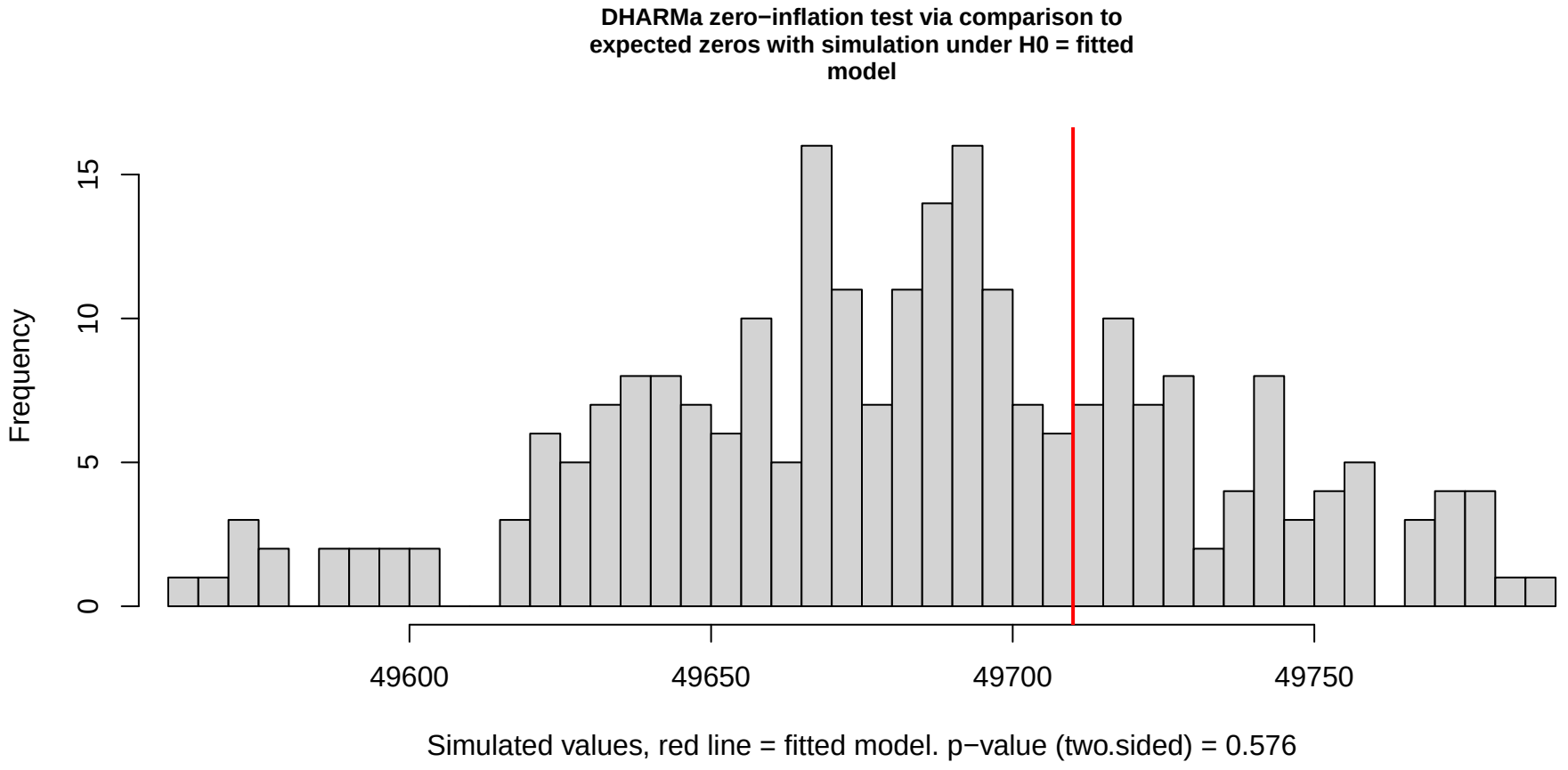

Fraxinus excelsior

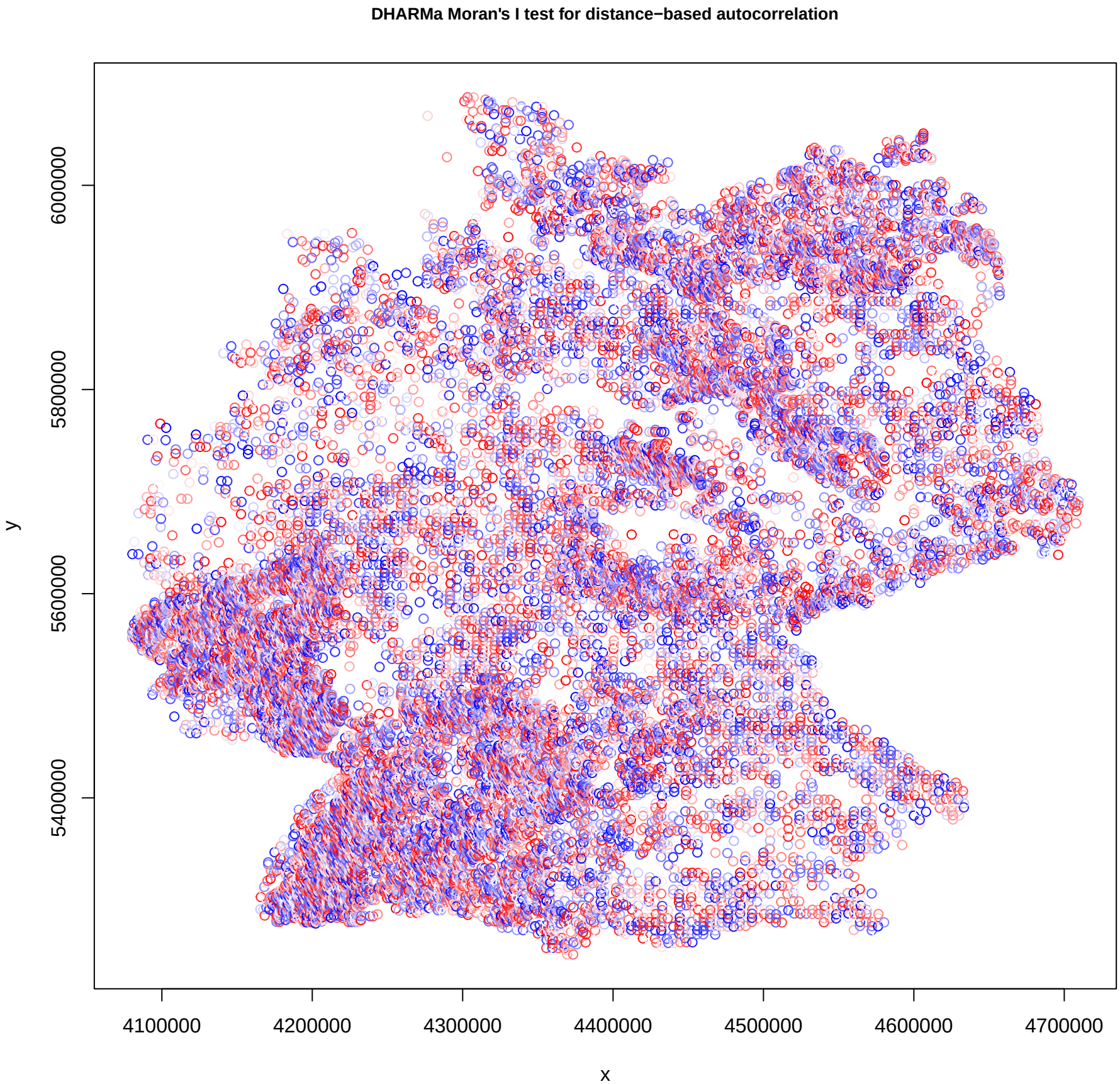

Populus x.canescens

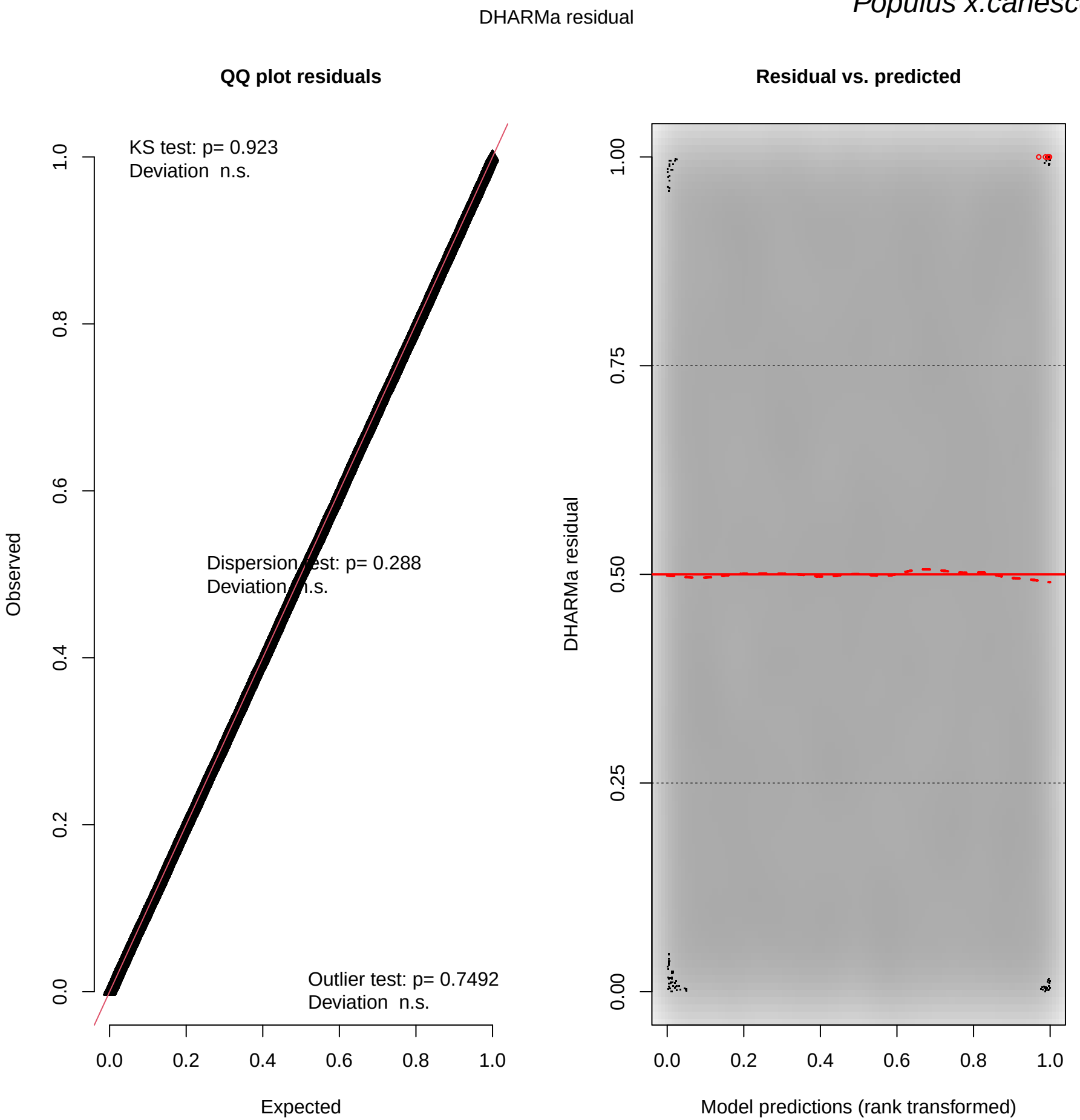

Populus x.canescens

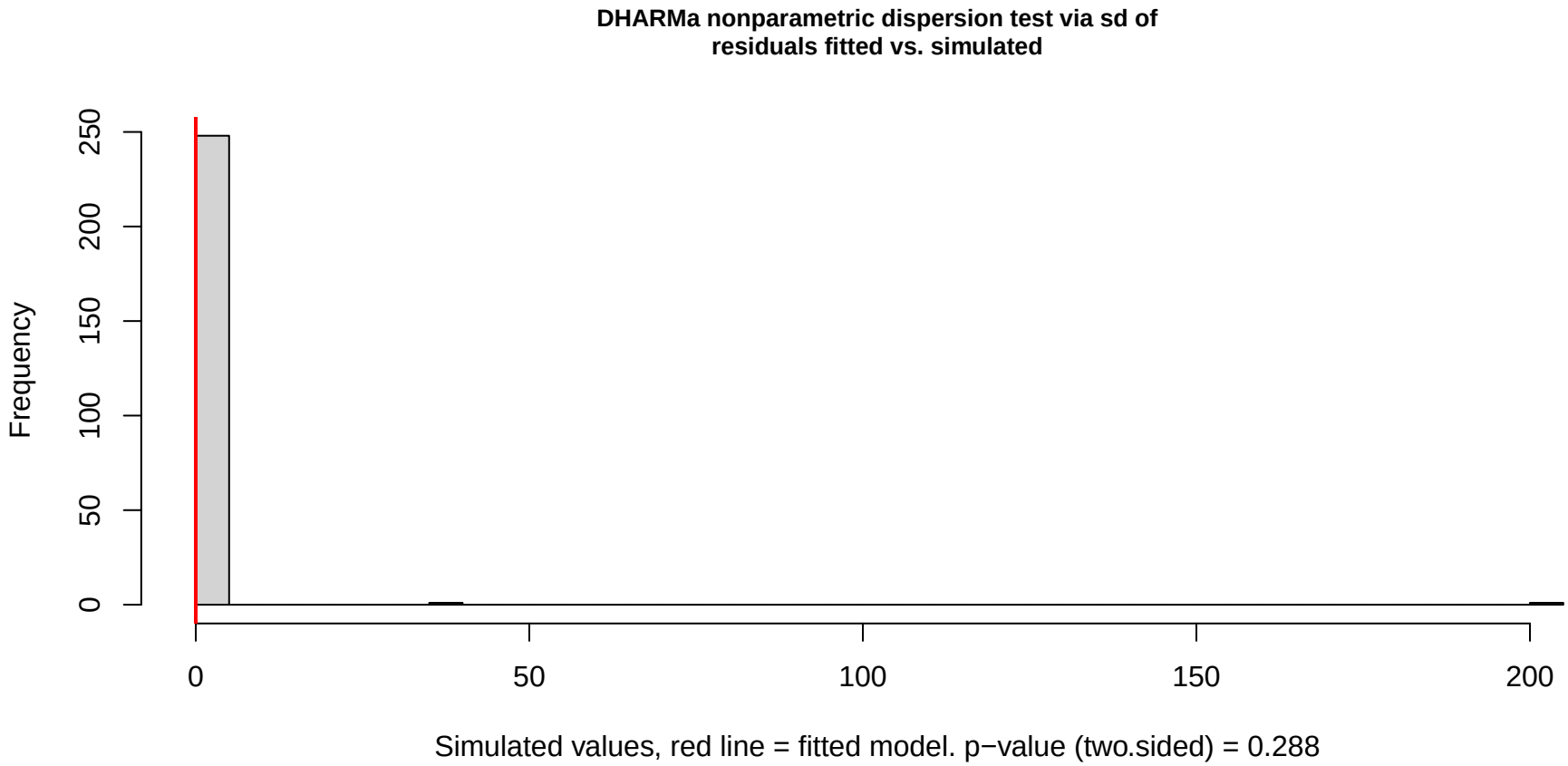

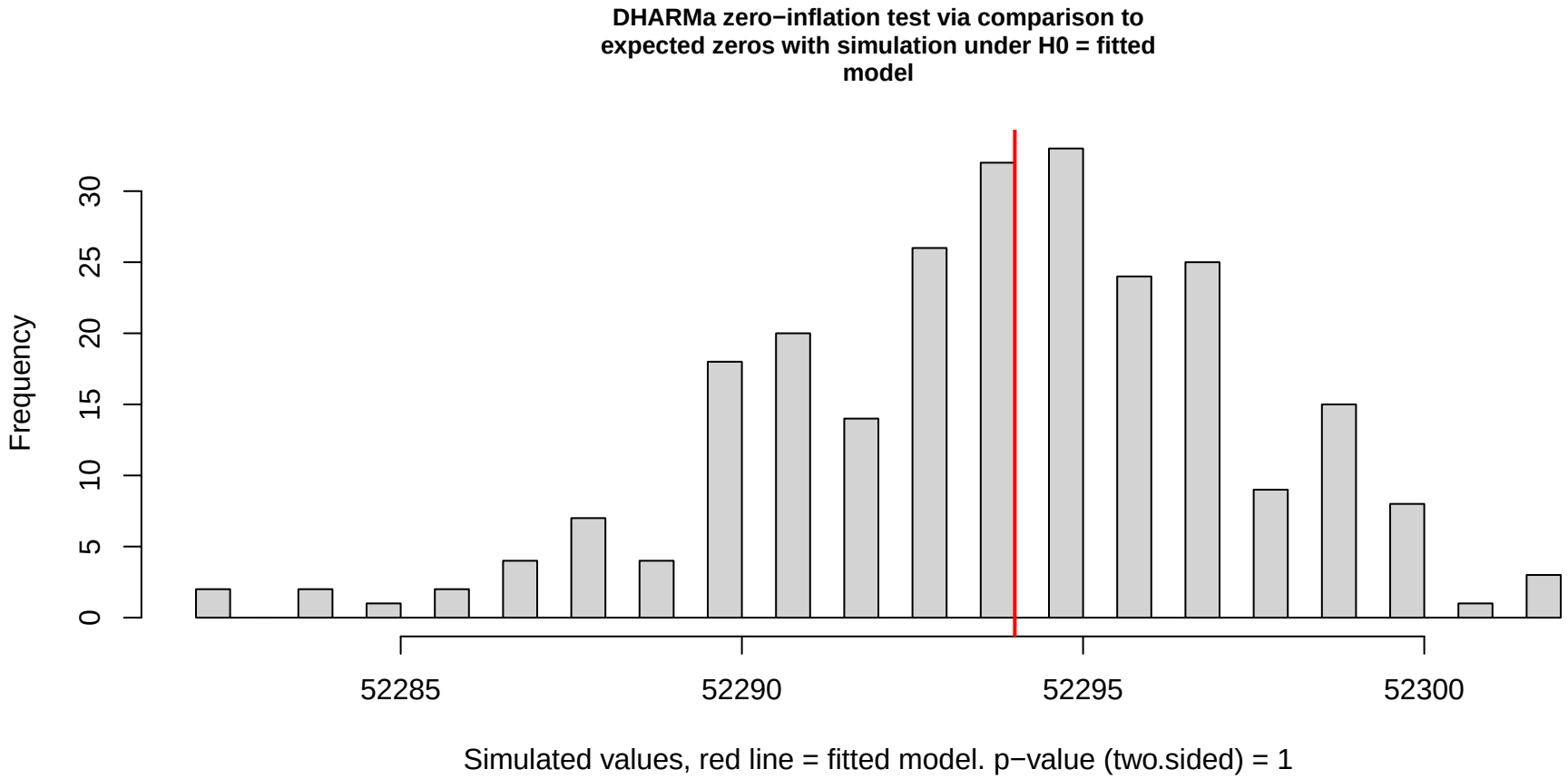

Populus x.canescens

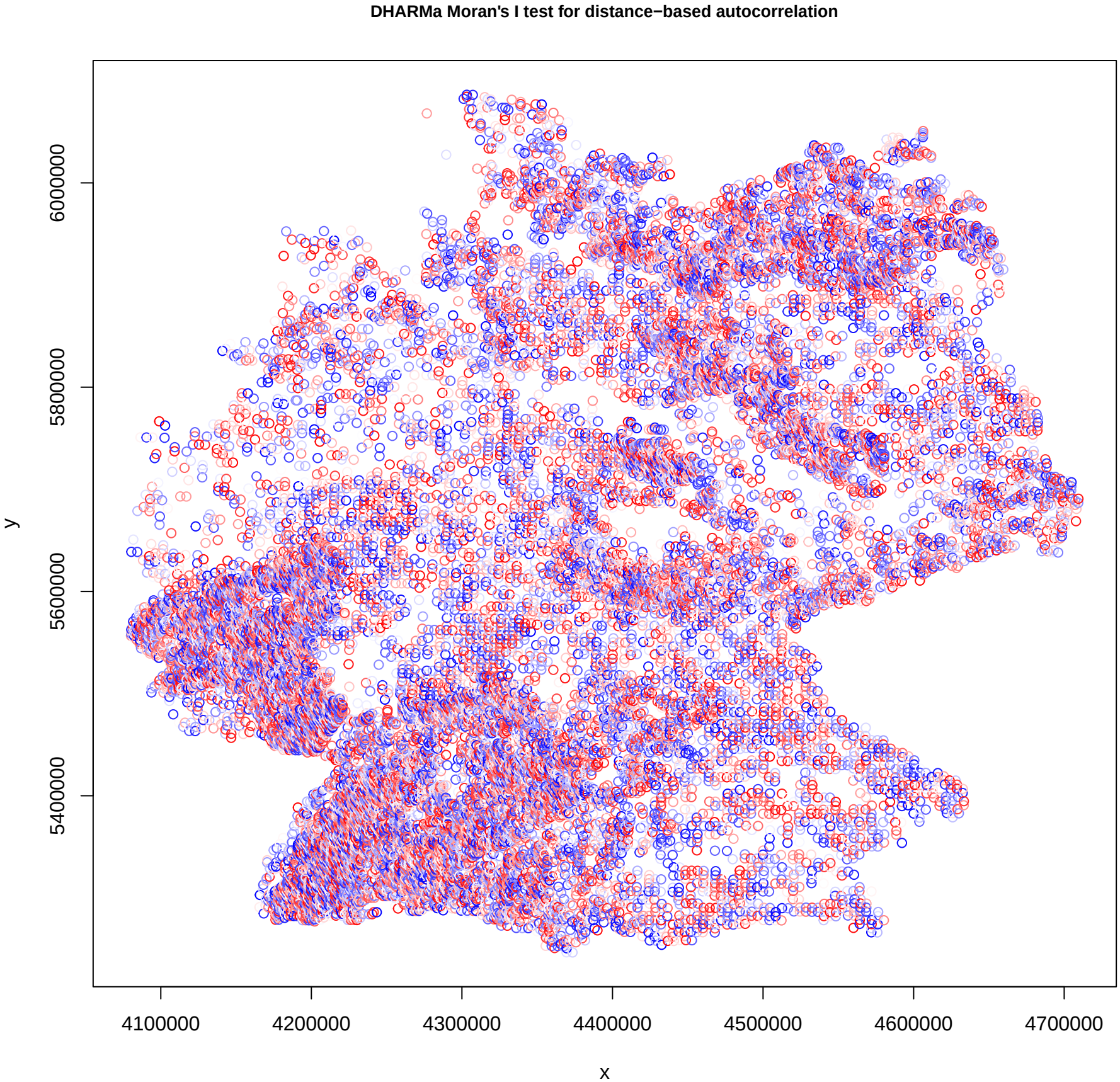

Populus tremula

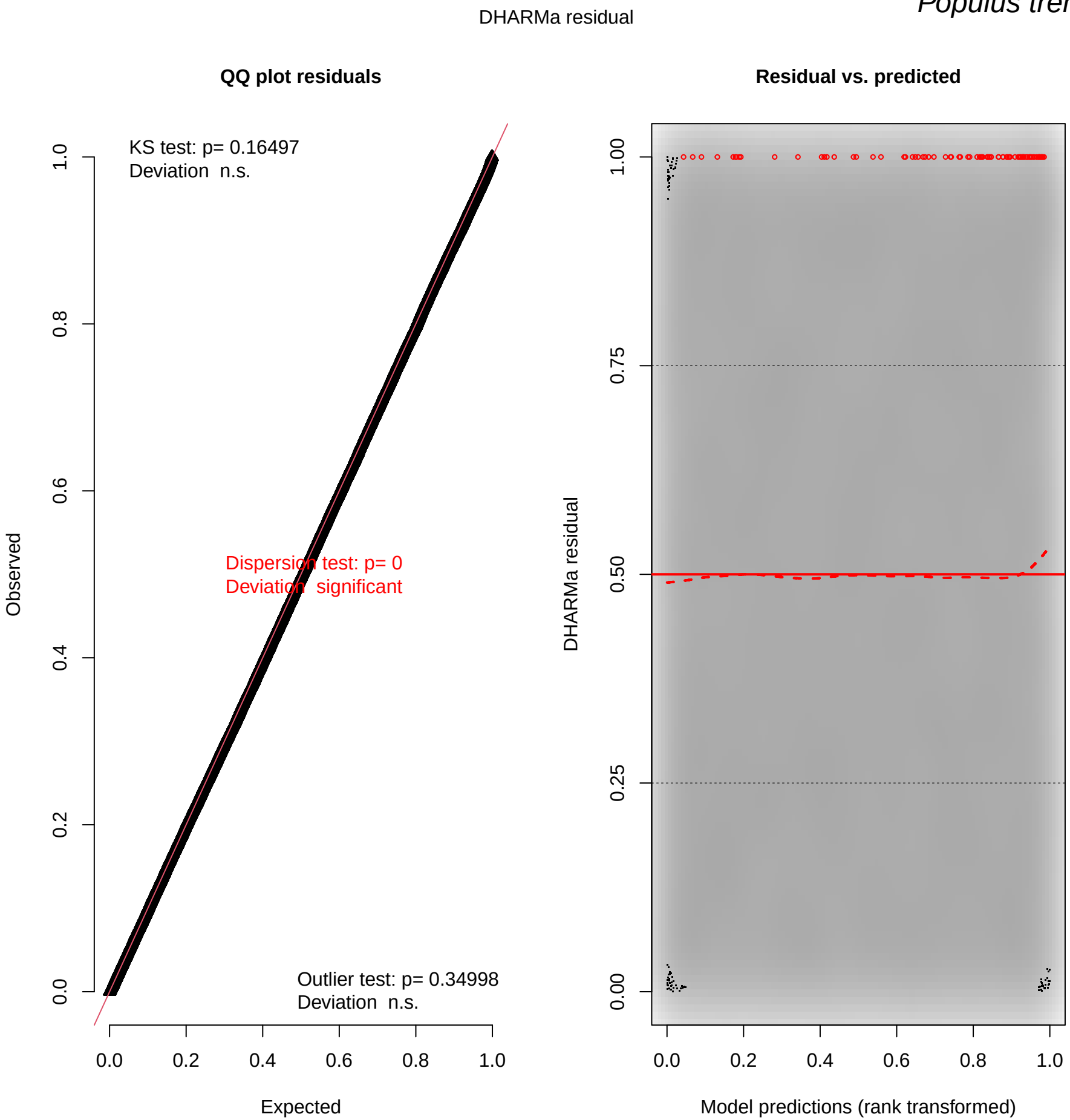

Populus tremula

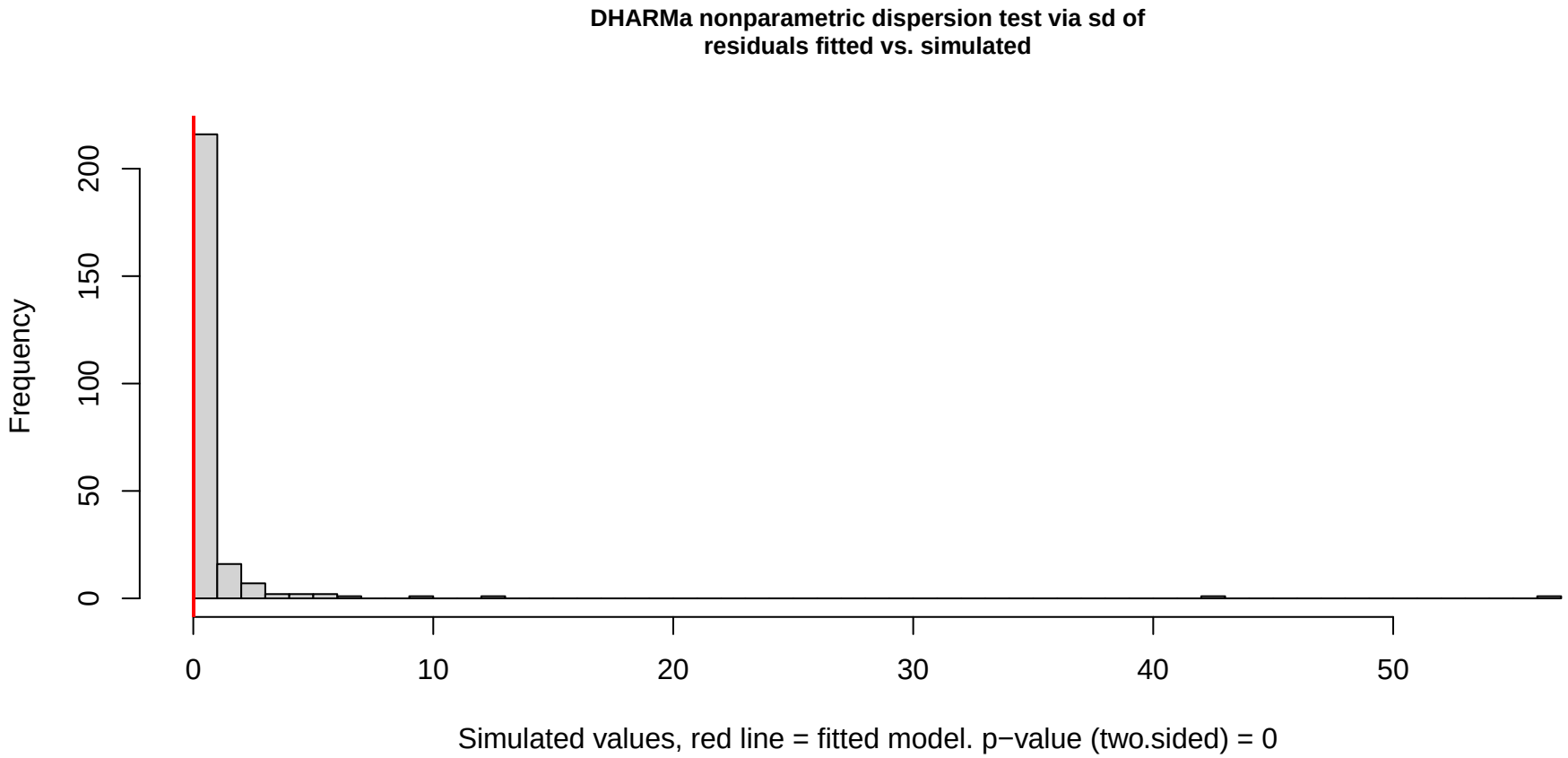

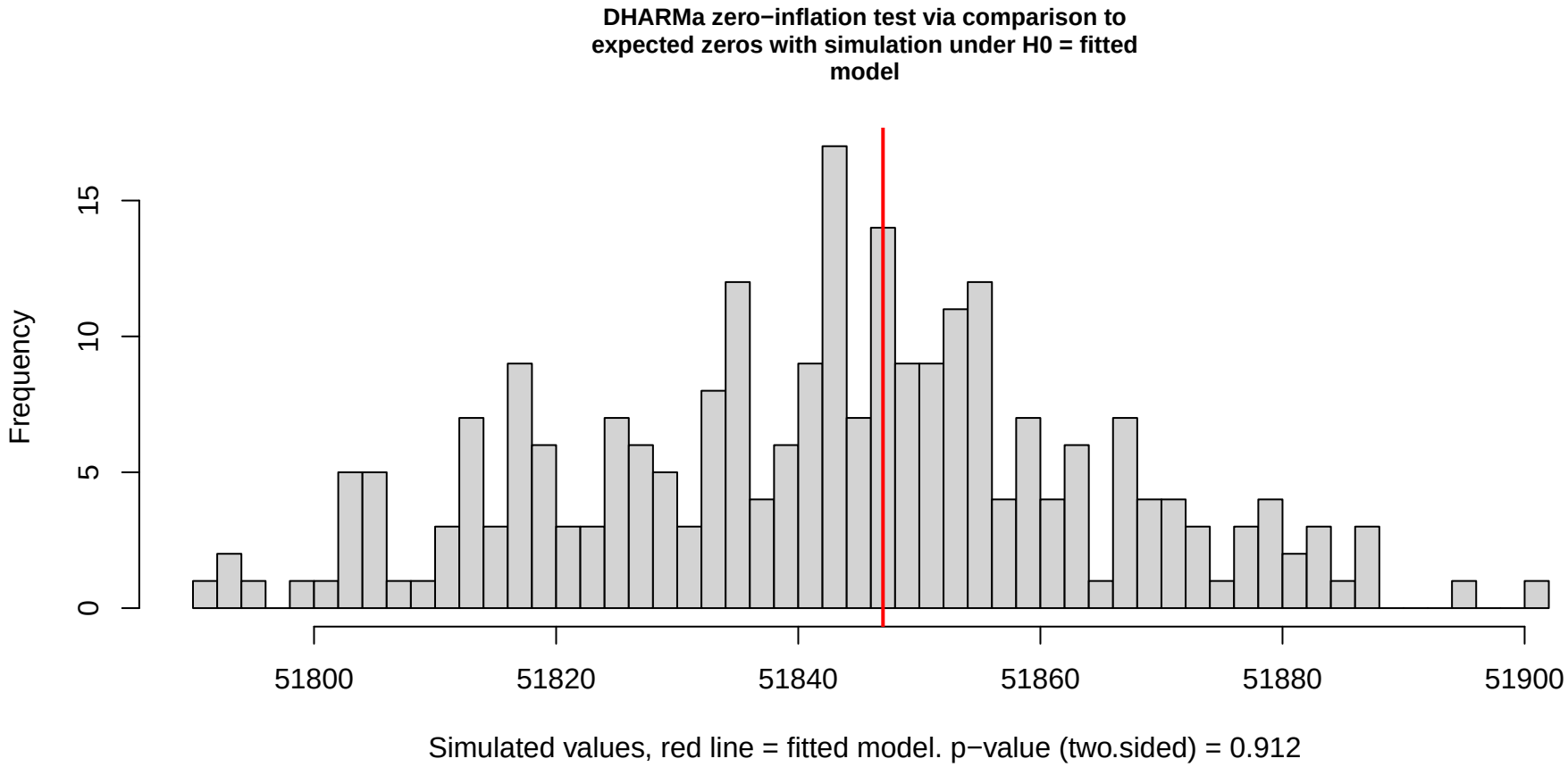

Populus tremula

Populus trichocarpa.x.maximoviczii

DHARMa residual

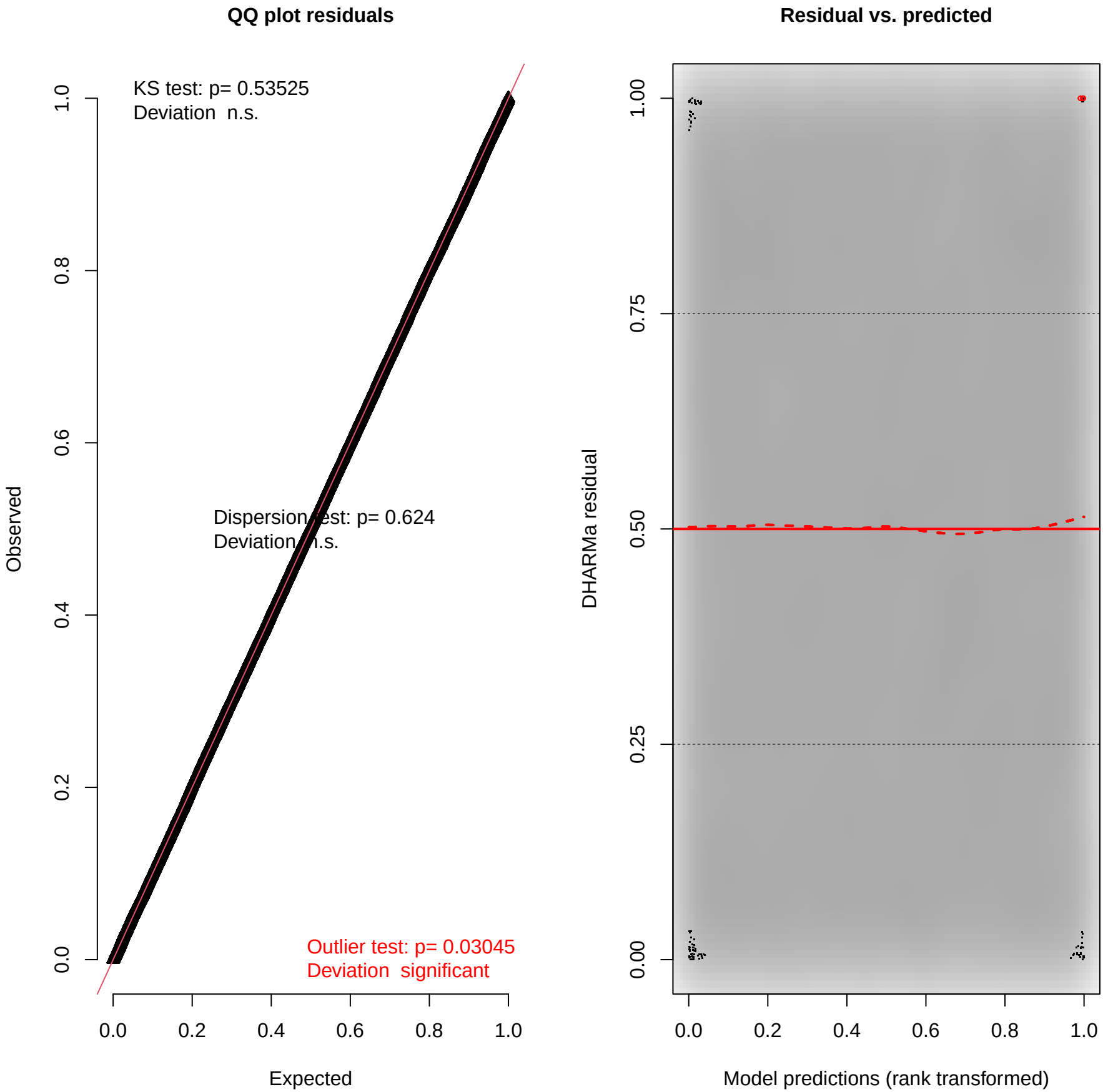

Populus trichocarpa.x.maximoviczii

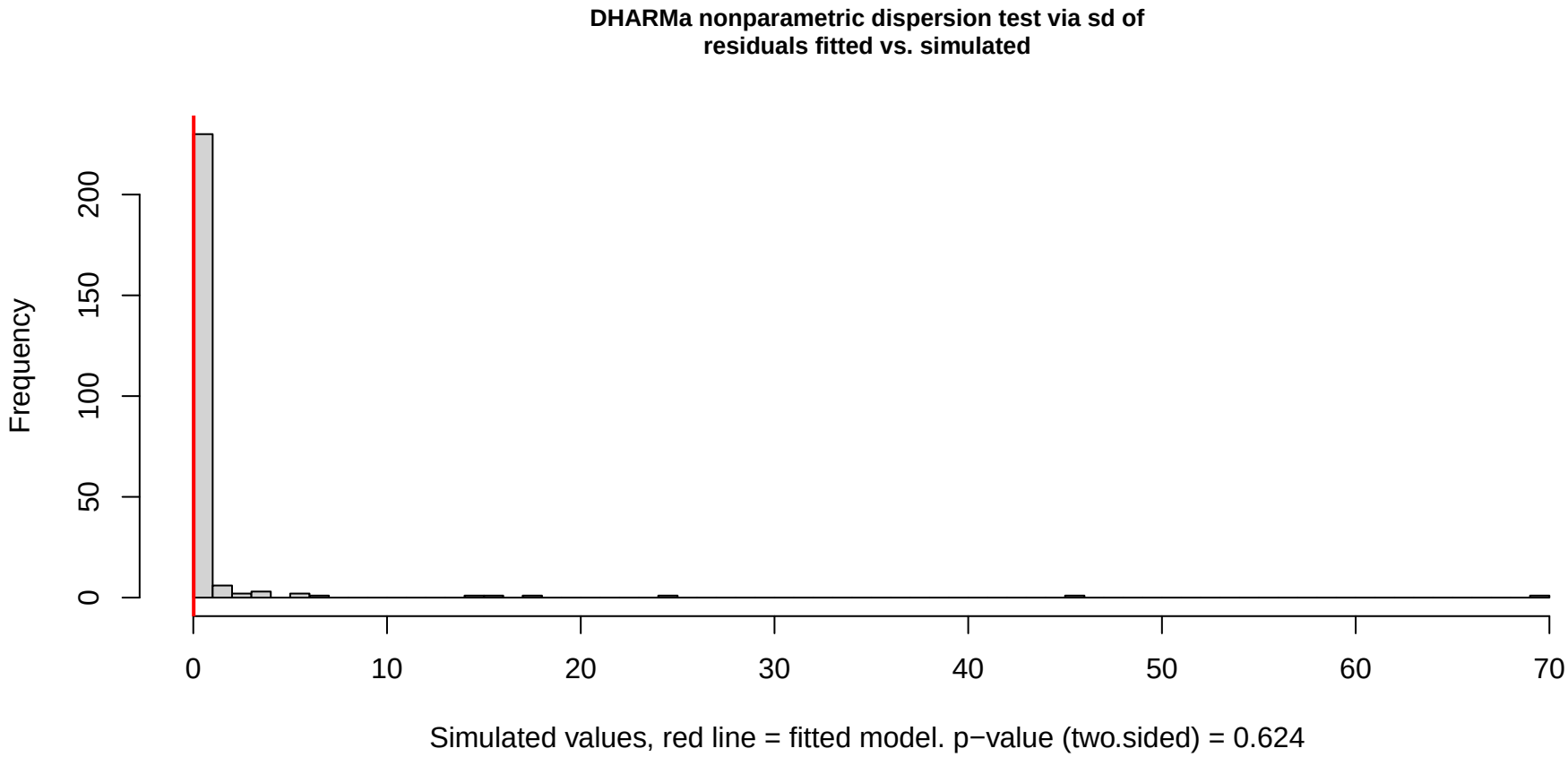

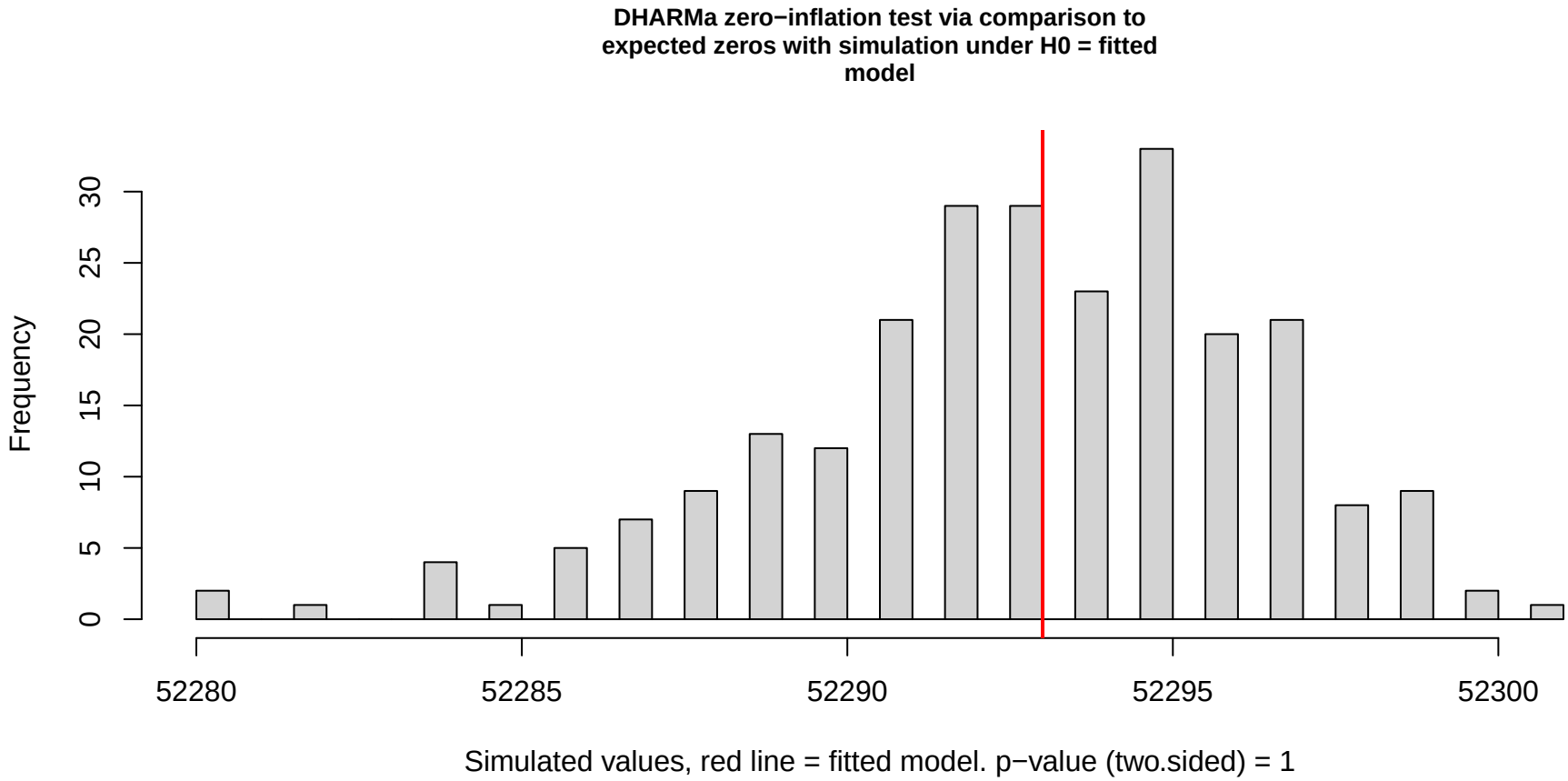

Populus trichocarpa.x.maximoviczii

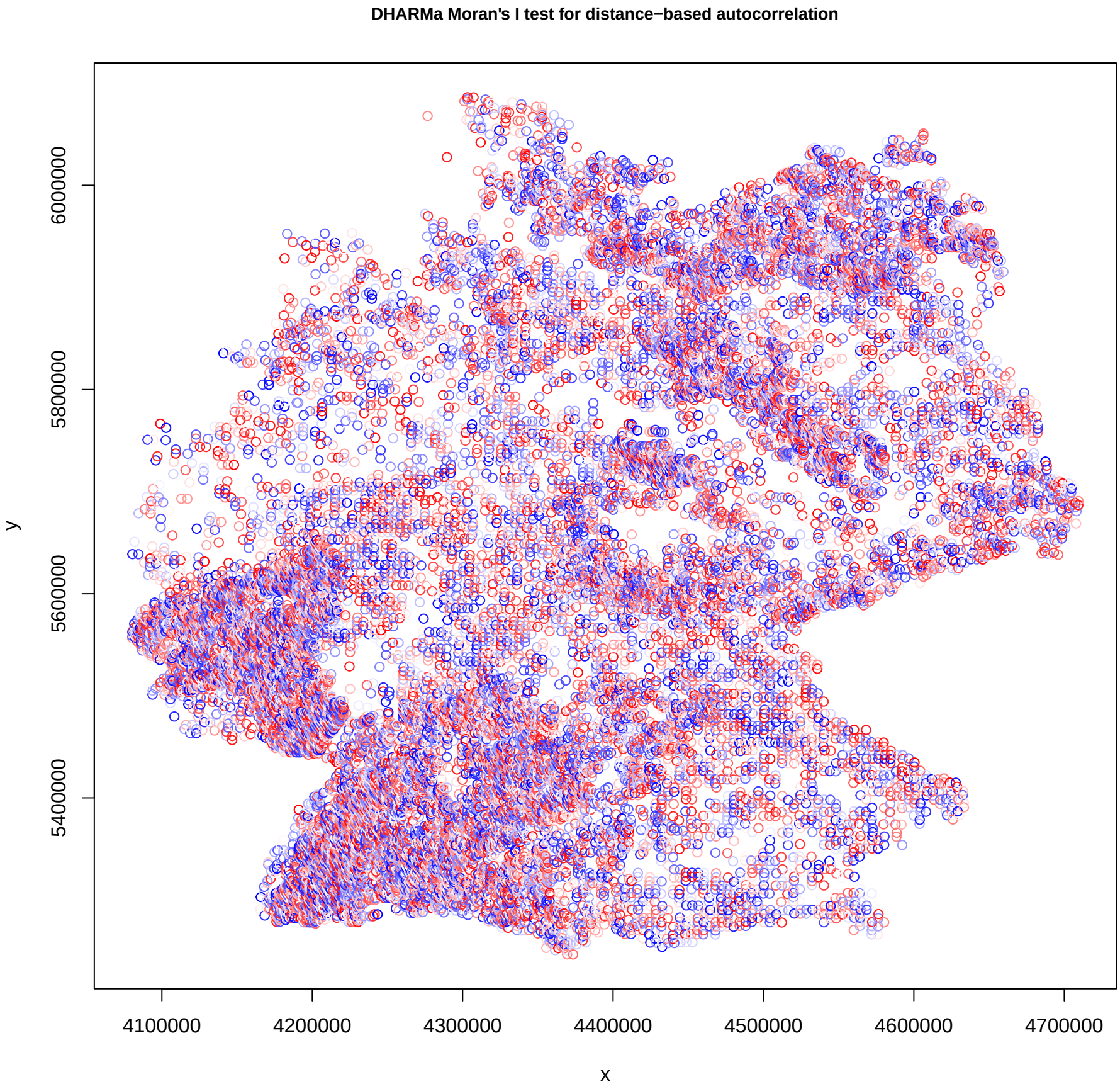

Populus nigra

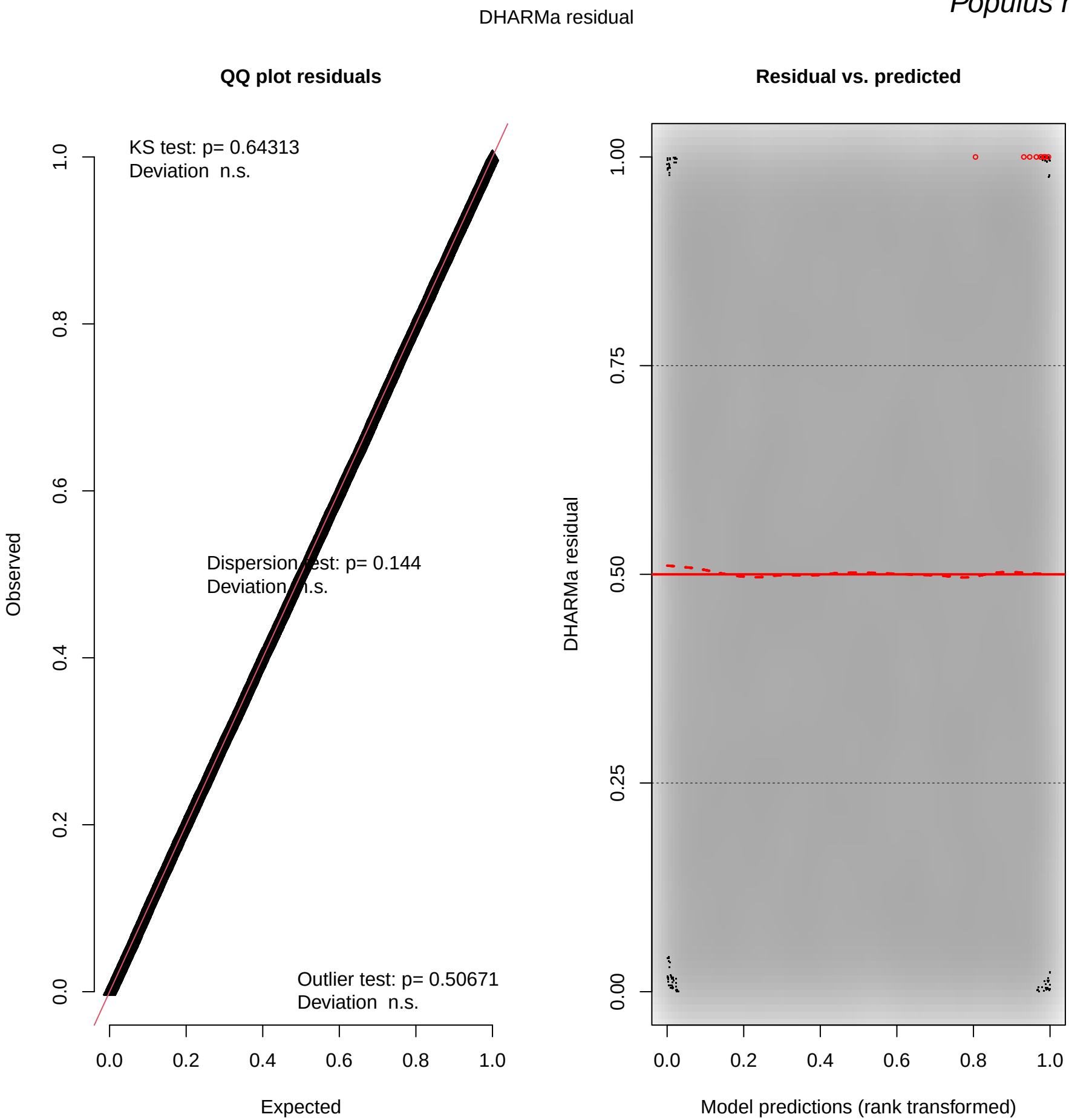

Populus nigra

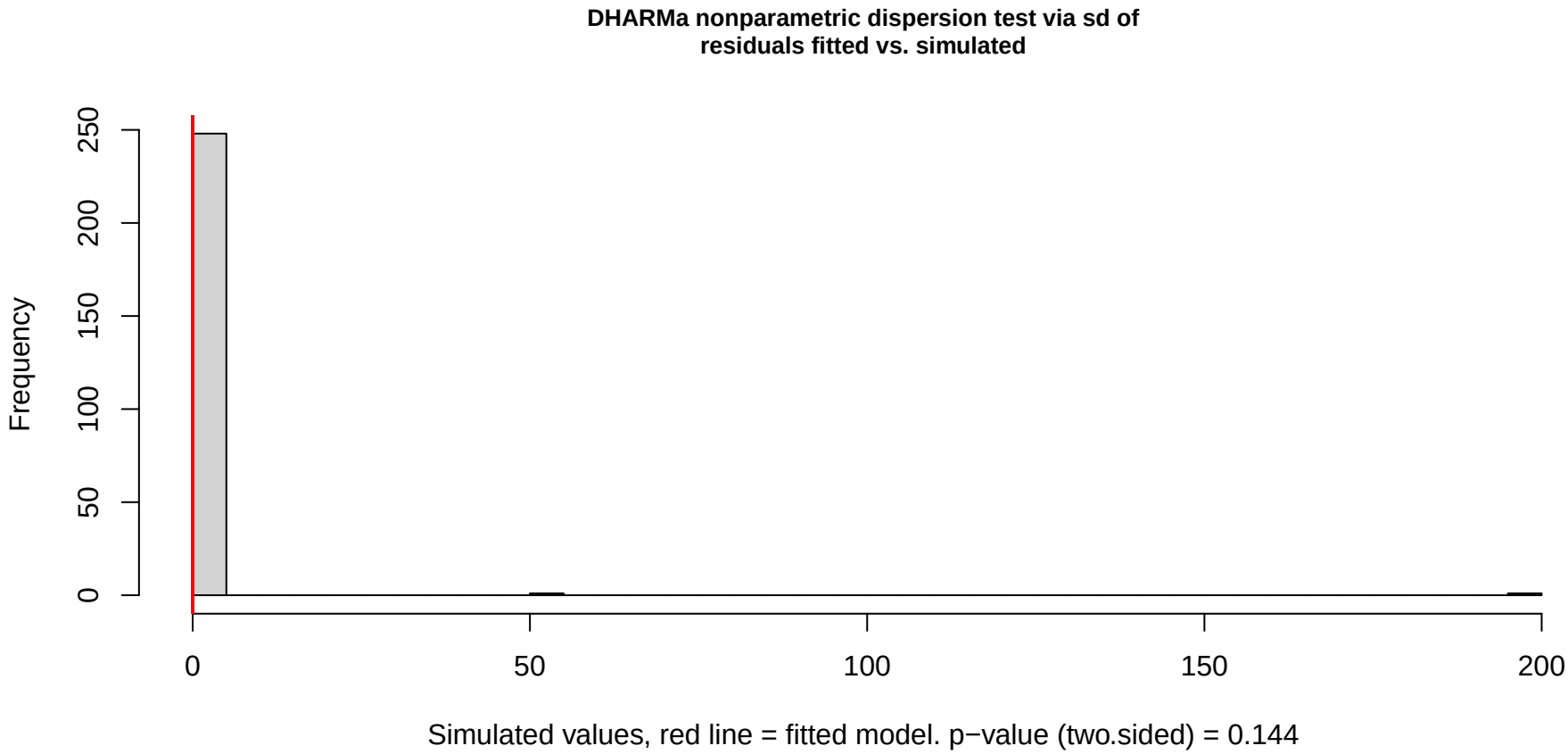

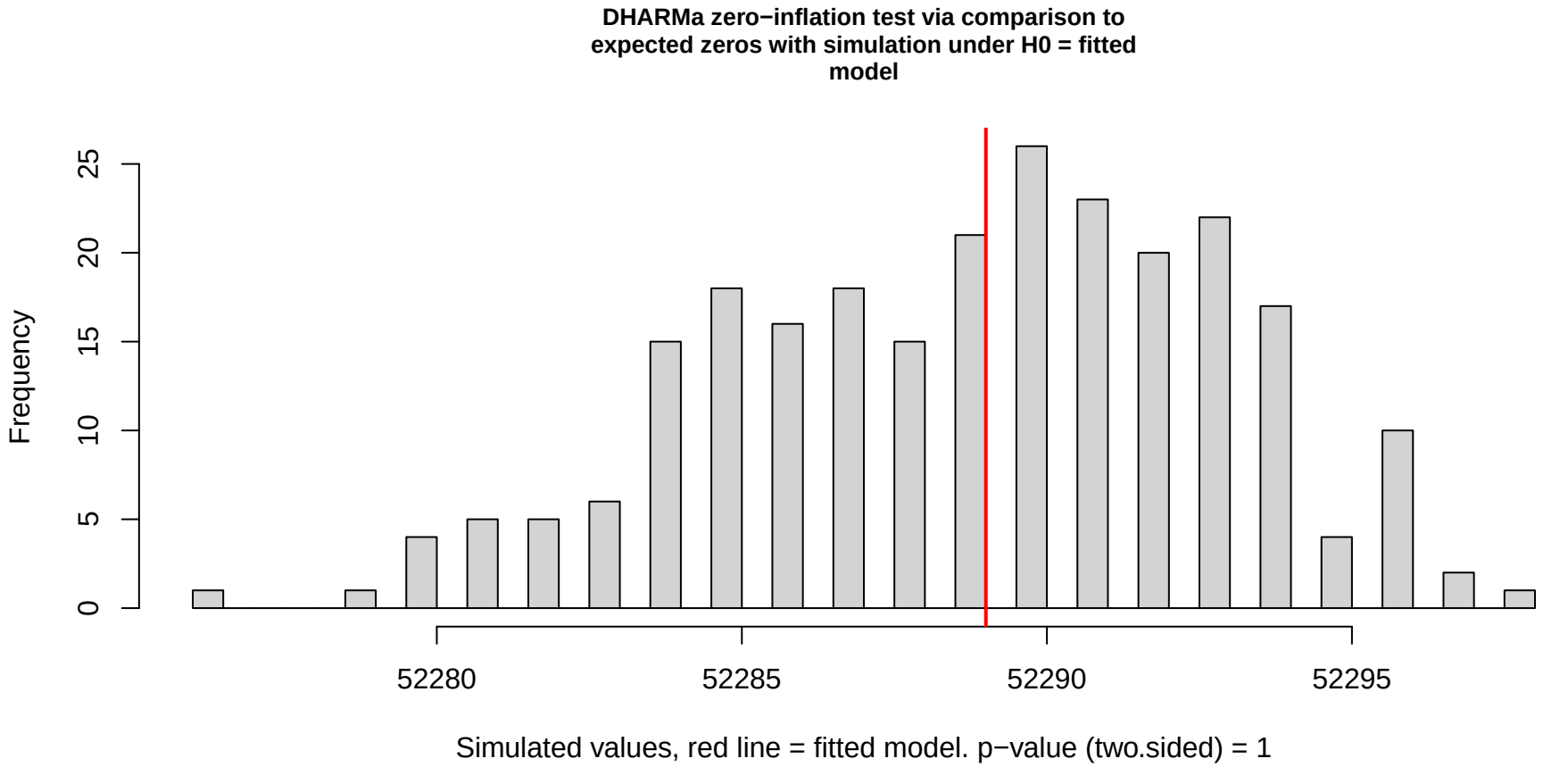

Populus nigra

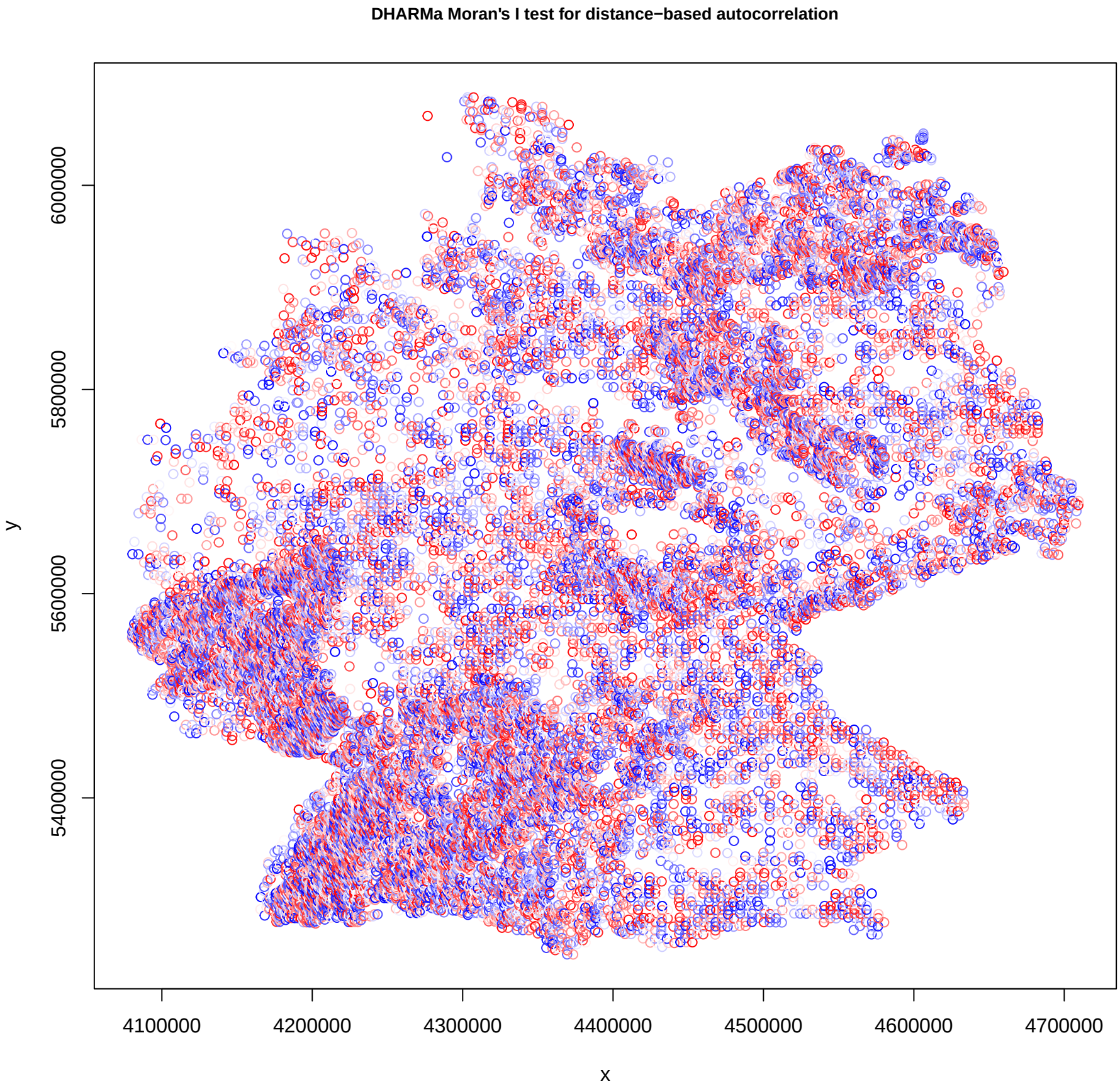

Populus alba

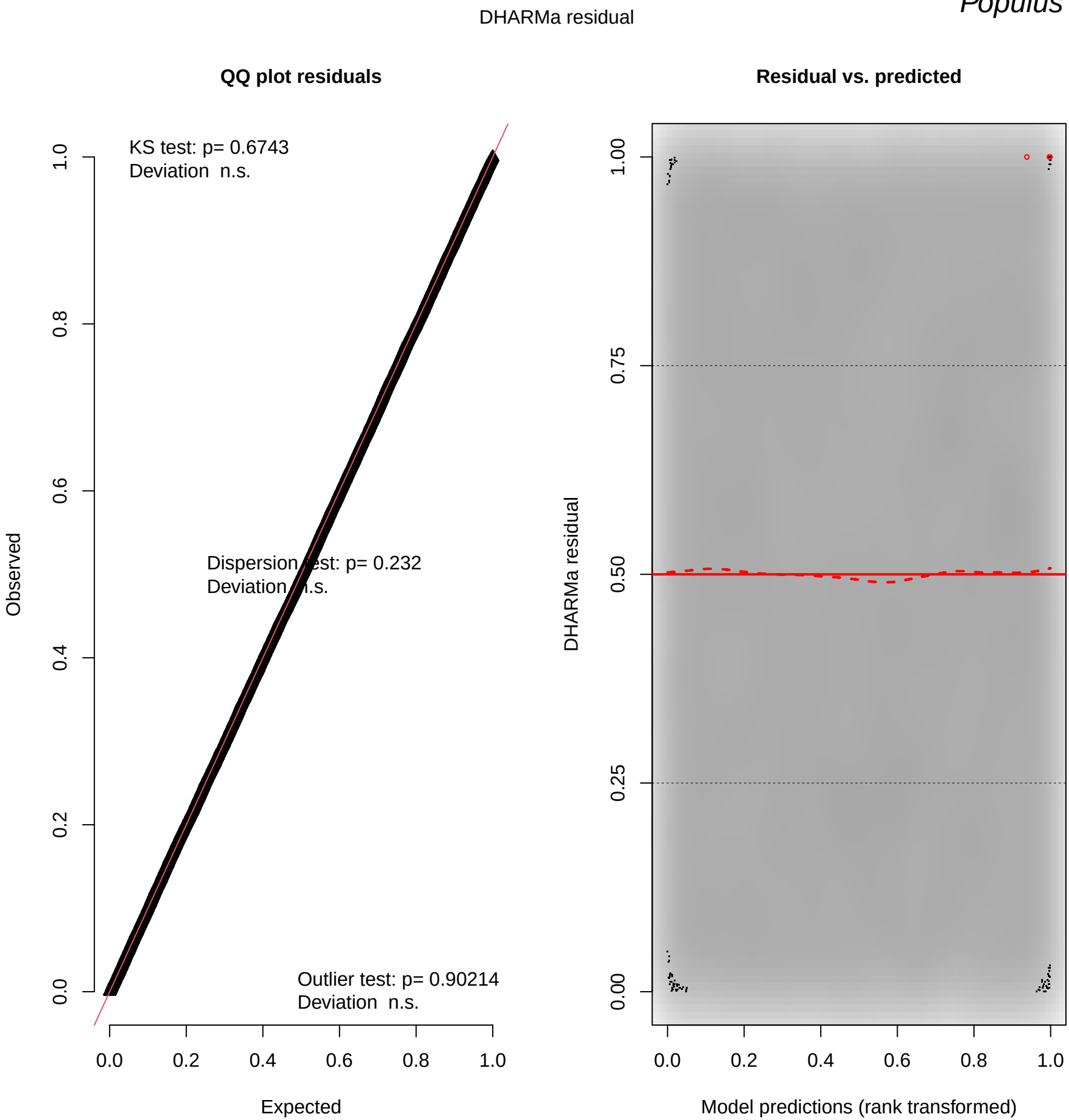

Populus alba

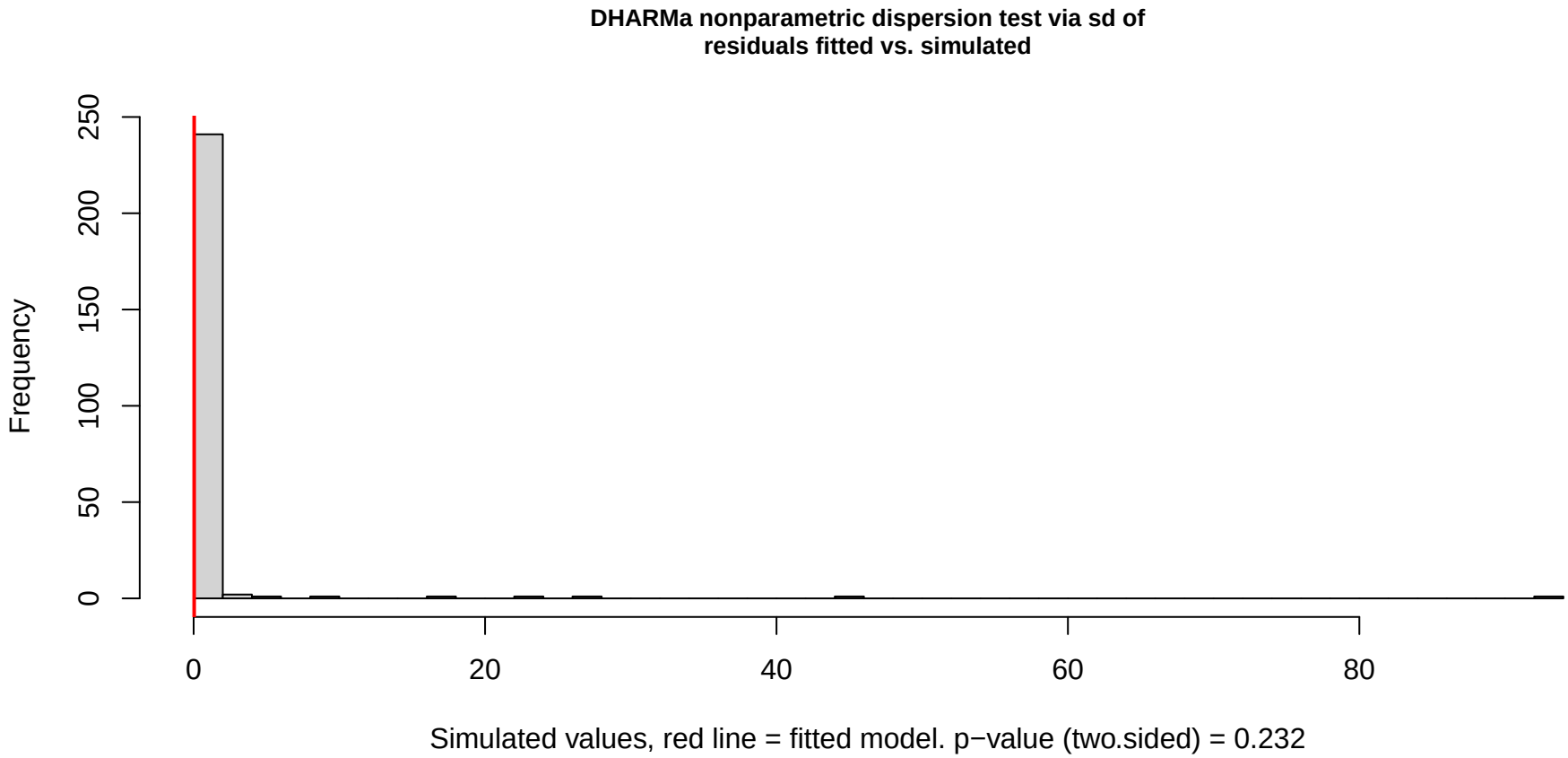

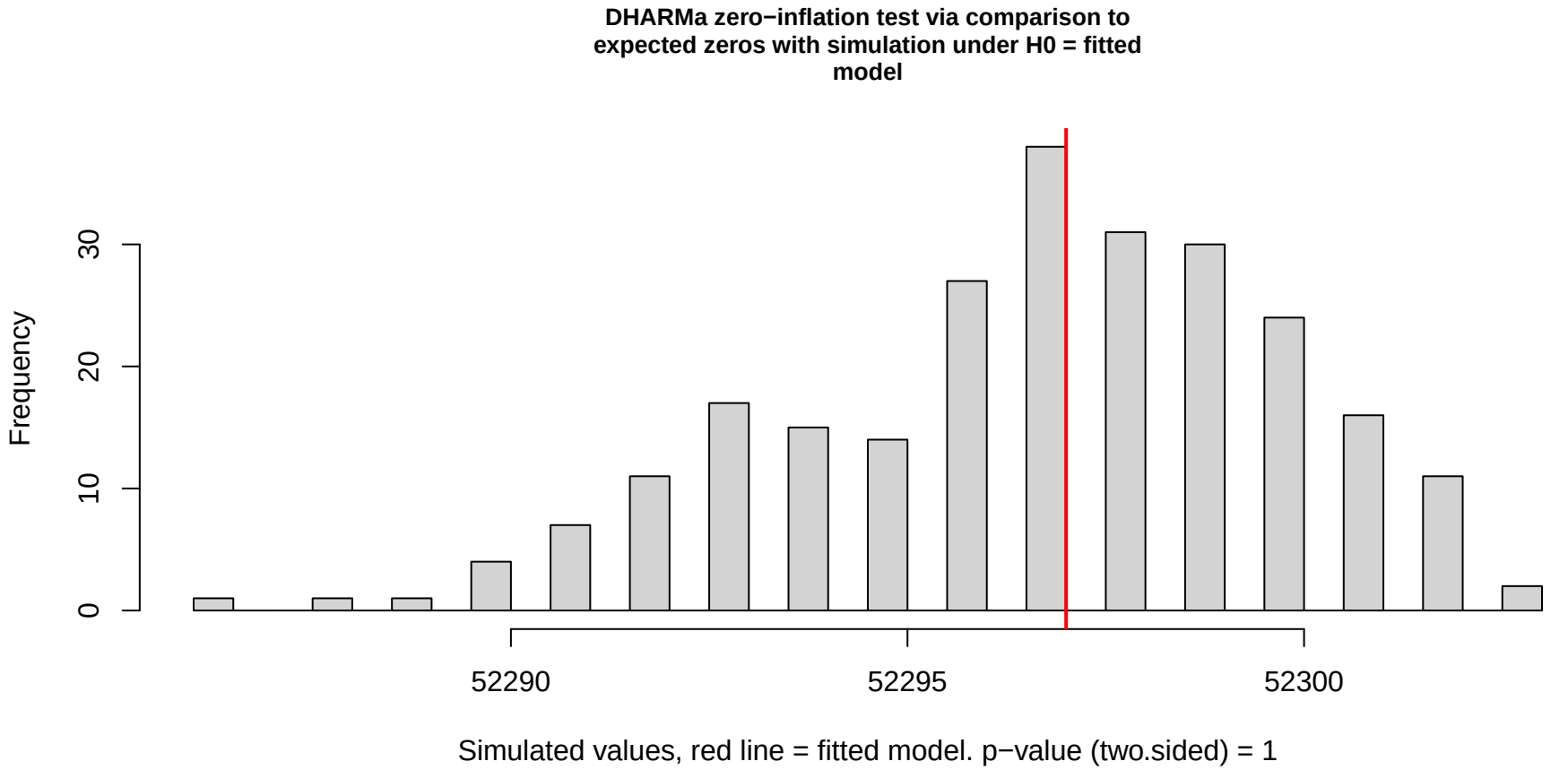

Populus alba

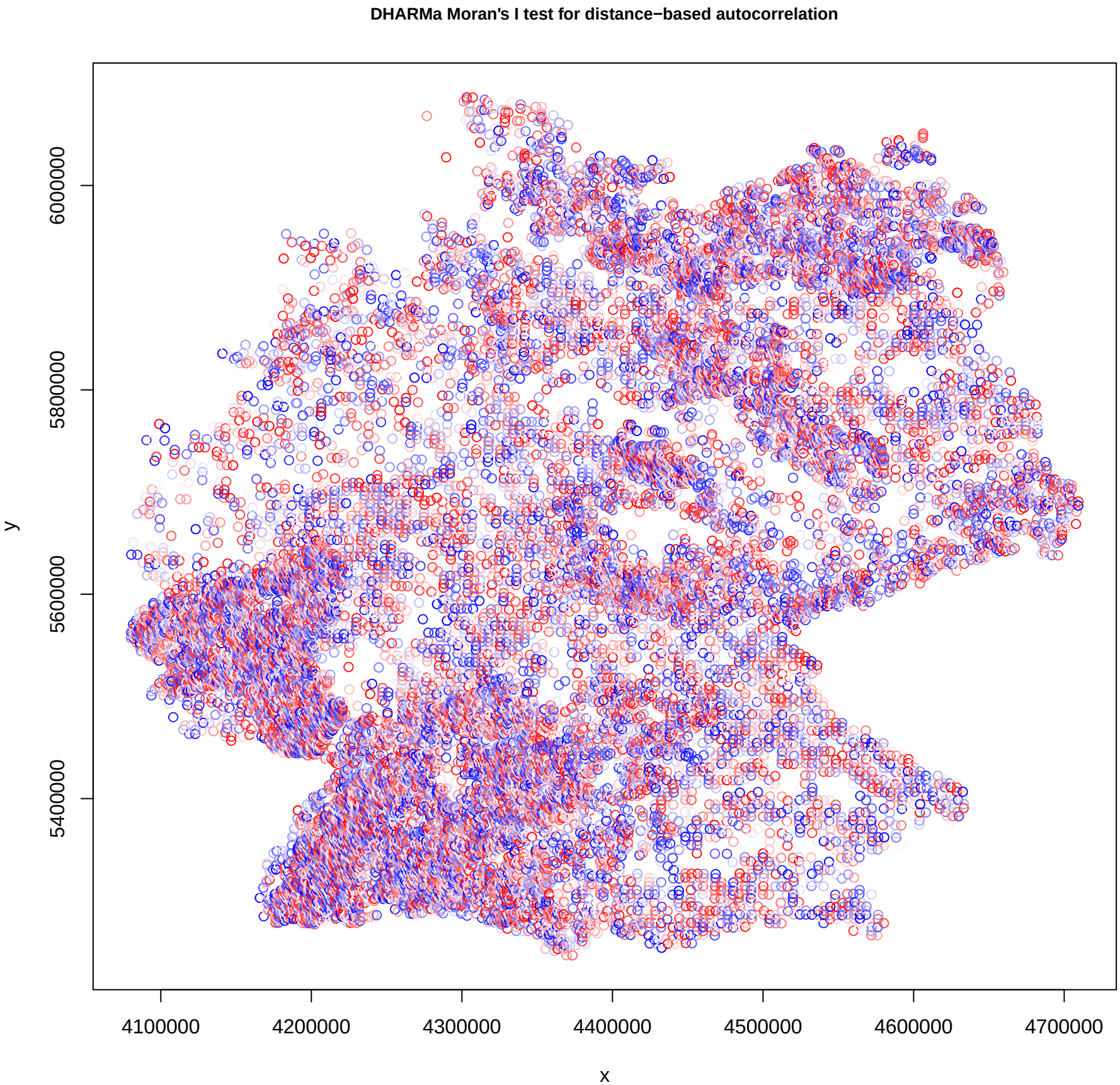

Alnus glutinosa

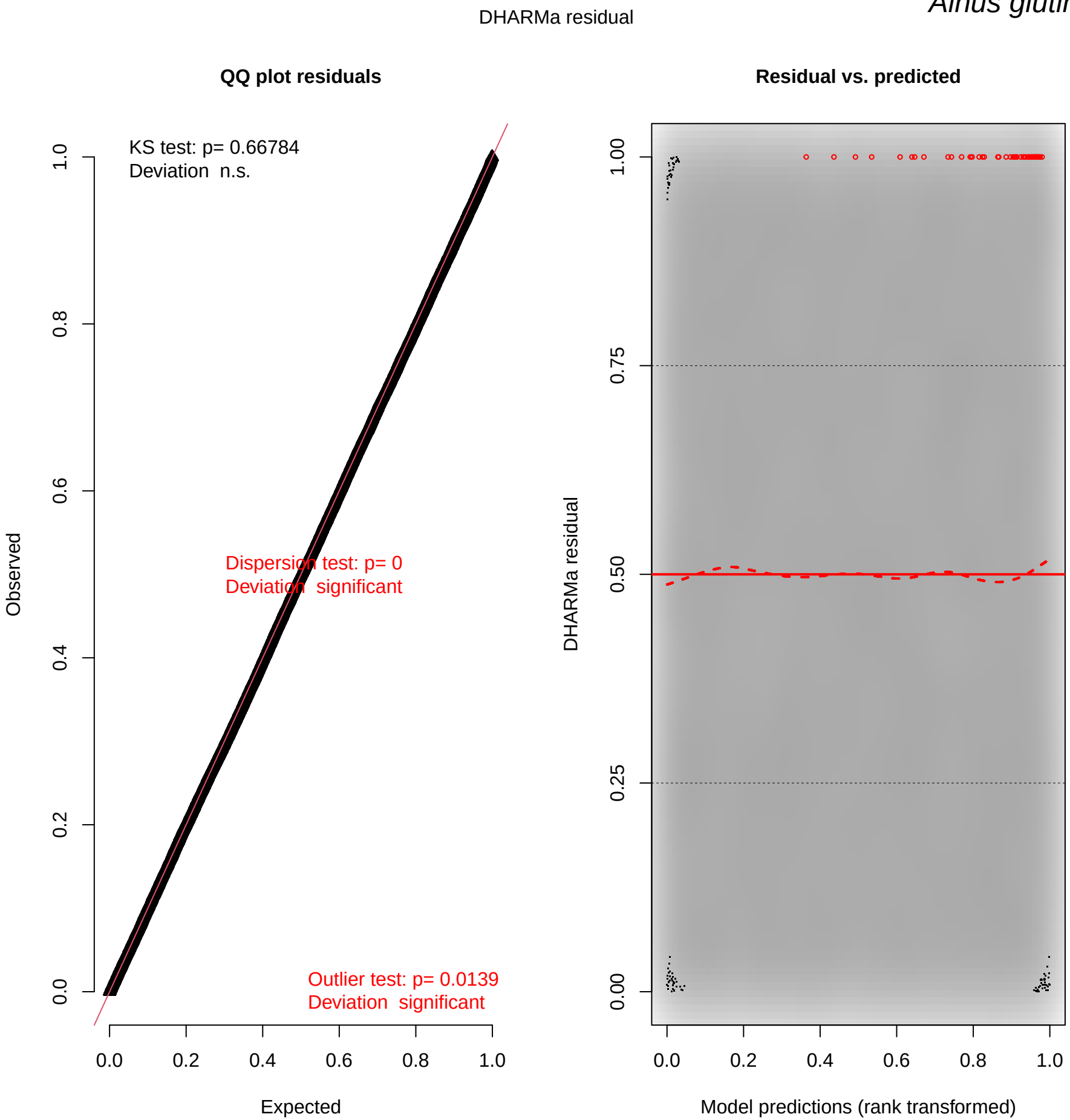

Alnus glutinosa

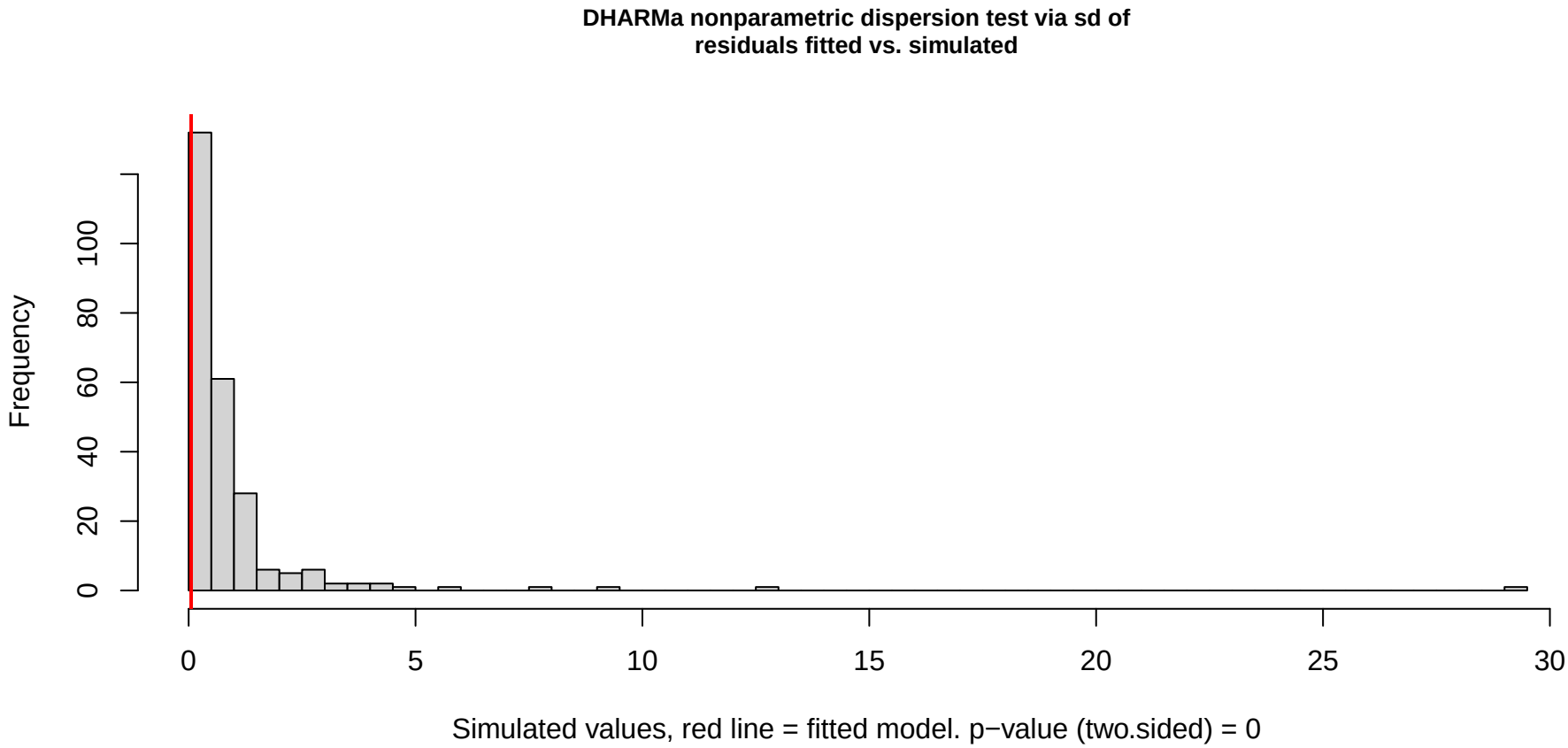

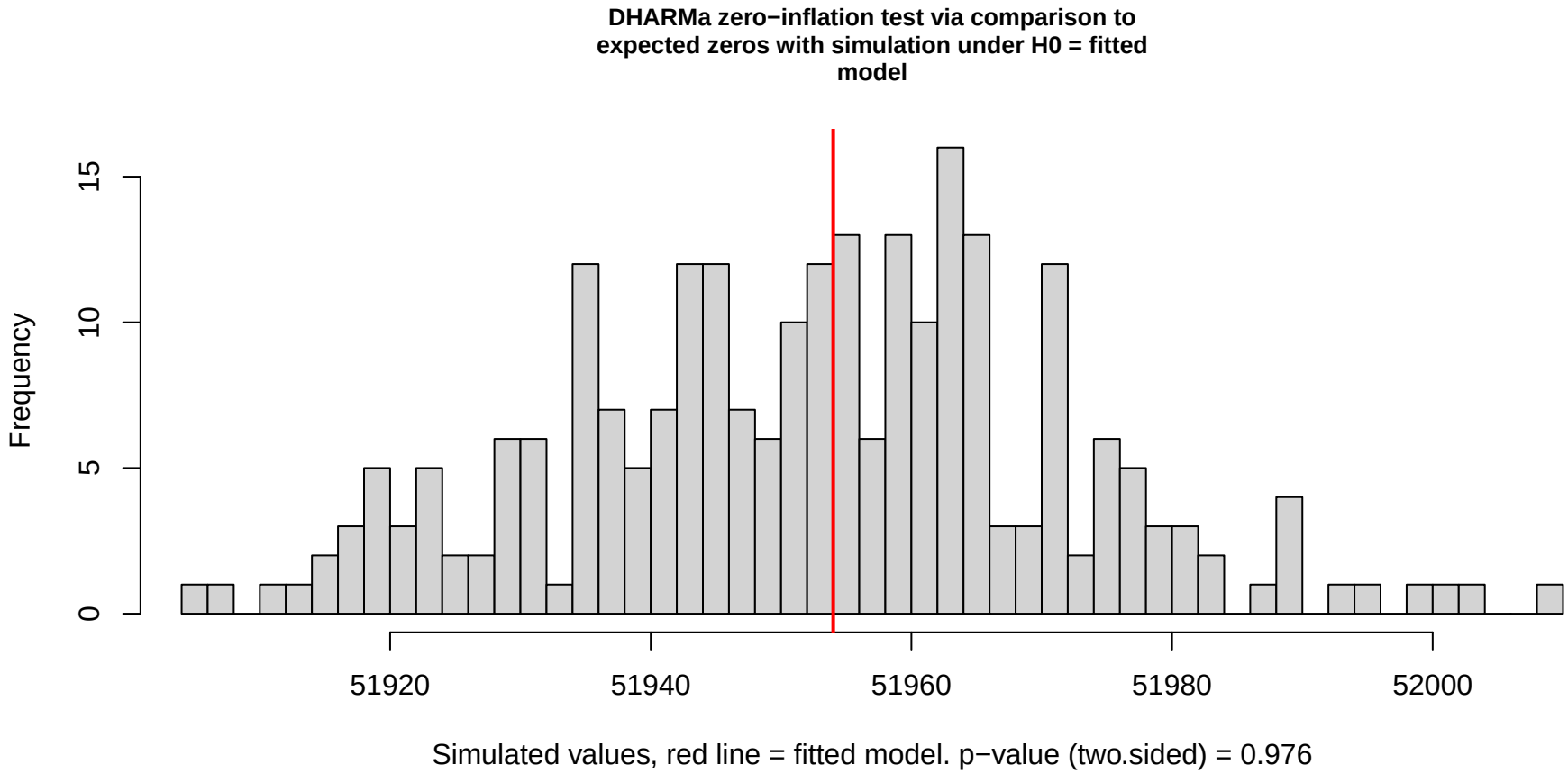

Alnus glutinosa

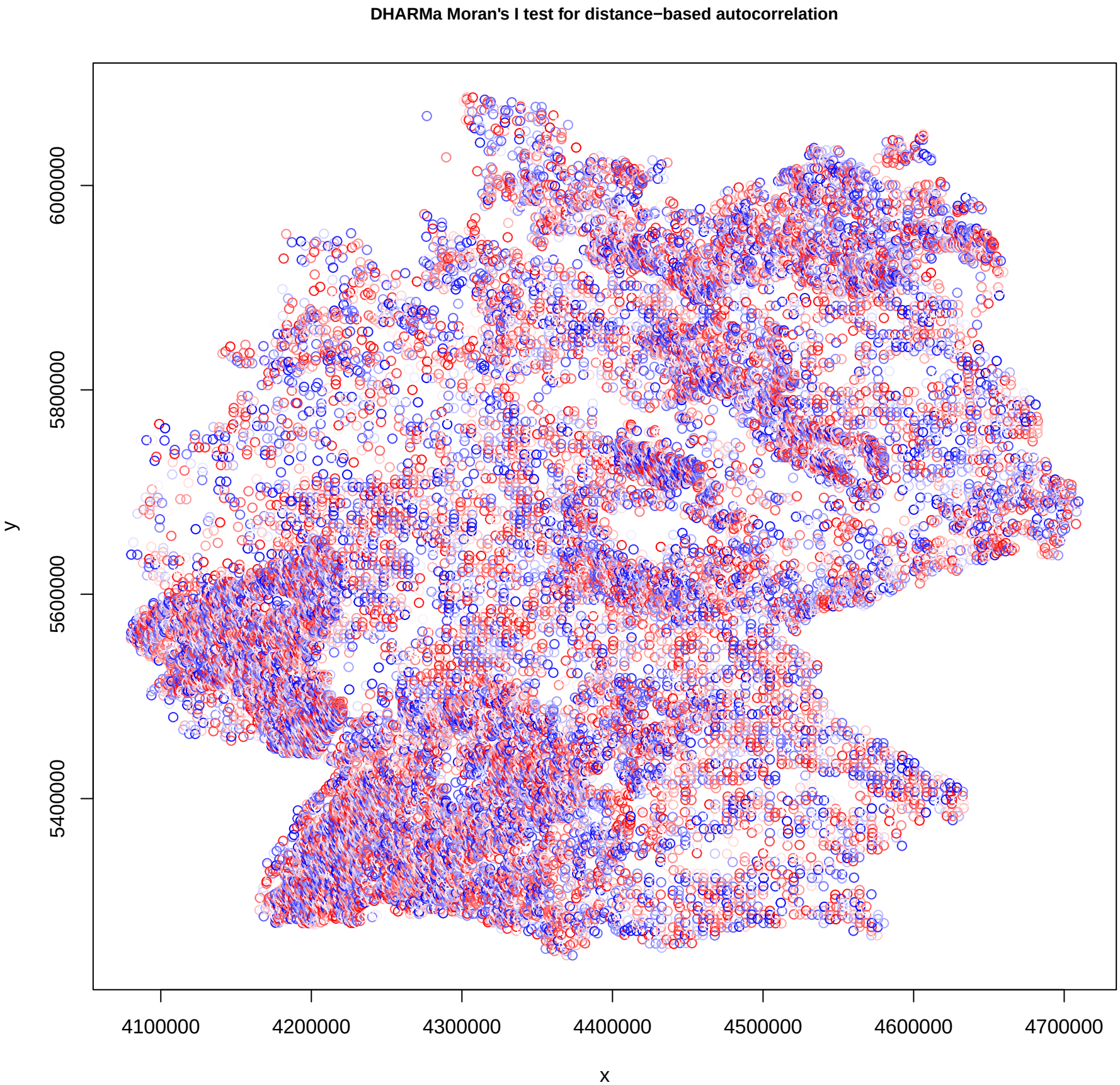

Alnus incana

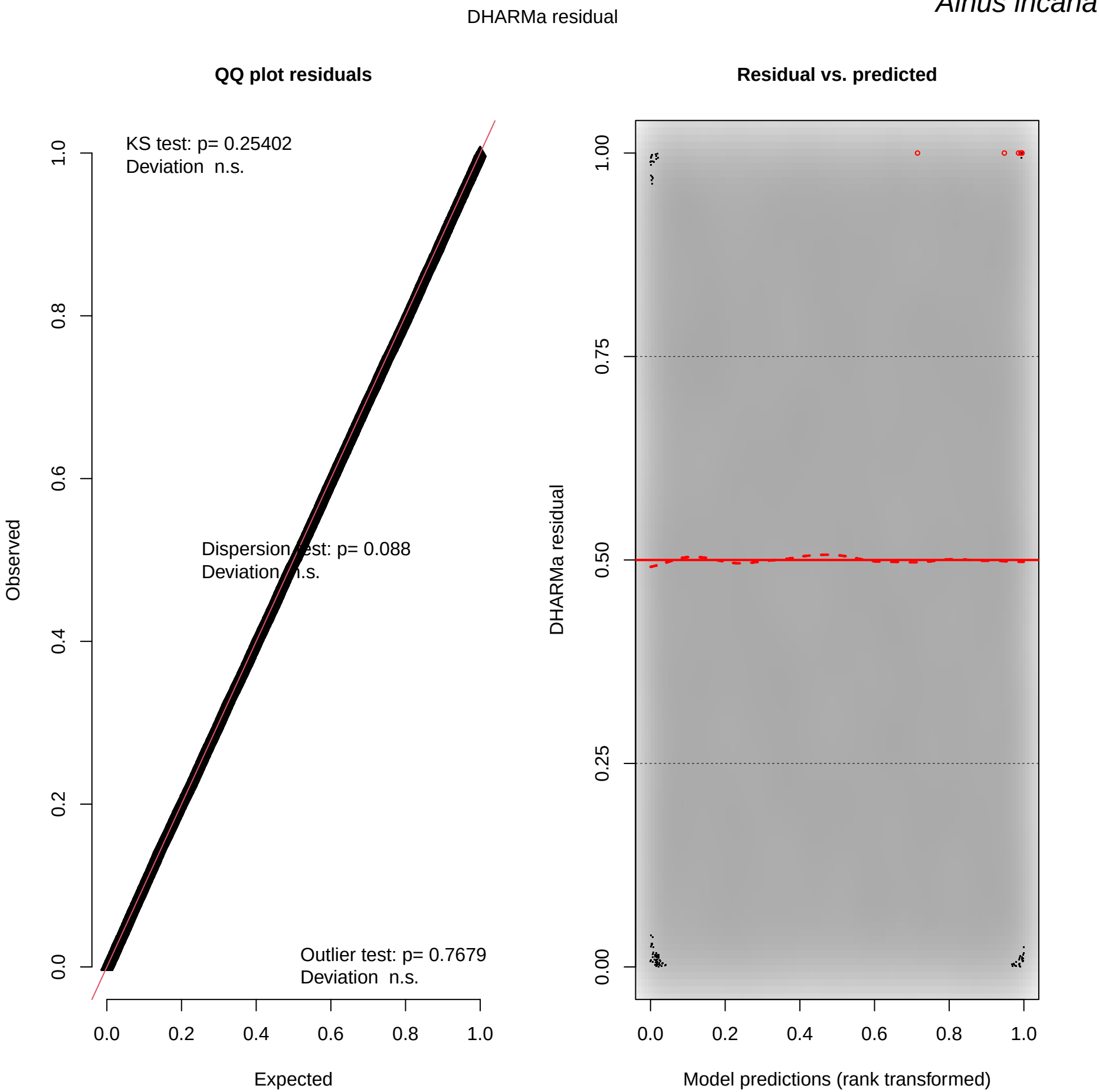

Alnus incana

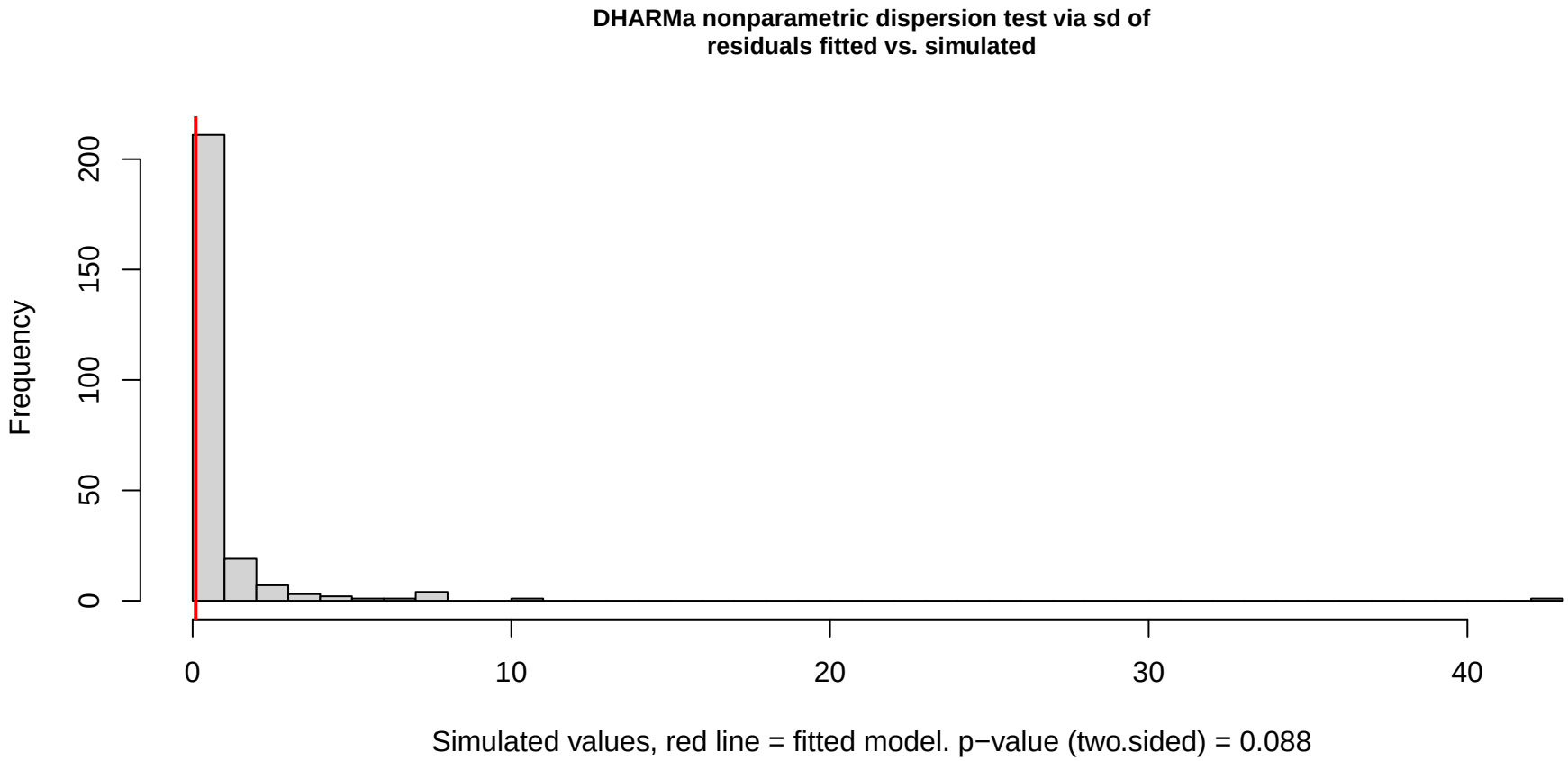

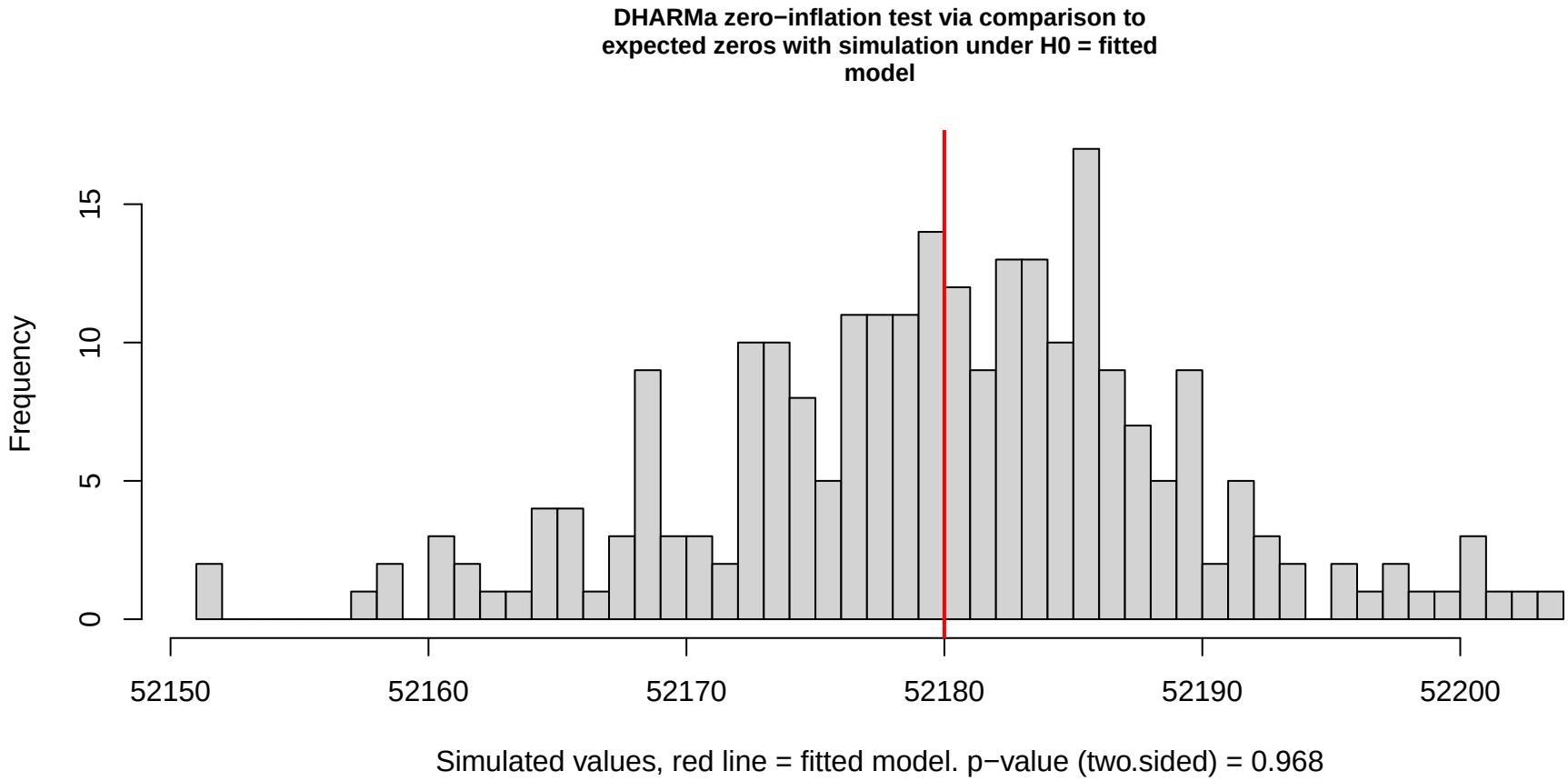

Alnus incana

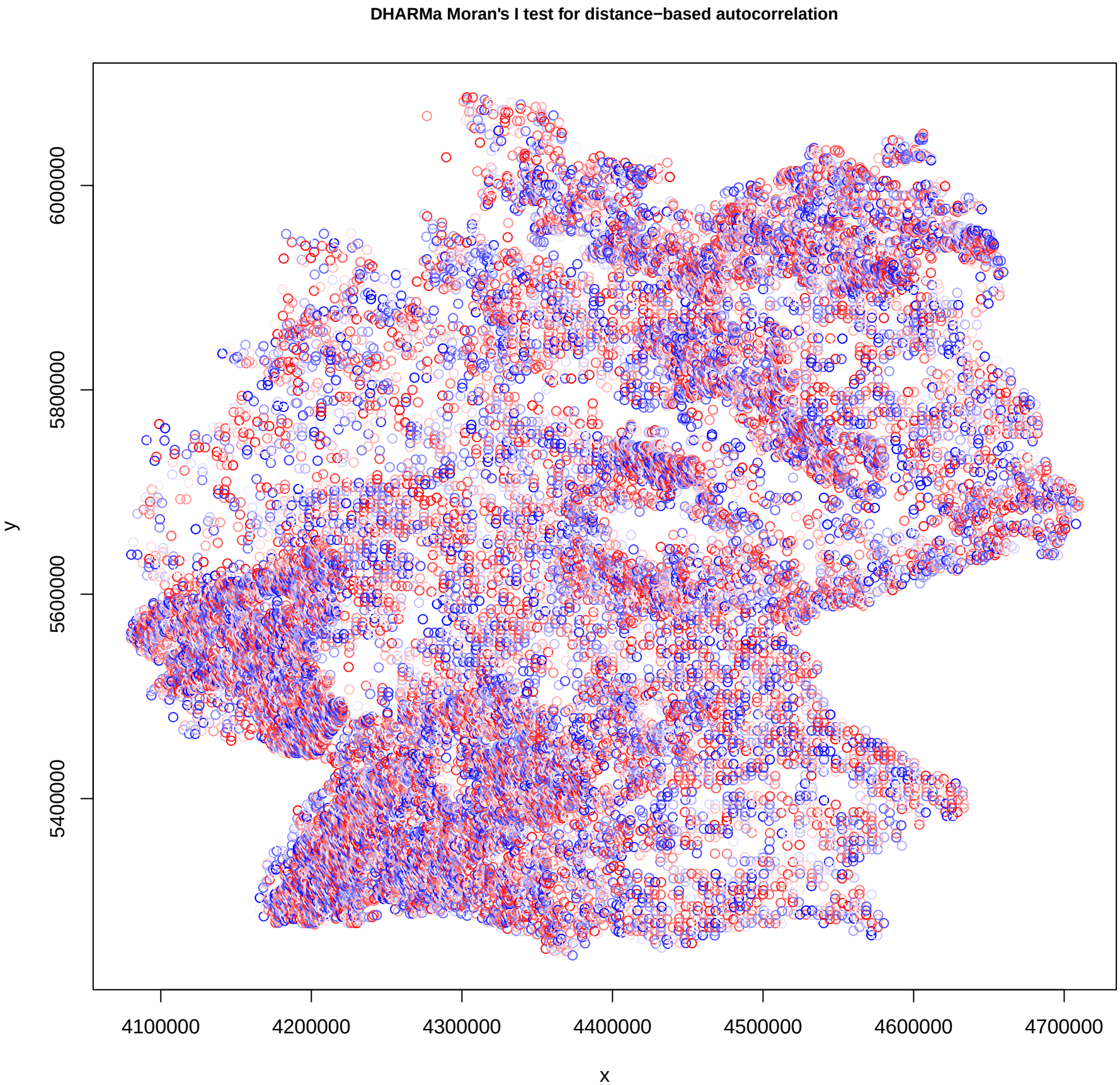

Fagus sylvatica

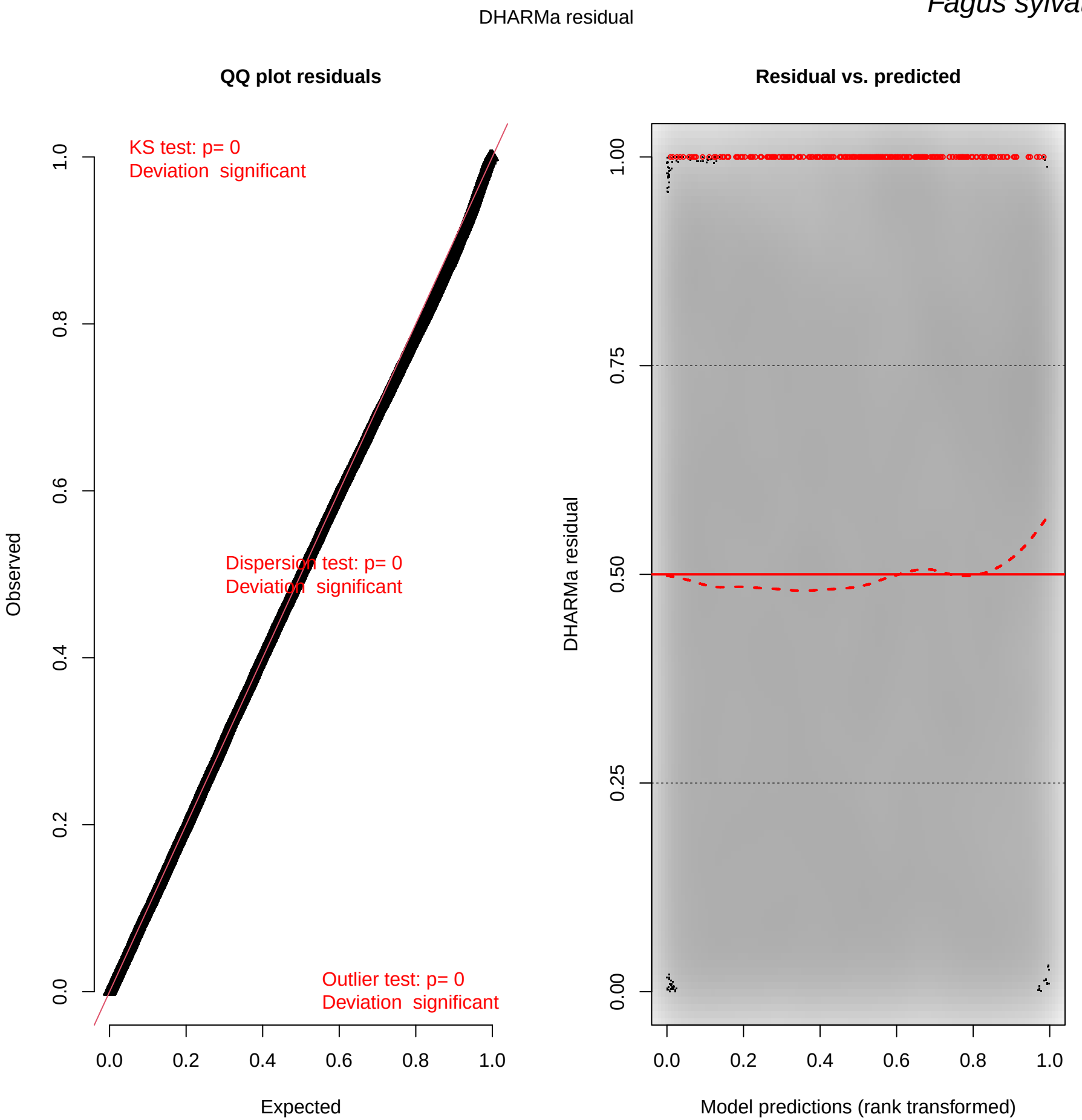

Fagus sylvatica

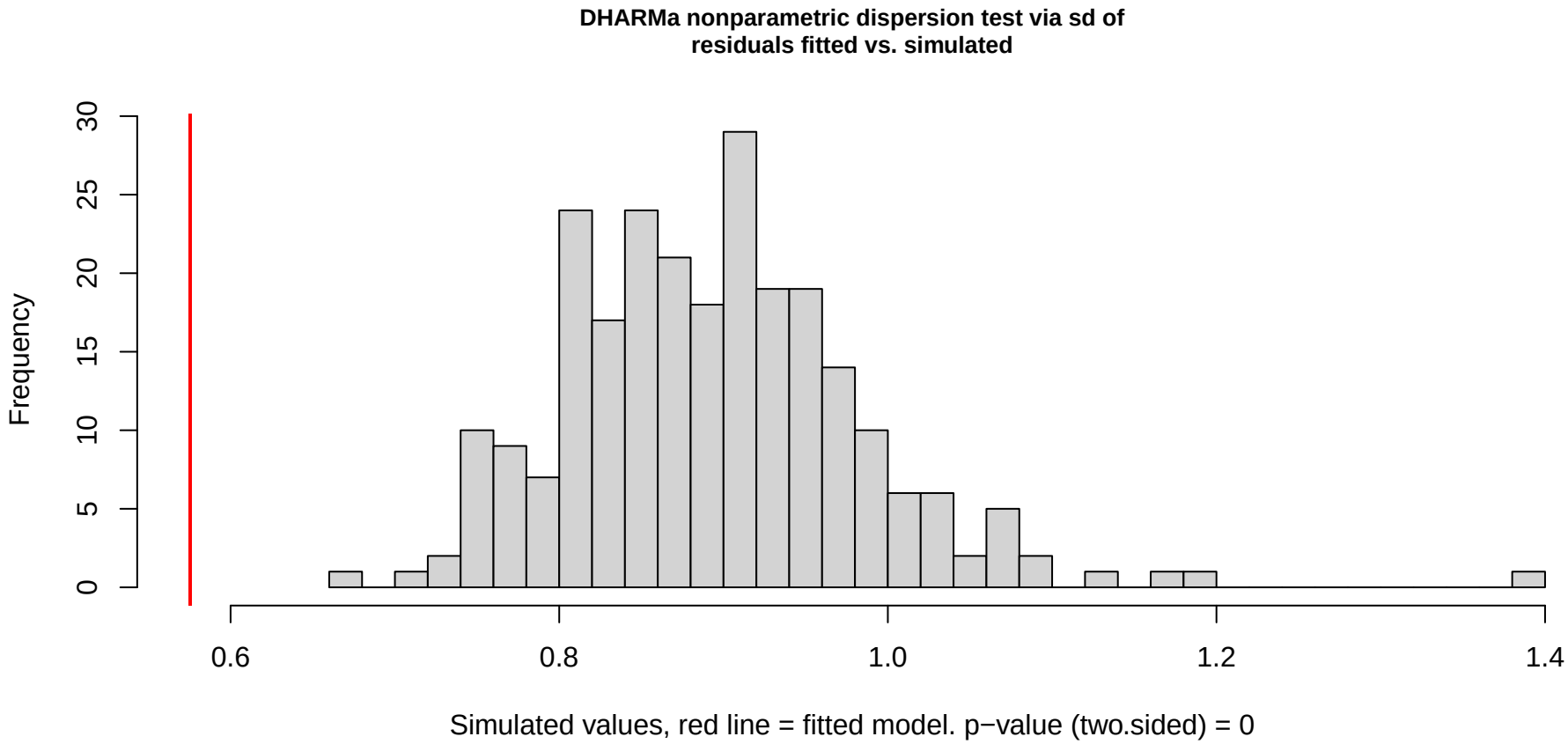

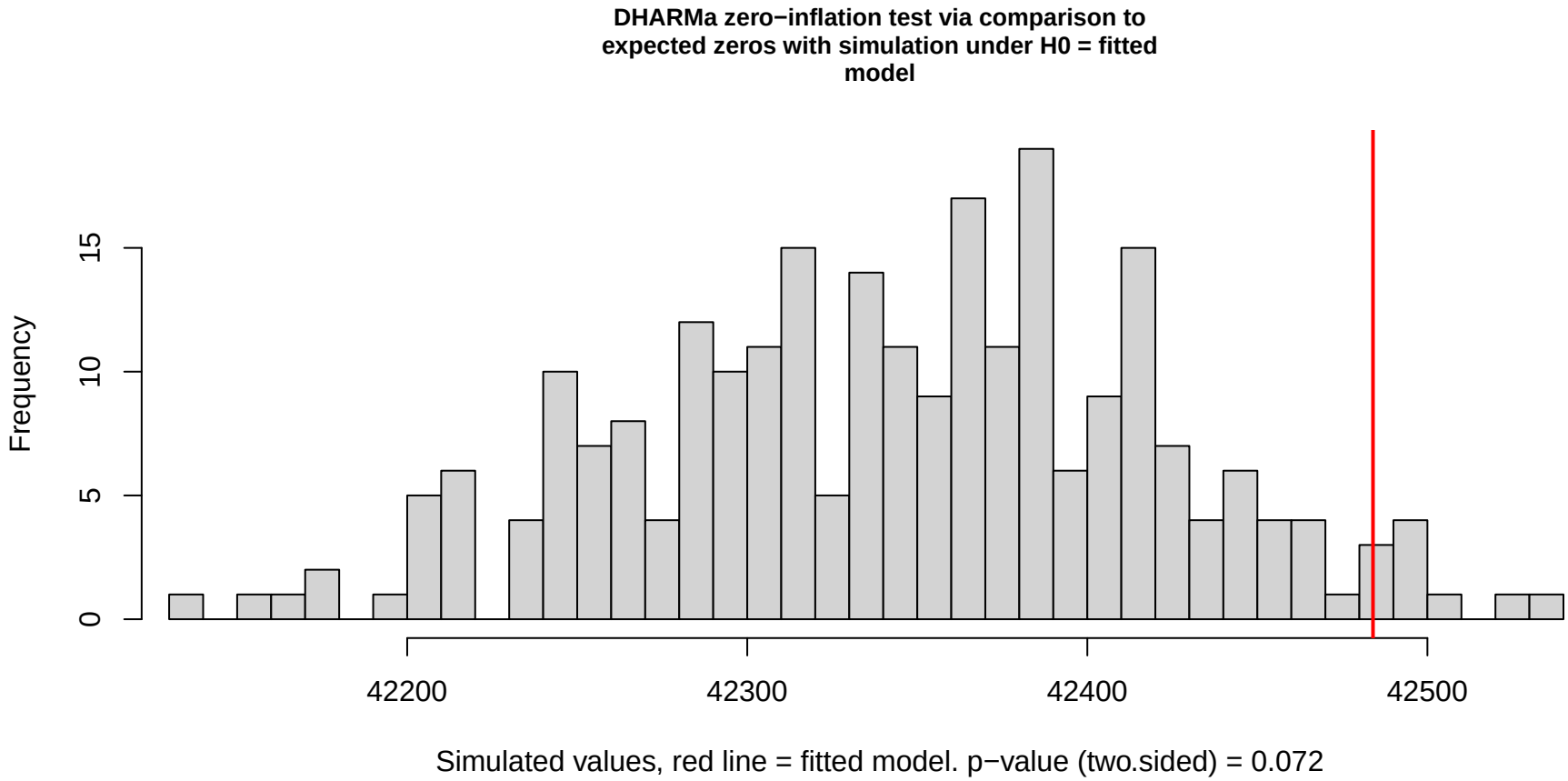

Fagus sylvatica

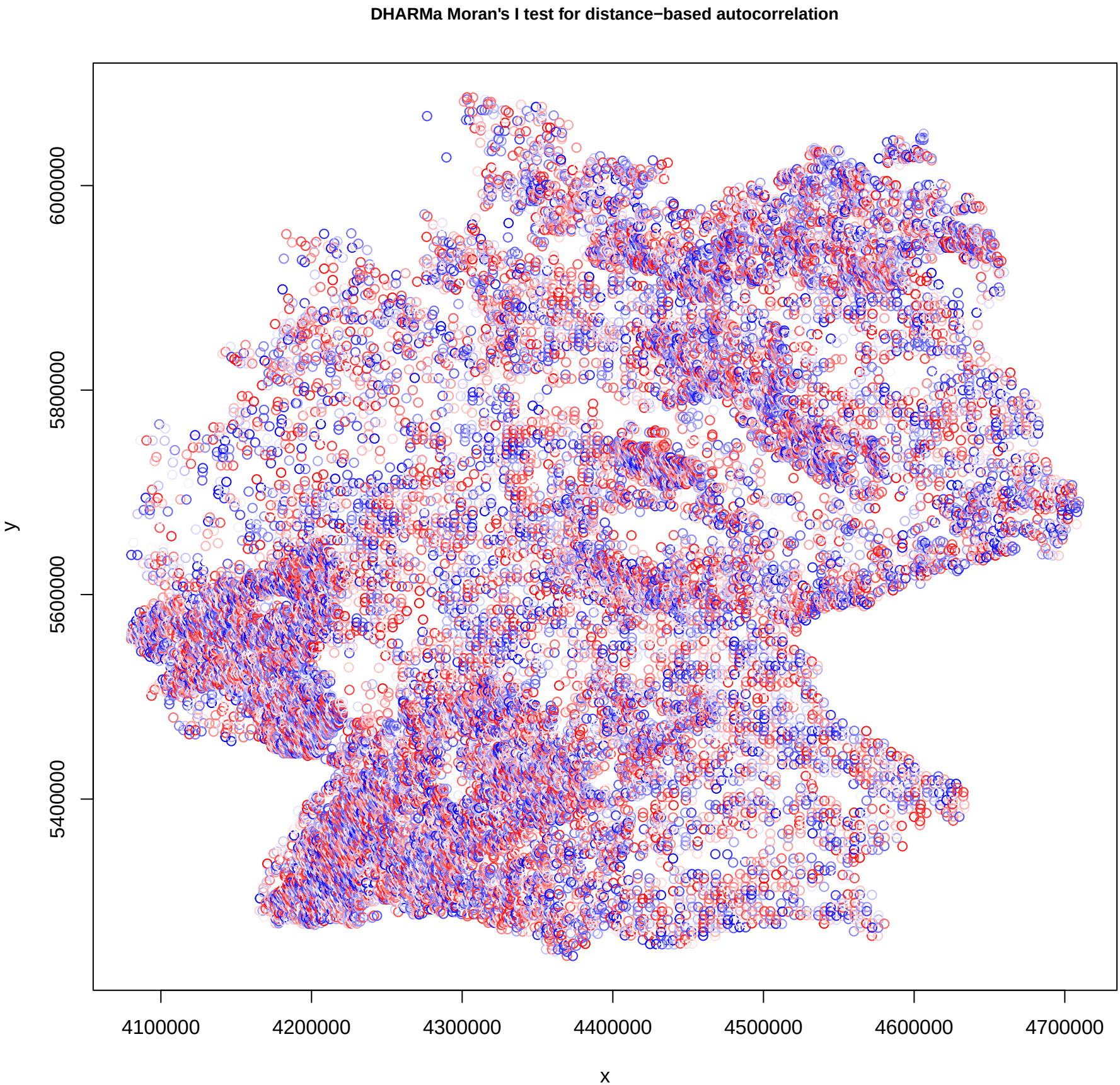

Prunus serotina

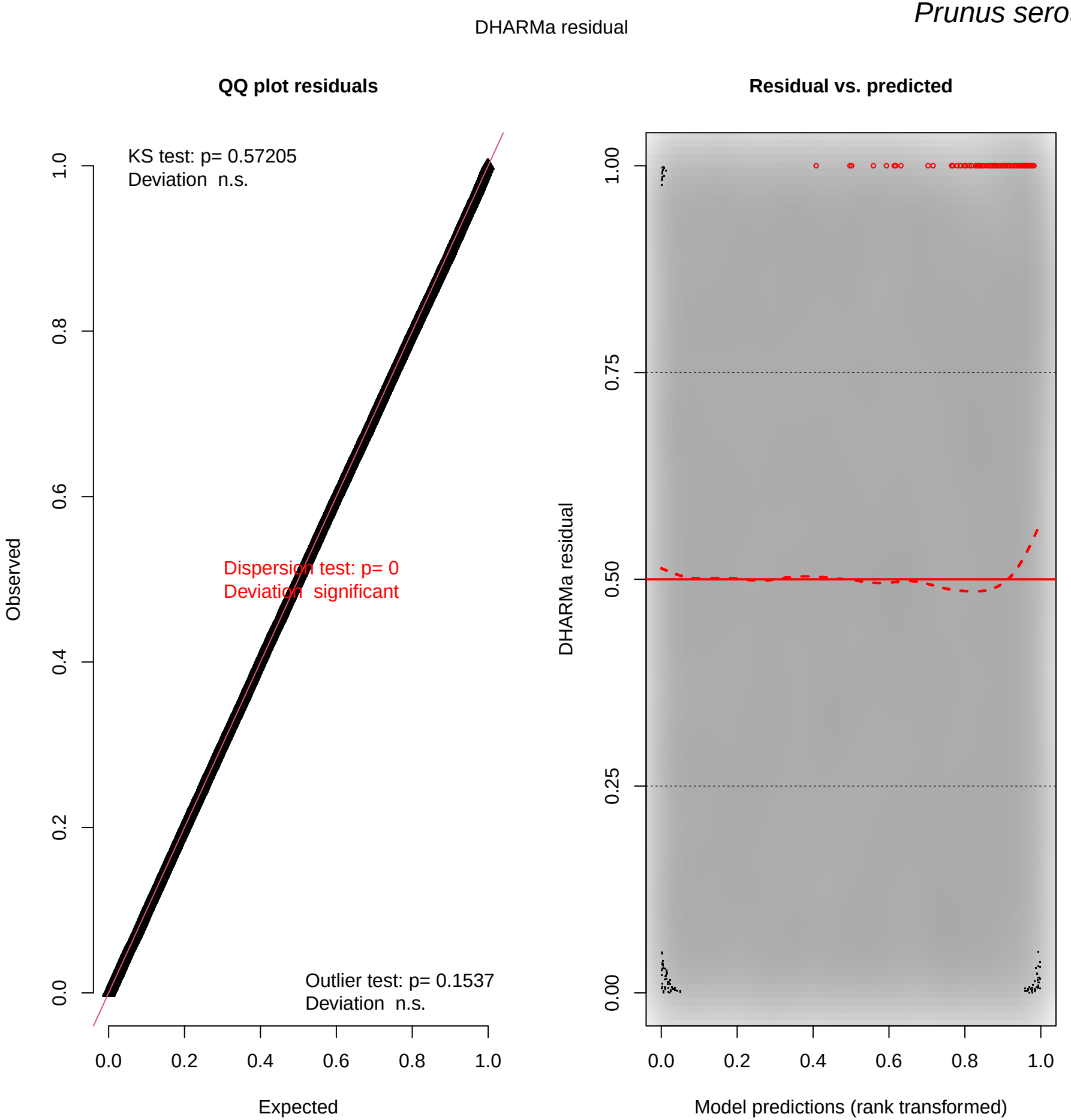

Prunus serotina

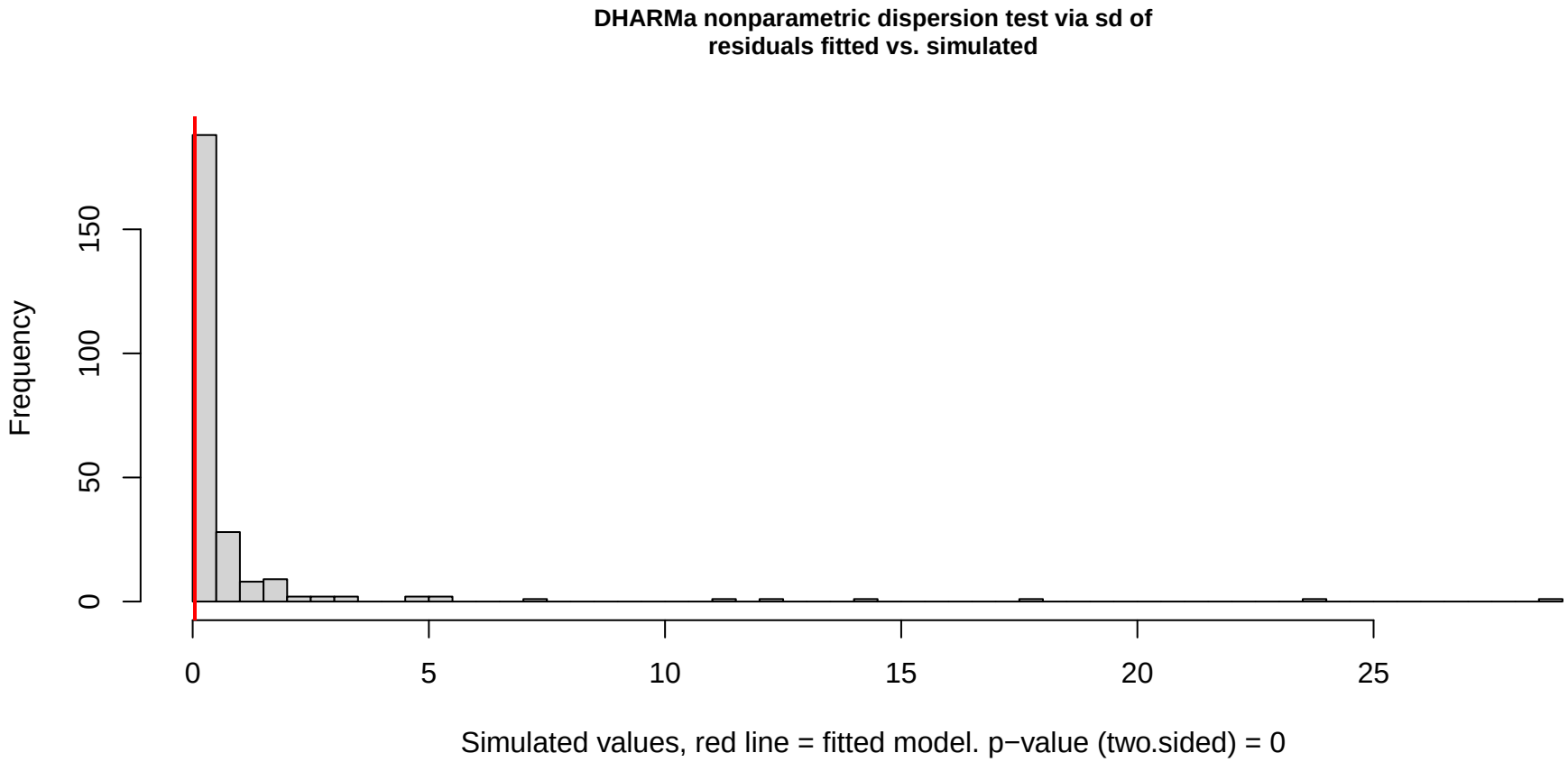

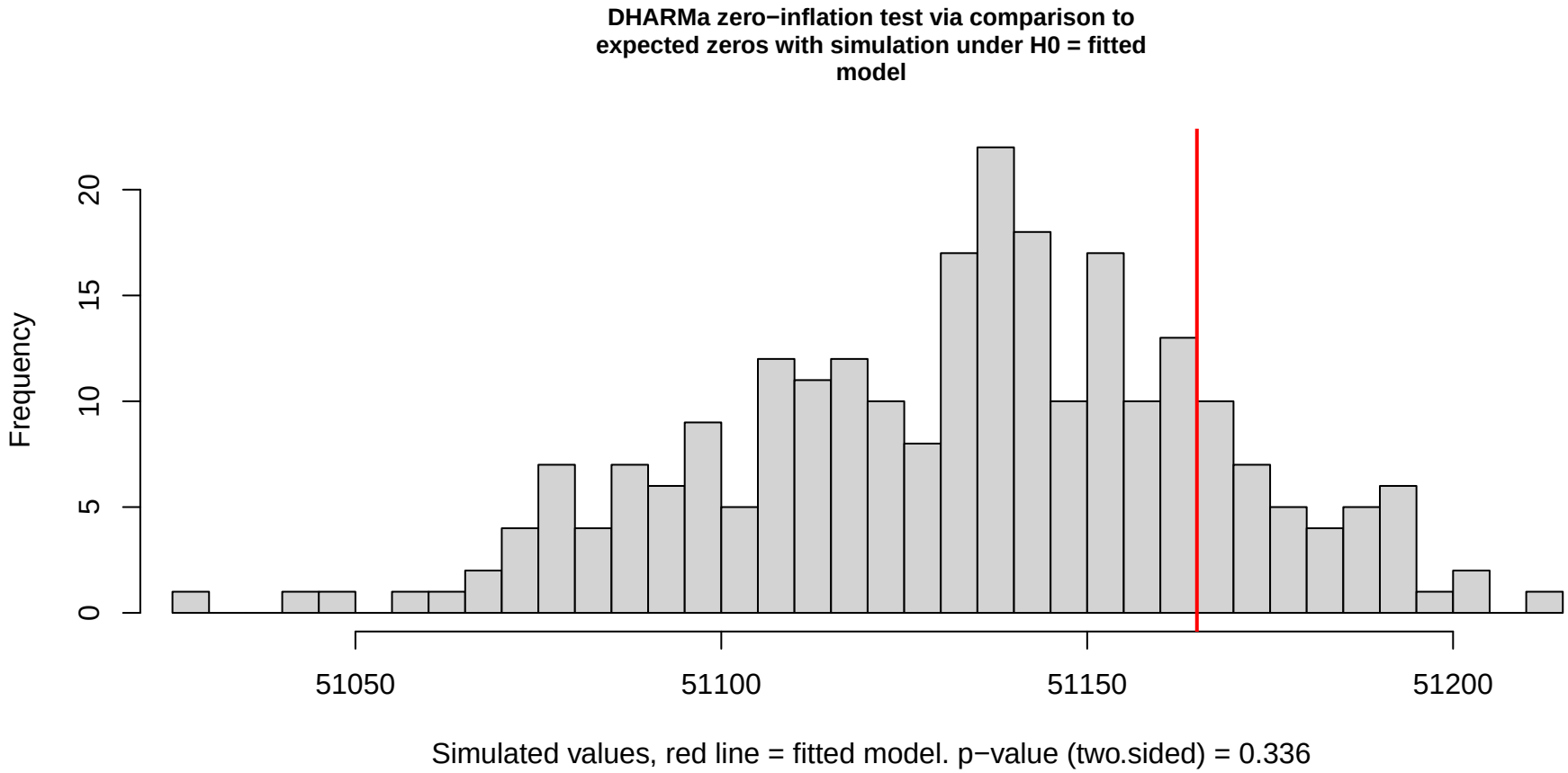

Prunus serotina

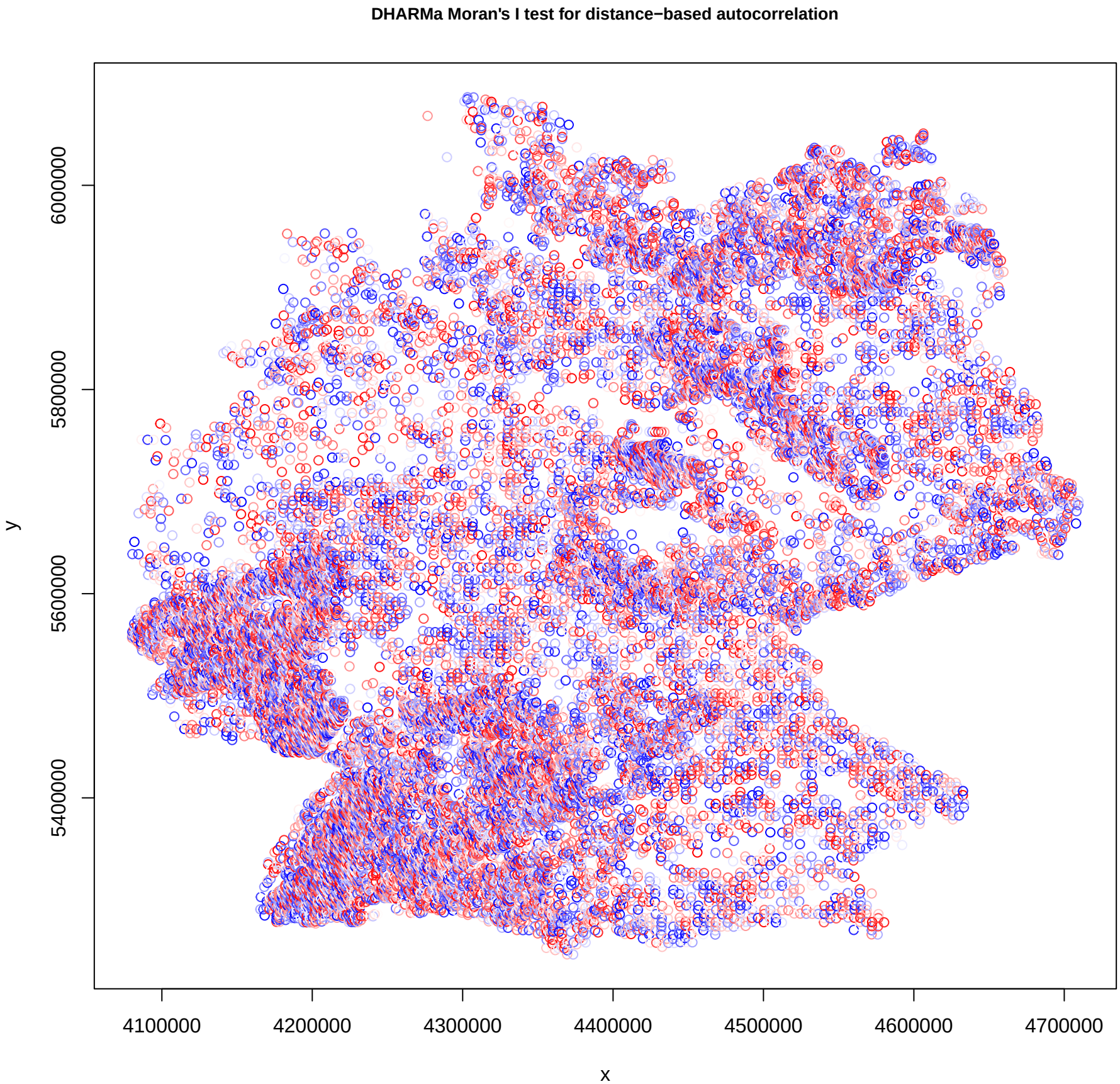

Sorbus aria

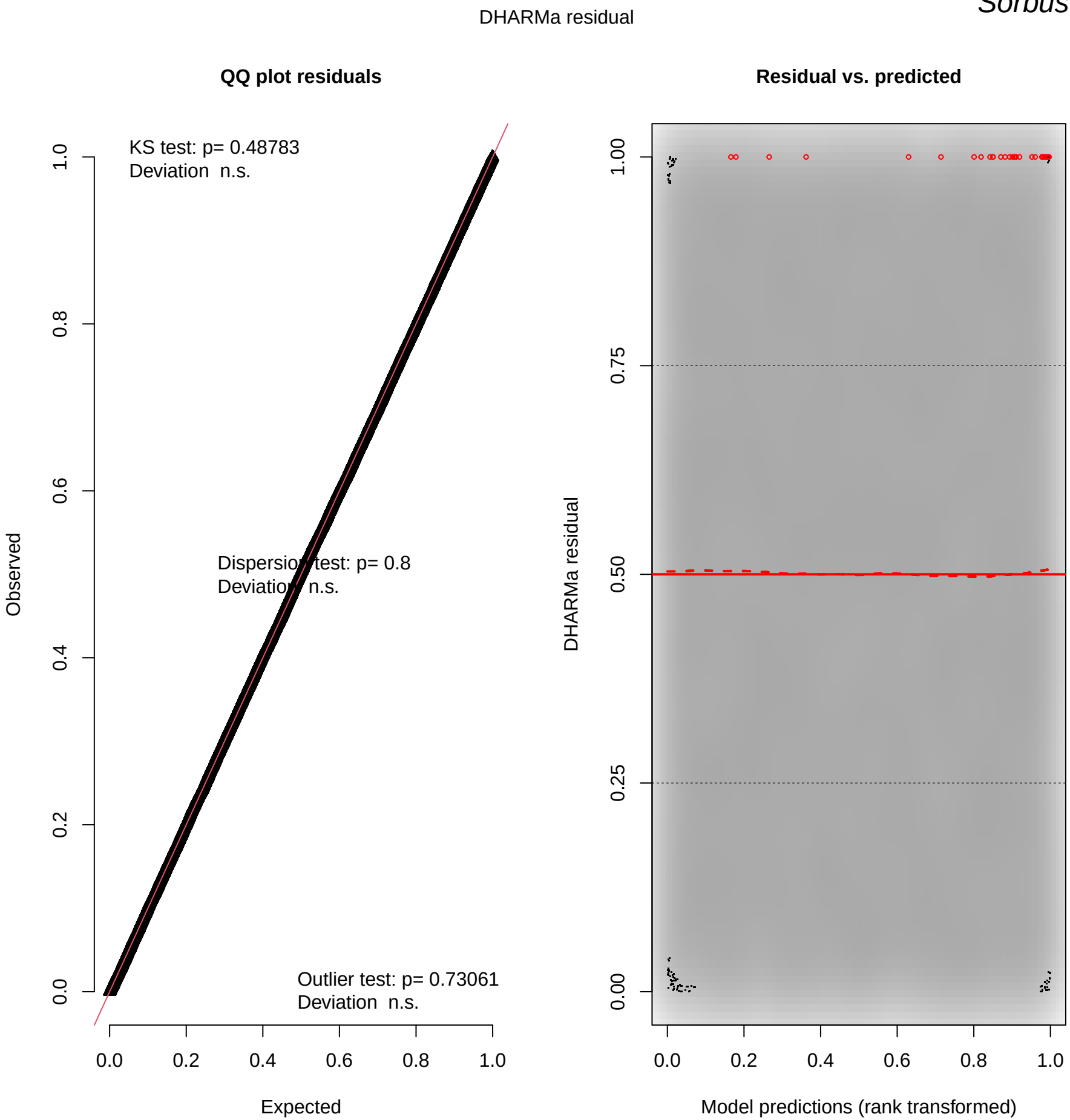
DHARMa residual
QQ plot residuals
KS test: p= 0.48783
Deviation n.s.
Dispersion test: p= 0.8
Deviation n.s.
Outlier test: p= 0.73061
Deviation n.s.
Observed
Expected
0.0
0.2
0.4
0.6
0.8
1.0
Residual vs. predicted
DHARMa residual
Model predictions (rank transformed)
0.00
0.25
0.50
0.75
1.00

Sorbus aria

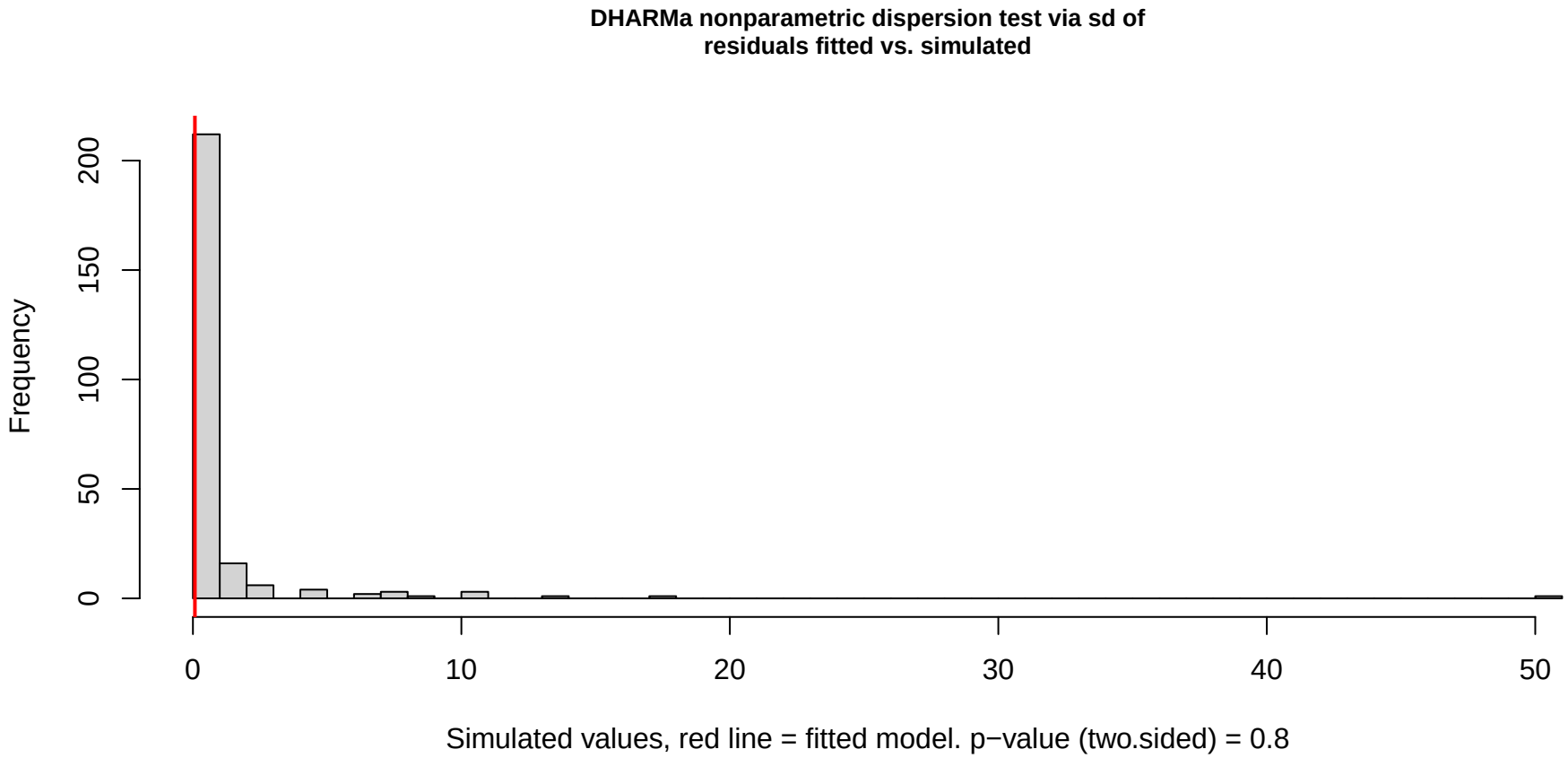
DHARMa nonparametric dispersion test via sd of residuals fitted vs. simulated
Frequency
0
50
100
150
200
0
10
20
30
40
50
Simulated values, red line = fitted model. p−value (two.sided) = 0.8

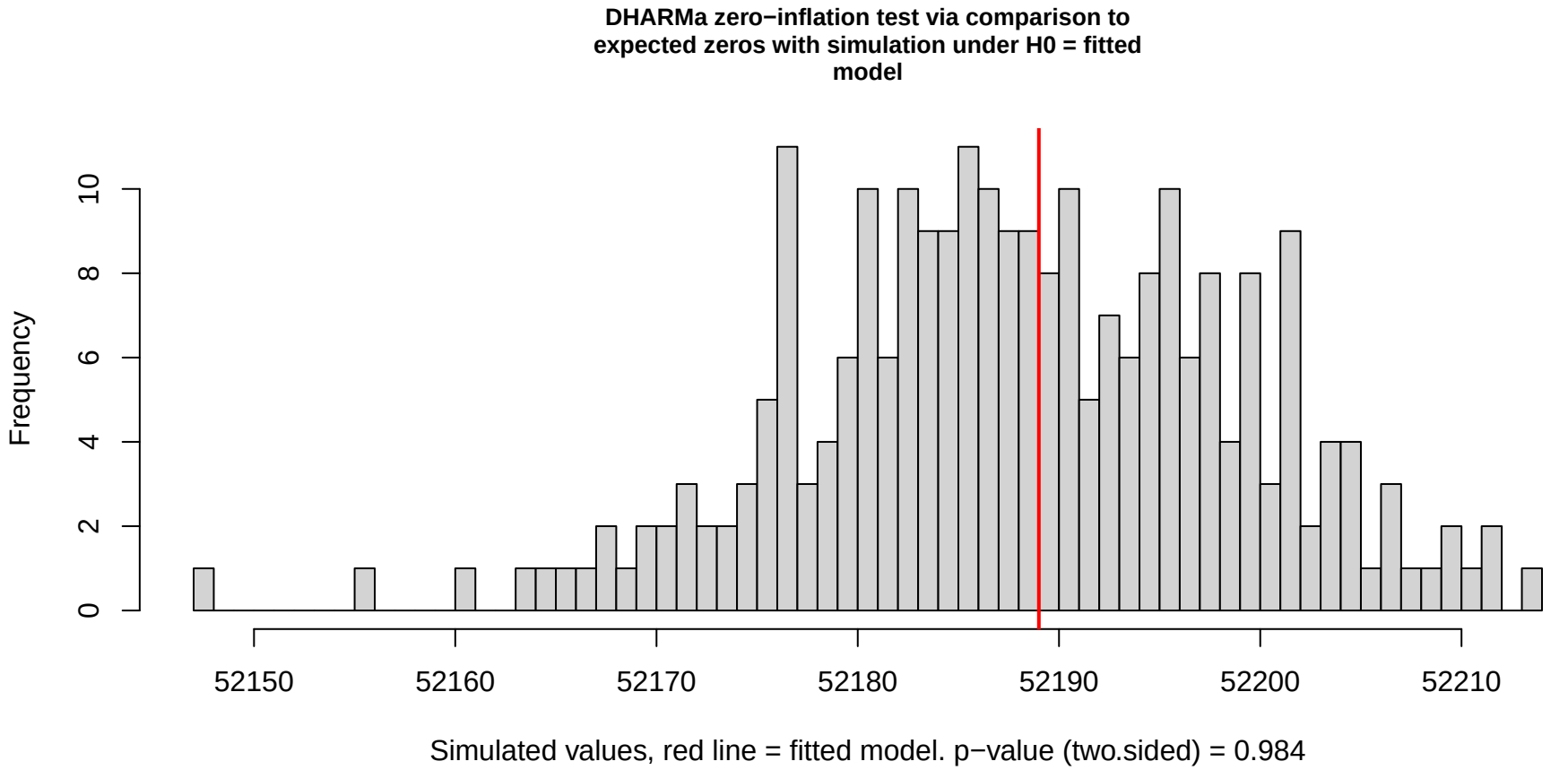
DHARMa zero−inflation test via comparison to expected zeros with simulation under H0 = fitted model
Frequency
0
2
4
6
8
10
52150
52160
52170
52180
52190
52200
52210
Simulated values, red line = fitted model. p−value (two.sided) = 0.984

Sorbus aria

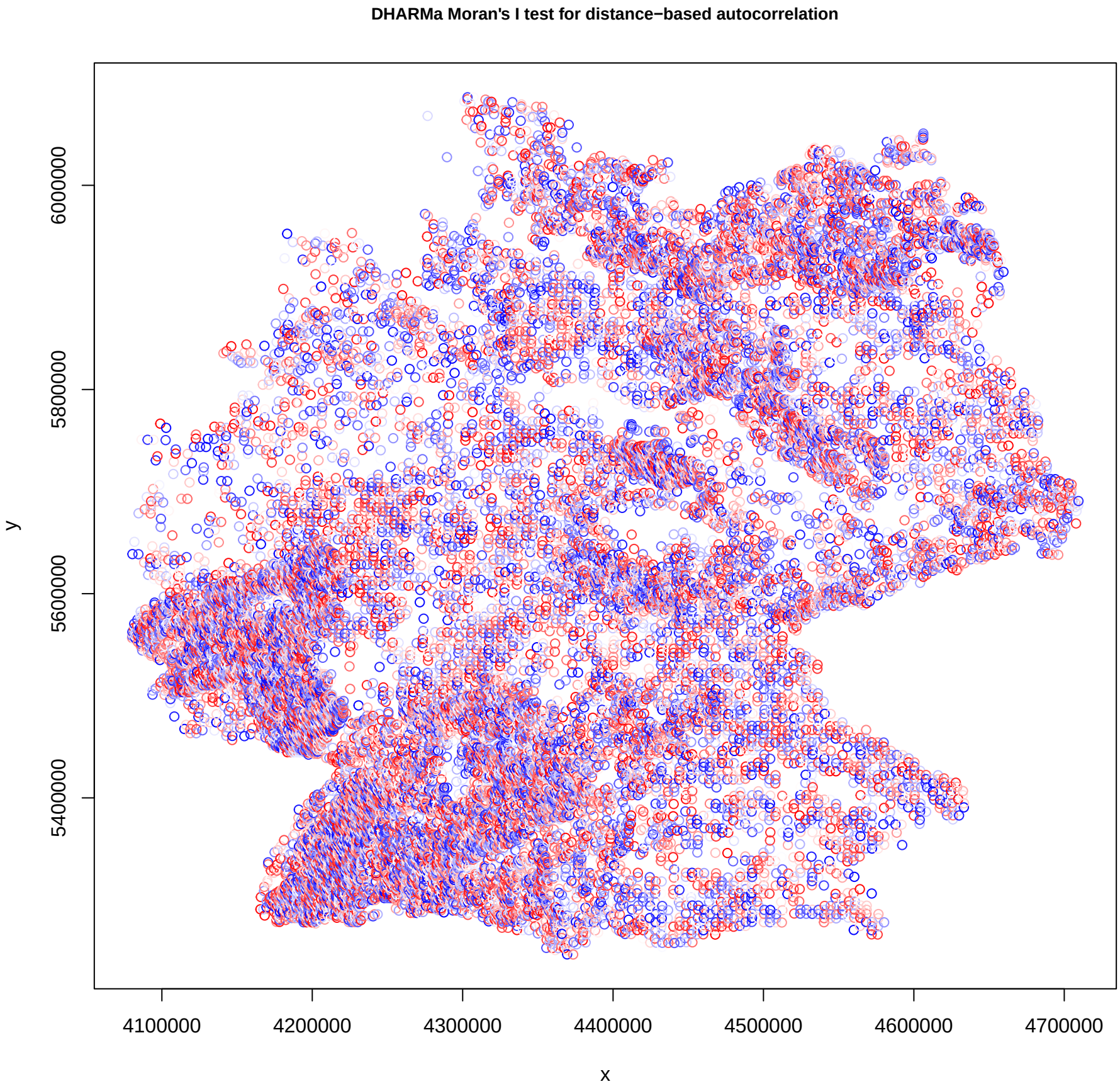
DHARMa Moran's I test for distance−based autocorrelation
6000000
5800000
5600000
5400000
y
4100000
4200000
4300000
4400000
4500000
4600000
4700000
x

Prunus avium

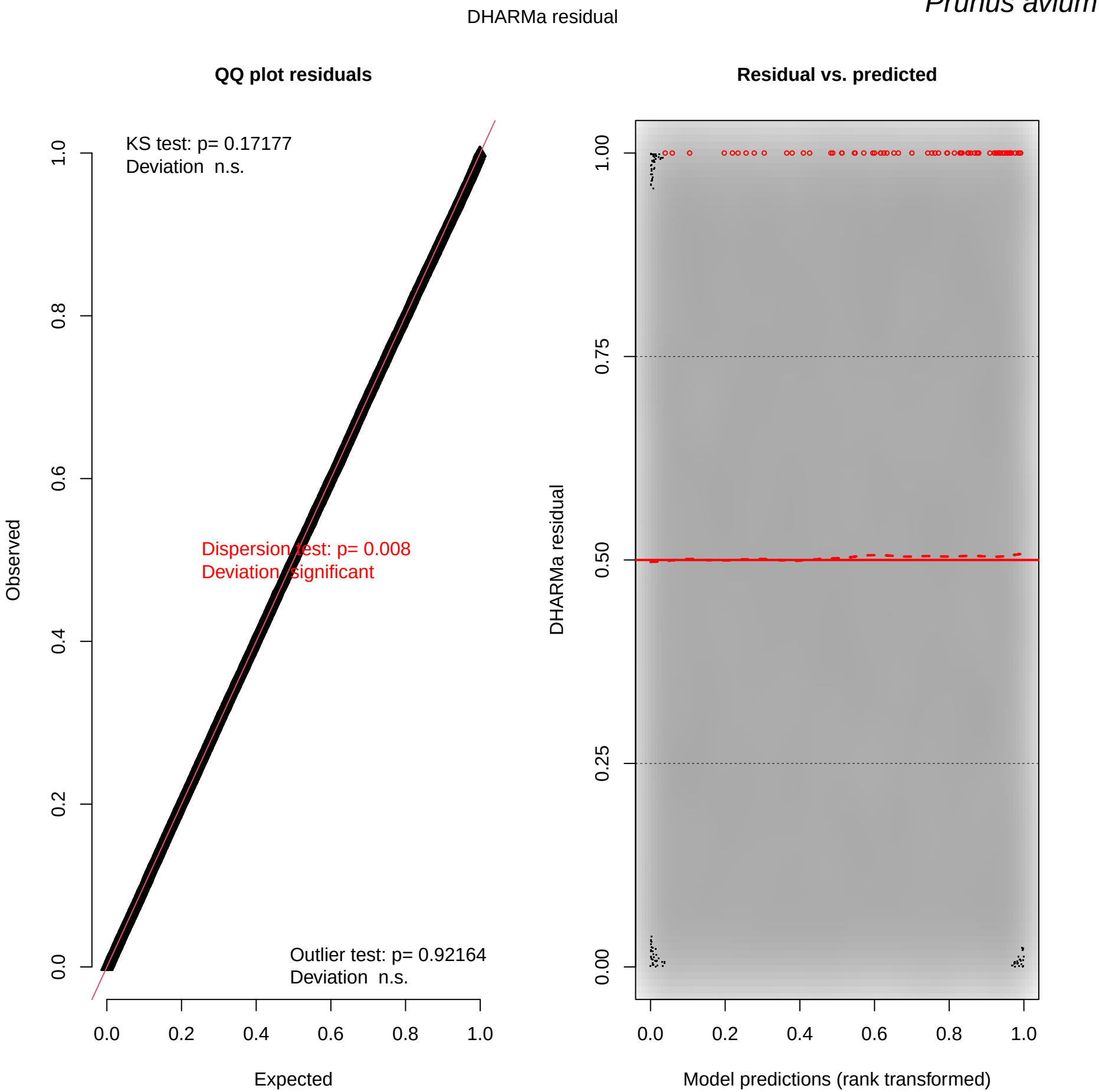

Prunus avium

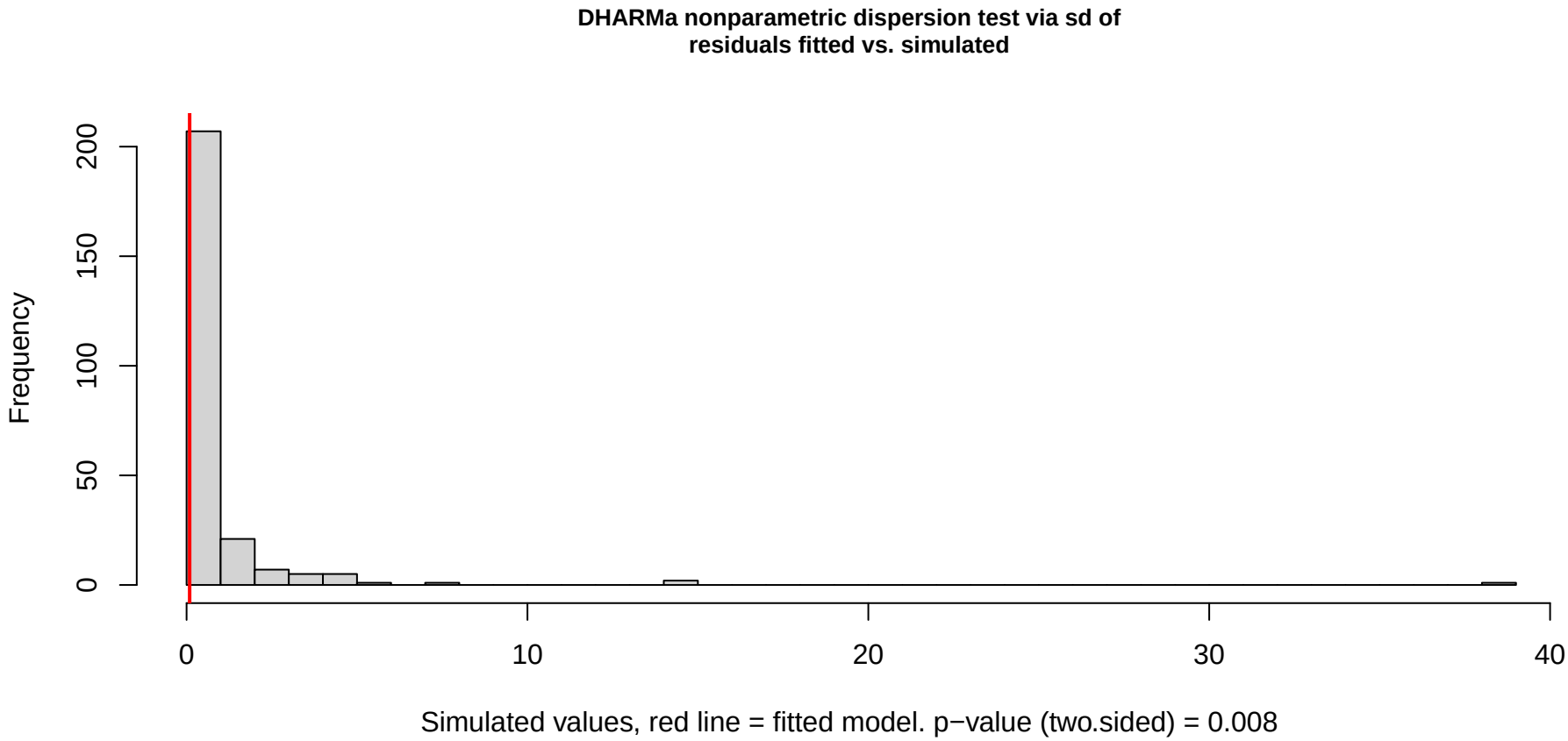

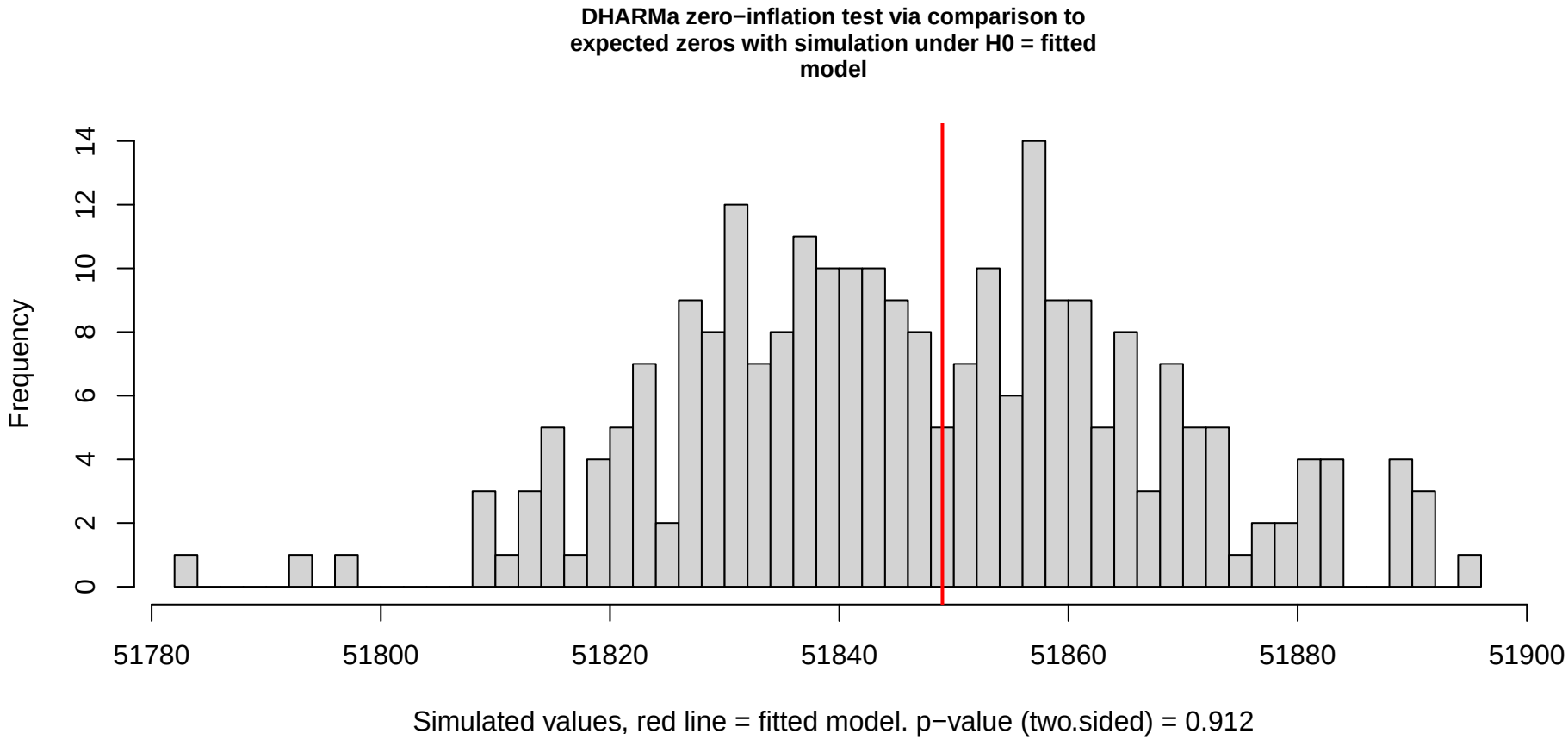

Prunus avium

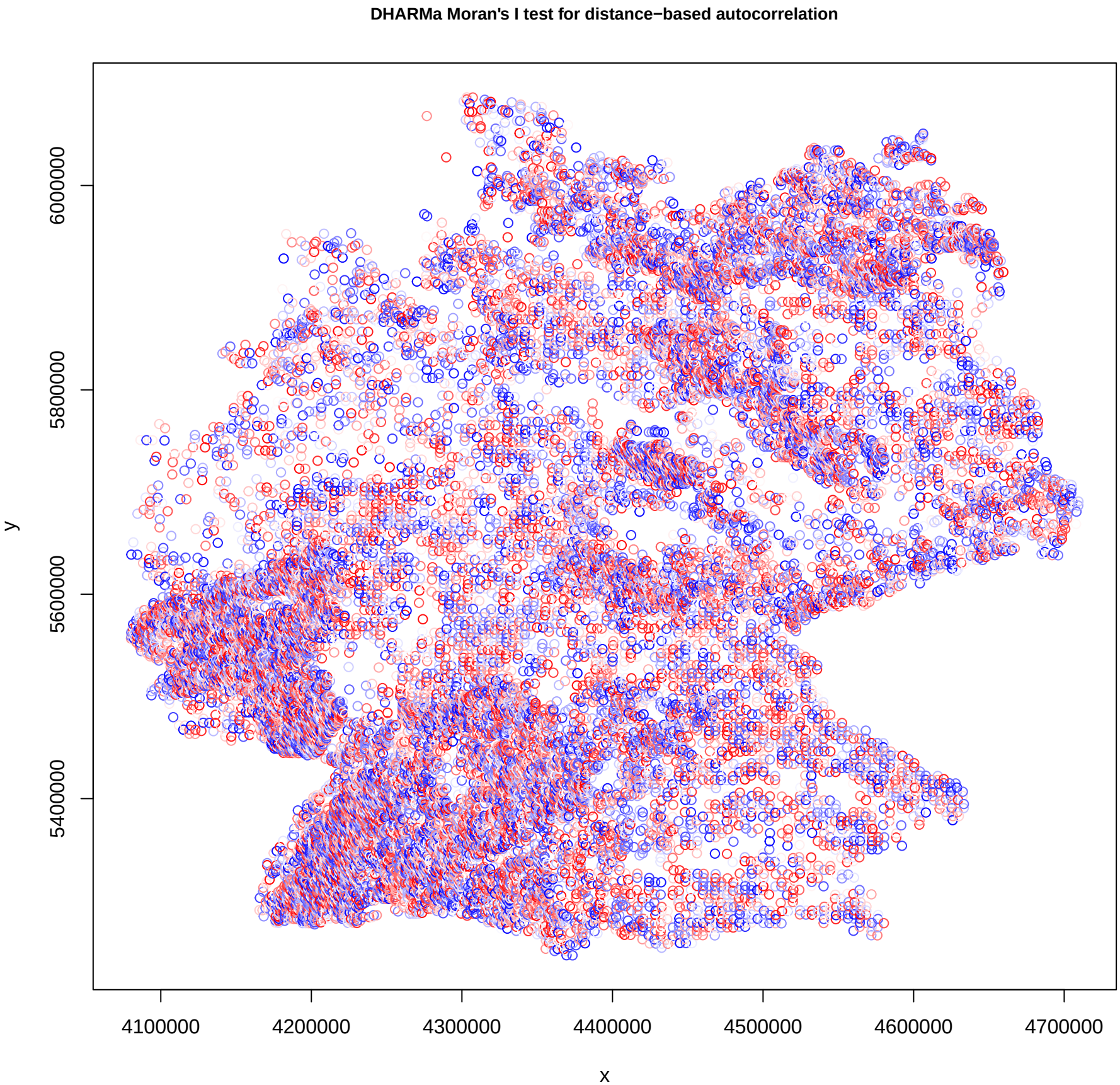

Prunus padus

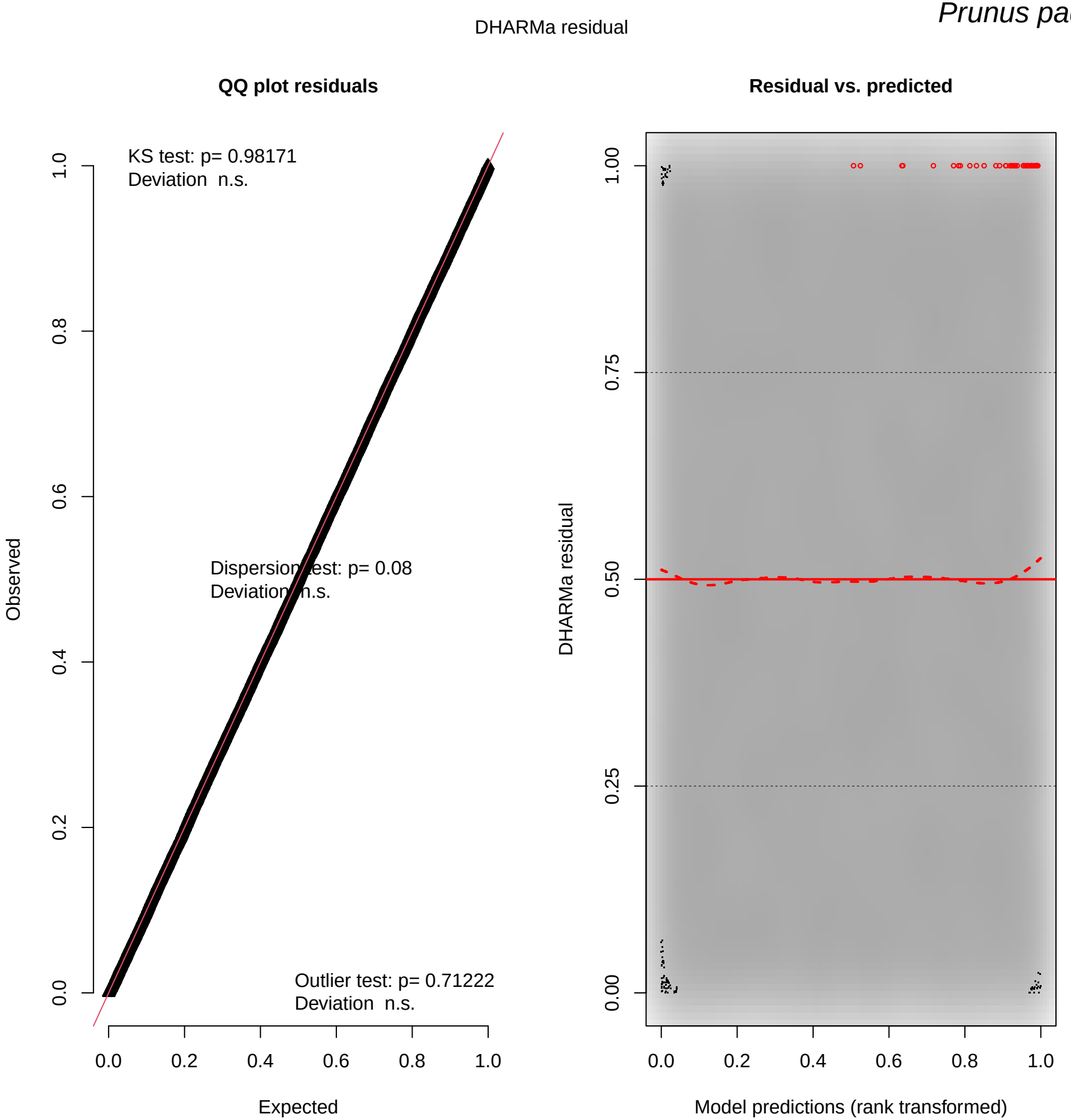

Prunus padus

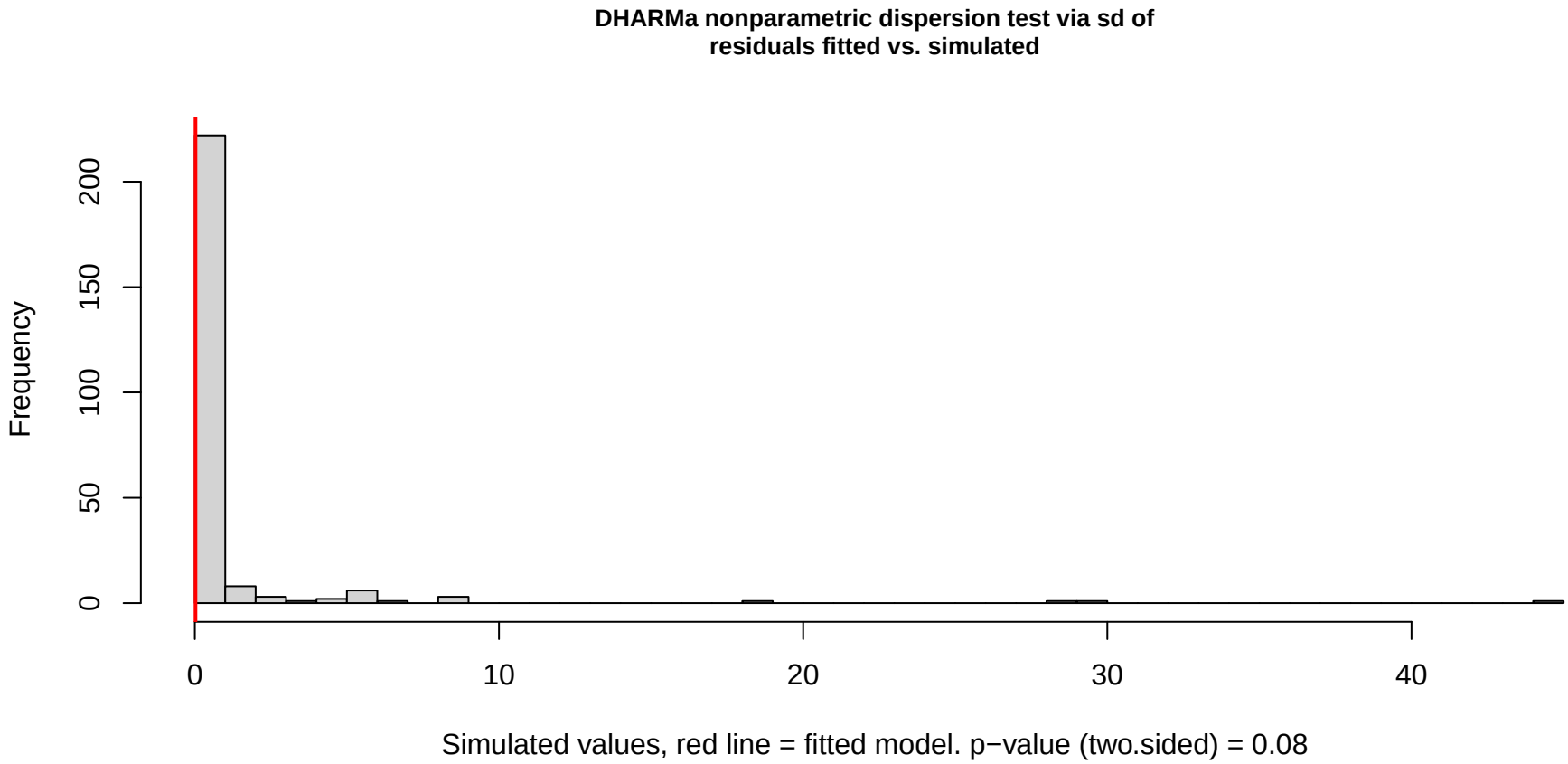

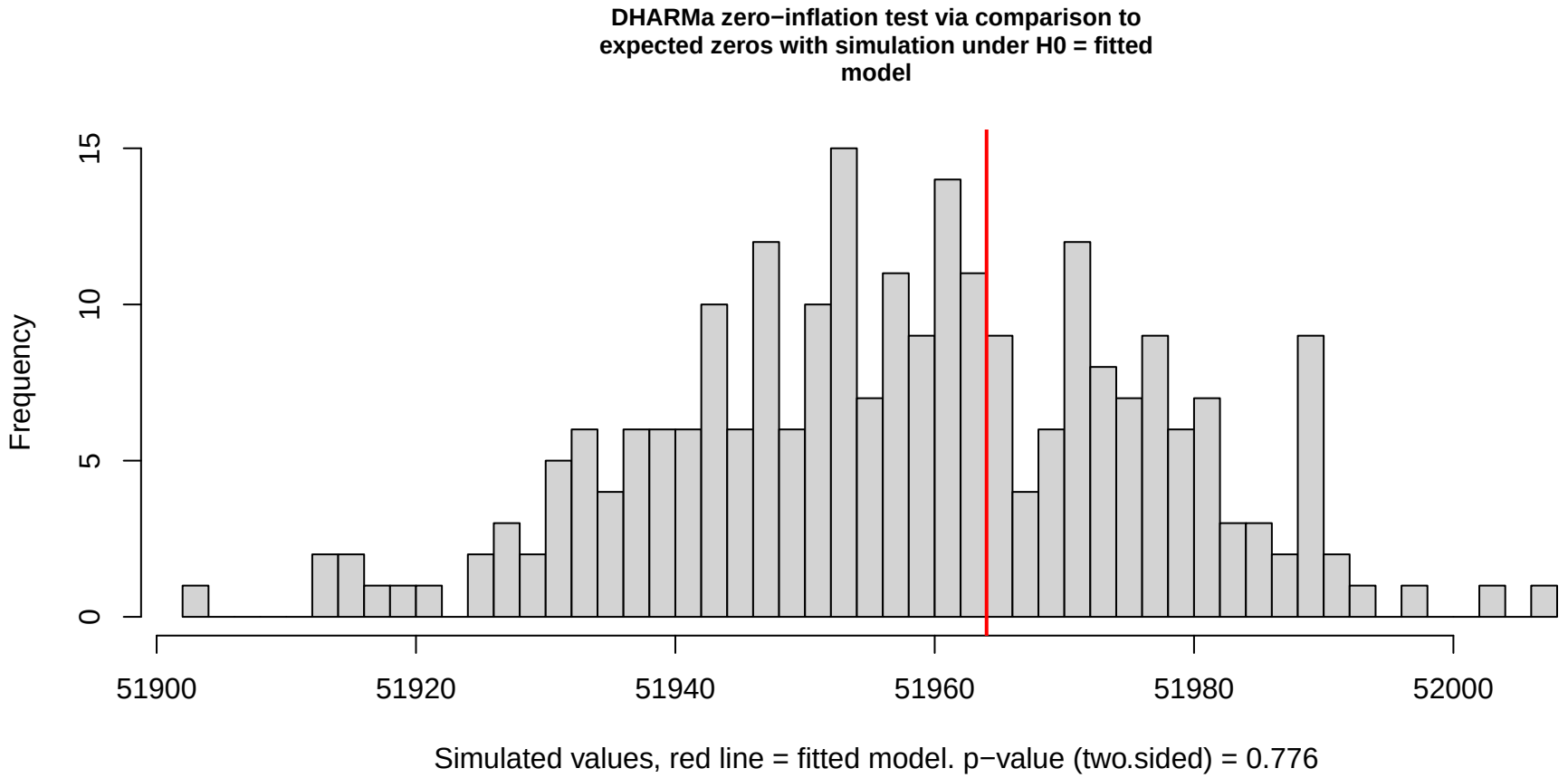

Prunus padus

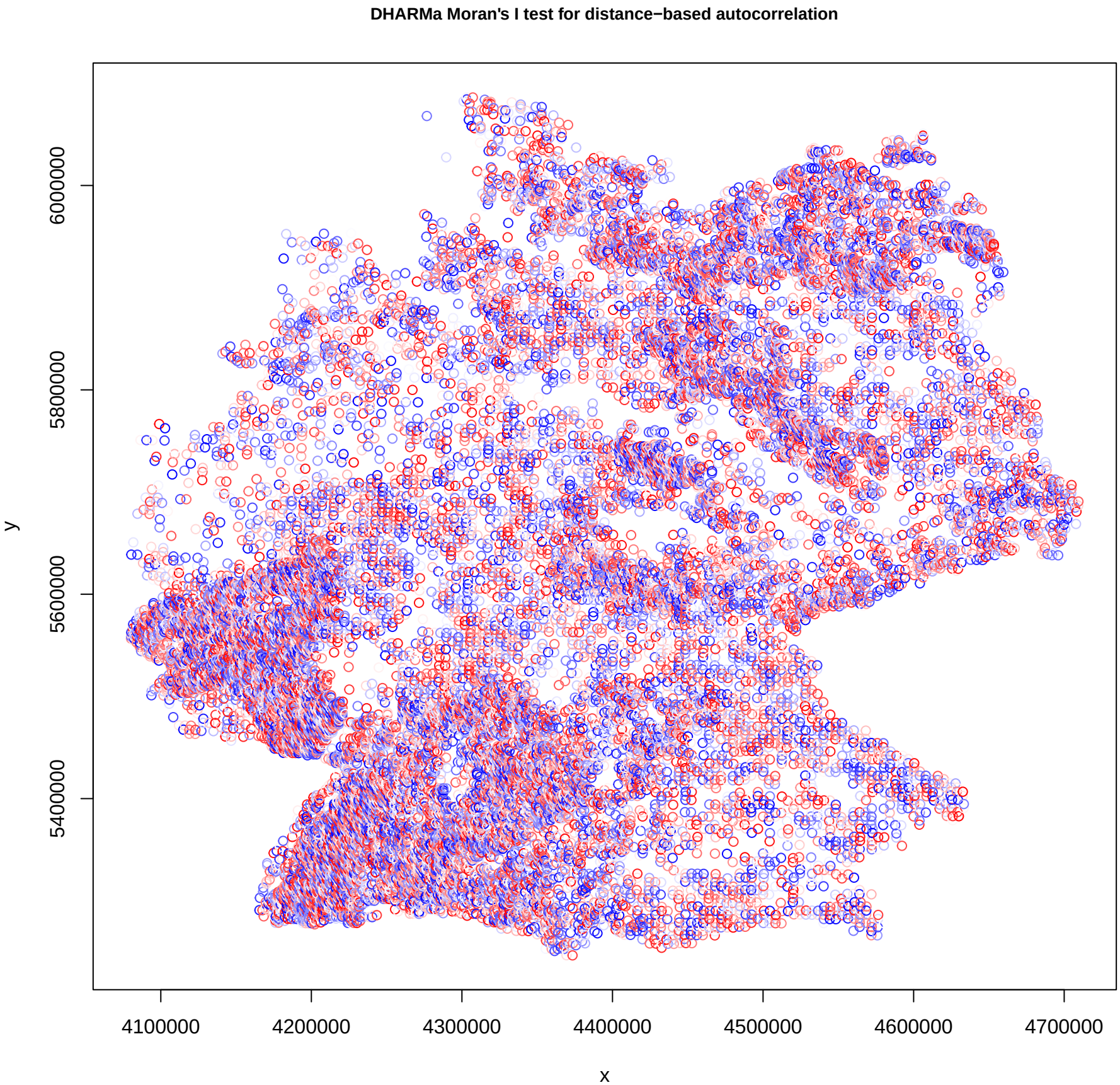

Sorbus aucuparia

DHARMa residual

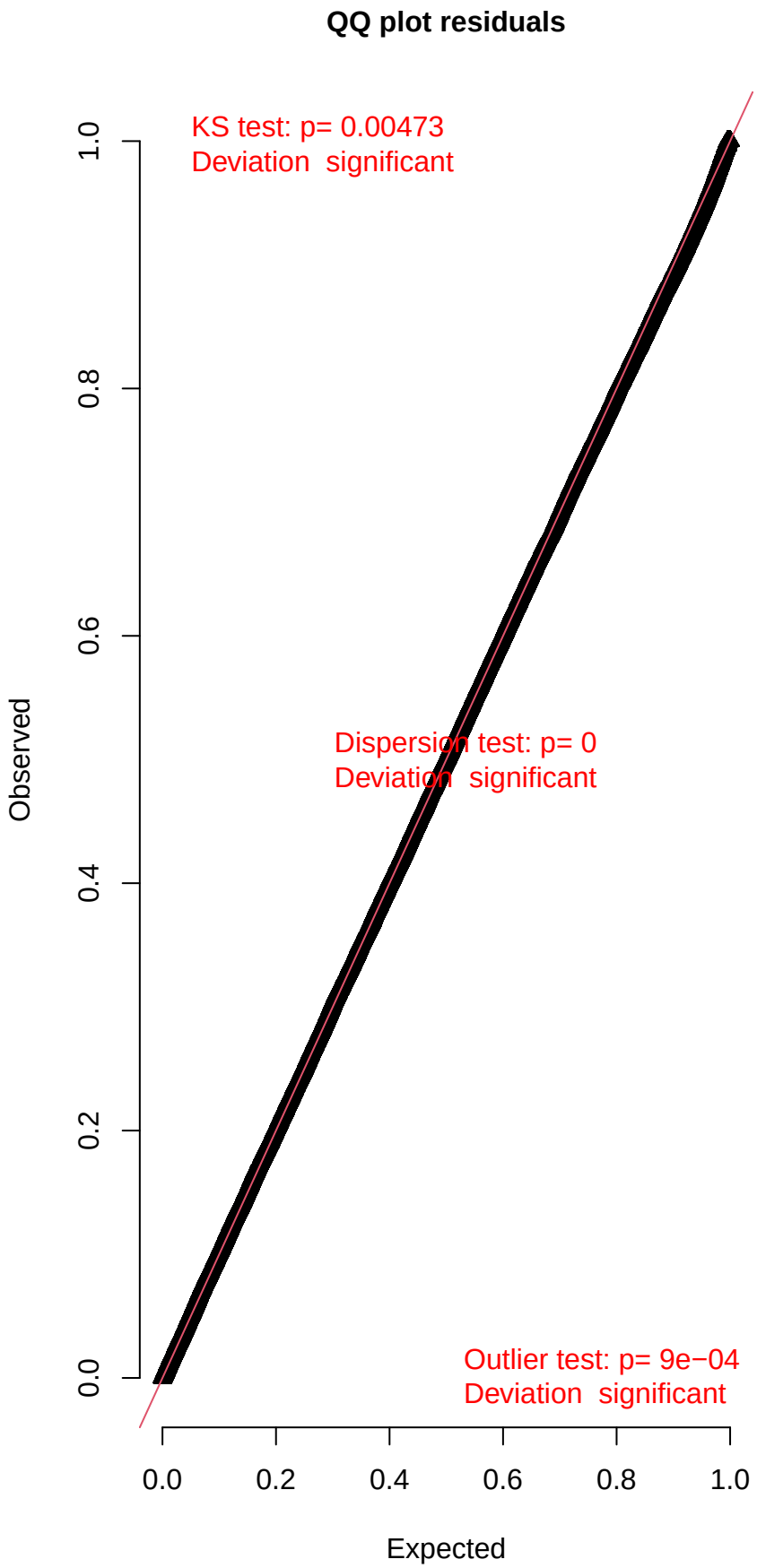

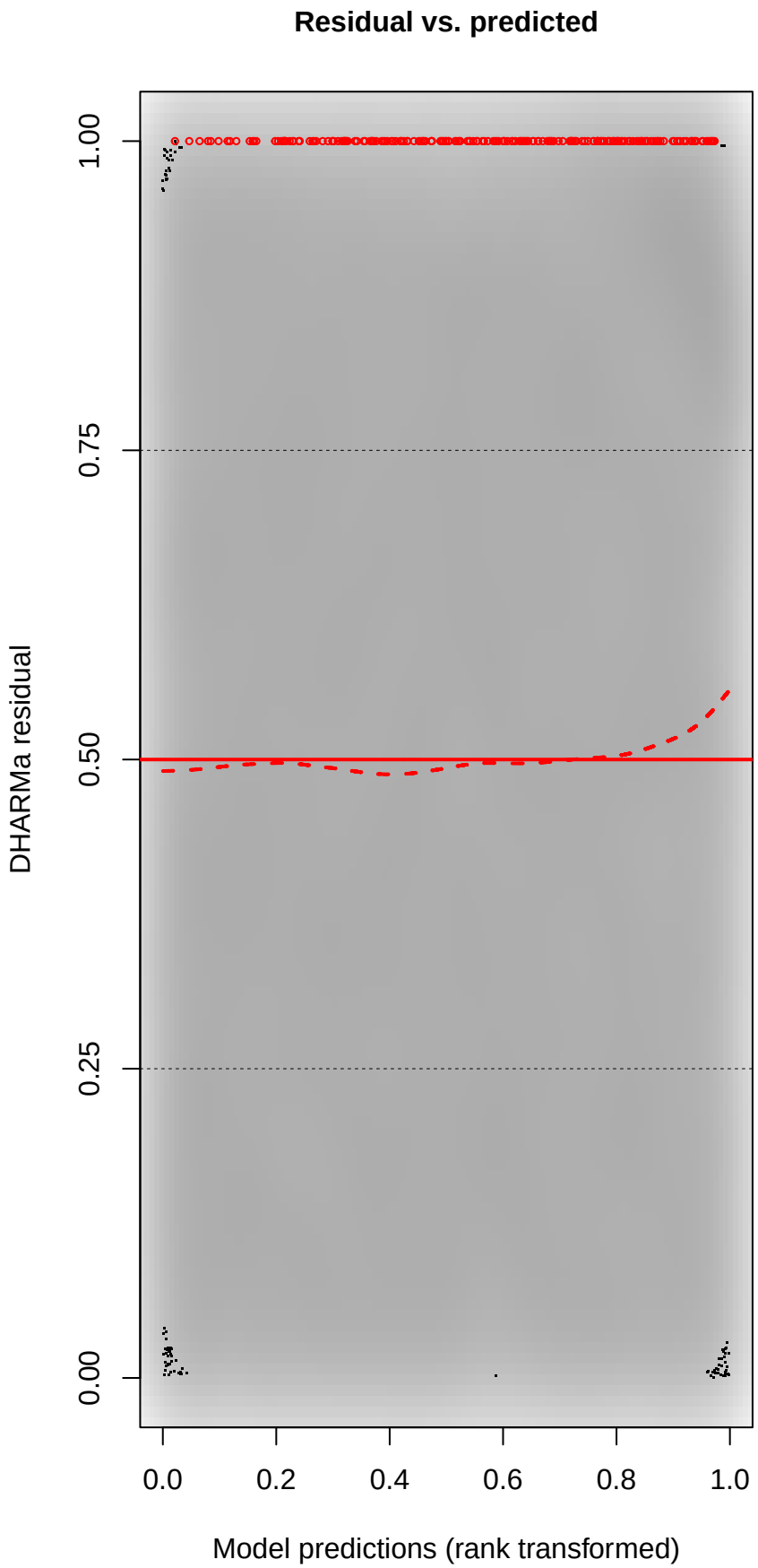

Sorbus aucuparia

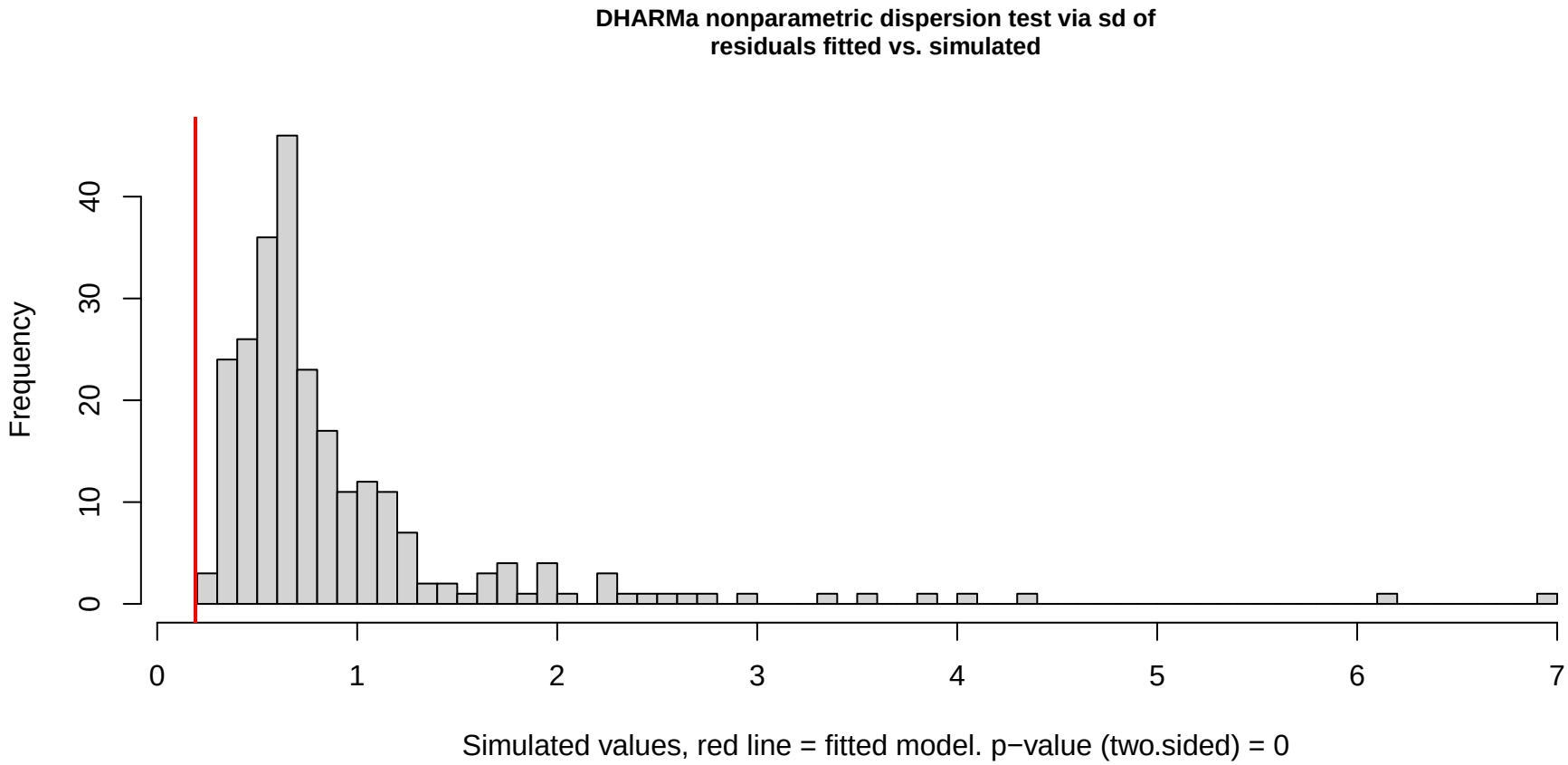

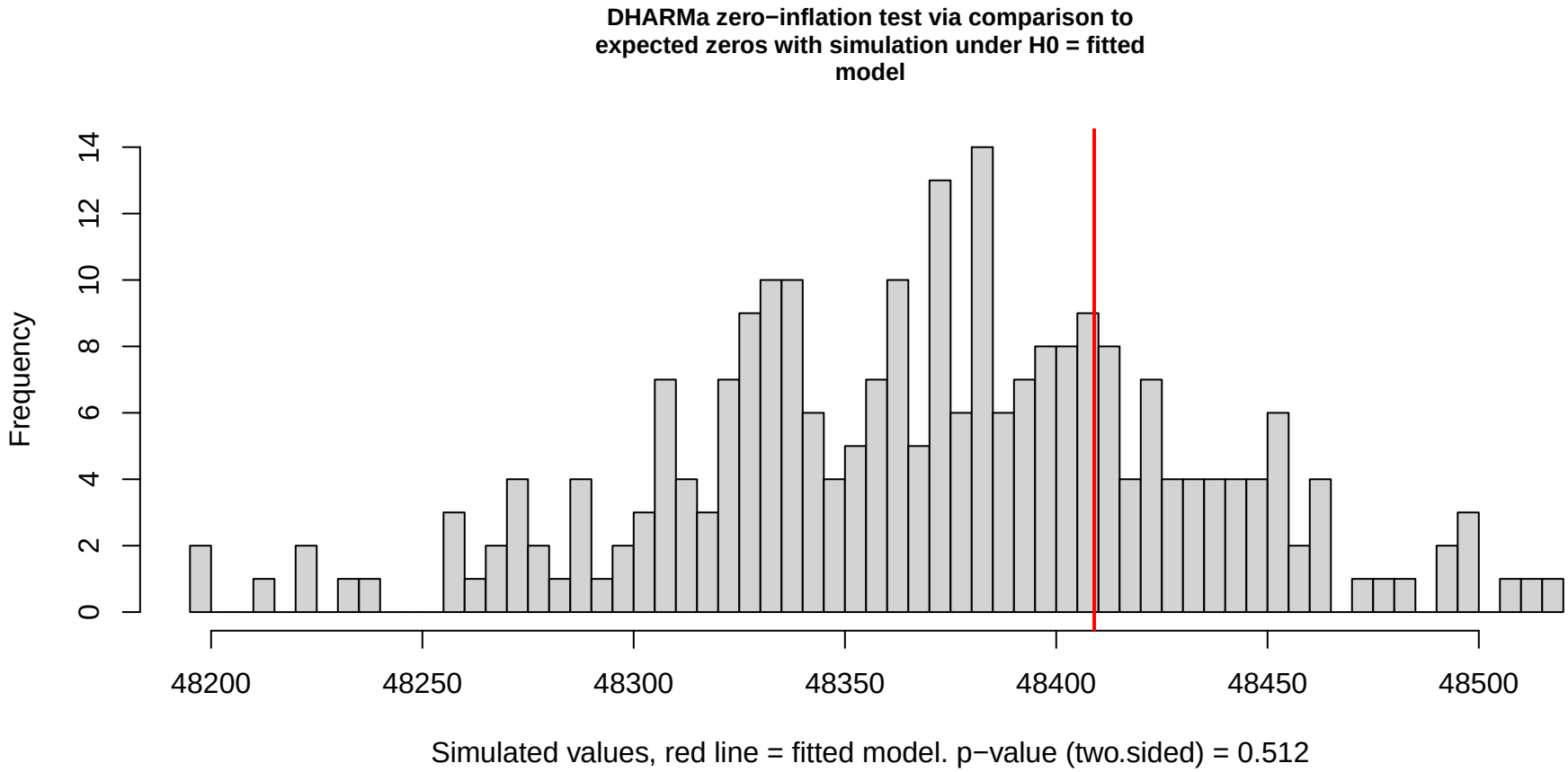

Sorbus aucuparia

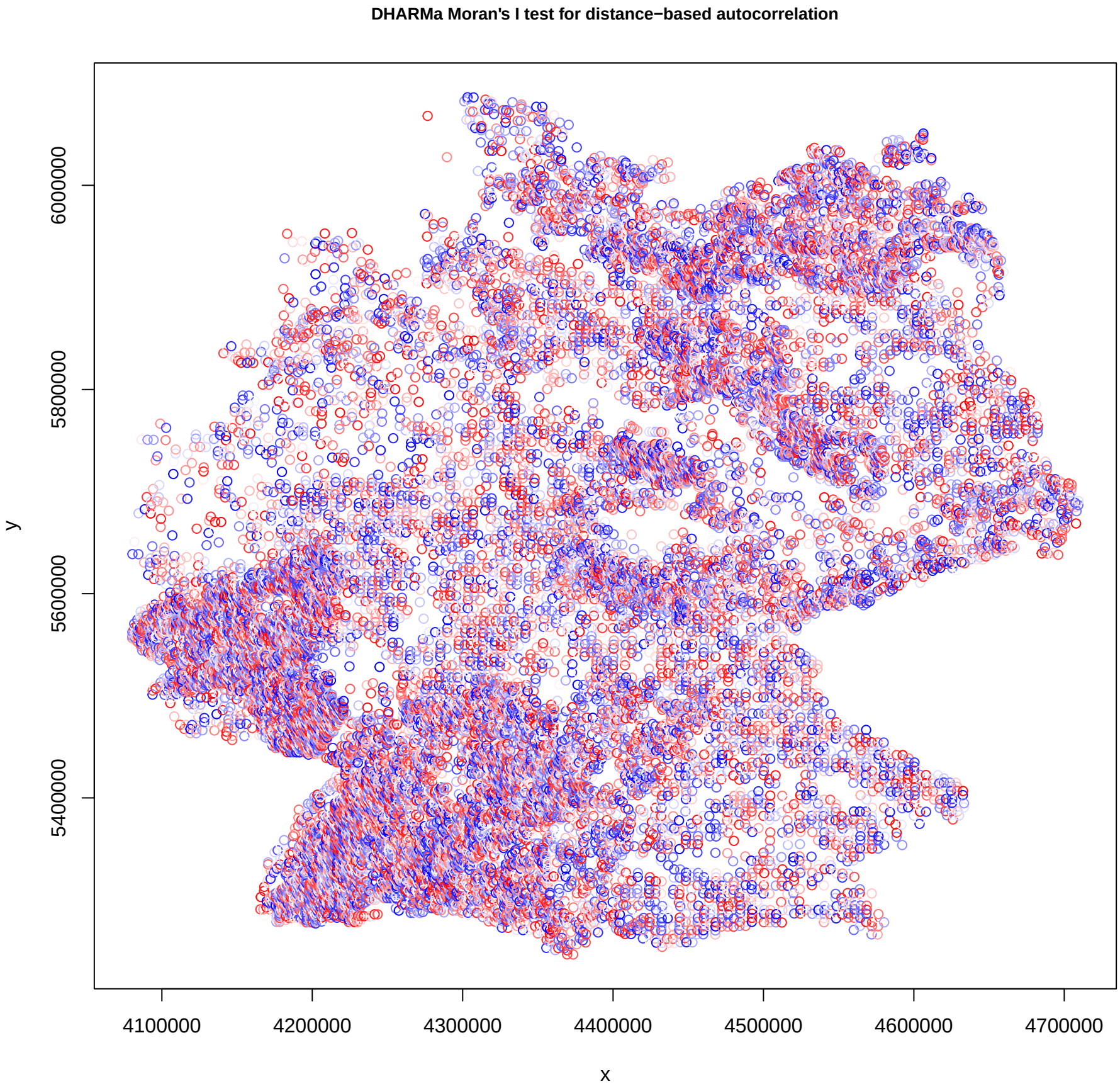

Quercus petraea.robur

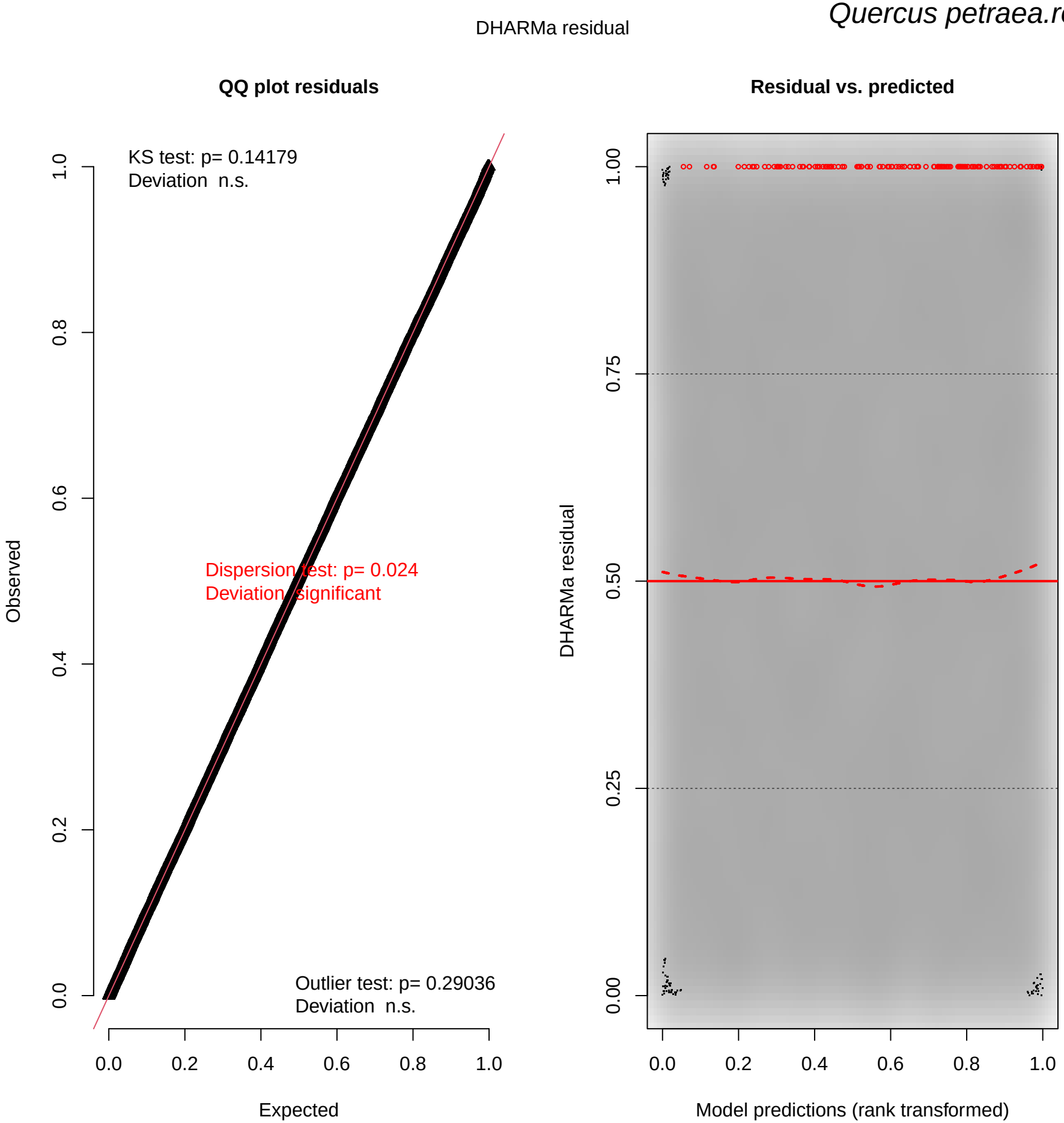

Quercus petraea.robur

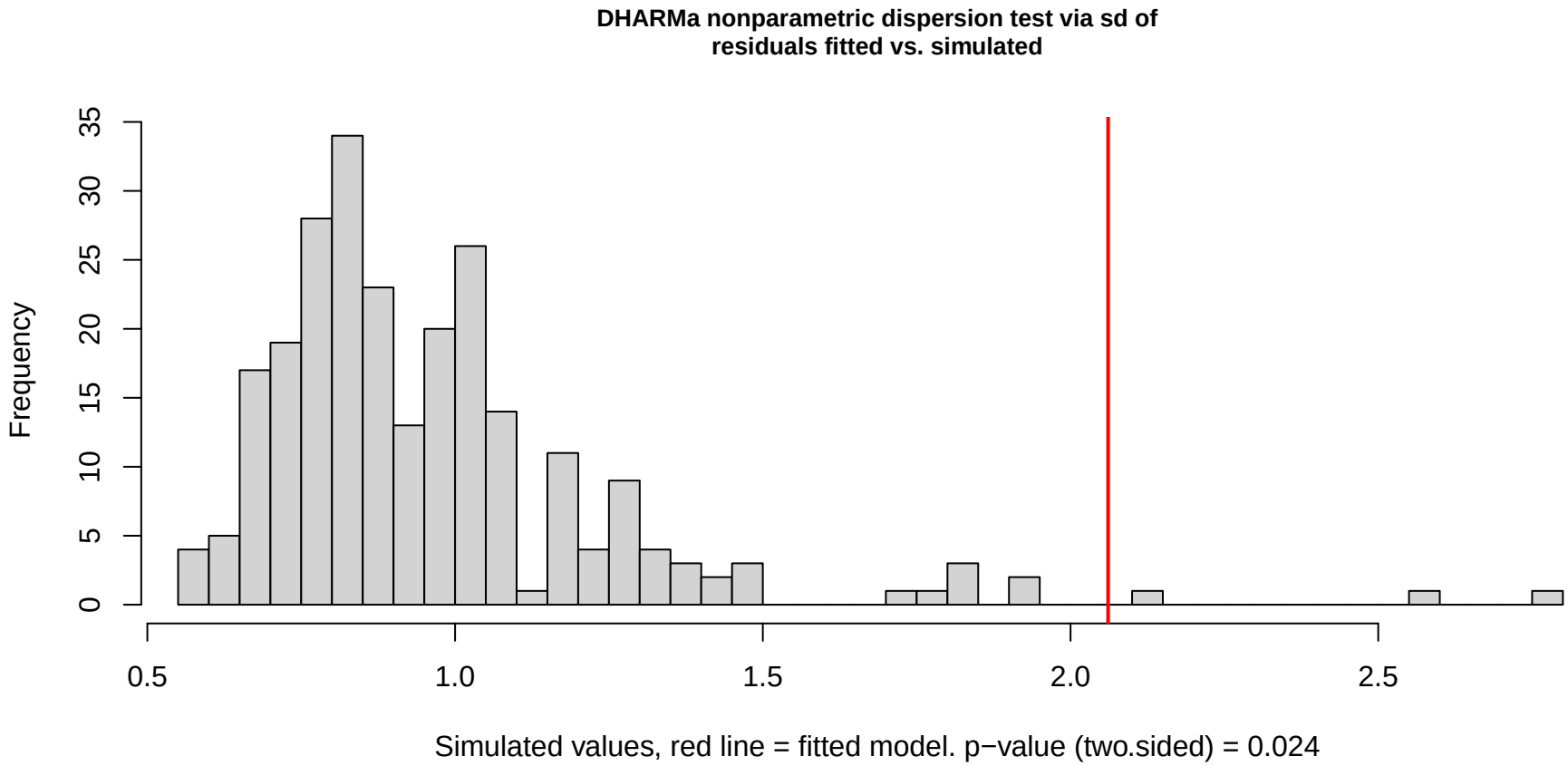

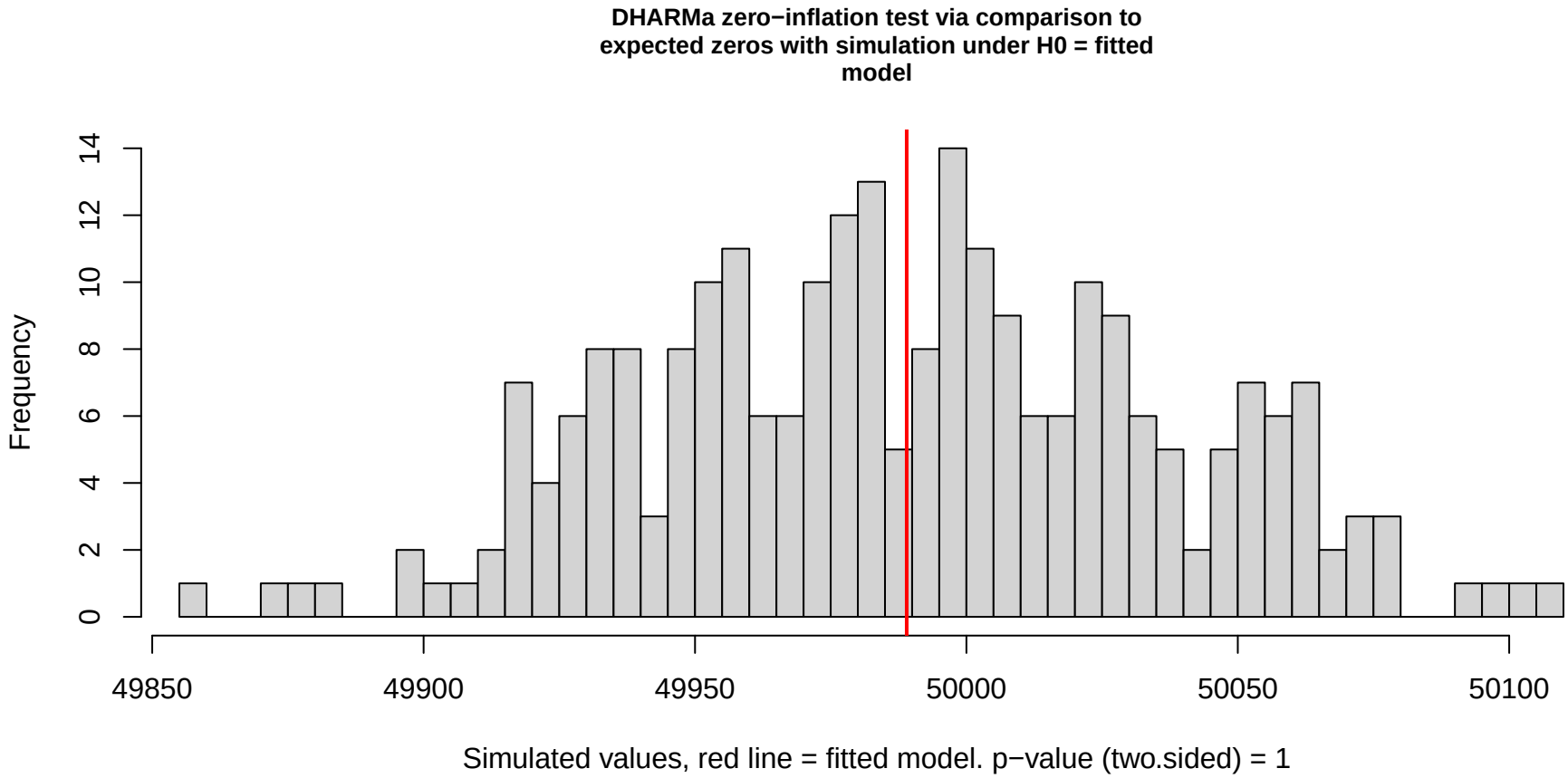

Quercus petraea.robur